HETEROGENEOUS CATALYSTS FOR THE ALKYLATION OF AMINES USING ALCOHOLS

SUBMITTED IN PART FULFILMENT OF THE
REQUIREMENTS FOR THE DEGREE OF
DOCTOR OF PHILOSOPHY

LUKA VICTORIA TALLON

SEPTEMBER 2015

DEPARTMENT OF CHEMISTRY

IMPERIAL COLLEGE LONDON

DECLARATION OF ORIGINALITY

I confirm that all work presented in this thesis is my own and other research is referenced in the text.

COPYRIGHT DECLARATION

The copyright of this thesis rests with the author and is made available under a Creative Commons Attribution Non-Commercial No Derivatives licence. Researchers are free to copy, distribute or transmit the thesis on the condition that they attribute it, that they do not use it for commercial purposes and that they do not alter, transform or build upon it. For any reuse or redistribution, researchers must make clear to others the licence terms of this work.

ABSTRACT

This PhD thesis describes the Au-catalysed alkylation of amines using alcohols (AAA). The work was broadly divided into two parts: (i) developing mechanistic and kinetic models for the reaction; and (ii) further catalyst development.

The introductory Chapter provides and overview of reported homogeneous and heterogeneous catalysts for the AAA reaction, with a comparison of their scope and limitations.

Chapter 2 begins with a summary of a previously reported mechanistic model using Au/TiO_2 to catalyse the model reaction of aniline with benzyl alcohol in flow. The Chapter proceeds by comparing the effects of O_2 and the use of different H_2O concentrations when performing the model reaction. Additionally, the stability and possible deactivation routes of the catalyst is interrogated.

In Chapter 3, the results from the mechanistic studies are used to further develop the previously reported kinetic model.

The effects of using different preparation techniques and supports on the catalyst structure and activity of Au/TiO_2 are detailed in Chapter 4 and 5, respectively. Chapter 6 presents the activities of different metal catalysts for the model reaction.

Chapter 7 contains experimental procedures for reactions and catalyst preparation methods.

In dedication to my parents and sister x

ACKNOWLEDGEMENTS

I would like to thank Dr Mimi Hii, Professor Klaus Hellgardt, Dr Peter Ellis and Dr James Cookson for the opportunity to work on this project and their invaluable guidance and support throughout. I am truly indebted to all of you all for the experience and knowledge I have gained. I also wish to express my gratitude to Dr John Brazier for his sound advice and help throughout the years. In terms of collecting data for my project, I would like to thank Dr Peter Ellis and the Johnson Matthey analytical department and Dr Ekaterina Ware for help with TEM imaging at Imperial College London.

To my family and friends- thank you for your encouragement and giving me confidence in times of doubt, without your support I would not have come this far.

To C-bear, Bee and Winnie- thank you for always making me smile and lifting my spirits during the difficult times along the journey xxx

TABLE OF CONTENTS

ABSTRACT iii
ACKNOWLEDGEMENTS v
LIST OF KEY ABBREVIATIONS viii
CHAPTER 1. Introduction 1
1.1 Synthetic methods for the alkylation of amines 2
1.2 The hydrogen borrowing method for the AAA reaction 4
1.2.1 Homogeneous catalysts for the AAA reaction 4
1.2.2 Heterogeneous catalysts for the AAA reaction 23
1.3 Conclusion 35
1.4 Project aims 37
CHAPTER 2. Mechanistic studies using Au/TiO_2 in flow 39
2.1 Background 40
2.2 Characterisation of Au/TiO_2 45
2.3 Results of the mechanistic studies using Au/TiO_2 47
2.3.1 The effect of H_2O on the AAA reaction using 2-methyl-2-butanol 47
2.3.2 The effect of H_2O and O_2 on the AAA reaction using 2-methyl-2-butanol 54
2.4 Results of the Au/TiO_2 deactivation and stability studies 62
2.5 Conclusion 67
CHAPTER 3. The development of a kinetic model for the AAA reaction 68
3.1 Background 69
3.2 Kinetic modelling of reaction data 73
3.3 Conclusion 84
CHAPTER 4. Preparation, characterisation and catalytic screening of Au/TiO_2 86
4.1 Background 87
4.1.1 Impregnation (IMP) 87
4.1.2 Deposition-Precipitation (DP) 88
4.1.3 Colloidal Synthesis (COL) 88
4.1.4 Spray Drying (SD) 89
4.1.5 Effect of thermal treatment conditions on particle size 89
4.2 The effect of the preparation technique on the structure of $Au//TiO_2$ 90
4.3 Catalyst screening results and analysis 96
4.3.1 Au/TiO_2 prepared by the DP method 97

4.3.2 Au/TiO_2 prepared the IMP method 99
4.3.3 Au/TiO_2 prepared by the COL method 100
4.4 Conclusion 102
CHAPTER 5. Investigation of Au supported catalysts for the AAA reaction 103
5.1 Background 104
5.2 The effect of the support on catalyst structure 106
5.3 Catalyst screening results and analysis 111
5.3.1 Au supported catalysts prepared by the DP method 111
5.3.2 Au supported catalysts prepared by the COL method 113
5.4 Conclusion 120
CHAPTER 6. Investigation of Au bimetallic and metal titania catalysts for the AAA reaction 121
6.1 Background 122
6.2 M/TiO_2 catalyst characterisation 123
6.3 M/TiO_2 screening results and analysis 125
6.3.1 Group 9: M/TiO_2 screening results 126
6.3.2 Group 10: M/TiO_2 screening results 127
6.3.3 Group 11: M/TiO_2 screening results 128
6.4 Preparation, characterisation and catalytic screening of additional Cu/TiO_2 catalysts 131
6.4.1 Cu/TiO_2 screening results 133
6.5 $Au,M/TiO_2$ catalyst characterisation 136
6.6 $Au,M/TiO_2$ screening results and analysis 139
6.6.1 Group 9: $Au,M/TiO_2$ screening results 139
6.6.2 Group 10: $Au,M/TiO_2$ screening results 140
6.6.3 Group 11: $Au,M/TiO_2$ screening results 141
6.6.4 Comparison of H-TPD data and screening results 141
6.7 Conclusion 143
6.8 Project summary and Future work 144
CHAPTER 7. Experimental 147
7.1 General 147
7.2 Catalyst characterisation 149
7.3 Catalytic reactions 150
7.4 Catalyst synthesis and calcination 155
REFERENCES 159

LIST OF KEY ABBREVIATIONS

AAA	Alkylation of amines using alcohols
API	Active pharmaceutical ingredients
BET	Brunauer Emmett Teller
Calc.	Calcination
CHN	Carbon, hydrogen, nitrogen
COL	Colloidal
Conv.	Conversion
CPME	Cyclopentyl methyl ether
DP	Deposition-precipitation
DPEphos	Bis-[2-(diphenylphosphino)phenyl]ether
DPPE	1,2-Bis(diphenylphosphino)ethane
Dppf	1,1'-Bis(diphenylphosphino)ferrocene
EDX	Elemental dispersive x-ray
FTIR	Fourier transform infrared
GC	Gas Chromatography
GC-FID	Gas Chromatography flame ionisation detector
GC-MS	Gas Chromatography mass spectrometry
Glc	Gas liquid chromatography
H-TPD	Hydrogen- temperature programmed desorption
ICP	Inductively coupled plasma
IMP	Impregnation
IWI	Incipient wetness impregnation
PBR	Packed bed reactor
PVA	Poly(vinyl) alcohol
RMS	Relative mean square
SD	Spray drying
SMSI	Strong metal support interactions
SPR	Surface plasmon resonance
TEM	Transmission electron microscopy
TOF	Turnover frequency

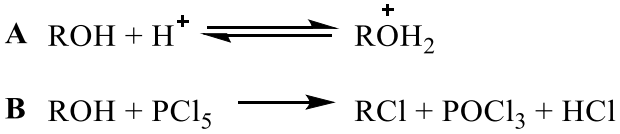
UV	Ultraviolet
WI	Wet impregnation
χi	Electronegativity of metal ions
χ0	Paulings electronegativity of the metal element
z	Valence of metal ions

CHAPTER 1. Introduction

As the global population continues to increase, so do the demands on the chemical industry, making current processes that are often hazardous to the environment unsustainable.[1] The key challenge is to create methods that limit the detrimental effects to the environment for future generations, yet allow for the needs of our current population to be met. This is the underlying theme of sustainable development, which the chemical industry has been working towards through employing 'green chemistry' strategies.[2]

In 1998, Anastas and Kirchoff developed a list of 12 green chemistry principles,[3, 4] with the basic message following, that methods should be designed which limit the use and generation of hazardous reagents in the manufacture and application of chemical products. In order to catalyse the integration of green chemistry and engineering, the American Chemical Society (ACS) Green Chemistry Institute (GCI) was established.[5] The Institute identified a list of key research areas were improvements are required, with the activation of alcohols for nucleophilic substitution being voted as the second most important topic.

Using alcohols as a feedstock is desirable as they are readily available and inexpensive, however, OH is a poor leaving group, and is generally replaced by a better one through methods such as protonation or halogenation (Scheme 1.1).[6] However, protonation can cause the incoming nucleophile to be deactivated in the acidic environment, and use of reagents such as PCl_5 leads to the generation of hazardous waste materials.



SCHEME 1.1. *Activating alcohols by* ***A)*** *protonation,* ***B)*** *halogenation.*

A 'green alternative' for the activation of alcohols is the hydrogen borrowing method (also known as the hydrogen auto transfer process).

This project aims to study the alkylation of amines using alcohols (AAA) employing this strategy. A background of common synthetic methods for the alkylation of amines is discussed next (Section 1.1) with the details of the hydrogen borrowing method presented in the following section (1.2).

1.1 Synthetic methods for the alkylation of amines

It has been estimated that roughly 64% of all nitrogen substitutions are alkylations in the pharmaceutical industry.[5] Indeed, the amine functionality brings essential activity to a wide range of pharmaceutical drugs (Figure 1.1).[7] Venlafaxine is used in the treatment of depression and generalised anxiety disorder, Chlorpheniramine is an alkylamine antihistamine used for relieving allergies, while Piribedil is used in the treatment of Parkinson's disease.[8-10] Nitrogen containing compounds also find applications in epoxy hardeners, vulcanising agents and in the preparation of detergents, fabric softeners and dyes.[2] For example, pH indicator Methyl orange and Lauryldimethylamine oxide, which is a detergent, emulsifier, foaming agent, softener and dyeing auxiliary.[11, 12]

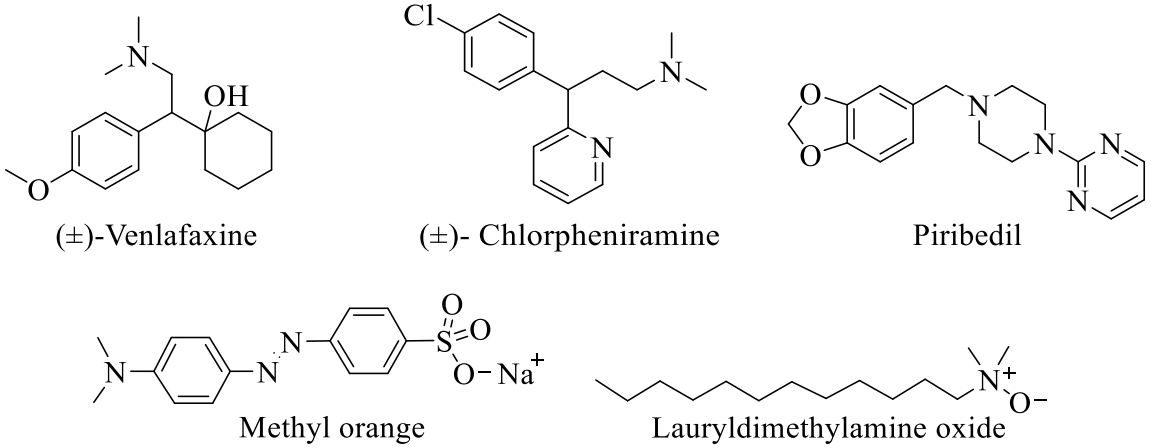


FIGURE 1.1. *Important pharmaceutical drugs containing amine functionalities.*

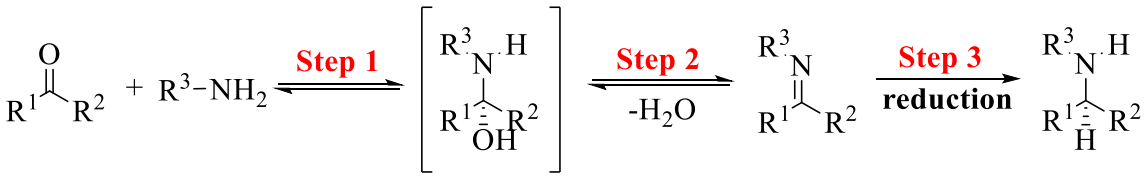
Amines and ammonia are nucleophilic species that readily undergo S_N2 substitutions with alkyl halides to generate newly alkylated amine compounds (Scheme 1.2).[13] The toxic nature of alkyl halides and the overalkylation commonly found makes this process unfavourable, especially in the pharmaceutical industry where there is strict control of residual impurities.[14] A way of avoiding overalkylation is to use an excess of amine, however this generates large amounts of waste.



SCHEME 1.2. *S_N2 substitution of amines using alkyl halides.*

An alternate strategy is the use of reductive amination of aldehydes and ketones (Scheme 1.3).[15, 16] Condensation of amine with the carbonyl species affords a carbinol amine (Step 1) which eliminates H_2O to yield imine (Step 2). The imine species is subsequently reduced to

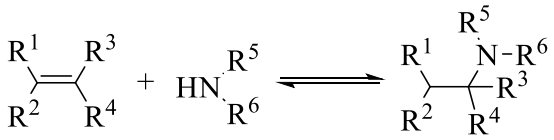
give the alkylated amine product (Step 3). Common hydride reducing agents are $NaCNBH_3$ or $Na(OAc)_3BH$, a more economical and effective method is to employ a catalyst, usually Pt, Ni or Pd based, with molecular H_2.[15]



SCHEME 1.3. *Reductive amination of carbonyl species to afford amine products.*

Overalkylation remains an issue with this technique and the use of reducing agents and hazardous molecular H_2, which requires containment, is disadvantageous. Furthermore, when employing reagents that contain multiple C-C bonds (double and triple) and other functional groups prone to reduction, the hydrogenation of imine is limited.

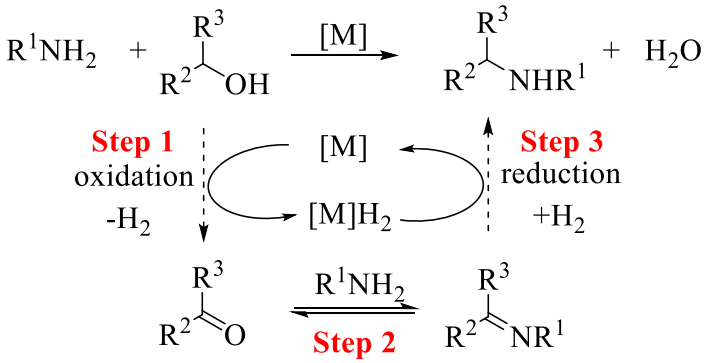
A more efficient process is hydroamination, which involves the addition of an amine to an unsaturated C-C multiple bond.[17-19] Nitrogen containing compounds are produced in one step, without the formation of side-products (Scheme 1.4). Hydroamination is widely used in industry,[2] yet reactions are hindered by the high activation barrier arising from the electrostatic repulsion of the electron pair on the nitrogen atom and the electron rich π-bond. The high reaction temperatures required to overcome the barrier shifts the equilibrium over to the starting materials, due to the negative reaction entropy ΔS°.[17] It is this combination that makes the design of catalysts for this reaction essential. Still the majority of the reported systems able to facilitate this process are difficult to synthesise, expensive, sensitive to air and moisture and/or are highly toxic.[17]



SCHEME 1.4. *Hydroamination of amines across C-C double bonds.*

1.2 The hydrogen borrowing method for the AAA reaction

In a hydrogen borrowing system, a catalyst (M) acts as both a hydrogen donor and acceptor (Scheme 1.5).[20] Hydrogen is abstracted from the alcohol to yield the more reactive carbonyl intermediate and metal hydride species (Step 1). The carbonyl compound then condenses with the amine to produce an imine intermediate (Step 2), to which the catalyst returns hydrogen forming the newly alkylated amine product (Step 3).



SCHEME 1.5. *The hydrogen borrowing method for the alkylation of amines using alcohols.*

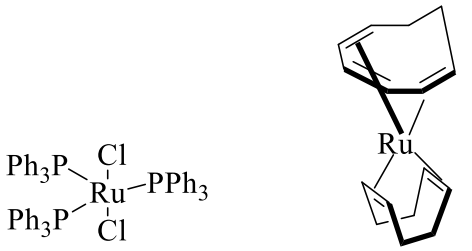
The overall process involves two redox steps, but performed in one operation. This concept of hydrogen shuttling is clearly superior to the aforementioned protocols for activating alcohols and for forming amine compounds. Extreme pH conditions can be avoided, H_2O is generated as the only stoichiometric by-product, it is a 'one-pot' process and the use of molecular H_2 is not necessary. There are numerous reports of catalysts facilitating the formation of amines using this technique, which will be introduced in the following Sections.

1.2.1 Homogeneous catalysts for the AAA reaction

Homogeneous processes, where the catalyst is in the same phase as the reactants (typically dissolved in a solvent) are advantageous as catalyst sites are generally single well-defined entities. Thus selectivity can be achieved by 'tuning' electronic and steric properties.

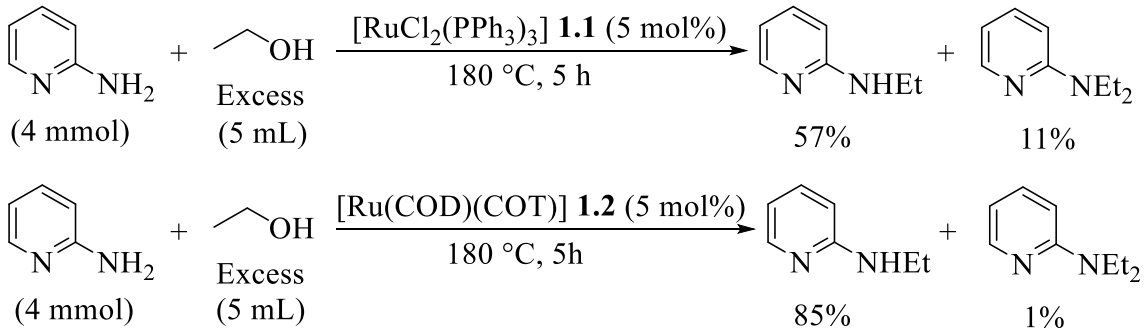
Grigg and Watanabe reported the first homogeneous catalysts for the AAA reaction in 1981, independently, using Ru and Ir based complexes.[21, 22] Early reports of the AAA reaction using Ru complexes, namely $[RuCl_2(PPh_3)_3]$ (**1.1**, Figure 1.2), suffered from the high reaction temperatures required (typically between 180-200 ˚C) and poor selectivity to the amine product.[22-24] The nature of the ligand may have contributed to the low selectivity of this catalyst. Certainly, it was shown that by employing [Ru(COD)(COT)] (**1.2**, Figure 1.2)

for the mono-alkylation of aminopyridines (relevant in the application of medicinally active compounds), an increased selectivity and yield could be obtained, compared to using **1.1** under the same reaction conditions (Scheme 1.6).[23]



1.1 **1.2**

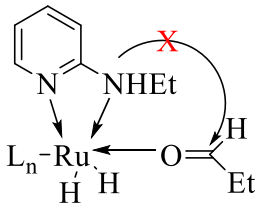
FIGURE 1.2. *Structures of [RuCl₂(PPh₃)₃] (**1.1**) and [Ru(COD)(COT)] (**1.2**).*



Yields determined by GLC.

SCHEME 1.6. *Mono and dialkylation of aminopyridine using [RuCl₂(PPh₃)₃](**1.1**) and [Ru(COD)(COT)] (**1.2**).*

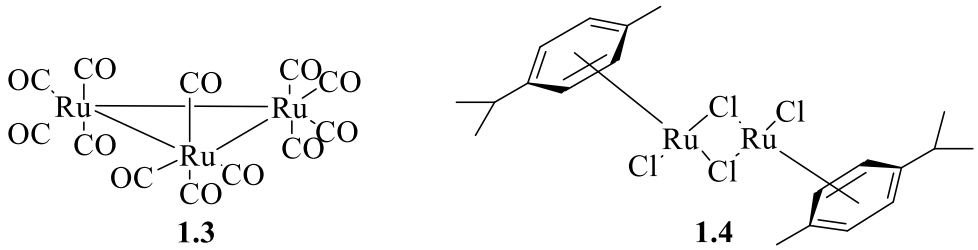
The increased selectivity afforded by complex **1.2** was ascribed to two causes, the first being the absence of phosphine ligands. Indeed when **1.2** was employed in the presence of various phosphine ligands (at 180 ˚C, for 5 h), the di-alkylated product was obtained.[23] The origin of this effect was not discussed in the study. However, in a separate report investigating the AAA reaction catalysed by **1.1**, it was suggested that phosphine might act to displace complexed aldehyde and facilitate its reaction in solution with amine.[25] The second cause was attributed to steric hindrance in the nucleophilic attack of aldehyde by the monoalkylated amine species, when employing **1.2**, leading to the monoalkylated amine being the major product (Scheme 1.7).



SCHEME 1.7. *Hindered nucleophilic attack of coordinated aldehyde by monoalkylated heteroaromatic amine, using [Ru(COD)(COT)]* ***(1.2)****.*

Overall, as well as the high reaction temperatures required, both **1.1** and **1.2** complexes have limited scope with regards to using less reactive secondary alcohols as substrates. Carbonyl compounds generated from secondary alcohols are generally less electrophilic and are more sterically hindered than primary carbonyl species, meaning more forcing conditions are often required.

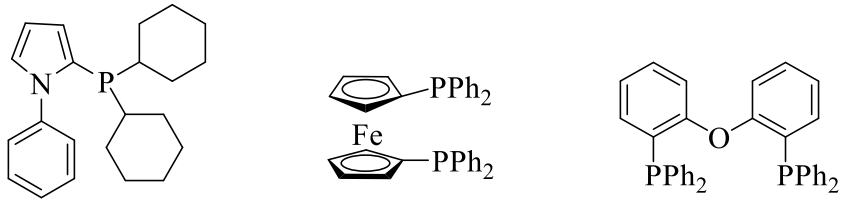
In this regard, $[Ru_3(CO)_{12}]$ (**1.3**) and $[Ru(p\text{-cymene})Cl_2]_2$ (**1.4**) (Figure 1.3), reported independently by Beller and Williams,[26-28] respectively, showed that these complexes can be used to catalyse reactions between secondary alcohols and amines under mild conditions.



1.3 **1.4**

FIGURE 1.3. *Structures of* $[Ru_3(CO)_{12}]$ ***(1.3)*** *and* $[Ru(p\text{-cymene})Cl_2]_2$ ***(1.4)****.*

In these examples, the presence of phosphine ligands were required (Figure 1.4). Using the Ru carbonyl complex **1.3**, pyrrole phosphine (**1.5**) was shown to give the highest reactivity. On the other hand, bidentate phosphines, 1, 1'-Bis (diphenylphosphino)ferrocene (dppf) or Bis-[2-(diphenylphosphino)phenyl]ether (DPEphos) (**1.6** and **1.7**, respectively) were employed in combination with Ru cymene complex **1.4**.



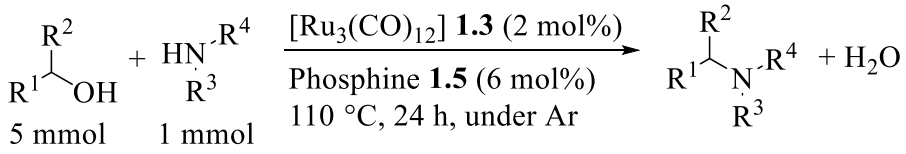
1.5 **1.6** **1.7**

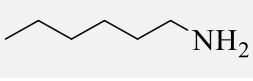
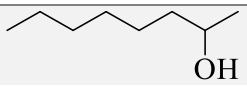
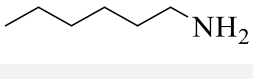
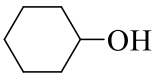
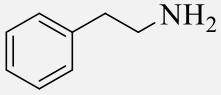
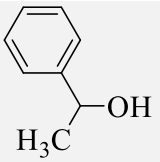
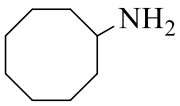
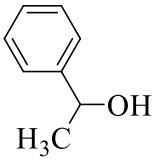
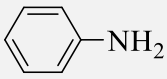
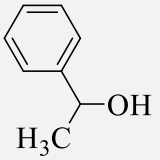
FIGURE 1.4. *Phosphine ligands used in combination with* $[Ru_3(CO)_{12}]$ ***(1.3)*** *and* $[Ru(p\text{-cymene})Cl_2]_2$ ***(1.4)****.*

In contrast to complexes **1.1** and **1.2** mentioned above, the combination of Ru complex **1.3** and phosphine ligand **1.5** was able to catalyse the alkylation of secondary aliphatic alcohols with *n*-hexylamine (Table 1.1, entries 1 and 2), as well as a variety of aliphatic amines with 1-phenylethanol, in excellent yields (Table 1.1, entry 3).[28] Amines containing long alkyl chains are particularly interesting as they are important in the detergent industry.[29]

However, the activity decreased as more hindered aliphatic amines were employed (Table 1.1, entry 3 vs. entry 4). The reaction also failed for poorly nucleophilic aniline (Table 1.1, entry 5), even ones containing electron-donating substituents.[28]

TABLE 1.1. *N-alkylation of amines with secondary alcohols using [$Ru_3(CO)_{12}$] (**1.3**) and phosphine **1.5**.*

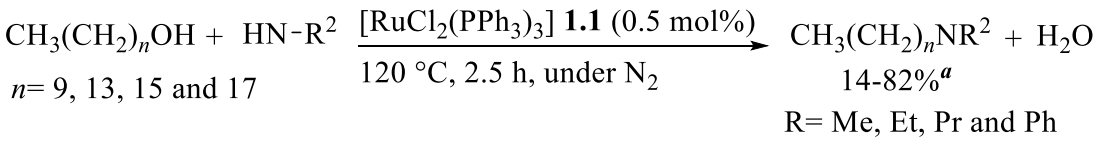


Entry	Amine	Alcohol	Yield (%)[a]
1[b]			98
2[c]			99
3			90
4			58
5			0

[a] *Determined by GC,* [b] *amine (1 mmol), alcohol (2 mmol),*[c] *100 ˚C.*

The reaction scope of **1.3**/**1.5** is interesting compared to catalyst **1.1**, which was able to facilitate the reaction of aniline and aliphatic amines with long chain aliphatic alcohols to afford tertiary amines (Scheme 1.8). In this case, aromatic amines were more active than aliphatic ones (47-52% yield vs. 14-28% yield). This is notable as reactions between anilines and aliphatic alcohols are typically challenging in AAA catalysis, due to the low nucleophilicity of the amine and poor reactivity of the alcohol. In contrast to complex **1.3**,

primary aliphatic alcohols were employed in these reactions which could explain the increased activity of this system. Indeed when secondary alcohols were used, the reaction failed.[25, 29]



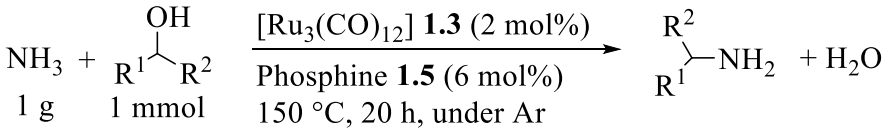
[a] *Determined by GC-MS*

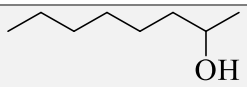
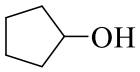
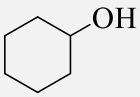
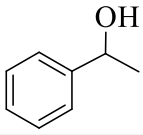
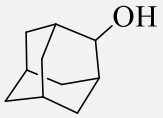
SCHEME 1.8. *N-alkylation of secondary amines using primary aliphatic alcohols and [RuCl₂(PPh₃)₃] (**1.1**).*

The application of catalyst **1.3**/**1.5** can be extended to allow the formation of primary amines from secondary alcohols using ammonia.[30] The production of primary amines is of significant importance, as they are useful intermediates for further derivitisation reactions.

Using **1.3**/**1.5**, modest to excellent yields were obtained employing aliphatic and aromatic alcohols (Table 1.2, entries 1-4); lower yields were observed for sterically hindered 2-adamantanol (Table 1.2, entry 5).

TABLE 1.2. *Formation of primary amines from aliphatic and aromatic alcohols using [Ru₃(CO)₁₂] (**1.3**) and phosphine **1.5**.*

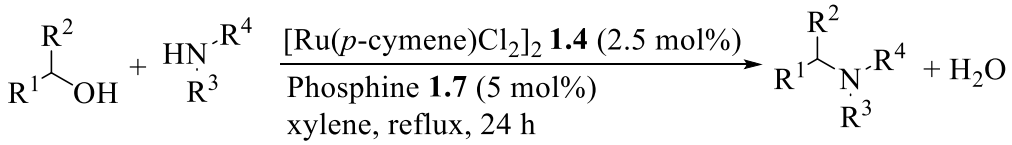


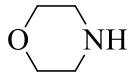
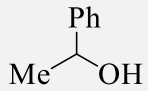
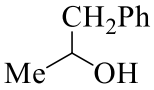
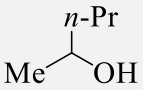
Entry	Alcohol	Yield (%)[a]
1		76
2[b]		69
3		87
4		62
5[b]		45

[a] *Determined by GC,* [b] *0.6 g NH₃*

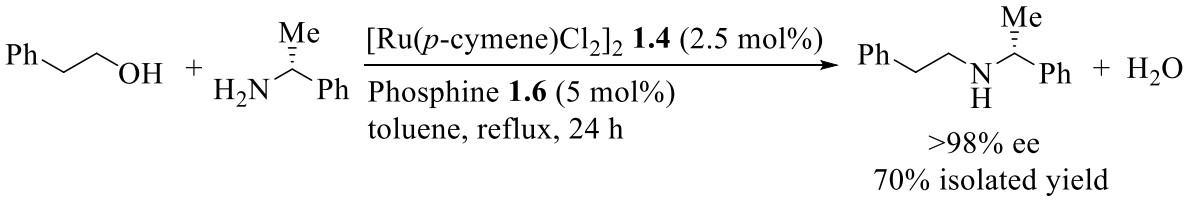
In comparison, [Ru(*p*-cymene)Cl_2]$_2$ (**1.4**), in combination with phosphine ligands **1.6** or **1.7**, demonstrated a wider substrate scope than the other Ru catalysts (**1.1**, **1.2** and **1.3**), predominantly with reactions between unbranched primary alcohols and unhindered amines.[27] The formation of cyclic tertiary amines from secondary alcohols was also accomplished using this system (Table 1.3), with non-benzylic alcohols giving higher yields (Table 1.3, entry 1 vs. entries 2 and 3).

***TABLE 1.3**. Formation of tertiary amines using secondary alcohols and [Ru(p-cymene)Cl_2]$_2$ (**1.4**) in combination with phosphine **1.7**.*



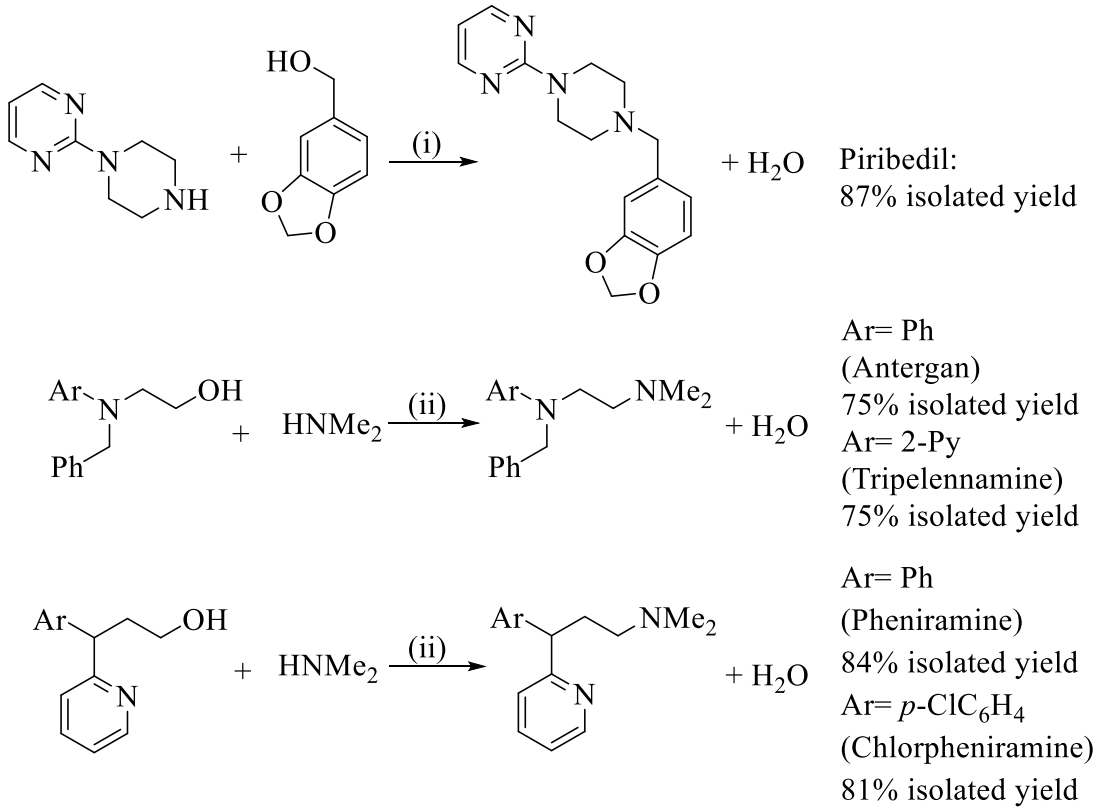
		Amine
		
Entry	**Alcohol**	**Isolated yield (%)**
1		65
2		86
3		88

Reactions with enantiomerically pure amines proceeded with retention of configuration (Scheme 1.9), which is imperative in the pharmaceutical industry as enantiomers can have different and even adverse physiological effects.[31] To the best of our knowledge, this is the only Ru catalytic system which was tested for its applicability in retaining stereochemical purity during the course of alkylation (compared to catalysts **1.1**, **1.2** and **1.3**).



***SCHEME 1.9.** Formation of enantiomerically pure amine using [Ru(p-cymene)Cl_2]$_2$ (**1.4**) and phosphine **1.6**.*

The preparation of active pharmaceutical ingredients (API's), including Piribedil and anti-inflammatory agents Antergan, Tripelennamine, Pheniramine and Chlorpheniramine, was also demonstrated using Ru cymene complex **1.4** with phosphine ligands **1.6** or **1.7** and excellent yields were afforded (75-87%) (Scheme 1.10).

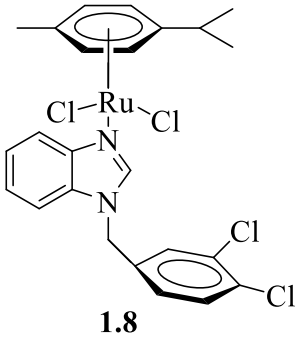


(i) [Ru(*p*-cymene)Cl_2]$_2$ **1.4** (1.25 mol%), **1.6** (2.5 mol%), toluene, reflux, 24 h

(ii) [Ru(*p*-cymene)Cl_2]$_2$ **1.4** (2.5 mol%), **1.7** (5 mol%), toluene, reflux, 24 h

SCHEME 1.10. *The preparation of pharmaceuticals using [Ru(p-cymene)Cl_2]$_2$ **(1.4)** and phosphine ligands **1.6** or **1.7**.*

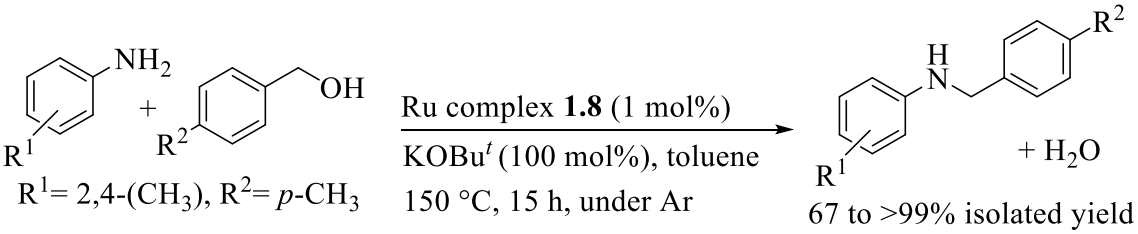
The presence of phosphine ligands are essential for the activity of most of the Ru based catalysts discussed thus far (**1.1**, **1.3** and **1.4**). More recently, a Ru cymene complex containing a benzimidazole ligand (**1.8**, Figure 1.5) has been reported to have certain catalytic activity).[32]



1.8

FIGURE 1.5. *Structure of Ru cymene complex (**1.8**).*

However, the reaction scope was rather limited to benzyl alcohol and aniline derivatives (Scheme 1.11). Long reaction times (15 hours) and the inclusion of 100 mol% base ($KOBu^t$) was required, presumably to expedite the dehydrogenation of alcohol to the carbonyl species.

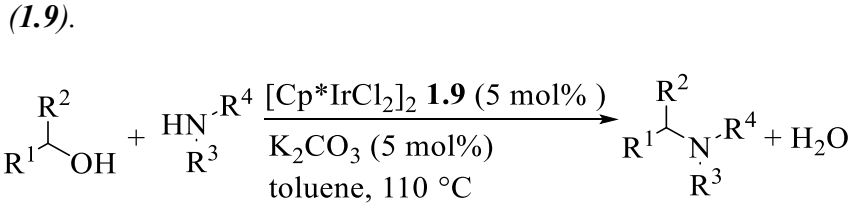


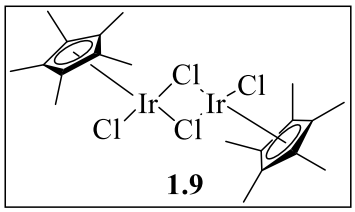
SCHEME 1.11. *N-alkylation of aniline with benzyl alcohol derivatives using [Ru(p-cymene)Cl_2]$_2$ bearing a benzimidazole moiety (**1.8**).*

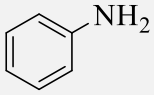
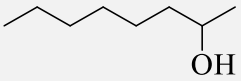
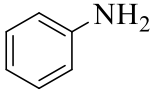
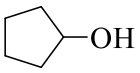
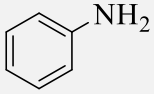
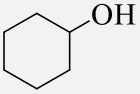
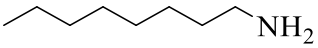
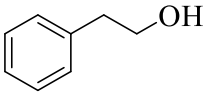
In terms of the broad reaction scope and the mild conditions employed, [Ru(*p*-cymene)Cl_2]$_2$ (**1.4**) used in combination with bidentate phosphines (**1.6** and **1.7**) appears to offer the best performance. This conclusion was also made in a study investigating various Ru based complexes for the amination of aliphatic and aromatic amines with benzyl alcohol.[33] Even so, the main limitation of Ru catalysts is their poor reactivity towards secondary alcohols and with aniline derivatives.

In this light, an Ir based complex, [Cp*$IrCl_2$]$_2$ (**1.9**, Table 1.4), was found to catalyse numerous AAA reactions employing aliphatic amines and anilines with primary and secondary alcohols (Table 1.4).[34] A moderate yield was achieved for the alkylation of 2-octanol with aniline (Table 1.4, entry 1) and better yields were generated for cyclic secondary alcohols (Table 1.4, entry 1 vs. entries 2 and 3). This is most likely due to the increased electrophilicity of the carbonyl compounds afforded from the dehydrogenation of the starting alcohols. Long chain aliphatic amine aminated by primary aliphatic alcohol gave a moderate yield and required a long reaction time (Table 1.4, entry 4).

TABLE 1.4. *N-alkylation of amines with primary and secondary alcohols using [Cp*IrCl$_2$]$_2$. **(1.9)**.*





Entry	Amine	Alcohol	Time (h)	Isolated yield (%)
1			40	69
2			17	85
3			17	92
4			48	61

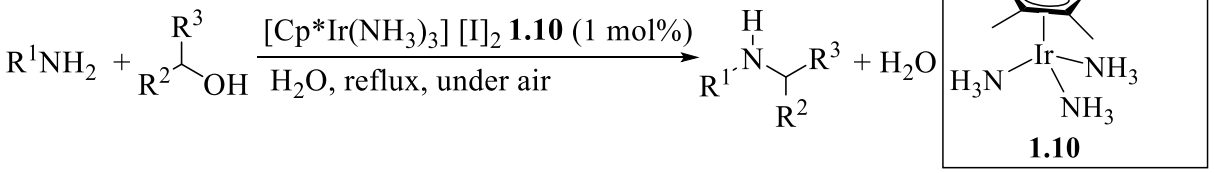
Although the system generated good to moderate yields for these challenging transformations, the reaction times were long, and base was required.

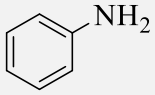
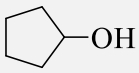
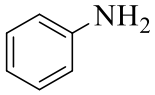
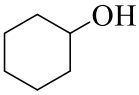
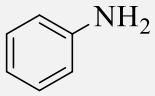
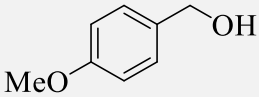
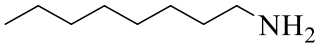
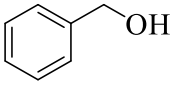
Employing H_2O as a solvent has benefits over using organic solvents, as H_2O is non-flammable and inexpensive. Thus recent developments of a $[Cp^*Ir(NH_3)_3][I]_2$ complex (**1.10**, Table 1.5) has allowed for the preparation of secondary and tertiary amines using H_2O as a reaction medium and without the need for base.[35]

Reactions involving aniline proceeded with lower amounts of catalyst compared to equivalent reactions using Ir complex **1.9** (Table 1.5, entries 1 and 2 vs. Table 1.4, entries 2 and 3), and in the case of employing cyclohexanol along with aniline, higher TOF's (turnover frequencies. Calculated by: turnover number/time, in this Chapter) were afforded (15.5 h^{-1} vs 1.1 h^{-1}).

This system has obvious advantages over the earlier Ru catalysts discussed not only due to the higher TOF's, but also because of its ability to facilitate reactions using secondary alcohols. For instance, 100 mol% (1 equivalent) of KOBu^t was required for the amination of aniline with benzyl alcohol derivatives using **1.8** at 150 ˚C for 15 hours (Scheme 1.11). Whereas the same reactions can be achieved with excellent yields in 6-14 hours, in the absence of base, using catalyst **1.10** (Table 1.5, entry 3). Aliphatic amines were also well tolerated (Table 1.5, entry 4).

TABLE 1.5. *N-alkylation of amines with primary and secondary alcohols using [Cp*Ir(NH$_3$)$_3$][I]$_2$ (**1.10**).*



Entry	Amine	Alcohol	Time (h)	Isolated yield (%)
1[a]			24	82
2			6	93
3			6	93
4			14	82

[a] *2 mol% of catalyst.*

In contrast to Ru complex **1.4**, the ability of **1.10** to catalyse the construction of API's and/or to retain the chirality of enantiomerically pure species was not demonstrated.

In this respect, [Cp*IrI$_2$]$_2$ (**1.11**, Figure 1.6) was employed in the synthesis of Fentanyl, an analgesic with approximately 100 times greater potency than morphine (Scheme 1.12).[36]

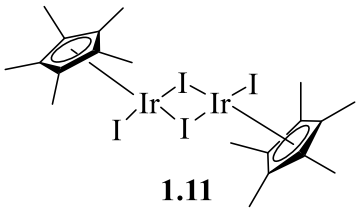
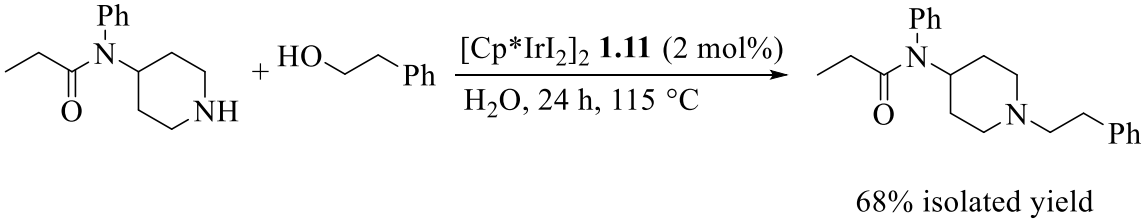


FIGURE 1.6. *Structure of [Cp*IrI$_2$]$_2$ (**1.11**).*

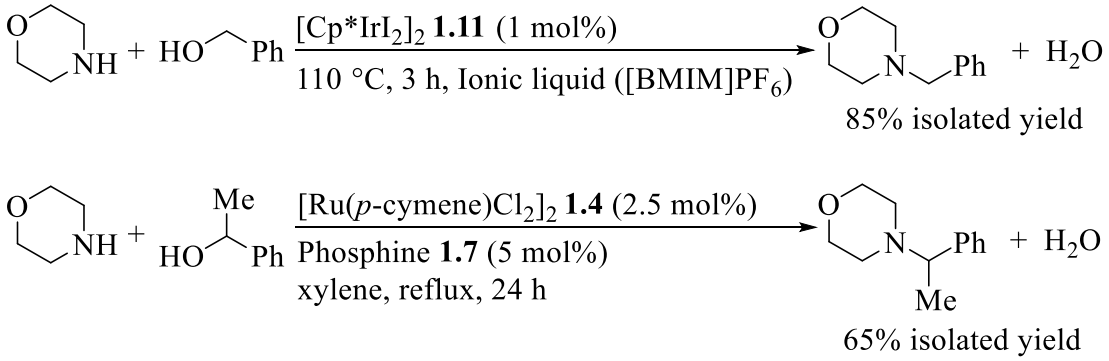


68% isolated yield

SCHEME 1.12. *Synthesis of Fentanyl using [Cp*IrI$_2$]$_2$ (**1.11**).*

Other pharmaceutical drugs were not synthesised in this study, but compared to the Ru catalyst (**1.4**), the use of ligands was not necessary and the reaction was conducted in H$_2$O

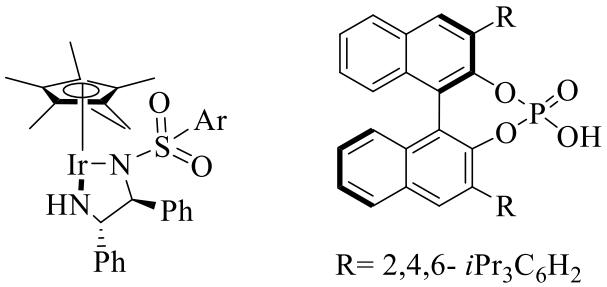
instead of toluene (Scheme 1.12 vs. Scheme 1.10). Furthermore, the formation of structurally similar tertiary amines occurred with significantly higher TOF's using complex **1.11** compared to the Ru catalyst (**1.4**) (28.3 h^{-1} vs. 1.1 h^{-1}, Scheme 1.13).



SCHEME 1.13. *Formation of tertiary amines using secondary alcohols catalysed by [Cp*IrI2]2 (**1.11**) and [Ru(p-cymene)Cl2]2 (**1.4**).*

The use of more challenging substrates, such as secondary alcohols, was not demonstrated in this study.

More recently, an enantioselective Ir catalyst (**1.12**) in combination with chiral phosphoric acid (**1.13**) (Figure 1.7) was reported for the synthesis of chiral amines starting from racemic mixtures of alcohol and amines.[37] Enantioselectivity was achieved in the hydrogenation of the imine, by a chiral Ir hydride intermediate.

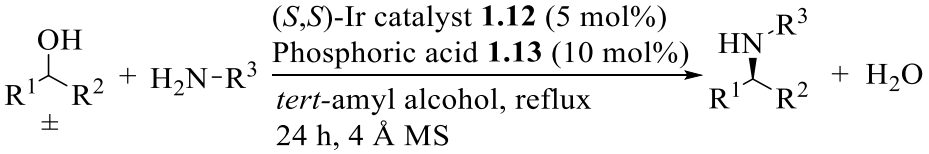


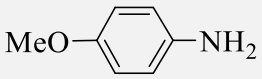
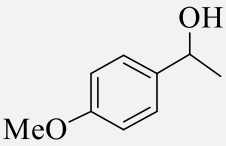
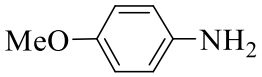
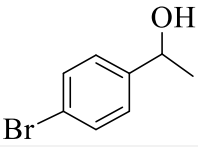
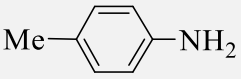
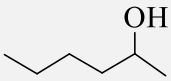
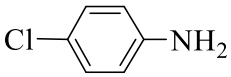
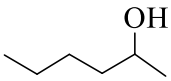
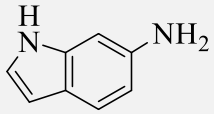
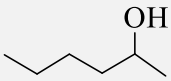
1.12 **1.13**

FIGURE 1.7. *Structures of enantioselective Ir catalyst **1.12** and chiral phosphoric acid **1.13**.*

Using this catalytic system, secondary alcohols bearing linear as well as aryl substituents reacted with aniline derivatives, to generate substituted amines in good to excellent yields and enantioselectivity (*ee*) (Table 1.6). Products containing electron-donating substituents were obtained with higher *ee* values (Table 1.6, entry 1 vs. entry 2). Substituted anilines containing electron withdrawing and donating groups afforded high yields (Table 1.6, entries 3 and 4), and notably the heterocyclic amine, 5-aminoindole, was successfully coupled with 2-hexanol (Table 1.6, entry 5).

TABLE 1.6. *Enantioselective animation using an Ir based catalyst (**1.12**) in combination with chiral phosphoric acid **1.13**.*

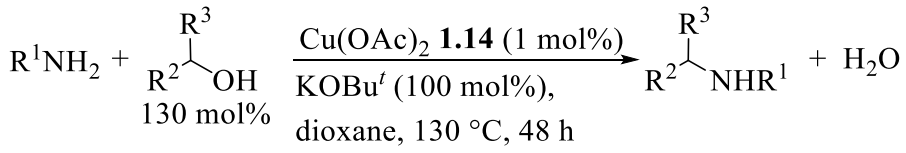


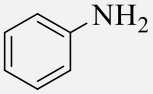
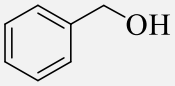
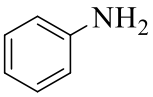
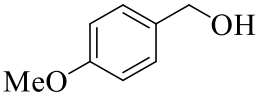
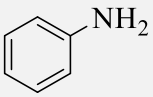
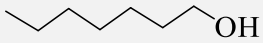
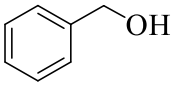
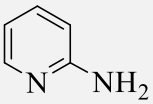
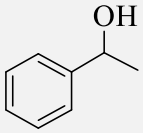
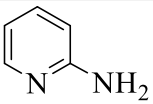
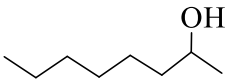
Entry	Amine	Alcohol	Isolated Yield (%)	ee (%)
1			72	96
2			69	83
3			97	88
4			81	83
5			84	81

Although the majority of homogeneous catalysts reported for the AAA reaction are based on Ru and Ir complexes, several groups have reported the use of other metals, for instance, Cu, Pd, Fe and Au.[38-42] Cu and Fe based catalysts are particularly attractive due to the ready availability of the metals and they allow for cost effective alternatives.

Ramon and co-workers demonstrated that $Cu(OAc)_2$ (**1.14**) was able to couple aromatic amines with primary and secondary alcohols.[38] Benzyl alcohol derivatives react with aniline to afford excellent yields (Table 1.7, entry 1 and 2). Yet compared to analogous reactions catalysed by the Ir complex **1.10**, much lower TOF values were generated, for example the alkylation of aniline by *p*-methoxy benzyl alcohol (1.8 h^{-1} vs. 15.5 h^{-1}). The amination of aliphatic alcohols with aniline gave lower yields contrasted to using aromatic ones, likely due to the decreased electrophilic nature of the carbonyl species afforded (Table 1.7, entry 3 vs. entries 1 and 2). The use of highly electron rich *tert*-butylamine as a reagent failed, even after 6 days, presumably due to steric hindrance (Table 1.7, entry 4). When secondary alcohols were employed with electron poor pyridine-2-amine, the yields were low, more base (200 mol%) and longer reaction times were required (Table 1.7, entries 5 and 6).[38]

TABLE 1.7. *N-alkylation of amines using primary and secondary alcohols and $Cu(OAc)_2$ **(1.14)**.*

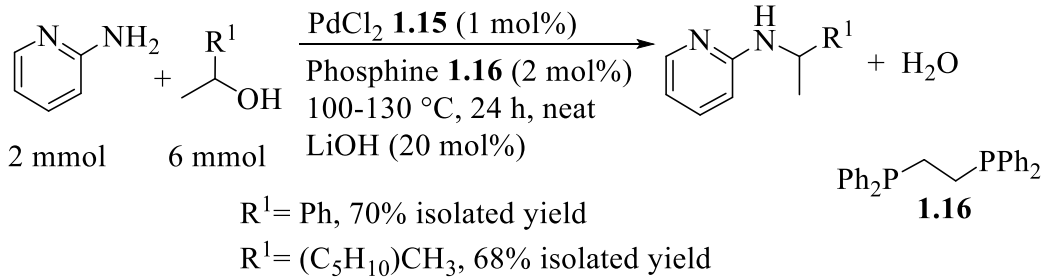


Entry	Amine	Alcohol	Isolated Yield (%)
1			>99
2			85
3			40
4[a]			0
5[b]			40
6[b]			25

[a] *6 days reaction time,* [b] *4 days reaction time and 200 mol% of KOBu^t.*

A mild approach for the synthesis of amines by secondary aromatic and aliphatic alcohols was demonstrated using $PdCl_2$ (**1.15**).[40] A lower mol% of base (required to generate the catalytically active Pd alkoxide precursor) was used and larger TOF's using the same substrates as catalyst **1.14** were yielded (Scheme 1.14 vs. Table 1.7, entries 5 and 6). For instance the alkylation of 2-aminopyridine with 1-phenylethanol proceeded with a value of 2.9 h^{-1} vs. 0.8 h^{-1} obtained by complex **1.14**.

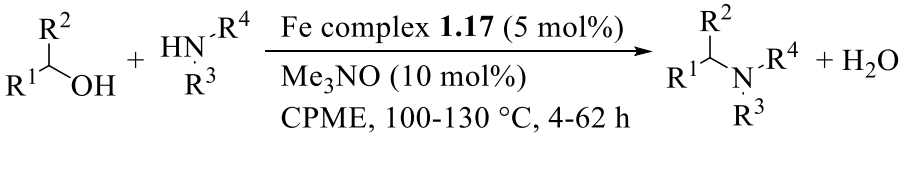
Although the system was more active than catalyst **1.14**, the addition of phosphine ligand (dppe, **1.16**, Scheme 1.14) was necessary (2 mol%). Also, compared to reactions catalysed by the Ir based complex (**1.9)** (Table 1.4), harsher reaction conditions were required (20 mol% of base instead of 5 mol%).

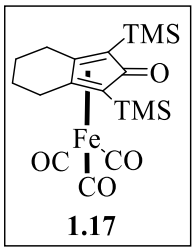


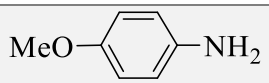
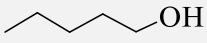
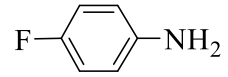
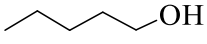
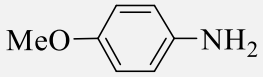
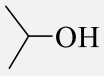
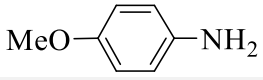
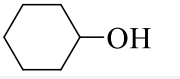
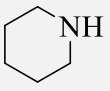
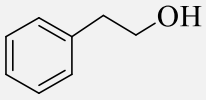
SCHEME 1.14. *N-alkylation of aromatic amines using secondary alcohols and $PdCl_2$ (**1.15**) and phosphine **1.16**.*

In terms of finding an inexpensive yet effective catalytic system, promising results for the alkylation of functionalised anilines with primary aliphatic alcohols were generated using an Fe complex (**1.17**) and Me_3NO (Table 1.8, entry 1 and 2).[42] However poor selectivities were obtained when secondary alcohols were used as alkylating agents (Table 1.8, entry 3 and 4) and the amination of secondary amines with alcohols gave modest results (Table 1.8, entry 5).

TABLE 1.8. *N-alkylation of amines with alcohols using an Fe based complex (**1.17**).*

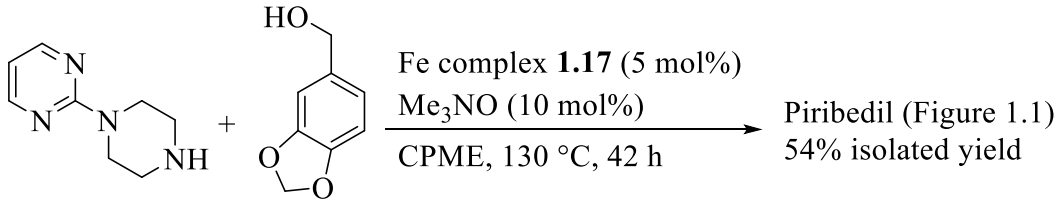




Entry	Amine	Alcohol	Yield (%)[a]
1			91
2			77
3[b]			12
4[b]			14
5[c]			53

[a] *Isolated yields,* [b] *GC-FID selectivity,* [c] *Molecular sieves were used.*

The synthesis of Piribedil was demonstrated using this Fe catalyst (Scheme 1.15), but the system was less efficient for this transformation compared to using [Ru(*p*-cymene)Cl_2]$_2$ (**1.4**), generating lower TOF values (0.3 h^{-1} vs. 2.9 h^{-1}).

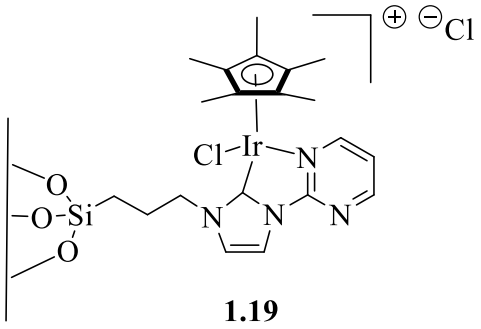


SCHEME 1.15. *Synthesis of Piribedil using an Fe complex (**1.17**).*

Au complex $[(Ph_3P)AuCl]$[41] (**1.18**) was shown to catalyse the reaction between benzyl alcohol and aniline derivatives (64-90% isolated yield, with electron withdrawing and donating groups). However, modest results were obtained using long chain aliphatic alcohols, (58-64% isolated yield) and the use of a secondary alcohols failed. Although a relatively low reaction temperature was used (100 ˚C), the inclusion of base ($KOBu^t$, 1 equivalent), large amounts of catalyst (10 mol%), long reaction times (up to 4 days) and additive AgOTf was necessary (to generate the active catalytic species).

In summary, the synthetic utility of most homogeneous catalysts reported for the AAA reaction are limited by the need for co-catalyst and base. The synthesis of organic ligands can be challenging and there are difficulties in the recovery process, which makes the use of these catalysts uneconomical. Even though it was shown that catalyst $[Cp^*IrI_2]_2$ (**1.11**) can be used along with ionic liquids or H_2O, without the use of co-catalyst and base, separation techniques (liquid-liquid extraction and/or column chromatography) are still required. In this context there has been much effort made in trying to immobilise organic ligands or metal complexes onto a solid support through chemical bonds.[43, 44] Such catalysts combine the advantages of both homogeneous and heterogeneous systems in that well-defined catalysts can be created which are easily separated from the reactants.

A recent example is a pyrimidine-substituted *N*-heterocyclic carbene Ir complex supported on mesoporous silica (SBA-15) (**1.19**) (Figure 1.8).[43]

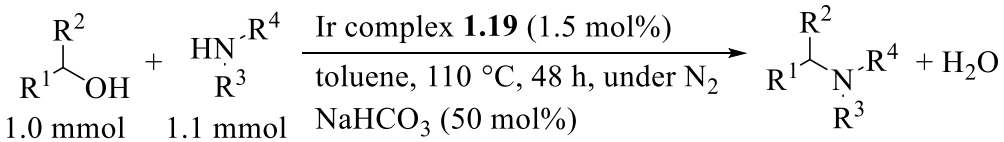


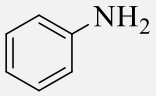
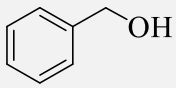
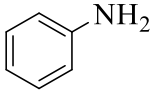
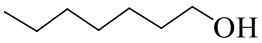
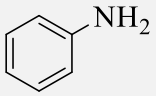
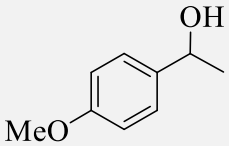
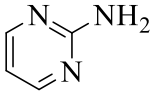
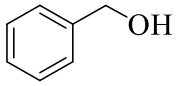
1.19

FIGURE 1.8. *Structure of the silica supported Ir complex (**1.19**).*

Mesoporous silica functions as an excellent support due to its high surface area, ordered structure and uniform pore diameter. In its absence, the obtained yield for the alkylation of aniline with benzyl alcohol decreased (~10%). Mild reaction temperatures of 110 ˚C were employed and even after 12 runs, the catalyst (**1.19**) was shown to retain its activity. On the other hand, the reaction scope was poor, as the majority of reactions described employed aniline and benzyl alcohol derivatives. Reaction times of 48 hours were necessary, as well as the inclusion of base (50 mol%, $NaHCO_3$). The activity of the system is comparable to the poorly active $Cu(OAc)_2$ catalyst (**1.14**), where the alkylation of aniline with benzyl alcohol afforded TOF's of 2.1 h^{-1} and 1.3 h^{-1} when using **1.14** and **1.19**, respectively (Table 1.7, entry 1 vs. Table 1.9, entry 1). When more challenging reactions were performed, such as the alkylation of aniline with secondary and aliphatic alcohols, or when heteroaromatic amines were used as substrates, modest to good yields were obtained (Table 1.9, entries 2-4).

TABLE 1.9. *N-alkylation of amines with alcohols using a supported Ir complex (**1.19**).*



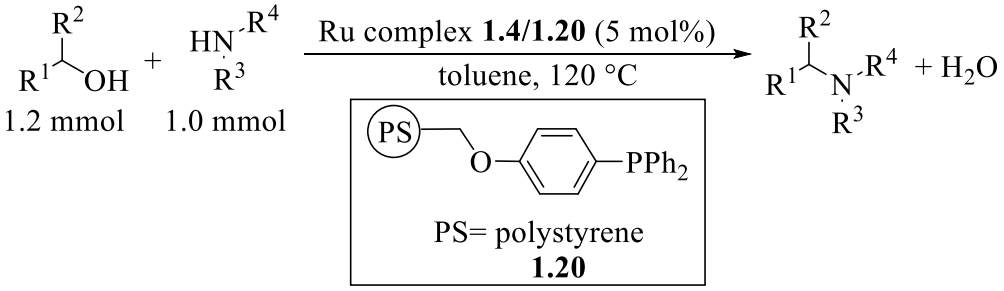
Entry	Amine	Alcohol	Isolated Yield (%)
1			93
2			52
3			78
4			70

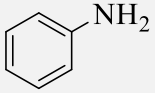
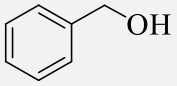
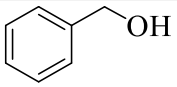
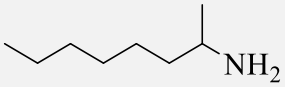
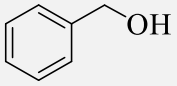
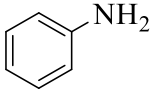
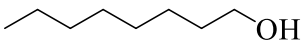
Alternatively, Ru complex **1.4** has been immobilised onto phosphine functionalised polystyrene (**1.20**) (Table 1.10).[44] The alkylation of primary and secondary amines along with alcohols proceeded in the absence of base using this system, yet the activity was generally lower than the unsupported Ru complex (**1.4**). The alkylation of aniline with benzyl alcohol generated a TOF of 1.6 h^{-1} for unsupported Ru (**1.4**), whereas 0.6 h^{-1} was achieved by this polymer bound system (Table 1.10, entry 1). Similarly, the TOF for the alkylation of

morpholine with benzyl alcohol (Table 1.10, entry 2) was larger for the homogeneous Ru catalyst (**1.4**) (2.8 h^{-1} vs. 1.0 h^{-1}).

Sterically challenging long chain aliphatic amines were tolerated well (Table 1.10, entry 3) as was the use of aniline with long chain aliphatic alcohols (Table 1.10, entry 4). However, the use of secondary alcohols gave poor yields (<30%) and the synthesis of Piribedil proceeded with a lower TOF than that afforded by the homogeneous Ru catalyst (**1.4**) (0.4 h^{-1} vs. 2.9 h^{-1}).

TABLE 1.10. *N-alkylation of amines with alcohols using a supported Ru complex (**1.20**).*



Entry	Amine	Alcohol	Time (h)	Isolated Yield (%)
1			24	69
2			18	87
3			24	73
4			24	88

In spite of the decreased activity of this catalyst, an interesting aspect of this work was the use of a flow reactor for the alkylation of piperidine with benzyl alcohol (Figure 1.9). In a typical procedure, reagents were pre-mixed with toluene and the resulting solution was pumped into a packed bed reactor (PBR) at 30 μL min^{-1}, giving a long residence times of ~ 90 minutes (the average contact time of substrates with the catalyst surface). This single pass set-up, where substrates are passed through the reaction zone once, allows for the generation of a time-on-line profiles, as shown in Figure 1.9 (product yield % plotted against time). Catalyst stability can be interrogated using this experimental set-up. In this study, the reaction proceeded smoothly for 6 hours until the yield decreased to 59% (Figure 1.9). No leached Ru species were detected by ICP analysis, thus the decrease in activity may be

ascribed to other deactivation routes, [45] for example by thermal degradation and/or poisoning of active sites by substrates and/or products.

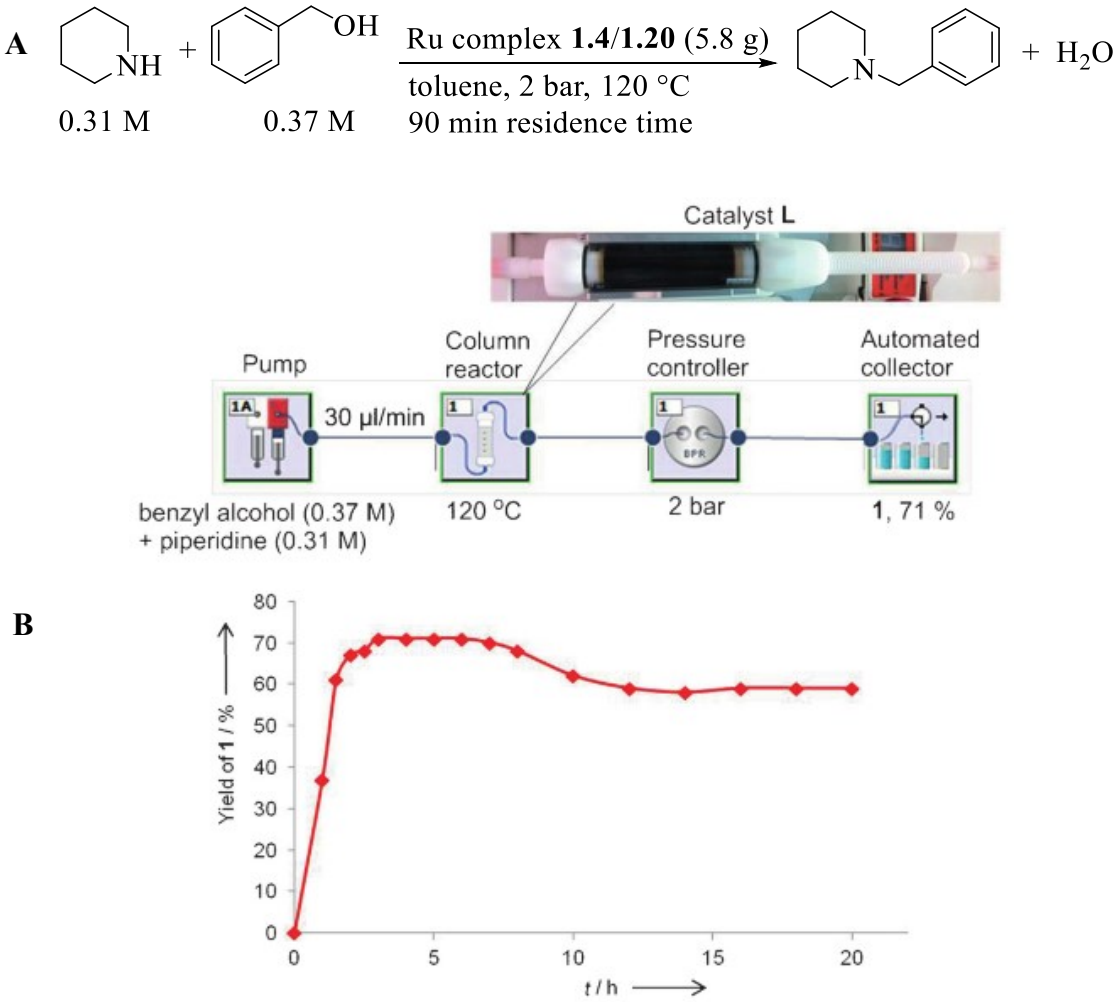


FIGURE 1.9. A) *Set-up for the alkylation of piperidine using a continuous flow system.* ***B)*** *Time-on-line profile monitoring product formation over time (% yield). Reproduced from reference* [44].

Catalyst deactivation was observed in a separate study using homogeneous Ru complex **1.4** supported on a phosphine bound polymer (**1.21**) using a flow reactor.[46] A mixture of morpholine and benzyl alcohol in toluene (pre-mixed with toluene) was pumped into the PBR at flow rates between 0.1 and 0.25 mL min^{-1}. Leached Ru species were detected (by ICP analysis) when operating the reactor under pressure (5 bar), instead of using atmospheric conditions. As pressure is required to keep the solvent in the liquid phase, this reduces the functionality of the catalyst in terms of employing higher temperatures, which are frequently required for more challenging transformations. It was observed that by using slower flow rates at higher temperatures and under atmospheric pressure (110 ˚C at 0.25 cm^3 min^{-1} vs.

150 ˚C at 0.1 cm^3 min^{-1}); increased conversions were yielded (15% vs. 98%). The facility to enhance conversion through altering the residence time is an attractive feature of using flow chemistry; however, the use of immobilised homogeneous complexes in flow is questionable. This is due to the low activities and catalyst deactivation observed and the scale-up for industrial applications is not trivial because of the enormous complexity in the ligand preparation and immobilisation. A more beneficial system is the use of a simple metal supported catalyst that could be employed in flow.

There is an increasing demand for processes to move towards using flow reactors particularly for continuous processing.[46] This is exemplified in an article in the Wall Street Journal, which stated that:

"*The pharmaceutical industry has a little secret: Even as it invents futuristic new drugs, its manufacturing techniques lag far behind those of potato chip and laundry-soap makers…*"[47]

There are numerous reports where the transition from batch processes to flow is encouraged, and the benefits are plentiful:

- It is easier to control reaction parameters such as heating and mixing.
- Catalysts are held in closed cartridges, which facilitates catalyst-product separation.
- It allows for a safer containment of materials when dealing with hazardous reactions, because smaller quantities are generated at a given time.
- It allows for improved reaction profiling meaning that a better understanding of the reaction mechanism can be achieved.
- An increased reaction space is afforded due to the increase in reagent: catalyst ratio.
- By-product formation can be prevented by moving reagents away from the reaction zone after they have formed the desired product.
- Conversion and selectivity can be controlled through altering the residence time.
- Inline analysis and purification is possible to follow the reaction progress, which is particular useful in multistep processes.

There are challenges to be overcome when introducing such processes into industry. In particular, once approval is given to produce a pharmaceutical drug that was developed in batch, it can be difficult to argue the need for a flow process due to concerns over producing any unwanted side reactions.[46]

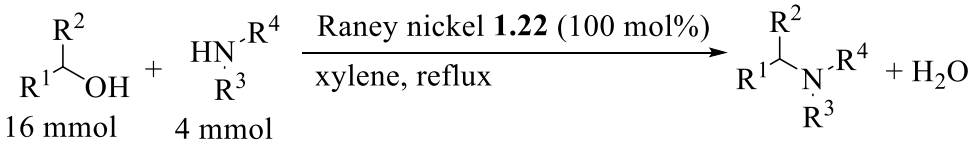
Heterogeneous catalysts for the AAA reaction, employing both batch and flow processes, are discussed in the following section (1.2.2).

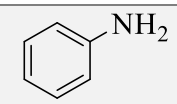
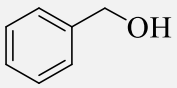
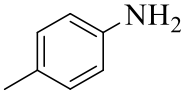
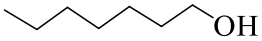
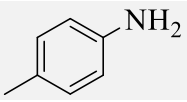
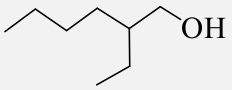
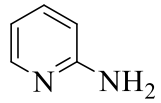
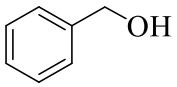
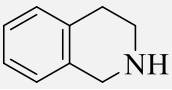
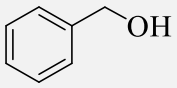
1.2.2 Heterogeneous catalysts for the AAA reaction

Heterogeneous processes are often favoured over homogeneous ones for their practicality, namely, the ease of product separation. This is very important, especially in the pharmaceutical industry, where the product is highly regulated for metal contamination.[14] Heterogeneous catalysts are scarcely used in industry for the AAA reaction as many systems suffer from poor product selectivity, limited substrate scope and the harsh reaction conditions required, especially when using zeolite, silica and alumina structures (temperatures up to 400 °C are required).[48-51]

Catalysts using cost effective metals such as Ni and Cu have been investigated for the AAA reaction.[52-57] A recent report using a Raney Ni catalyst (**1.22**), prepared from a Ni and Al alloy, has shown promising results.[58] Although reactions proceeded in the absence of base, a large amount of catalyst was required (100 mol%). Aliphatic alcohols were generally more reactive than aromatic ones (Table 1.11, entry 1 vs. 2 and 3) and there were no examples of using more challenging secondary alcohols. When employing 2-ethylhexanol with amine, lower yields were generated contrasted to using *n*-heptanol, likely due to steric hindrance (Table 1.11, entry 2 vs. 3). Heteroaromatic and secondary amines generated good to modest yields, but required long reactions times (up to 32 hours) (Table 1.11, entries 4 and 5).

TABLE 1.11. *N-alkylation of amines with alcohols using a Raney Ni catalyst (**1.22**).*



Entry	Amine	Alcohol	Time (h)	Isolated Yield (%)
1			24	90
2			12	78
3			12	67
4			24	84
5			32	65

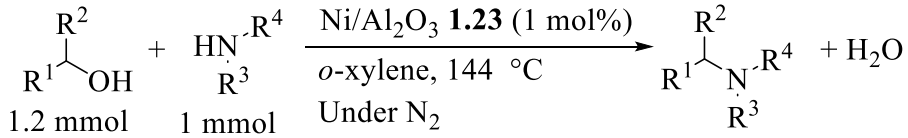
The synthesis of Piribedil was demonstrated using the same conditions outlined in Table 1.11, yielding 85% product in 24 hours. This system is much less efficient (TOF value of 0.04 h^{-1}) compared to the notable homogeneous Ru complex (**1.4**) which has a TOF value of 2.9 h^{-1}. The process is further limited by the necessity for large amounts of catalyst and increased reaction times when using less activated substrates.

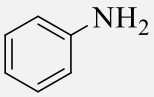
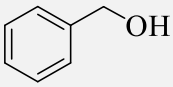
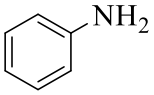
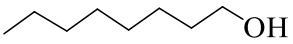
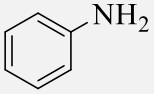
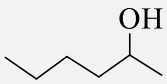
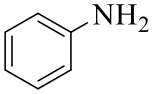
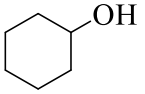
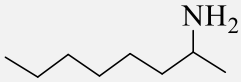
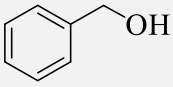
In this light, two separate reports (both by Shimizu and co-workers) using Ni/θ-Al_2O_3 (**1.23**)[59] and Ni/$CaSiO_3$ (**1.24**)[60], demonstrate that the selective formation of primary, secondary and tertiary amines can be achieved under mild conditions and with higher TOF's than the excellent homogeneous Ir and Ru catalysts (**1.9** and **1.4**, respectively).

Ni/θ-Al_2O_3 (**1.23**) was active for the formation of secondary and tertiary amines using a wide range of primary and secondary alcohols along with aromatic and aliphatic amines, affording good to excellent yields (74-99%) (Table 1.12). A TOF value of 33 h^{-1} was achieved for the formation of *N*-phenylbenzylamine (Table 1.12, entry 1) which is much larger than the value generated by the Ir complex **1.9** (1.5 h^{-1}). The same TOF was realised for the reaction of aniline with *n*-octanol (Table 1.12, entry 2), which is impressive because many catalytic systems are unsuccessful for reactions between anilines and aliphatic alcohols. Indeed TOF values of 0.7 and 0.8 h^{-1} were achieved when employing *n*-heptanol with aniline using Ir (**1.19**) and Cu (**1.14**) based catalysts, respectively.

Longer reaction times were necessary when employing aliphatic secondary alcohols with aniline (Table 1.12, entries 3 and 4), yet the TOF values achieved were still better than that of the homogeneous Ir catalyst (**1.9**). The coupling of cyclohexanol with aniline proceeded with a TOF of 3.9 h^{-1}, which is compared to 1.1 h^{-1} afforded by **1.9**. Aliphatic amines along with benzyl alcohol were also well tolerated (Table 1.12, entry 5).

TABLE 1.12. *N-alkylation of amines with alcohols using Ni/ θ-Al_2O_3 (**1.23**).*



Entry	Amine	Alcohol	Time (h)	Yield (%)[a]
1			3	99
2			3	99
3[b]			24	81
4[b]			24	94
5[c]			24	74

[a] *Determined by GC, based on aniline,* [b] *130 ˚C,* [c] *amine (0.5 mmol), alcohol (2.0 mmol), catalyst (2 mol%).*

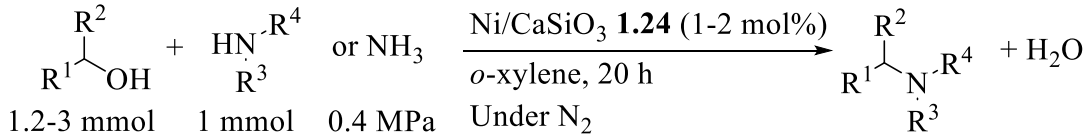
This system was not tested for its ability in producing API's or chiral amines, and the catalyst required a pre-reduction step (at 500 ˚C under H_2 for 30 minutes). The alkylation reaction of aniline with 1-octanol was annihilated in the absence of this treatment, indicating that metallic Ni is the active species in the reaction.

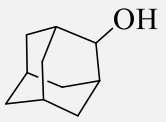
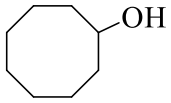
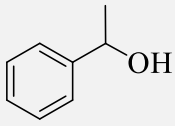
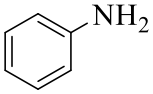
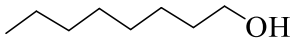
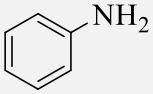
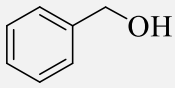
The same observation was found in the study using Ni supported on $CaSiO_3$ (**1.24**).[60] The alkylation of 2-octanol with ammonia did not occur when **1.24** was exposed to air, which was ascribed to O_2 generating inactive Ni^{2+} species. Following the activation procedure (600 ˚C under H_2 for 30 minutes), **1.24** was shown to catalyse the amination of ammonia with aliphatic and aromatic alcohols to yield primary amines in good to high yields (70-80%). As previously discussed, the selective formation of primary amines by the hydrogen borrowing method is rarely reported. Thus, a cost effective system that is active for this reaction is particularly noteworthy.

The amination of 2-adamantanol has a TOF of 4.4 h^{-1} (Table 1.13, entry 1), which is higher than the value achieved for the analogous reaction using the homogeneous Ru complex (**1.3**) (1.1 h^{-1}). Although increased reaction temperatures were required compared to using catalyst **1.3** (150 ˚C vs. 170 ˚C), an order of a magnitude lower amount of ammonia was employed (2.2 vs. 35-59 equivalents). Reactions using less sterically hindered alcohols were performed at lower temperatures (140 ˚C) (Table 1.13, entries 2 and 3). The scope of the catalyst was

also demonstrated using aliphatic and aromatic alcohols with aniline, generating good to excellent yields (77- 96%) (Table 1.13, entries 4 and 5). However, the TOF for the reaction of aniline with *n*-octanol was considerably lower than that of the other Ni catalyst (**1.23**) reported by the group (2.4 h^{-1} vs. 33 h^{-1}). This highlights the effect that changing the support can have, and suggests that it plays an active role in tuning the activity of the catalyst. Higher activities were found when using supports that are amphoteric in nature, such as Al_2O_3.[59] In a study investigating the oxidation of alcohols, it was postulated that both acidic and basic sites were required to facilitate the reaction: A basic site to abstract the hydroxyl hydrogen from the alcohol to form the alkoxide species, and an acid site to remove hydrogen from the alkoxide as a hydride.[61, 62]

TABLE 1.13. *N-alkylation of amines with alcohols using Ni/CaSiO₃* (**1.24**).



Entry	Amine	Alcohol	Temp (˚C)	Yield (%)[a]
1	NH_3		170	88
2	NH_3		140	71
3[b]	NH_3		140	74
4			155	96
5[c]			155	78

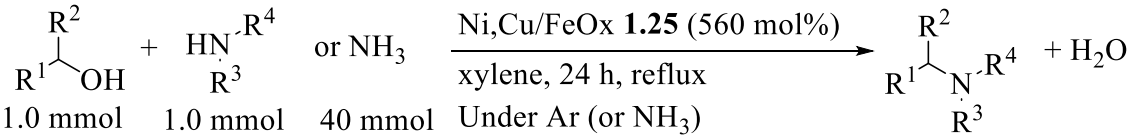
[a] *Determined by GC, based on alcohol,* [b] *catalyst (5 mol%),* [c] *17 hours.*

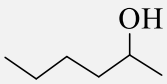
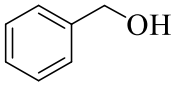
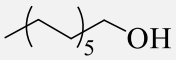
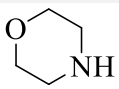
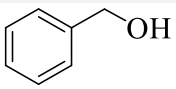
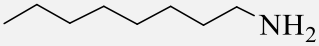
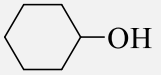
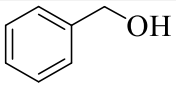
Both of these Ni catalysts exhibit excellent generality for the AAA reaction, but operate using batch processes meaning that product separation is not as facile as it could be.

In this regard a bimetallic Ni,Cu/FeO_x (**1.25**) catalyst enabled the alkylation of ammonia or amines with primary and secondary alcohols. The catalyst has the advantage of being easily removed from the reaction mixture, using a magnet.[63] It was suggested that the synergism between the Ni, Cu and Fe species was crucial for the AAA reactions; therefore

the mol% values were calculated taking into account all three species. By doing this, it can be seen that an excessive amount of catalyst was employed in the reactions (up to 936 mol%), resulting in a very inefficient system. The TOF value of 33 h^{-1} for the formation of *N*-phenylbenzylamine by Ni/θ-Al_2O_3 (**1.23**) was significantly larger than that yielded by this bimetallic system (7.0 x 10^{-3} h^{-1}). Even so, the generality of the catalyst was good. Ammonia was coupled with various primary and secondary alcohols, and although the di-alkylated product was obtained for many of the reactions (Table 1.14, entry 1), primary amines were formed by using an excess of ammonia (40 mmol) (Table 1.14, entries 2 and 3). Other amines, including morpholine and long chain aliphatic amines reacted smoothly with aliphatic and aromatic primary or secondary alcohols (Table 1.14, entries 4 and 5). Dimethyl amine was also tested (which is a structure found extensively in functional compounds, such as Venlafaxine, Figure 1.1) along with benzyl alcohol derivatives and aliphatic alcohols with yields of 65 to 92% (Table 1.14, entry 6).

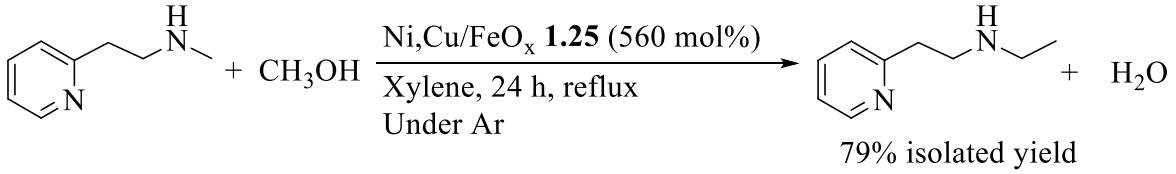
TABLE 1.14. *N-alkylation of amines with alcohols using Ni,Cu/FeO$_x$ (**1.25**).*



Entry	Amine	Alcohol	Yield (%)[a]
1[a]	NH_3		76
2[b]	NH_3		77
3[b]	NH_3		59
4			89
5			86
6			83

[a] *Catalyst (936 mol%), ammonia (1.2 mmol),*[b] *12 hours*

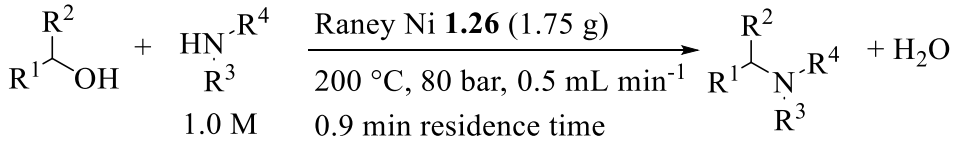
The synthesis of a variety of API's (using the general conditions outline in Table 1.14) was demonstrated, including Piribedil, Pheniramine and *N*-methyl-2-(pyridin-2-yl)-ethanamine, a drug used in the treatment of Meniere's disease and vertigo (Scheme 1.16).

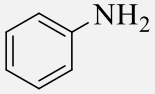
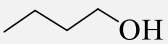
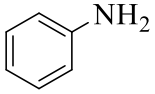
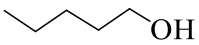
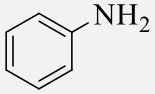
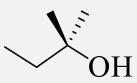


SCHEME 1.16. *Synthesis of N-methyl-2-(pyridin-2-yl)-ethanamine using Ni,Cu/FeO$_x$ (**1.25**).*

The use of a magnet for catalyst recovery is novel, but what would be even better is the use of a PBR, where the catalyst is held in a closed cartridge allowing for effortless product separation. This has been demonstrated using inexpensive Raney Ni (**1.26**) for the amination of aniline with various long chain aliphatic amines as the reaction solvent.[64] High yields were afforded by using a flow reactor (in single pass) (Table 1.15), however the reaction mixture was passed through the catalyst cartridge twice, leading to a rather inefficient system. Reactions with more sterically encumbered alcohols did not afford any products (Table 1.15, entries 1 and 2 vs. entry 3).

TABLE 1.15. *N-alkylation of amines with alcohols in flow using Raney Ni in flow (**1.26**).*



Entry	Amine	Alcohol	Yield (%)[a]
1			87
2			93
3			0

[a] *Determined by GC-MS.*

Other heterogeneous catalysts using noble metals such as Ag and Pd have been reported for the AAA reaction, but many suffer from poor generality and reaction selectivity.[65-70] Some of the studies using Ag catalysts (**1.27**-**1.29**) are highlighted in Table 1.16, which shows the general reaction conditions employed in the AAA reactions, the substrate scope and TOF values achieved for the alkylation of benzyl alcohol with aniline. The reaction scope

for all of these catalysts was mostly limited to the use of primary alcohols with aniline derivatives, with the need for large amounts of base (Table 1.16, entries 1-3).

Poor selectivity towards the amine product was found for many of the reactions catalysed by the Ag/Al_2O_3-Ga_2O_3 system (**1.29**) (Table 1.16, entry 3), where the formation of imine as well amide was detected. Compared to the cost effective Ni/θ-Al_2O_3 catalyst (**1.23**), the TOF's for the generation of *N*-phenylbenzylamine were considerably lower for the Ag based systems (33 h^{-1} vs. 0.4-2.2 h^{-1}) (Table 1.16, entries 1-3).

TABLE 1.16. *The general reaction conditions, substrate scope and TOF for the formation of N-phenylbenzylamine using Ag based catalysts (**1.27-1.29**).*

Entry	Catalyst	Conditions	Substrate scope	TOF (h^{-1})
1	$Ag_6Mo_{10}O_{33}$ (**1.27**) [71]	20 mol% catalyst, 20-40 mol% $KOBu^t$, 160 ˚C, 12-20 hours	Primary amines (mostly aniline derivatives) coupled with primary aliphatic and benzylic alcohols	0.4
2	Ag/Al_2O_3 (**1.28**) [66]	2.4 mol% catalyst, 20 mol% Cs_2CO_3, 120 ˚C, 19 hours, under N_2 or He (1 atm)	Primary and secondary amines (mostly aniline) coupled with primary aliphatic and benzylic alcohols	2.2
3	Ag/Al_2O_3-Ga_2O_3 (**1.29**) [67]	3 mol% catalyst, 28 mol% NaH, 110 ˚C, 26-48 hours, under Ar	Primary aliphatic and aromatic amines (mostly aniline derivatives, one example using morpholine) coupled with benzylic and aliphatic primary alcohols	1.1

Catalyst pre-reduction in a hydrogen flow (at 300 ˚C for 30 minutes) was required for the Ag/Al_2O_3 (**1.28**) catalyst to generate active metallic Ag species. Without this step the conversion and selectivity towards the formation of *N*-phenylbenzylamine was reduced. Similarly, reduction of Ag in the Ag/Al_2O_3-Ga_2O_3 system was necessary for catalytic activity (**1.29**).

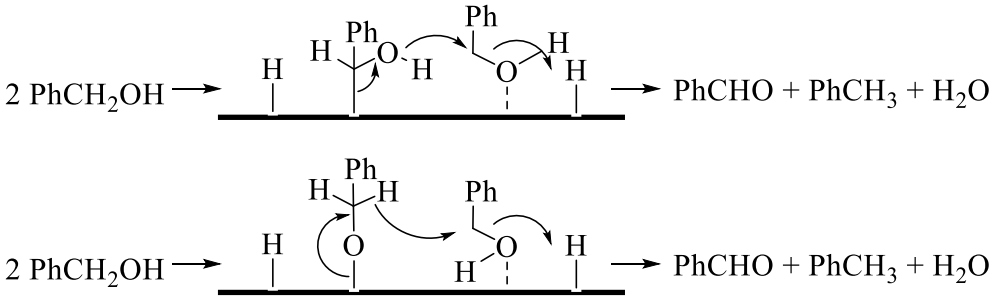
Pd supported on MgO and Fe_2O_3 (**1.30** and **1.31**, respectively),[68, 70] were shown to be amongst the most active materials for the alkylation of aniline with benzyl alcohol. Much larger TOF values were obtained than those generated by the excellent Ru, Ir and Ni catalysts, although higher temperatures were required (Table 1.17, entries 1 and 2 vs. 3-5).

TABLE 1.17. *Comparison of catalysts for the N-alkylation of aniline with benzyl alcohol.*

Entry	Catalyst	Cat. (mol%)	T(˚C)	Time (h)	Yield (%)	TOF (h^{-1})
1	Pd/MgO (**1.30**)	0.8	180	0.25	79	421
2	Pd/Fe_2O_3 (**1.31**)	0.4	160	2	90	105
3	Ni/θ-Al_2O_3 (**1.23**)	1.0	144	3	99	33
4	Ru Complex (**1.4**)	2.5	110	17	95	2.9
5	Ir complex (**1.9**)[a]	2.0	110	17	97	1.5

[a] *$NaHCO_3$ (2 mol%)*

Toluene was formed as a side product in the amination of aniline along with benzyl alcohol (7% yield) in the reaction catalysed by Pd/MgO (**1.30**), and greater amounts (up to 16% yield) were detected when higher Pd loadings were employed (1 wt.% vs. 2-10 wt.%). A possible route for its generation is the disproportionation of benzyl alcohol. This was reported in a separate study investigating the oxidation of benzyl alcohol over Au,Pd/TiO_2, Scheme 1.17 shows the two mechanisms that were proposed.[72]



SCHEME 1.17. *Possible mechanisms for toluene formation over a Au,Pd/TiO_2 catalyst for the oxidation of benzyl alcohol.*

The scope of the Pd/MgO catalyst (**1.30**) was limited to using aniline along with long chain primary aliphatic alcohols.[68] Even though this is a challenging reaction and good conversions were achieved (65-99%), the selectivities to the alkylated amine product were low to moderate (8-79%), long reaction times were necessary (up to 24 hours) and less reactive secondary alcohols were not tested. The system also required activation under H_2 (for 2 hours at 250 ˚C) prior to its use in reactions to generate active Pd^0 species.

Pd/Fe_2O_3[70] (**1.31**) exhibited a larger reaction scope than Pd/MgO (**1.30**), aniline as well as heteroaromatic and aliphatic amines undergo reactions with primary aliphatic alcohols, to furnish very good yields (72-99%) but the reaction times were long (up to 28 hours) and no examples of secondary alcohol substrates were provided.

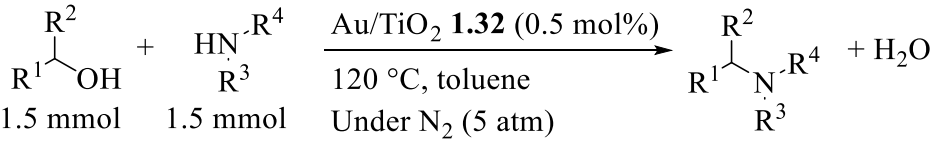
Overall, the pre-reduction of the Ni, Pd and Ag containing catalysts is a significant hindrance in terms of practicality. In this regard, the use of Au heterogeneous catalysts has demonstrated to be a very effective protocol as catalyst pre-activation is not necessary.

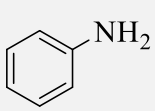
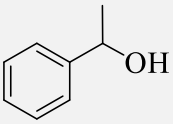
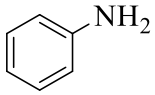
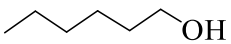
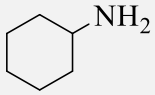
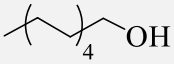
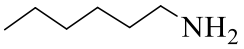
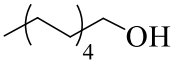
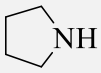
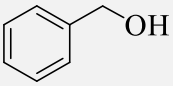
Au is an interesting catalyst material as it is relatively inert in its bulk form, yet displays excellent activity for a range of reactions when dispersed onto a solid support as nanoparticles in dimensions less than 10 nm.[73] It is well known that the activity of Au catalysts are strongly dependant on the size of the particles, with smaller ones generally being more active.[73] Haruta [74, 75] and Corma [68] studied a variety of Au supported catalysts (including Au supported on MgO, NiO, ZrO_2, TiO_2) for the formation of *N*-phenylbenzylamine from benzyl alcohol and aniline, however the major product obtained in most of these systems was the imine intermediate.

A broader reaction scope using Au/TiO_2 with very small Au particles (**1.32**) (mean particles size ~1.8 nm) has been reported (Table 1.18).[76] The system was able to operate under base free conditions, catalysing the reaction of various amines with alcohols. Although the TOF for the generation of *N*-phenylbenzylamine was lower than that of the Pd and Ni catalysts (**1.23**, **1.30** and **1.31**) (13.1 h^{-1} vs. 33-421 h^{-1}), lower reaction temperatures were employed (120 ˚C vs. 144-180 ˚C).

In comparison to the Pd systems (**1.30** and **1.31**), challenging substrates such as secondary aromatic and aliphatic alcohols generated excellent yields with aniline (Table 1.18, entries 1 and 2). Aliphatic amines, which were reluctant to react in previous systems, proceeded smoothly using an increased amount of catalyst and reaction temperature (5 mol% and 140 ˚C) (Table 1.18, entries 3 and 4). The reaction of pyrolidine, which is a structure found in many natural products and pharmaceuticals,[76] gave the desired tertiary amine when used along with benzyl alcohol (Table 1.18, entry 5).

TABLE 1.18. *N-alkylation of amines with alcohols using Au/TiO₂ (**1.32**).*

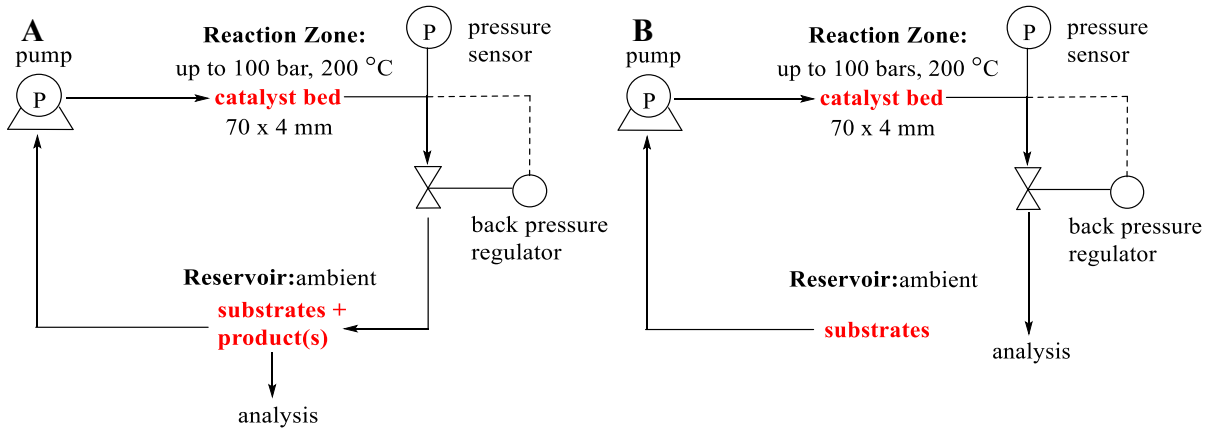


Entry	Amine	Alcohol	Time (h)	Yield (%)[a]
1			36	93
2			40	94
3[b]			55	53
4[b]			63	50
5[c]			50	97

[a] *Determined by GC,* [b] *amine (0.15 mmol), alcohol (0.15 mmol), catalyst (5 mol%), 140 ˚C,* [c] *catalyst (1 mol%), 140 ˚C.*

The main limitation of this system is the use of very long reaction times (up to 63 hours). By expanding the reaction space (higher temperature and pressure), afforded by employing a flow reactor, it has previously been shown that selective direct alkylation of a range of amines can be achieved in very good selectivity by using commercial Au/TiO_2 catalyst (Strem AUROlite^{TM}) (**1.33**).[77]

In this work, reactions were operated in batch-recycle mode, which involves the continual recycling of products through the reaction zone. Scheme 1.18 shows the configurations of single pass and batch-recycle modes and Table 1.19 highlights the general differences of these methods.



SCHEME 1.18. *Configuration of the flow reactor showing* ***A)*** *Batch-recycle mode and* ***B)*** *Single pass mode.*

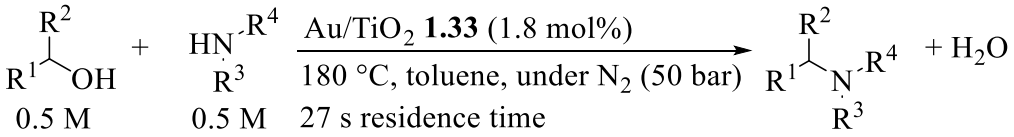
TABLE 1.19. *Advantages and disadvantages of using batch-recycle and single pass modes.*

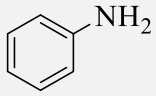
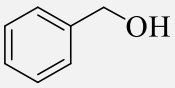
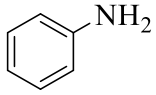
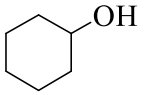
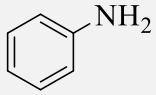
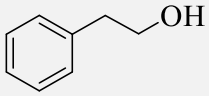
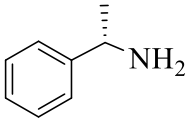
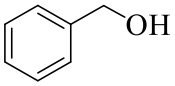
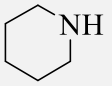
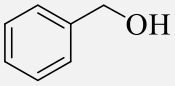
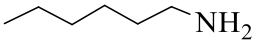
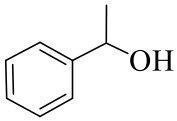
Reactor Set-up	Advantages	Disadvantages
Batch-recycle mode	• Reaction progress can be monitored over time, allowing for changes in selectivity and/or conversion to be studied.	• Does not give information regarding catalyst deactivation easily. • Aliquots are collected manually. • Products may require separation from substrates contained in the reaction reservoir.
Single pass mode	• Catalyst stability can be monitored over time. • Samples can be collected automatically using a fraction collector.	• Changes in selectivity and conversion over the course of a reaction cannot be monitored.

Using this system the alkylation of aromatic, aliphatic and chiral amines was achieved with excellent selectivity using a number of primary and secondary alcohols (Table 1.20). Primary and secondary aliphatic alcohols reacted smoothly, but required longer reaction times and when using phenylethanol as a reagent, lower conversions were afforded (Table 1.20, entries 2 and 3).

The reaction of benzyl alcohol and optically active α-methylbenzylamine gave the desired product with complete retention of stereochemistry (Table 1.10, entry 4) and secondary amines were well tolerated (Table 1.10, entry 5). The applicability of the system was further demonstrated by employing long chain aliphatic amines with secondary alcohols (Table 1.20, entry 6).

TABLE 1.20. *N-alkylation of amines with alcohols using Au/TiO₂ (**1.33**).*



Entry	Amine	Alcohol	Time (h)	Conversion (%)[a]	Selectivity (%)[b]
1[c,d]			3	99	97
2			7	85	100
3			7	59	>99
4[d]			7	91	98
5			6	98	100
6			7	85	>99

[a] *Determined by GC,* [b] *determined by* ^{1}*H NMR,* [c] *catalyst (0.9 mol%),* [d] *180 ˚C.*

Additionally, the synthesis of Piribedil can be achieved using this system (77% isolated yield) and occurred with a TOF of 1.8 h^{-1}.[77] This is slightly lower than that achieved by the homogeneous Ru complex (**1.4**) (2.9 h^{-1}), however the reaction methodology is much more advantageous as product purification can be easily achieved. Compared to the Raney Ni catalyst used in flow (**1.26**) a much broader reaction scope was demonstrated.

1.3 Conclusion

In summary, it was found that homogeneous systems using noble metals, Ru and Ir, were more active than those bearing base metals, such as Cu and Fe. In particular, [Ru(*p*-cymene)Cl_2]$_2$ (**1.4**) demonstrated a wide substrate scope and was applicable for the production of API's. However, the use of phosphine ligands was essential for this catalyst as well as for the majority of the other systems. Generally, the synthetic utility of homogeneous catalysts for the AAA reaction is limited by the need for organic ligands, the addition of base and the requirement for product separation techniques.

Immobilising homogeneous Ru and Ir complexes onto solid supports, allows for easier product separation. However, catalysts were found to deactivate under more forcing conditions, which are generally required for more challenging reactions, and the synthesis of complex ligands remains an issue. A highlight from the work was the demonstration of using immobilised Ru catalysts (**1.4**/**1.20** and **1.4**/**1.21**) in flow. Flow chemistry has many advantages over using batch processes, mainly conversion and selectivity can be fine-tuned by altering the residence time and it allows for greener and safer protocols. Moreover, product separation is very facile as the catalyst is held in a closed cartridge.

By using simple metal supported catalysts, the issues of product separation and complex ligand synthesis can be overcome. A drawback of using heterogeneous catalysts is the difficulty in achieving well-defined catalyst sites. Thus the majority of the heterogeneous catalysts were not tested for their ability in retaining enantioselectivity. This is not a major issue as there have also been very few homogeneous systems reported to facilitate these transformations for the AAA reaction; the only recent example being a homogeneous Ir based catalyst (**1.12**) in combination with chiral phosphoric acid (**1.13**). A clear disadvantage of the heterogeneous systems lies in the harsh reaction conditions required, with temperatures up to 400 ˚C reported and for some of the Ni based catalysts (**1.22** and **1.25**) a large excess of catalyst was required.

Ni supported on Al_2O_3 and $CaSiO_3$ (**1.23** and **1.24**) were shown to operate with low catalyst loadings (1-2 mol%) and displayed excellent reaction generality, with higher activities than analogous reactions performed by notable homogeneous Ru and Ir complexes (**1.4** and **1.9**). However, these materials required a pre-reduction step, which was also necessary for Ag and Pd based catalysts, and reactions were only performed in batch reactors.

In this regard, it has been shown that Au/TiO_2 has remarkable activity for the AAA reaction and does not require a time consuming pre-reduction step.[77] A flow reactor was

employed in the studies allowing for a wider reaction scope, a greener system than previously reported catalysts and the synthesis of Piribedil was demonstrated.

Fundamentally, reactions performed using batch methods are limited by the size of the reactor, due to their inability to recycle reagents efficiently.[46] In a flow process the turnover of the catalyst is only restricted by its lifetime, as a continuous feed of reagents over the catalyst surface can be realised. Therefore, by adopting a flow reactor, the formation of amines can be realised in a safer and sustainable manner compared to using batch techniques. One of the major challenges in this field is the development of a non-noble catalyst that is able to operate in flow with high activity and the development of a kinetic model, which would support in the understanding of the reaction mechanism.

1.4 Project aims

This project is divided into two main topics, namely mechanistic and catalyst development studies.

Mechanistic studies

It has previously been demonstrated that Au/TiO_2 (using toluene as a solvent) is a very active system for the AAA reaction in flow (Section 1.2.2).[77] However, there is little known regarding the mechanism occurring over the catalyst surface. Following on from the previous work, commercial Au/TiO_2 (Strem AUROlite^{TM}) will be used to investigate the effects of changing reaction parameters on catalyst activity (conversion and selectivity), with the aim of gaining a better understanding of the mechanism. The reaction of benzyl alcohol and aniline will be used for these studies, employing a flow reactor (X-Cube Thales Nano, as described in Chapter 7). Benzyl alcohol and aniline were chosen as the model substrates because Au/TiO_2 can catalyse the coupling of these species in a relatively short period of time (Table 1.20, entry 1); and as this is commonly reported in literature, it will allow direct comparisons to be made.

The effects of H_2O and O_2 will be studied in batch-recycle mode and the reaction progress monitored over time. These two parameters have been selected as it has previously been demonstrated that the AAA reaction is affected by H_2O when using this catalyst (discussed in Chapter 2) and it is anticipated that the reaction atmosphere may also influence activity. 2-Methyl-2-butanol will replace toluene in these studies as it allows for increased H_2O solubility (120 g L^{-1} vs. 0.5 g L^{-1}), and it is a greener solvent.[78]

It is hoped that these results will aid in the development of the previously reported kinetic model,[77] and lead to the formation of a predictive model using the new solvent system (Chapter 3). A predictive model for the AAA reaction will enable future reactions, using Au/TiO_2, to be designed as to achieve the maximum output and capability of the catalyst. Additionally, the stability and possible deactivation modes of the catalyst will be interrogated by performing the model reaction in single pass mode (Scheme 1.18). It is important to know the catalyst lifetime and possible degradation pathways for industrial applications, as solutions may be engineered to try to reduce the effects of deactivation and increase catalytic performance.

Catalyst development studies

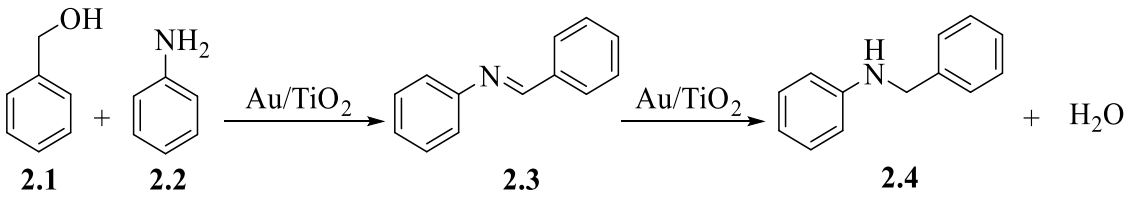
In this part of the project (described in Chapters 4, 5 and 6) a variety of different catalysts will be prepared and tested for their activity towards the AAA reaction in a batch reactor. Au supported on TiO_2 will be prepared using numerous well-established techniques in order to identify the effects that this has on the activity and structure of the catalyst. By gaining a better knowledge of any influences that preparation techniques may invoke, the development of an overall more active system can be realised.

Different Au supported catalysts will be synthesised to understand whether the support plays an active role in the reaction and to distinguish the effects that changing the support has on the particle structure.

To discover if there are any systems more active, selective and/or cost effective compared to using Au based systems, different metal supported catalysts will be prepared, including Au bimetallic catalysts.

CHAPTER 2. Mechanistic studies using Au/TiO_2 in flow

The main objective of the work described in this Chapter was to achieve a deeper understanding of the reaction occurring over 1 wt.% Au/TiO_2 (Strem AUROlite^{TM}), using the model reaction between **2.1** and **2.2**, conducted using a ThalesNano X-cube^{TM} flow reactor (Scheme 2.1).



SCHEME 2.1. *The alkylation of* ***2.2*** *with* ***2.1*** *catalysed by* Au/TiO_2.

The precise mechanism for the AAA reaction using Au/TiO_2 remains largely unknown. It is important to understand how the reaction occurs over Au/TiO_2, as it will allow a comprehensive model to be constructed (Chapter 3). Additionally, the stability and possible deactivation modes of the catalyst were interrogated because by understanding the cause(s) of degradation, solutions may be engineered to try to reduce any detrimental effects.[79]

Kinetic and mechanistic models for the alkylation of **2.2** with **2.1** have been proposed.[77] The details of these are discussed in the following Section (2.1), which provides a background for the studies performed in this work.

2.1 Background

Previous studies[77] investigated the effects of temperature (130-180 ˚C) and pressure (5-50 bar) for the alkylation of **2.2** with **2.1** using the X-cube flow reactor in batch-recycle mode (Scheme 1.18). No effect of pressure on conversion or selectivity was detected, suggesting that H_2 was not generated during the process, and that it was adsorbed hydrides (from the oxidation of **2.1**) which were responsible for the reduction of **2.3** to **2.4**. Concurrently, a substantial influence of temperature on the selectivity of the reaction was discovered. At low temperatures (130 ˚C) the formation of the oxidised species (imine (**2.3**) and PhCHO) was found to accumulate over the course of the reaction, whereas at high temperatures (150-180 ˚C) this effect was avoided and imine behaved as a reaction intermediate, leading to higher selectivities for **2.4** (from 65% at 130 ˚C vs. ~94% at 150-180 ˚C). This can be observed in Figure 2.1, where the formation of imine (**2.3**) is plotted against time for the three different reaction temperatures investigated (130, 150 and 180 ˚C). Note that the conversions achieved were 65% and >99% for reactions conducted at 130 ˚C and 150-180 ˚C, respectively.

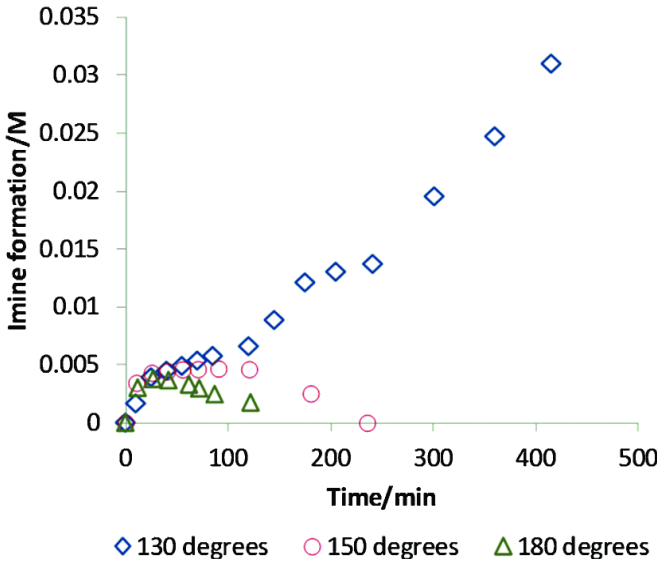
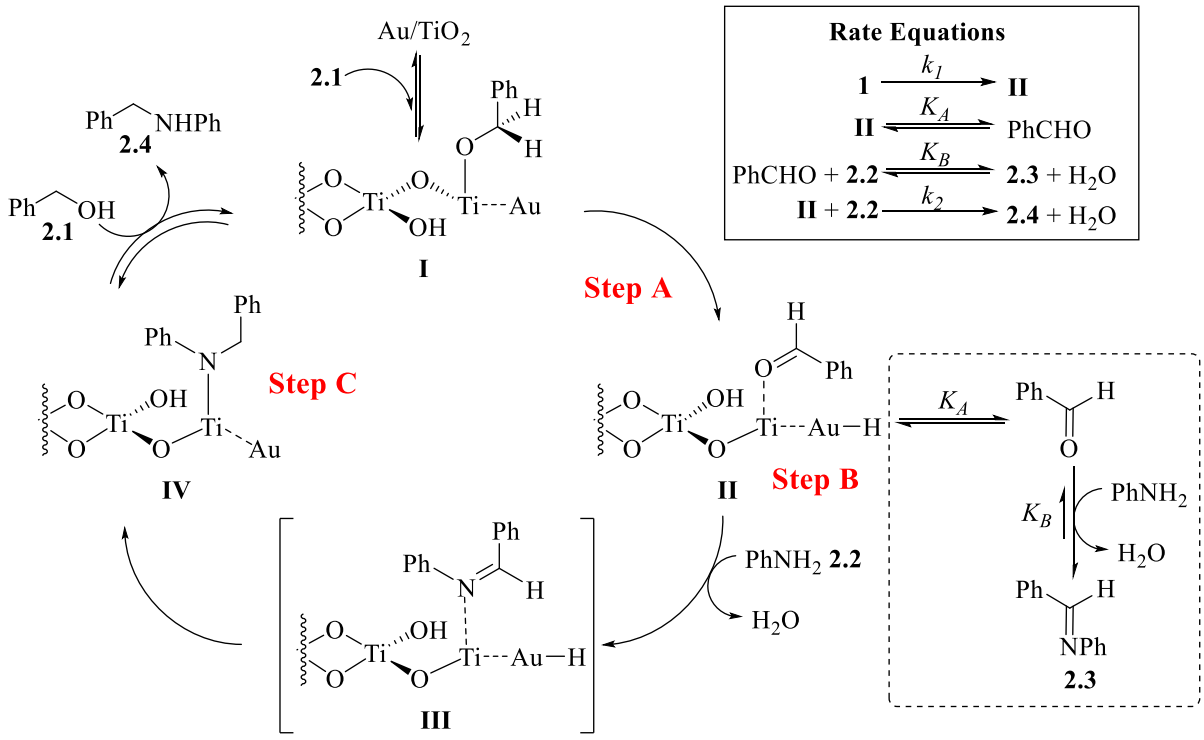


FIGURE 2.1. *Effect of temperature on the evolution of imine (**2.3**) over the course of the reaction.* ***Reaction conditions:*** *A mixture of **2.1** (0.29 M) and **2.2** (0.16 M) in toluene (10 mL) was re-circulated through a cartridge of Au/TiO_2 (2.7 mol% Au) at a flow rate of 1.5 mL min^{-1} and 50 bar pressure.*[77]

Based on these observations, the following catalytic cycle and rate equations were constructed (Scheme 2.2):



SCHEME 2.2. *Previously reported catalytic cycle and associated rate equations.*[77]

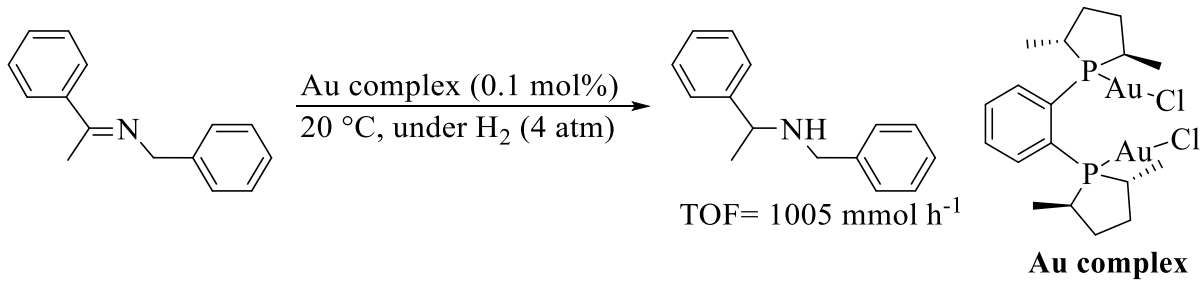
Step A: ***Oxidation/dehydrogenation of alcohol:*** The first step in the model, involves the reversible binding of alcohol to generate the alkoxide intermediate (**I**). An irreversible scission of the C-H alkoxide bond affords bound aldehyde (**II**) and metal hydride on the catalyst surface. The formation of this species was identified to be the rate determining step (k_1), with a measured rate of 4.5 x 10^{-4} s^{-1} and an activation energy of 93.7 kJ mol^{-1} (Table 2.1, entry 1).[77] The calculated activation energy is comparable to that of a later study investigating the amination of myrtenol, a natural terpene alcohol, over Au/ZrO_2 (87.7 kJ mol^{-1}) (Table 2.1, entry 2).[80]

TABLE 2.1. *Previously derived rates and activation energies for the dehydrogenation of* ***2.1****.*

Entry	Catalyst	Conditions	Rate (s^{-1})	E_{act} (kJ mol^{-1})
1	1 wt.% Au/TiO_2 (0.9 mol%) [77]	**2.1** and **2.2** (1:1, 0.5 M), 180 ˚C, 50 bar (in flow), toluene	4.5 x 10^{-4}	93. 7
2	3 wt.% Au/ZrO_2 (1.4 mol%) [80]	myrtenol and **2.2** (1:1, 1mM), 180 ˚C, under N_2 (9 bar) in a stainless steel reactor, toluene	7.4 x 10^{-2}	87.7

Step B: ***Formation of imine:*** As highlighted earlier, it was only at high temperatures (>150 ˚C) where imine begins to behave as a reactive intermediate. Therefore it was proposed that the bound aldehyde species (**II**) can desorb from the surface and condense with aniline (**2.2**) in solution to form 'free' imine (**2.3**), and that only bound aldehyde (**II**) can react with **2.2** to generate **2.4**, and H_2O as a by-product. Data fitting results showed that at low temperatures (130 ˚C) the formation of **2.4** (k_2) was sufficiently slow (5.7 x 10^{-2} $M^{-1}s^{-1}$) such that the formation of **2.3** (K_A•K_B) became competitive (1.46). At higher temperatures, the formation of **2.3** becomes disfavoured. The consequence of this is to increase the amount of reactive bound aldehyde (**II**) in the system, which enhances the selectivity for **2.4**. The large reaction space afforded by using a flow reactor allows for excellent catalyst efficiency.

Step C: ***Formation of the amine product:*** The cycle completes with the reduction of bound imine to generate **2.4**. To the best of our knowledge, there are no known reports of heterogeneous Au catalysts facilitating the hydrogenation of imines. However, there has been a report of a homogeneous Au complex catalysing the hydrogenation of *anti*-N-benzyl(1-phenylethylidene)imine in the presence of H_2 (Scheme 2.3), with comparable TOF's to that of Ir and Pt analogues (11365 and 1118 mmol h^{-1}, respectively).[81]



SCHEME 2.3. *Hydrogenation of imine using a homogeneous Au complex.*

In addition to the temperature affecting the reaction, it was previously demonstrated that the alkylation of **2.1** with **2.2** was curtailed by employing a desiccant cartridge fitted to the outlet of the reactor (Figure 2.2).[77]

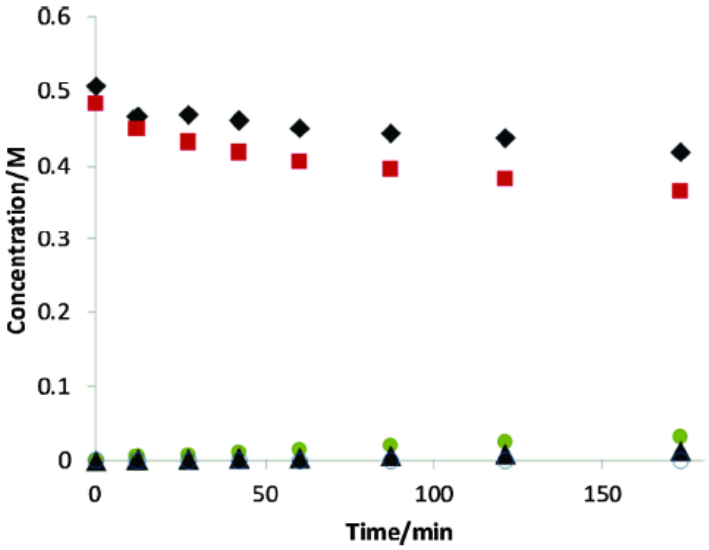


FIGURE 2.2. *Alkylation of* ***2.1*** *with* ***2.2*** *under anhydrous conditions. (■=**2.1**, ▲=**2.4**, ●=**2.3**, ○=PhCHO, ♦=**2.2**).* ***Reaction conditions:*** *A mixture of* ***2.1*** *(0.5 M) and* ***2.2*** *(0.5 M) in toluene (10 mL) was re-circulated through a cartridge of Au/TiO_2 (1 mol% Au) at a flow rate of 1.5 mL/ min at 180 ˚C and 50 bar pressure.*[77]

This result is surprising given that H_2O is formed as a by-product in the reaction (from the condensation of **2.3** with PhCHO) and hence it is expected that its removal would give rise to an increase in conversion to maintain the reaction equilibrium. The loss of catalytic activity, however, signified that the presence of H_2O was crucial for the activity of Au/TiO_2.

The interaction of H_2O with TiO_2 has been extensively studied, due to the central role it plays in many important applications such as solar-hydrogen production.[82] H_2O is known to adsorb molecularly and to dissociate over TiO_2 to generate OH and H functionalities, which greatly influence the chemistry of the catalyst surface. Indeed, theoretical calculations have shown that surface OH species promote catalytic activity by participating directly in the catalytic pathway and by reducing the overall activation barrier in the oxidation of methanol and isopropanol using Pt/C.[83] Similarly, it was demonstrated in a separate study that adsorbed OH species lower the barrier of activation for the scission of alcohol C-H bonds in the oxidation of alcohols over Au.[84] As the first step in the AAA reaction involves the oxidation of alcohol to the carbonyl species, it can be hypothesised that surface OH groups may be involved in catalysing this step. H_2O is found to exert important effects in many catalytic reactions other than the oxidation of alcohols, such as CO oxidations and hydrogenation reactions.[85-87]

In this Chapter, a more detailed study of the mechanism was performed by changing reaction conditions and analysing their effect, on conversion and/or selectivity.

The effect of H_2O in 2-methyl-2-butanol was not particularly well understood at the beginning of the project because previous studies used toluene as a reaction medium. To investigate the effect of H_2O in the reaction, experiments were designed specifically using a range of different H_2O concentrations (2-200 mM), including the use of a desiccant cartridge, and reaction progress monitored by sampling aliquots during the course of the reaction. The motivation for assessing a series of concentrations was because earlier work only interrogated the removal of H_2O from the system (Figure 2.2). Thus, more detailed investigations were important to enable the effect of moisture to be elucidated fully. Experiments were conducted in batch-recycle mode as it allows changes in selectivity and conversion through the course of a reaction to be monitored (Scheme 1.18 and Table 1.19).

In the presence of O_2, the metal hydrides generated on the catalyst surface (Scheme 2.2, step A) can be removed by the formation of H_2O as a by-product. Hence, the AAA reaction is generally performed under de-oxygenated (N_2-purged) conditions, to suppress the formation of oxidised by-products. Thus, in order to interrogate the effect of O_2 on catalytic activity, experiments were performed either under air or N_2, by purging the reaction mixture with the respective gas.

To study the stability of Au/TiO_2 and to understand whether any species may deactivate the catalyst, the flow reactor was operated in single pass mode to generate time-on-line profiles (Scheme 1.18). Intermediates and products (**2.3**, **2.4** and H_2O) were introduced separately (after 2 hours) into the reaction vessel containing **2.2** and **2.1**, and the concentration of **2.1** was monitored. An experiment conducted without the introduction of species into the vessel, containing **2.1** and **2.2**, was used to compare against these experiments. If species are involved in deactivating Au/TiO_2, perhaps via blocking active sites, an increase in the concentration of **2.1** over time is expected, as less will be converted to products and/or intermediates. The time-on-line profile conducted without the introduction of species into the vessel will also allow for the stability and lifetime of Au/TiO_2 to be monitored.

All of the studies were performed with commercially available 1 wt.% Au/TiO_2 (Strem AUROlite^{TM}) catalyst. The characterisation data of this system is presented next (Section 2.2), followed by the mechanistic (Section 2.3) and catalyst stability studies (Section 2.4).

2.2 Characterisation of Au/TiO₂

Note that all characterisation of the Au/TiO₂ (Strem AUROlite™) catalyst was conducted at Imperial College London. The catalyst was thermally pre-treated at 150 ˚C for 24 hours prior to its use in all reactions. This was to ensure that comparisons between experiments conducted using anhydrous conditions (i.e. dried catalyst, solvent and desiccant) could be made against reactions involving the addition of H_2O.

TEM analysis was performed on untreated Au/TiO₂ as received from the supplier, dried Au/TiO₂ (at 150 ˚C in static air for 24 hours) and catalyst that was employed in a reaction (a mixture of **2.1** and **2.2** recycled over Au/TiO₂ at flow rate of 1.5 mL min^{-1}, 180 ˚C, 50 bar, 3 hours). This was done in order to assess whether the thermal treatment of the catalyst caused growth in particle size and to evaluate if the particle sizes changed during the reaction.

The drying of the catalyst did not significantly increase the Au particle size (Figure 2.3, and Table 2.2, entry 1 vs. entry 2). However, the average Au particle size did increase following the reaction (Figure 2.3 C and Table 2.2, entry 3), likely due to the combination of high pressure and temperature causing particle agglomeration.

TABLE 2.2. *Mean Au particle sizes of Au/TiO₂ under various conditions (~200 particles counted).*

Entry	Conditions	Average particle size (nm)
1	As-supplied	3.2 ± 0.1
2	Dried	3.4 ± 0.1
3	Used	4.2 ± 0.1

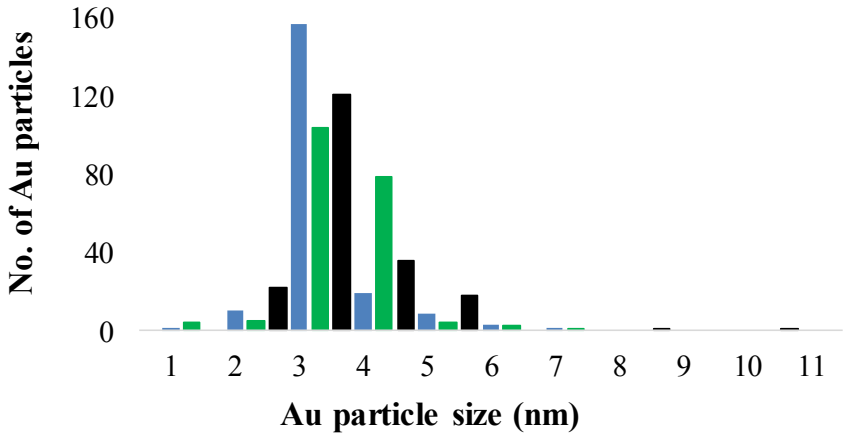


FIGURE 2.3. *Particle distribution graphs of Au/TiO₂ showing mean Au particle sizes (■=As-supplied, ■= Dried (at 150 ˚C for 24 hours), ■=Used (180 ˚C, 50 bar, batch-recycle mode, 3 hours).*

The surface area of Au/TiO_2 was measured using the BET method by physisorption of N_2. A surface area of 47 m^2 g^{-1} was revealed, which is in good agreement with our previously reported value for the Au/TiO_2 catalyst (40 m^2 g^{-1}).[77]

As-supplied and dried (150 ˚C for 24 hours) Au/TiO_2 was analysed by Fourier transform infrared (FTIR) spectroscopy in order to determine whether the temperature pre-treatment was effective in removing H_2O species. A similar investigation has been reported in the literature where FTIR analysis showed that pre-treating Au/TiO_2 under varying thermal conditions (150-350 ˚C, using various mixtures of O_2 and H_2) resulted in H_2O desorption from the surface.[88]

In this work it was found that the vibration band for adsorbed H_2O (1600 cm^{-1}) and the OH stretching region (3800-2500 cm^{-1}) both decreased following the drying procedure (Figure 2.4 A vs. B). These changes are attributed to the loss of adsorbed H_2O and surface hydroxyl groups on Au/TiO_2.[88] Thus it can be concluded that the temperature pre-treatment was effective in surface dehydroxylation and dehydration.

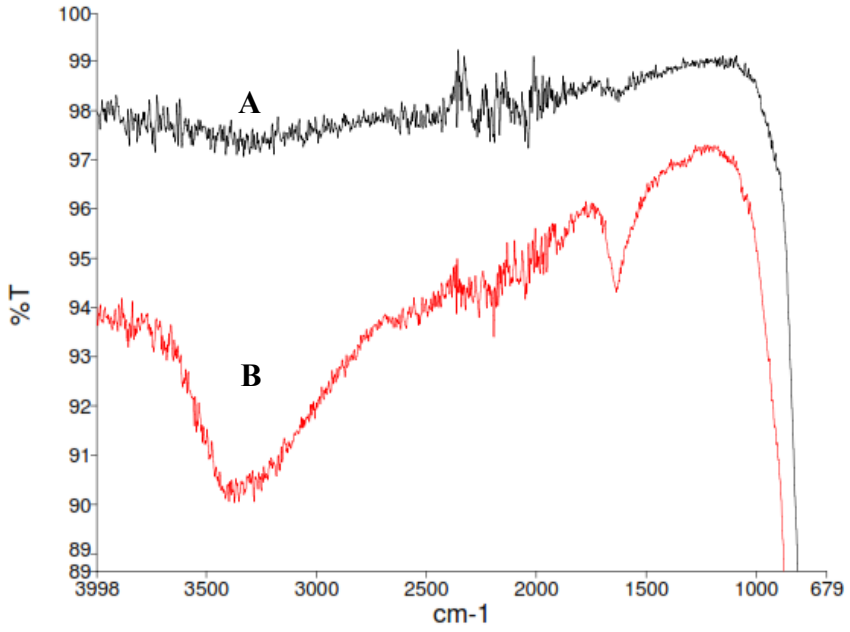


FIGURE 2.4. *FTIR analysis of* ***A)*** *Dried (150 ˚C for 24 hours) Au/TiO_2,* ***B)*** *As-supplied Au/TiO_2.*

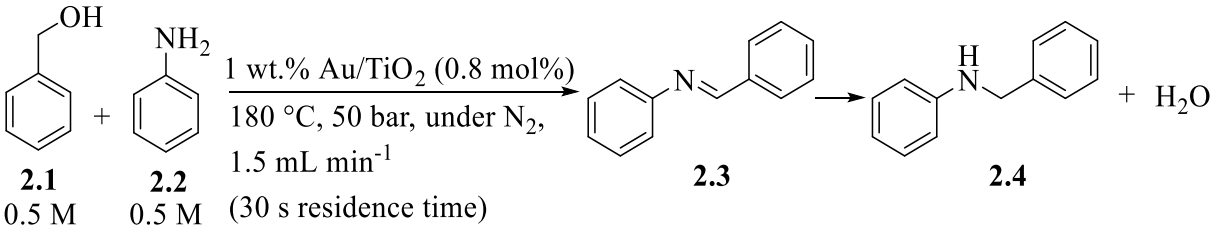
2.3 Results of the mechanistic studies using Au/TiO_2

To study the effect of H_2O on the reaction, a desired amount of H_2O was added to the solvent, before it was used to condition the catalyst and flow reactor up to the chosen temperature and pressure (180 ˚C at 50 bar). The same solvent mixture was used to prepare the reaction mixture, which was subsequently delivered into the reactor at a flow rate of 1.5 mL min^{-1}. For experiments conducted under anhydrous conditions, dry solvent was used to condition Au/TiO_2 and the reactor, and a desiccant line was fitted to the outlet of the reactor.

It should be noted that the residual concentration of H_2O in anhydrous 2-methyl-2-butanol was 2 mM. The H_2O content was determined using a Karl Fischer titrator, prior to the addition of **2.1** and **2.2**. Although batch-recycle mode was used for the majority of experiments detailed in this Chapter, single pass mode was used to validate the results of reactions, with sample fractions collected at set time intervals using a fraction collector.

2.3.1 The effect of H_2O on the AAA reaction using 2-methyl-2-butanol

The model system of **2.1** with **2.2** was chosen to test the activity of the Au/TiO_2 catalyst using the same reaction conditions adopted in previous studies,[77] (purging the reaction mixture with N_2) to allow for a direct comparison of results (Scheme 2.4).



SCHEME 2.4. *The alkylation of **2.2** with **2.1** for the mechanistic studies of Au/TiO_2, using a flow reactor.*

Initial H_2O concentrations of 2, 45, 180 and 200 mM in 2-methyl-2-butanol were used. Note that conversion of **2.1** was based on the generation of products. Under these conditions, the conversion of **2.1** to products and intermediates (**2.4**, **2.3**, PhCHO) was shown to be dependent on the concentration of H_2O in the system, with increasing H_2O content (>2 mM) leading to reductions in conversion (Figure 2.5). However, the rate of consumption of **2.1** remained the same for all of the experiments (Table 2.3) (calculated by linear regression of **2.1** vs. time). A consistent rate of **2.1** depletion should generate the same conversion to

products over time; therefore, the results imply that the mass balances did not close fully for the reactions. Indeed, the mass balances for experiments conducted with H_2O concentrations higher than 2 mM did not close to 100% and became gradually worse when employing higher levels of H_2O in the solvent (Table 2.3, entry 1 vs. entry 4).

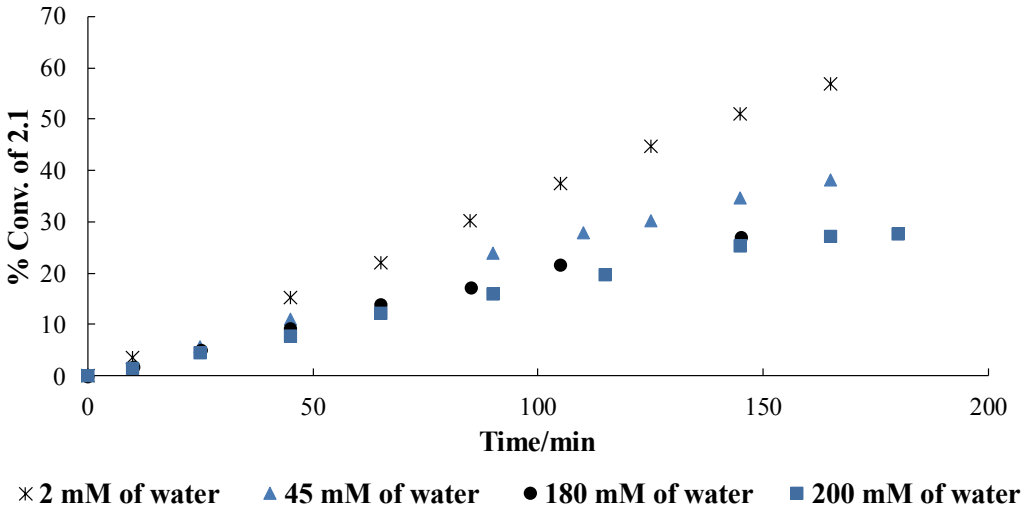


FIGURE 2.5. *Time conversion profile for the % Conversion of* ***2.1*** *to products, demonstrating the effect of using different initial H_2O concentrations in 2-methyl-2-butanol.*

TABLE 2.3. *Rate of* ***2.1*** *disappearance for experiments conducted using different H_2O concentrations in 2-methyl-2-butanol and the mass balances achieved.*

Entry	H_2O conc. (mM)	Mass balance (%)	d[1]/dt (M s^{-1})[a]
1	2	100	-1.3×10^{-3}
2	45	81	-1.3×10^{-3}
3	180	78	-1.4×10^{-3}
4	200	67	-1.2×10^{-3}

[a] *Conversion rate of* ***2.1*** *(M s^{-1}), calculated by linear regression of the concentration of* ***2.1*** *over the reaction time.*

When the concentration of **2.4** is plotted against time, it can be seen that lower amounts of the amine product **2.4** were detected for experiments using increased H_2O concentrations (>2 mM) (Figure 2.6). The decreased amounts of **2.4** found for these reactions accounts for the incomplete mass balances (Table 2.3, entries 2-4); however, it does not explain why lesser amounts of **2.4** were detected. As the rate of **2.1** disappearance remained unchanged for all of the reactions, it can be expected that products were generated at the same rate.

Therefore **2.4** was presumably lost in the system for reactions conducted with high H_2O concentrations. Indeed, **2.4** is insoluble in H_2O and thus it can be postulated that an emulsion and/or precipitation of **2.4** was formed with H_2O in the solvent, which subsequently was deposited within the reactor. Certainly, the reaction reservoir turned cloudy for experiments conducted with high H_2O concentrations. To elucidate this fully, further experiments are required to determine the solubility of **2.4** in 2-methyl-2-butanol/H_2O mixtures.

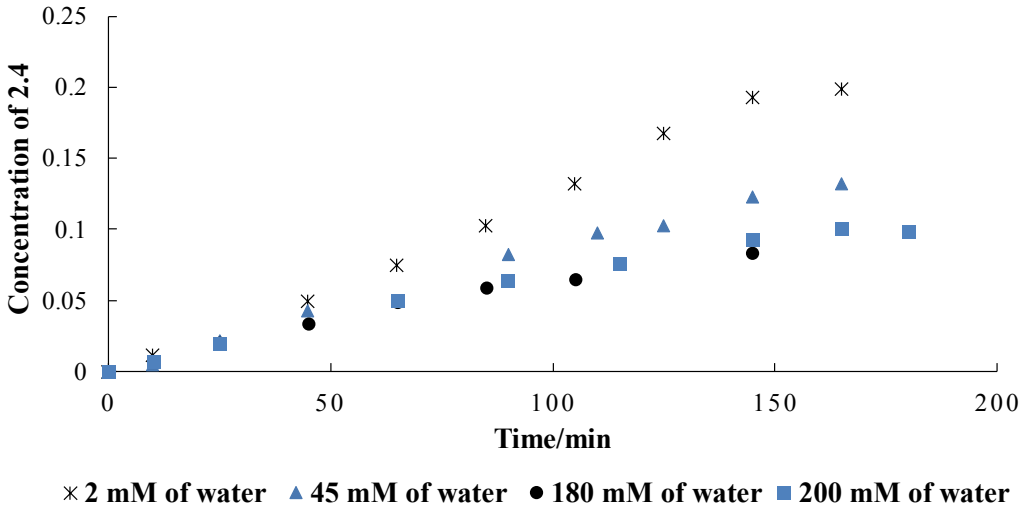


FIGURE 2.6. *Concentration of **2.4** over time for experiments using different initial H_2O concentrations in 2-methyl-2-butanol.*

Removing H_2O from the reaction, using a desiccant cartridge fitted to the outlet, resulted in a decreased conversion (by ~20%) and formation of **2.4** compared to the experiment using the same initial H_2O concentration, but without the use of a desiccant (Figure 2.7 A and B). Furthermore, an induction period of around 20 minutes was observed (highlighted in Figure 2.7 A). This result is similar to that previously reported by our group where the removal of H_2O resulted in the annihilation of the reaction (Figure 2.2). However, in this experiment, a mass balance of 73% was found, in contrast to the full mass balance achieved for the experiment conducted without desiccant (Table 2.3, entry 1). Yet the rate of **2.1** disappearance was comparable for both of the reactions (1.4×10^{-3} M s^{-1} and 1.3×10^{-3} M s^{-1}, with and without desiccant, respectively) implying that products were formed at the same rate. As a lower amount of **2.4** was detected when removing H_2O from the system with desiccant, it can be suggested that any residual H_2O held in the desiccant could have acted to trap **2.4**. This conclusion is similar to that drawn above where it was postulated that increased

H_2O concentrations in the solvent precipitated and/or formed an emulsion of **2.4**, due to the poor solubility of this species in H_2O.

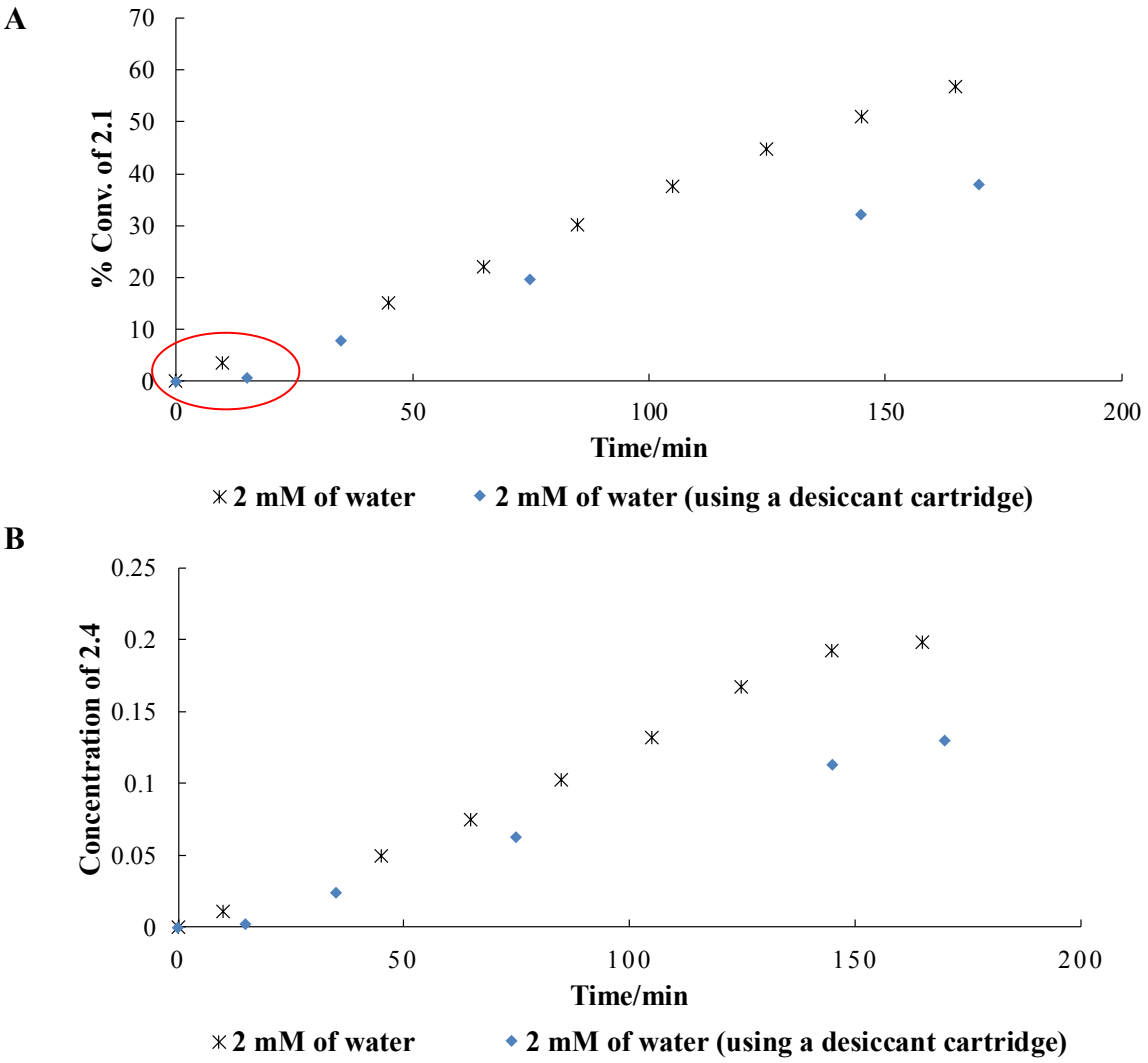


FIGURE 2.7. *The effect of removing H_2O using a desiccant (compared against an experiment using the same initial H_2O concentration but without the use of desiccant),* ***A)*** *% Conversion of* ***2.1*** *to products and* ***B)*** *Concentration of* ***2.4*** *over time.*

Although increased H_2O concentrations led to a loss of **2.4** (Figure 2.6), it was found that the selectivity for this species was enhanced by using higher levels of H_2O in the solvent (Figure 2.8). While this effect was small (2% increase in the selectivity for **2.4** by using 200 mM of H_2O, compared to 2 mM of H_2O), the results suggest that H_2O was able to facilitate the formation of **2.4**, perhaps by acting as a reductant.

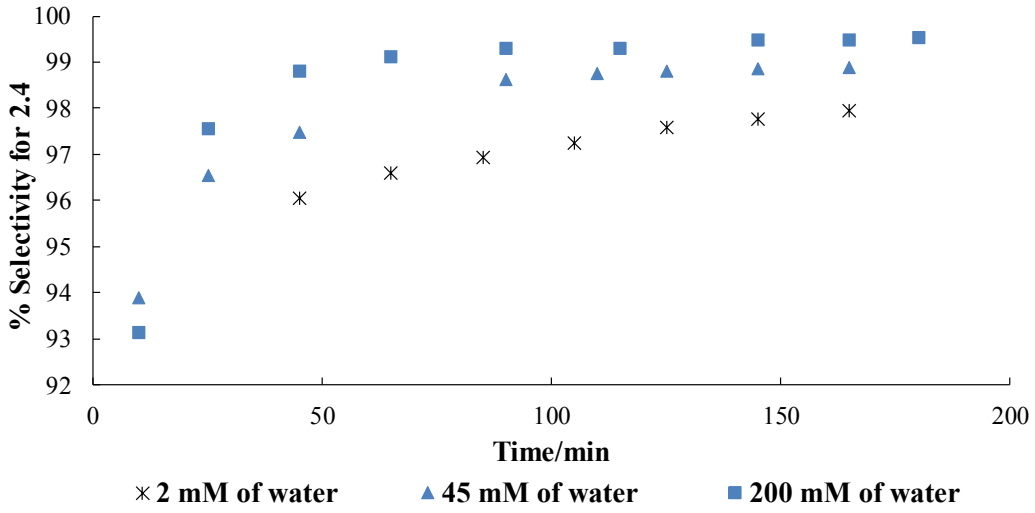
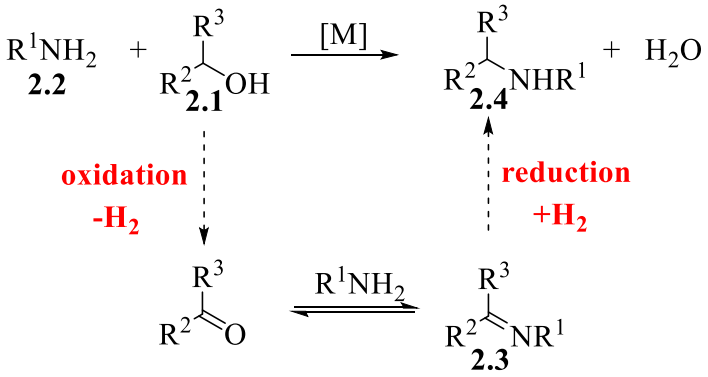


FIGURE 2.8. *Graph showing the % Selectivity for* ***2.4****, demonstrating the effect of using different H_2O concentrations in 2-methyl-2-butanol.*

In the hydrogen borrowing mechanism, it is understood that hydride generated from the initial dehydrogenation of **2.1** is used to reduce **2.3** to **2.4** (Scheme 2.5).



SCHEME 2.5. *The hydrogen borrowing mechanism.*

As H_2O is known to dissociate on the TiO_2 surface into OH and H species (Section 2.1), it is possible that it is able to act as a reductant in the reaction via these dissociated species. Indeed, the hydrogenation activity of PhCHO over Au supported on TiO_2, Al_2O_3 and ZrO_2 was shown to increase in the presence of H_2O, which was attributed to the increased availability of dissociated hydrogen species.[87]

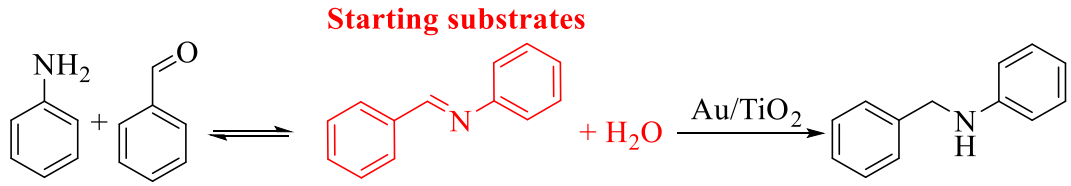
In order to study this, separate experiments were devised using mixtures of:

1. **2.3** (0.2 M) and H_2O (2 mM) in 2-methyl-2-butanol (under N_2)

and

2. **2.3** (0.2 M) and H_2O (200 mM) in 2-methyl-2-butanol (under N_2)

The solutions were passed over Au/TiO_2 (0.8 mol%) in batch-recycle mode at 1.5 mL min^{-1}, 180 ˚C and 50 bar for 2.5 hours (Scheme 2.6). It was predicted that if H_2O is able to act as a reductant, increased amounts of **2.4** would be generated in the second reaction, where a higher amount of H_2O was employed (200 mM vs. 2 mM of H_2O).



SCHEME 2.6. *Experiment designed to assess whether H_2O is able to act as a reductant.*

In the previously reported kinetic cycle, an equilibrium constant value of 1.46 was derived for the reversible formation of **2.3** from the condensation of desorbed PhCHO with **2.2** (at 180 ˚C, 50 bar, 1.5 mL min^{-1} using toluene as a solvent). As similar reaction conditions were employed to test for the formation of **2.4** from **2.3** and H_2O, it was anticipated that **2.2** and PhCHO would also be generated (Scheme 2.6).

As expected, PhCHO and **2.2** were produced through the hydrolysis of **2.3** in the second reaction, where 200 mM of H_2O was employed (Figure 2.9), confirming the reversibility of this process under the conditions employed.

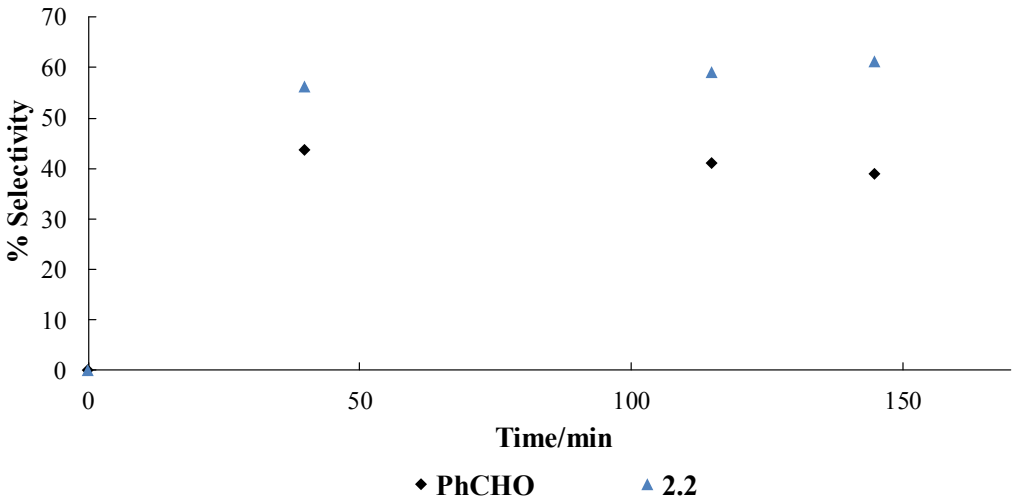


FIGURE 2.9. *Graph showing the % Selectivity for PhCHO and **2.2** when starting with **2.3** and H_2O (200 mM) in 2-methyl-2-butanol.*

Gratifyingly, the formation of **2.4** was detected in higher amounts for the experiment which employed 200 mM of H_2O compared to that using 2mM of H_2O (Figure 2.10). This shows that in the presence of high H_2O content, H_2O is able to act as a reductant.

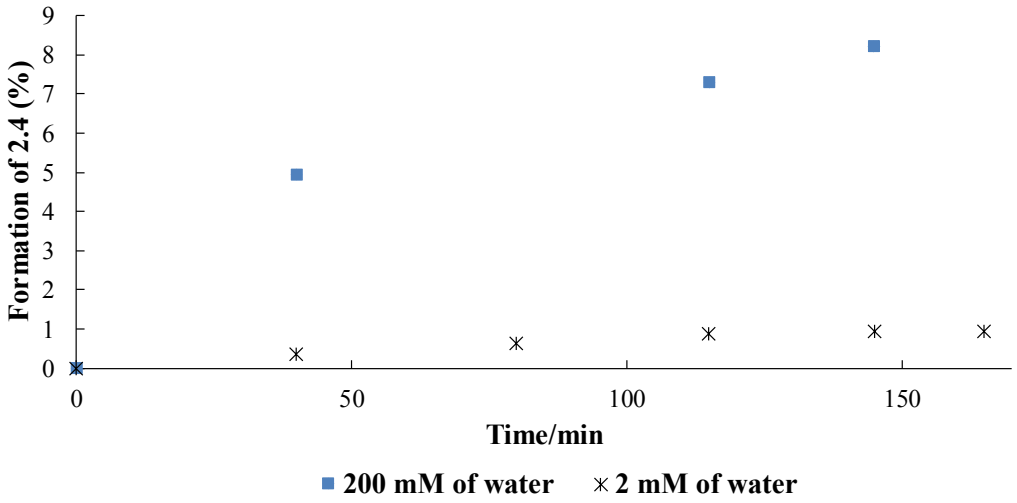


FIGURE 2.10. *Graph showing the percentage of* ***2.4*** *formed when starting with* ***2.3*** *in the presence of 2 mM and 200 mM of H_2O in 2-methyl-2-butanol.*

The key observations and conclusions made so far are listed below:

- Increased H_2O concentrations (>2 mM) led to decreased detection of **2.4**. The mass balances of reactions were incomplete for these reactions, yet the rate of **2.1** disappearance remained constant.

  H_2O was likely inducing an emulsion with ***2.4*** *and/or a precipitate (due to the poor solubility of this species in H_2O) with the species becoming trapped in the system, leading to a lower detection of* ***2.4*** *and subsequent reduction in conversion.*
- An induction period was found using a desiccant cartridge during the reaction and the detection **2.4** was lower (with an incomplete mass balance) compared to a reaction using the same initial H_2O concentration, but without a desiccant.

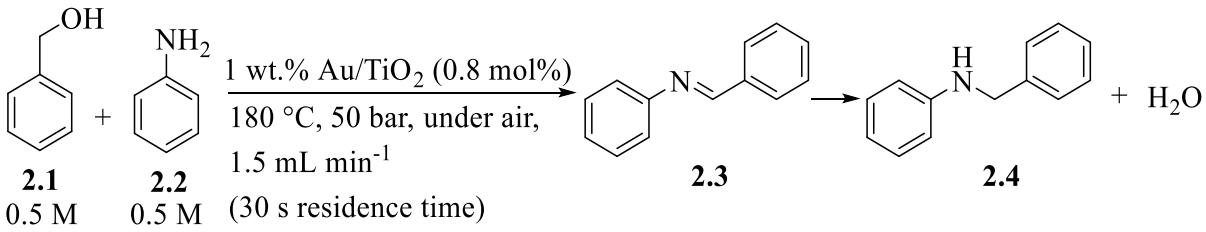
  2.4 *was likely being trapped by residual H_2O in the desiccant line. Thus leading to a lower detection of* ***2.4*** *and subsequent reduction in conversion.*
- In the presence of high H_2O content (>2 mM), the selectivity for **2.4** was enhanced. By starting with **2.3** in the presence of high H_2O levels (200 mM), **2.4** was formed (and correspondingly **2.3** and PhCHO).

  H_2O was able to act as a reductant, likely through dissociated hydrogen species on the catalyst surface, enhancing the selectivities when in high concentrations in the system.

  Overall, there appears to be two main functions of H_2O, namely acting to precipitate and/or form an emulsion with **2.4** when present in high levels (>2 mM) and as a reductant for the formation of **2.4** from **2.3**.

2.3.2 The effect of H_2O and O_2 on the AAA reaction using 2-methyl-2-butanol

The effects of H_2O and O_2 on conversion and selectivity were analysed using the same conditions employed in the previous studies, but purging the reaction mixture with air (Scheme 2.7).



SCHEME 2.7. *The alkylation of* ***2.2*** *with* ***2.1*** *for the mechanistic studies of Au/TiO_2, using a flow reactor.*

Experiments were performed using 2, 100 and 180 mM of H_2O, and interestingly, there appeared to be no influence on the conversion by increasing the moisture in the reaction (Figure 2.11). Under these three different H_2O concentrations used, the conversion of **2.1** remained essentially unchanged with closing mass balances for all reactions.

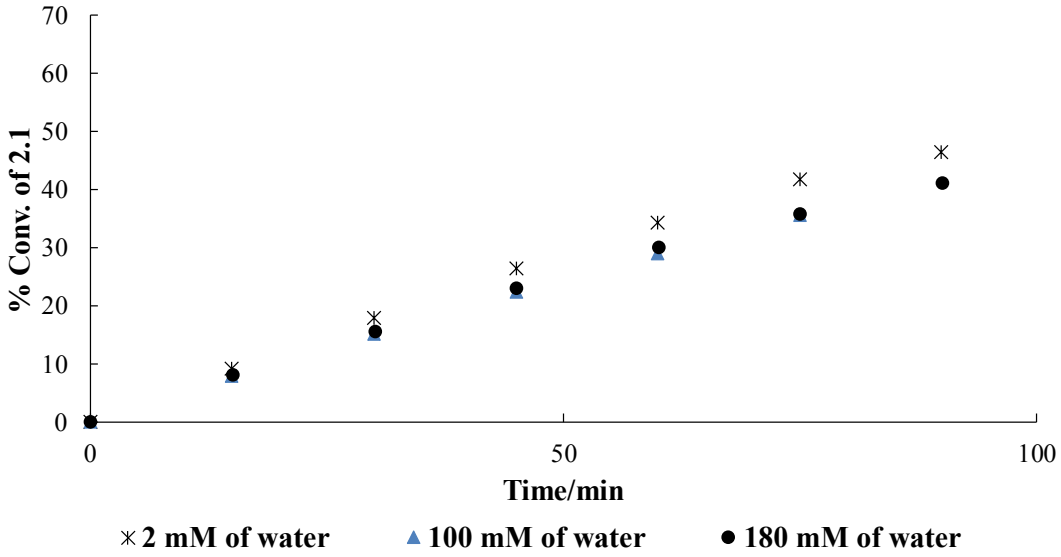


FIGURE 2.11. *Time conversion profile for the % Conversion of* ***2.1*** *to products, demonstrating the effect of different initial H_2O concentrations in 2-methyl-2-butanol under aerobic conditions.*

This result is in stark contrast to experiments performed under N_2, where the detection of amine product was decreased upon increasing the H_2O level, presumed to be due to the poor solubility of **2.4** at high H_2O concentrations (Figure 2.6). A reasonable explanation for this observation could be that O_2 facilitates in the solubility of **2.4** at higher H_2O concentrations, resulting in a complete mass balance.

In terms of the effect of H_2O content on reaction selectivity, it was shown that by using 180 mM of H_2O in the system, the selectivity for **2.4** was enhanced by 6% (at 90 minutes) compared to using 2 mM of H_2O (Figure 2.12).

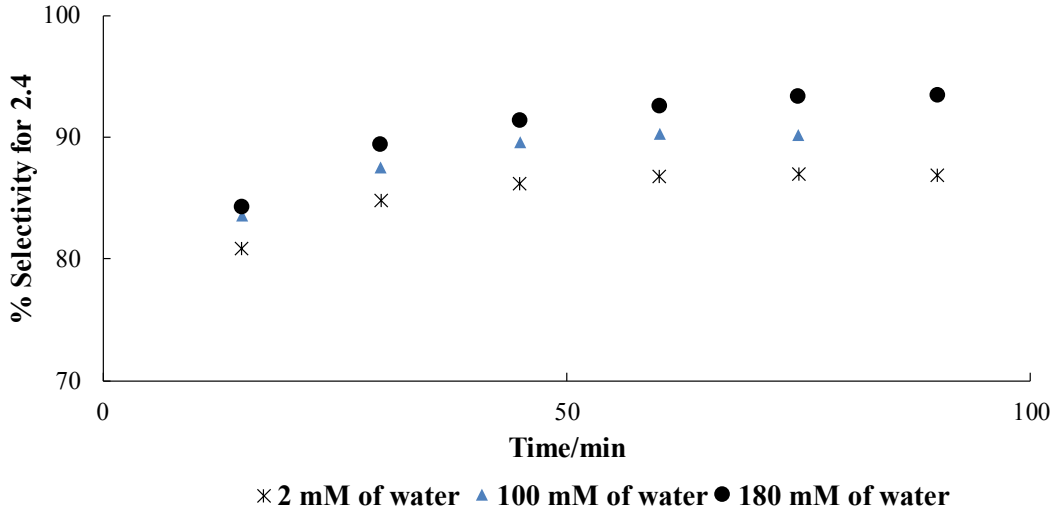


FIGURE 2.12. *Graph showing the % Selectivity for **2.4**, demonstrating the effect of different initial H_2O concentrations in 2-methyl-2-butanol under aerobic conditions.*

This is the same effect witnessed when reactions were performed under N_2 (Figure 2.8), where it was shown that H_2O is able to act as a reductant. However, there are differences in the magnitude of the influence of H_2O between reactions performed under air and N_2. Firstly, the effect of H_2O acting as a reductant was more prominent with reactions performed under air, compared to reactions performed under N_2 (Table 2.4, entry 1 vs. entry 2). There was a higher difference in the % selectivity for **2.4** between using 2 mM and 180 mM of H_2O for experiments performed under air compared to reactions conducted under N_2 (Table 2.4, entry 1 vs. entry 2).

TABLE 2.4. *Differences in the % Selectivity for* ***2.4*** *between experiments using 2 mM and 180 mM of H_2O, performed under air and N_2.*

Entry	Reaction atm.	% Selectivity for 2.4 (2 mM of H_2O)	% Selectivity for 2.4 (180 mM of H_2O)	Difference between 2 mM and 180 mM of H_2O (%)
1	Under air [a]	87	93	6
2	Under N_2 [b]	97	99	2

[a] *at 90 min,* [b] *at 85 min.*

Secondly, the selectivity for **2.4** was significantly lower over the course of the reaction when employing aerobic conditions, compared to reactions using the same H_2O concentration (2 mM) but under N_2 (Table 2.4, entry 1 vs. entry 2 and Figure 2.13).

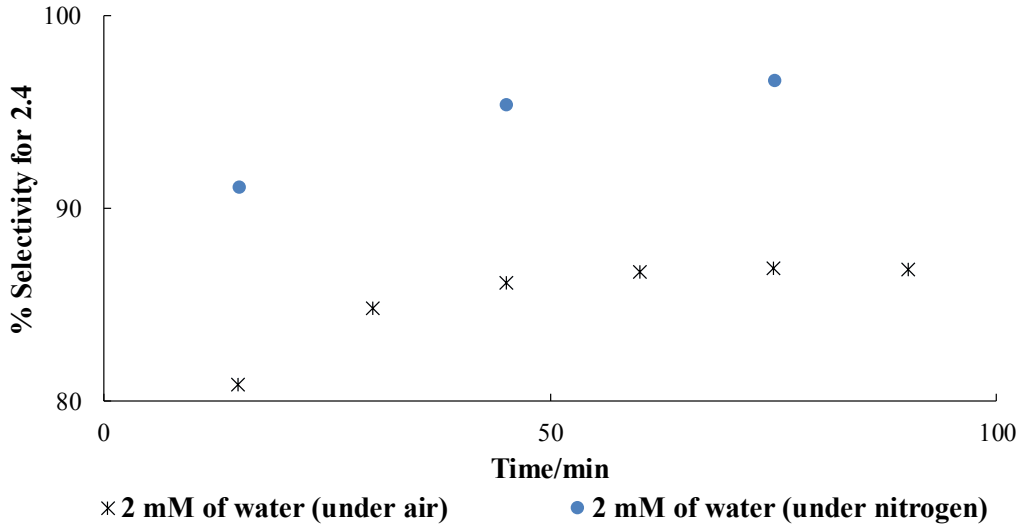
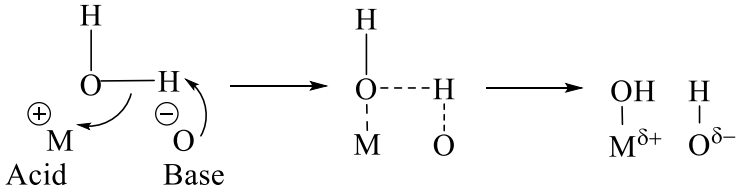


FIGURE 2.13. *Graph showing the differences in % Selectivity for* ***2.4*** *over the course of reactions performed under air and N_2 (using 2 mM of H_2O).*

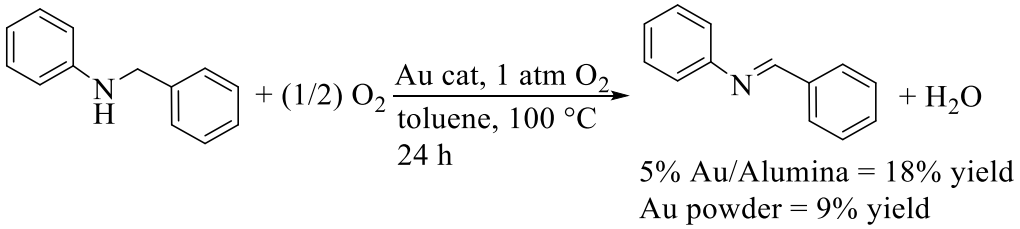
To clarify, the overall selectivity for **2.4** was higher over the course of the reaction for experiments performed under N_2 compared to reactions conducted under air using the same H_2O concentrations. However, the ability of H_2O to function as a reductant when using high H_2O contents (>2 mM) was increased when air was present in the reaction mixture. This suggests that O_2 promotes the ability of H_2O to act as a reductant; however, at the same time it interferes with the overall reduction of **2.3** to **2.4** by oxidising **2.4** to **2.3**. An explanation for the increased ability of H_2O to act as a reductant under air, could be that adsorbed O_2 species aid in the dissociation of molecular H_2O into OH and H species, resulting in more surface hydrogen species available to reduce **2.3** to **2.4**. Indeed, it is known that on certain metals, such as Cu and Au, pre-adsorbed O_2 has a promotional effect in the cleavage of O-H H_2O

bonds.[89, 90] The concerted mechanism proposed in the study using Cu, which has also been proposed to occur on Au,[89, 90] proceeds such that Cu atoms act as Lewis acid sites and adsorbed O_2 species as Brönsted base sites for proton abstraction from H_2O (Scheme 2.8).



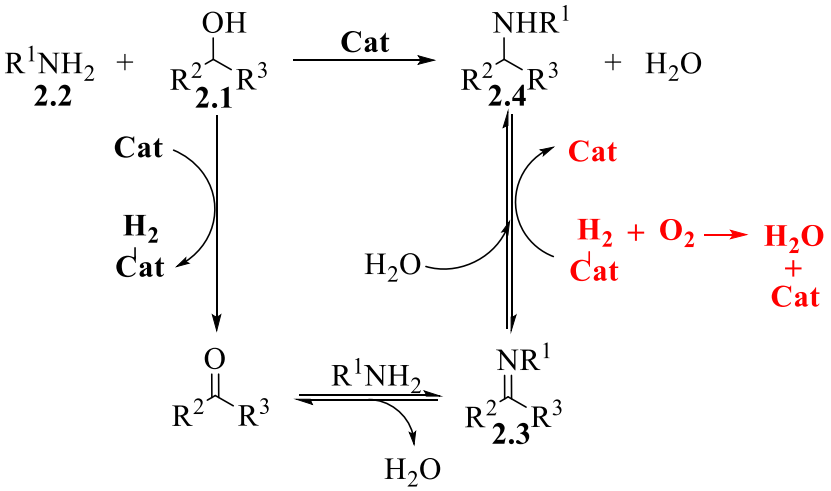
SCHEME 2.8. *Schematic for the dissociation of H_2O via an acid-base interaction.*[89]

In terms of the decrease in the overall selectivity to **2.4** when performing reactions under air, it has been demonstrated in the literature that by using an atmosphere of O_2, bulk Au powder and Au supported on alumina are active for the aerobic oxidative dehydrogenation of **2.4** to **2.3** (Scheme 2.9).[91] Therefore it would not be unreasonable to suggest that this reaction could have occurred in the experiments presented above.



SCHEME 2.9. *Au catalysed aerobic oxidation of N-phenylbenzylamine to the corresponding imine.*

Additionally, in the previous model,[77] the generation of **2.4** (reduction step) was presumed to be irreversible (Section 2.1). If this step was reversible under the conditions used in these studies, it can be hypothesised that the surface hydrides formed on generating **2.3** from **2.4** could be removed by O_2 (Scheme 2.10), thus making them inaccessible for the reduction of **2.3** and leading to lower selectivity for **2.4**.

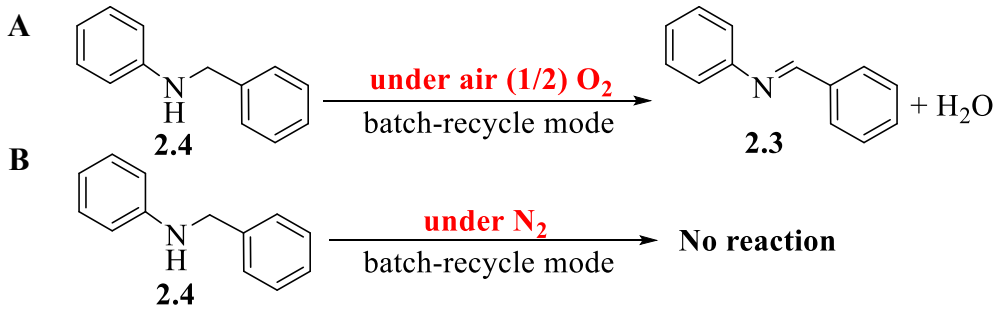


SCHEME 2.10. *Hydrogen borrowing scheme showing the removal of surface hydrides by O_2 to generate H_2O.*

To interrogate whether O_2 interferes in the formation of **2.4**, the following experiments were devised:

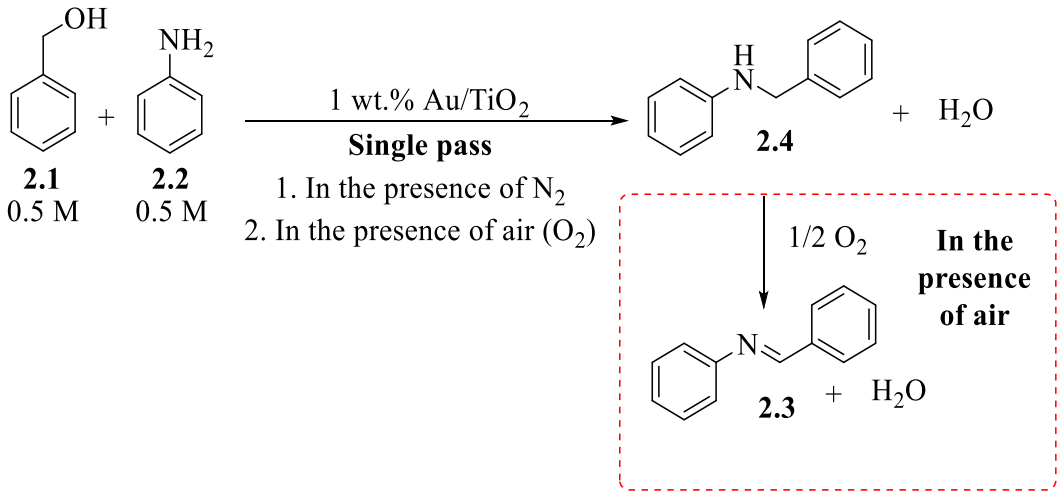
1. **2.4** (0.5 M) in 2-methyl-2-butanol (2 mM of H_2O) in the presence of O_2
2. **2.4** (0.5 M) in 2-methyl-2-butanol (2 mM of H_2O) in the absence of O_2 (reaction mixture purged with N_2)

The solutions were passed over Au/TiO_2 (0.8 mol%) in batch-recycle mode at 1.5 mL min^{-1}, 180 ˚C and 50 bar for 3 hours. It was predicted that if O_2 is able to oxidise **2.4** to **2.3** and/or if O_2 removes hydride species from the catalyst surface, **2.3** will be detected in the reaction performed in the presence of O_2 (Scheme 2.11 A), while under inert conditions **2.4** will remain unreacted (Scheme 2.11 B). If **2.3** is formed, the generation of PhCHO and **2.2** is also anticipated.



SCHEME 2.11. *Experiments to assess whether O_2 is able to oxidise **2.4** in batch-recycle mode.*

In addition to these experiments, single pass reactions (Scheme 1.18) were designed starting with **2.1** and **2.2** (0.5 M) under air and N_2 at 180 ˚C, 50 bar and 0.2 mL min^{-1} (Scheme 2.12). By operating the reactor in this manner, the amine product (**2.4**) formed is not recycled through the catalyst cartridge. Thus any interferences of O_2, i.e. whether it acts to remove surface hydride species and/or oxidises **2.4** to **2.3** may be avoided.



SCHEME 2.12. *Experiments to assess whether O_2 interferes with the reduction step (**2.3** to **2.4**) in single pass mode.*

As expected, the batch-recycle experiments showed an increasing conversion of **2.4** (12% at 180 min) and formation to **2.3** over time when passing **2.4** over Au/TiO_2 under aerobic conditions (Figure 2.14 A and B). This is in contrast to the same experiment conducted under inert conditions, which afforded 1% of **2.4** at 180 minutes. **2.4** was converted to **2.3**, with **2.2** and PhCHO also being detected in the reaction conducted in air (5% and 3% formed, respectively at 180 minutes). The results demonstrate that O_2 is able to oxidise **2.4** to **2.3**. Additionally, it highlights the reversibility of the formation of **2.4** as small amounts of **2.3**, PhCHO and **2.2** were generated when passing **2.4** over Au/TiO_2 under inert conditions. Therefore, it was confirmed that O_2 might be acting to remove surface hydride species upon the reversible formation of **2.3** from **2.4**, as well as oxidising **2.4** to **2.3**.

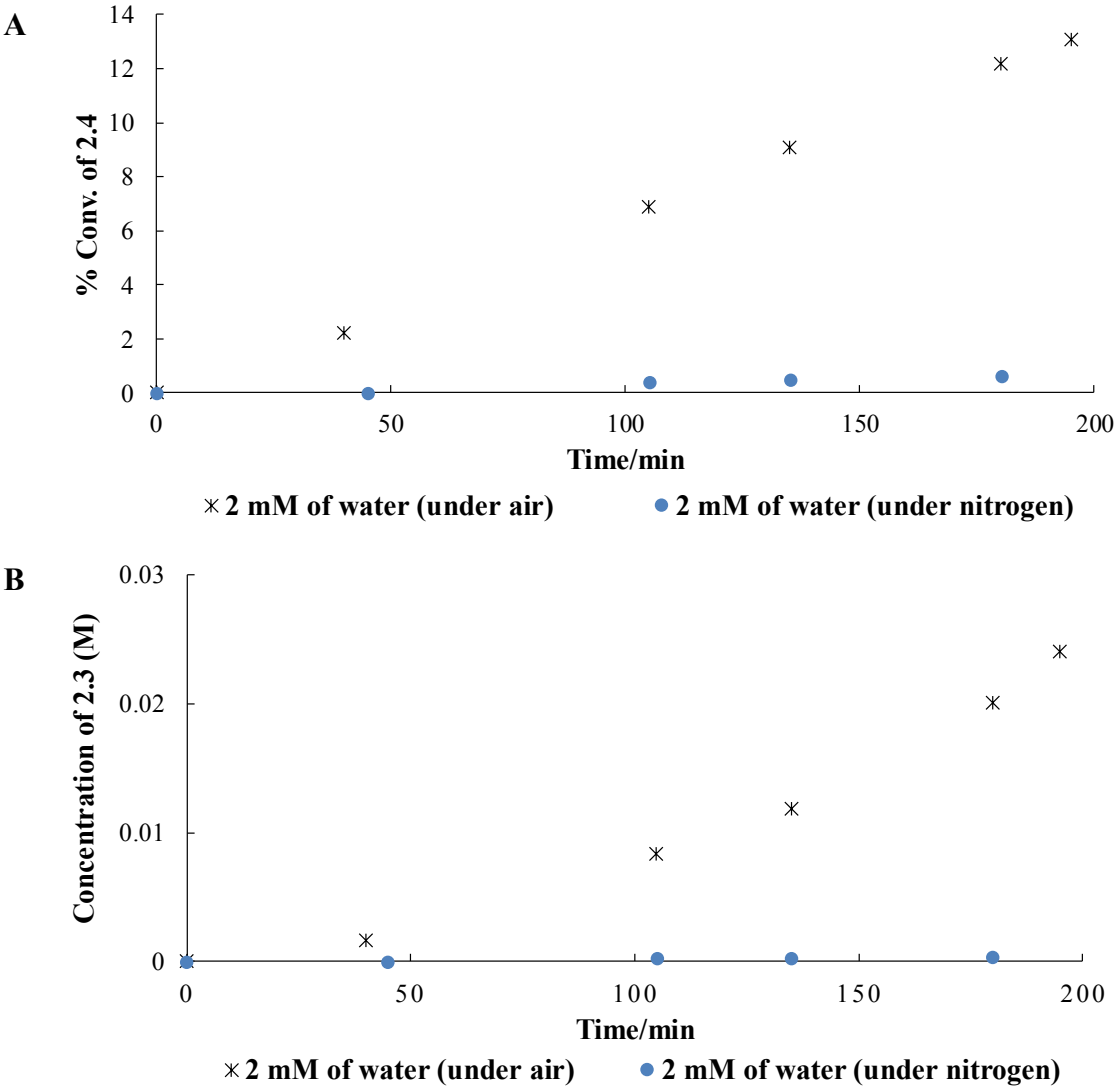


FIGURE 2.14. *Graphs showing that under aerobic conditions* ***2.4*** *is converted to* ***2.3****,* ***A)*** *% Conversion of* ***2.4*** *and* ***B)*** *Formation of* ***2.3*** *(M) over time.*

Notably, the selectivity for **2.4** remained unaltered when O_2 was introduced into the system in single pass mode. This can be seen by comparing the selectivity of reactions performed under N_2 and aerobic conditions using this experimental set-up (Figure 2.15). This result supports the proposal that it is the recycling of **2.4** through Au/TiO_2 in the presence of O_2 that leads to the decrease in overall selectivity (due to removal of surface hydride species and/or oxidation of **2.4**). In single pass mode, O_2 does not have an effect on the selectivity because **2.4** does not re-enter the reaction space.

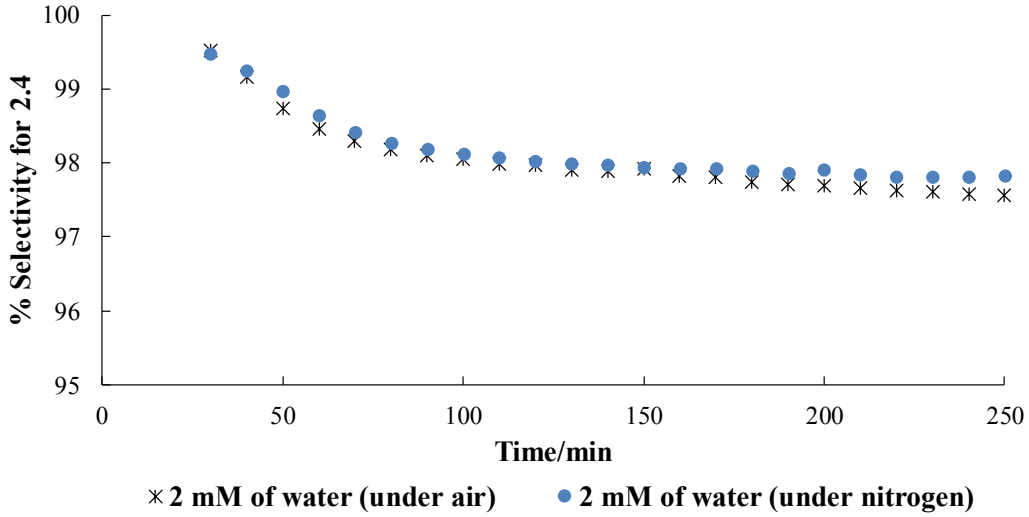


FIGURE 2.15. *Time-on-line profile showing the % Selectivity for* ***2.4*** *under air and N_2 using 2-methyl-2-butanol.*

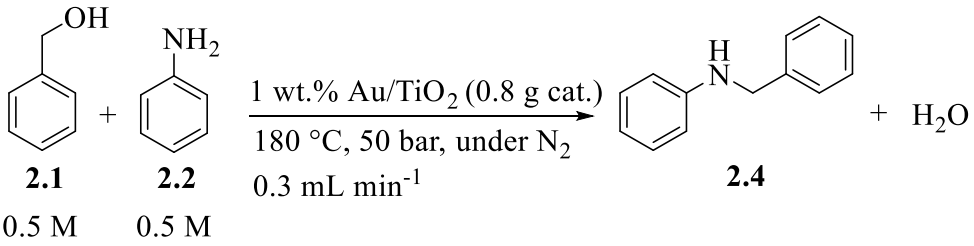
In summary, the following key observations and conclusions have been made:

- In contrast to experiments performed under N_2, there was no effect on the detection of **2.4** upon increasing the H_2O content in the reaction. However the selectivity for **2.4** was increased with H_2O concentrations higher than 2 mM due to H_2O acting as a reductant.
  Under inert conditions it was hypothesised molecular H_2O serves to precipitate and/or form an emulsion with ***2.4*** *at high moisture levels. Under air, it can be suggested that O_2 facilitates in the solubility of* ***2.4****, thus no apparent effect of increased H_2O concentration is detected.*
- The ability of H_2O to act as a reductant was more prominent when reactions were performed under air, compared to reactions performed under N_2.
  In the presence of O_2, if H_2O dissociation is increased, it follows that there will be more surface hydrogen species available to reduce ***2.3*** *to* ***2.4*** *compared to reactions performed under N_2.*
- The overall selectivity for **2.4** was significantly lower over the course of the reaction, when aerobic conditions were employed in batch-recycle mode, compared to reactions using the same H_2O concentration (2 mM) under N_2.
  O_2 interferes with the reduction of ***2.3*** *to* ***2.4*** *most likely due to oxidation of* ***2.4*** *to* ***2.3*** *and/or the removal of surface hydride species. By performing reactions in single pass mode, this can be avoided as* ***2.4*** *is not recycled through the catalyst bed.*

2.4 Results of the Au/TiO_2 deactivation and stability studies

Four different time-on-line single pass experiments (Scheme 1.18) were performed to investigate the stability and possible deactivation routes of Au/TiO_2 (Strem AUROlite^{TM}) using dry 2-methyl-2-butanol as the solvent (2 mM of H_2O). The first reaction was performed using **2.1** and **2.2** as model reagents. This experiment enables the stability of the catalyst to be assessed over time, and allows for comparisons against experiments where products and/or intermediates are introduced into the reaction. More specifically, in the following three studies, the amination of **2.2** with **2.1** was conducted and after 2 hours, intermediate or product (**2.3**, **2.4** or H_2O) was introduced into the reaction vessel (Scheme 2.13).

16 mM of **2.3**, **2.4** or H_2O were introduced into the reaction vessel after 2 hours



SCHEME 2.13. *Reaction parameters used for interrogating the stability of Au/TiO_2 and the possible deactivation modes.*

The concentration of **2.1** was monitored over the course of ~10 hours to study whether the introduction of the species into the mixture had an adverse effect on catalytic activity. If species are involved in deactivating Au/TiO_2, perhaps via blocking active sites, a decrease in the conversion of **2.1** is expected, which correlates to a decrease in activity. Note that the characterisation of Au/TiO_2 was presented in Section 2.2.

2.3, **2.4** and H_2O are known products and intermediates in the alkylation of **2.2** with **2.1**, therefore analysing the effects that an excess of these components have on activity is essential. It has been demonstrated that increased H_2O concentrations in 2-methyl-2-butanol (>2 mM) results in the loss of **2.4** (Section 2.3.1), however it is not known whether it also functions to deactivate Au/TiO_2. PhCHO is a known intermediate in the AAA reaction; however, introduction of this species into a vessel containing **2.2** will result in generation of **2.3** and H_2O through a condensation reaction.

Species were introduced in concentrations of 16 mM, as this was the approximate concentration calculated, based on the dimensions of **2.1**, to produce a monolayer over Au/TiO_2 (Full details can be found in Chapter 7). As higher residence times increase the

amount of intermediates and products being formed, a flow rate that allowed for low conversions of **2.1** ~30% (0.3 mL min^{-1}) was used. This is because if all of the reaction species are involved in deactivating the catalyst, it makes it difficult to isolate deactivation induced by species that are introduced into the reaction.

The time-on-line profile for the alkylation of **2.2** with **2.1**, without the introduction of products or intermediates into the vessel, is presented below (Figure 2.16). Note that the increase in concentration of **2.1** at 40 minutes (breakthrough) is due to the time taken for substrates and products to flow through the internal volume of the reactor (~4 mL). The concentration of **2.1** remains reasonably steady with minor deactivation observed over the course of the reaction. A slow deactivation rate of 7 x 10^{-5} M min^{-1} was calculated, by linear regression of the concentration over the reaction time, confirming the excellent lifetime characteristics of Au/TiO_2.

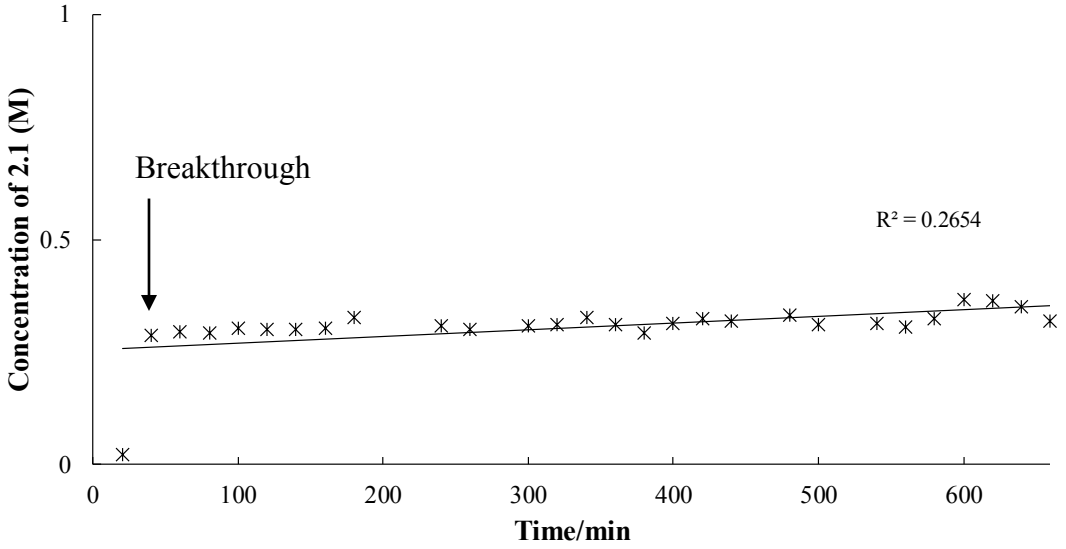


FIGURE 2.16. *Time-on-line profile showing the alkylation of* ***2.2*** *with* ***2.1*** *using Au/TiO_2 in 2-methyl-2-butanol.*

ICP and TEM analysis was conducted on the catalyst following this reaction. The results revealed that the Au loading remained unaltered (1 wt.% Au) and an increase of ~2 nm in Au particle size occurred (from 3 to 5 nm). The increase in particle size could be the cause for the gradual catalyst degradation, as small particles are known to be more active in the AAA reaction,[73] but to eliminate deactivation from products and/or intermediates, the experiments presented below were conducted.

There was no difference in the rate of deactivation when amine product (**2.4**) was introduced in the reaction vessel. This can be observed by comparing the profile for the

experiment shown in Figure 2.16, where no products or intermediates have been introduced into the reaction, against the same reaction where **2.4** has been added in the mixture after 2 hours (Figure 2.17)

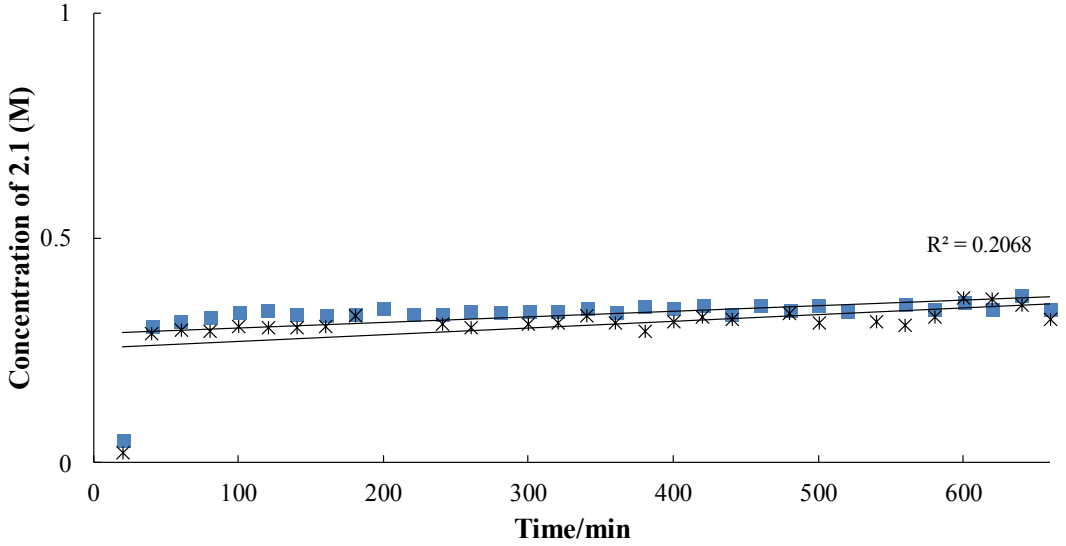


FIGURE 2.17. *Time-on-line profile showing the alkylation of **2.2** with **2.1** using Au/TiO_2 in 2-methyl-2-butanol.* ✳ *= no intermediate or product introduction,* ■ *= introduction of **2.4**.*

Similarly, there was no difference in the concentration of **2.1** or the rate of catalyst deactivation in the presence of H_2O (Figure 2.18).

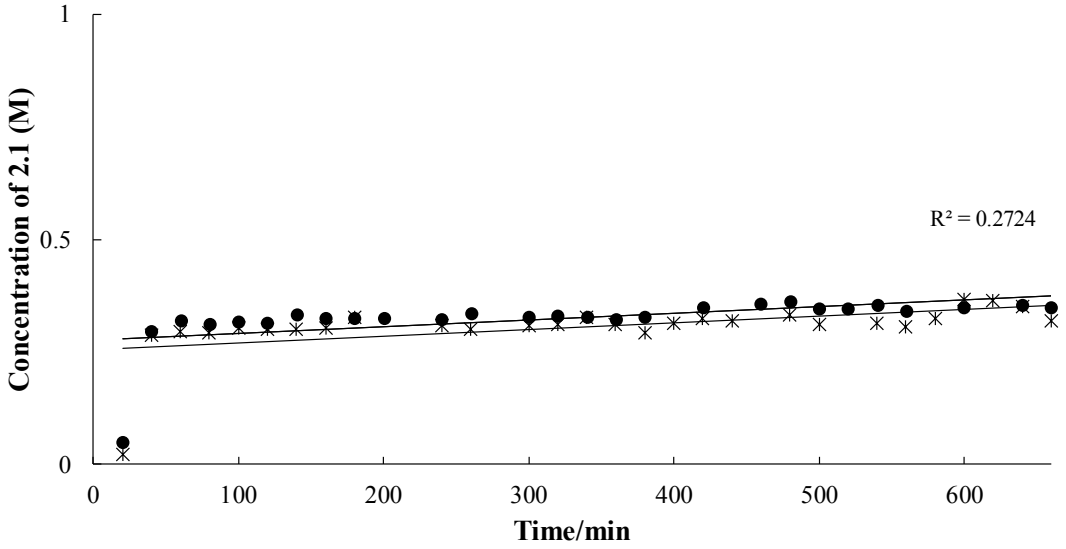


FIGURE 2.18. *Time-on-line profile showing the alkylation of **2.2** with **2.1** using Au/TiO_2 in 2-methyl-2-butanol.* ✳ *= no intermediate or product introduction,* ● *= introduction of H_2O.*

Employing high H_2O concentrations in 2-methyl-2-butanol (>2 mM), resulted in incomplete mass balances for the alkylation of **2.2** with **2.1** in batch-recycle mode (Section 2.3.1). In this experiment, a complete mass balance was achieved and the concentration of **2.4** remained constant over time (Figure 2.19).

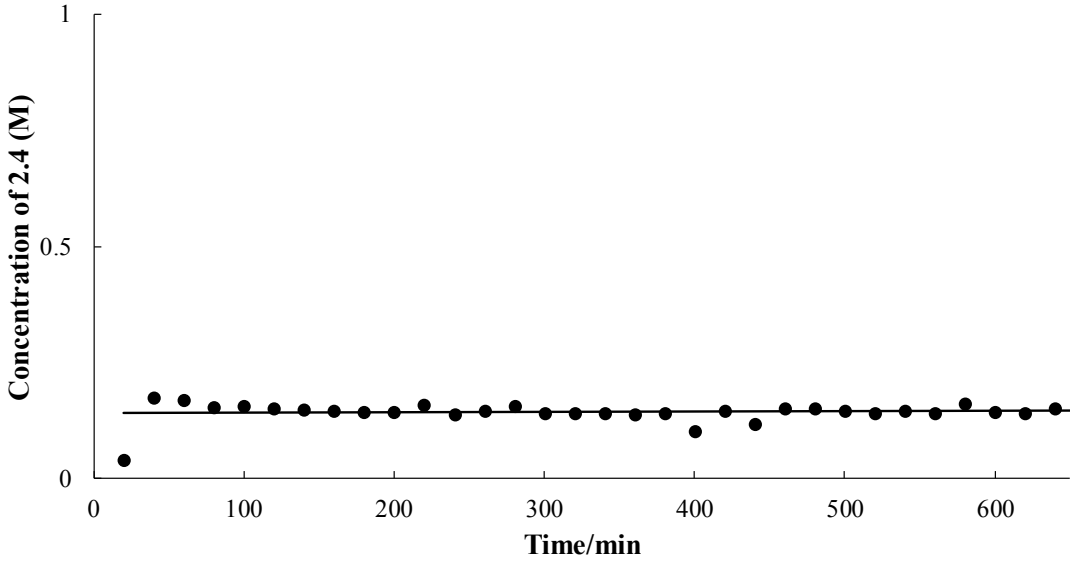


FIGURE 2.19. *Time-on-line profile showing the concentration of **2.4** following the introduction of H_2O into the reaction mixture after 2 hours.*

This could be due to the fact that in batch-recycle mode, the reaction mixture has the opportunity to cool in the reaction reservoir (held at room temperature) before being re-introduced into the catalyst cartridge, whereas in single pass mode the mixture is consistently heated. The drop in temperature may have induced precipitation of **2.4**; indeed the reaction mixture did turn cloudy in appearance after exiting the reactor in the batch-recycle experiments.

The introduction of **2.3** had no effect on the alkylation of **2.1** with **2.2** (Figure 2.20). It has been proposed in the literature that deposits of imine over catalytic sites results in the deactivation of Au/ZrO_2 during the amination of myrtenol.[80] However, these studies cannot be fairly compared because a different support and reaction substrates (myrtenol and **2.2**) were employed.

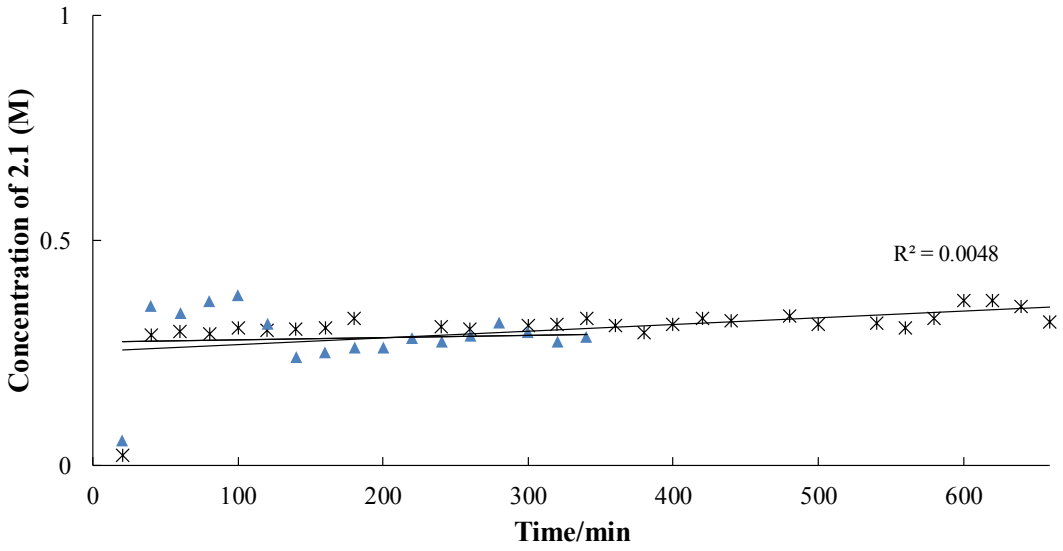


FIGURE 2.20. *Time-on-line profile showing the alkylation of* ***2.2*** *with* ***2.1*** *using Au/TiO_2 in 2-methyl-2-butanol.* ✳ *= no intermediate or product introduction,* ▲ *= introduction of* ***2.3****.*

Overall, the results suggest that **2.4**, **2.3** and H_2O do not deactivate Au/TiO_2 in single pass mode and that the minor and gradual loss of activity observed is most likely due to increases in Au particle size.

2.5 Conclusion

In summary, the results demonstrate that the careful control of reaction conditions during the AAA reaction is necessary for achieving good yields of the amine product. It was shown that H_2O, O_2 and even the way the reaction is performed (single pass vs. batch-recycle) can affect the selectivity and conversion of the reaction. It was hypothesised that high H_2O contents, when employing 2-methyl-2-butanol as a solvent, may induce precipitation of **2.4** and/or formation of an emulsion, causing incomplete mass balances. In order to fully elucidate this, further experiments are required to investigate the solubility of **2.4** in H_2O/2-methyl-2-butanol mixtures.

Even though H_2O is detrimental for the solubility of **2.4**, it is able to function as a reductant in the reaction when present in large amounts (45, 180 and 200 mM), presumably through hydrogen species generated by the dissociation of H_2O. Although the effect of this was small under inert conditions (2% increase in the selectivity for **2.4** by using initial H_2O concentrations of 200 mM instead of 2 mM), by using aerobic conditions the ability of H_2O to act as reductant was increased, which was attributed to O_2 facilitating in the dissociation of H_2O.

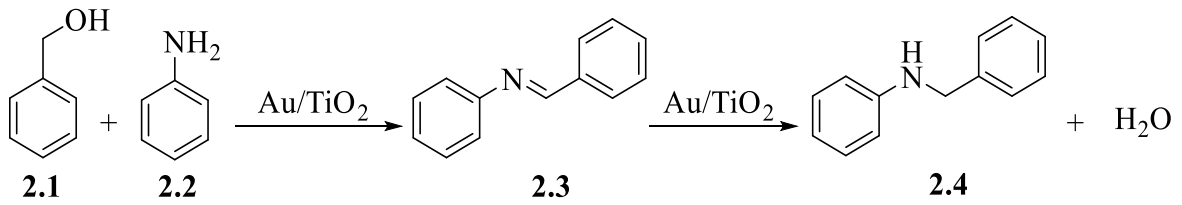
O_2 was also shown to have a secondary effect on reactions in batch-recycle mode. The overall selectivities for **2.4** were lower in the presence of O_2 compared to reactions performed under anaerobic conditions. This was attributed to O_2 interfering in the reduction step (**2.3** to **2.4**), presumably by removing surface hydride species and/or oxidising **2.4** to **2.3**. However, by operating the reactor in single pass mode, the selectivity for **2.4** remained unaffected in the presence of O_2.

Au/TiO_2 displayed very good stability over the course of the reaction between **2.1** and **2.2** in single pass mode, showing a slow deactivation rate over time. The gradual decrease in activity over time was attributed to increases in Au particle size, as there was no effect on catalytic activity when introducing reaction intermediates and product into the system.

Overall, the observations are crucial as they have not only allowed for a better insight into the mechanism, but they have also provided a basis for designing experiments in terms of optimising product selectivity and yields. The concepts learnt can be incorporated into an existing kinetic model, to allow a predictive model to be formed (Chapter 3).

CHAPTER 3. The development of a kinetic model for the AAA reaction

The objective of this Chapter is to develop a kinetic model using Berkeley Madonna software™ (Section 3.1) to describe the reaction profiles of the Au/TiO_2 catalysed alkylation of **2.2** with **2.1** (Scheme 3.1).



SCHEME 3.1. *The alkylation of **2.2** with **2.1** catalysed by Au/TiO_2.*

Preliminary kinetic and mechanistic models for the amination of **2.2** with **2.1** had been previously produced using toluene as a solvent (described in Chapter 2).[77] In this project, the kinetic model was developed further, using data obtained from reactions performed in 2-methyl-2-butanol under N_2 (Chapter 2). It was hoped that a predictive model could be produced that may be used in the design of future experiments to yield the best selectivity and conversion possible.

The summary below gives a background of the key steps from the previously reported kinetic model compared to relevant literature and the main conclusions derived from the mechanistic studies from the work described in Chapter 2.

3.1 Background

There are very few reports of kinetic models for the AAA reaction using heterogeneous catalysts. Since the paper describing the kinetic and mechanistic model (described in Chapter 2),[77] to the best of our knowledge, there has only been one other kinetic model reported using a Au-based heterogeneous catalyst. Au/ZrO_2 was employed for the amination of myrtenol (a natural terpene alcohol) with aniline (**2**).[80] The details of this work and the key steps from the previously derived kinetic model (Figure 3.1) are discussed below.

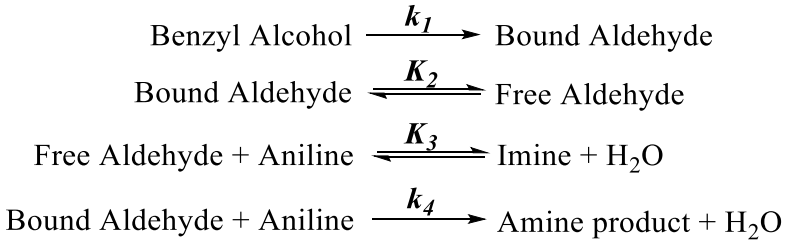


FIGURE 3.1. *Our previously reported kinetic model.*

***k_1*:** k_1 describes the irreversible formation of bound aldehyde species to the catalyst surface. This step was shown to be the slowest step of the catalytic cycle with a value of 4.5×10^{-4} s^{-1} at 180 ˚C.

K_2*•*K_3: The formation of imine (**2.3**) from the condensation of amine (**2.2**) with free aldehyde (generated from desorption of bound aldehyde) is represented by the combination of the two equilibrium constants, K_2 and K_3. Bound and free aldehyde terms were required in the kinetic model as it was demonstrated that, at low temperatures (130 ˚C), the formation of **2.3** steadily increases during the reaction. However, by using higher temperatures (150 and 180 ˚C) the formation of **2.3** becomes an intermediate process, i.e. the concentration increases initially but then decreases subsequently. Thus an equilibrium term was required to account for the free aldehyde species re-entering the catalytic cycle. An equilibrium constant of 1.5 was found for this step at 180 ˚C.

***k_4*:** k_4 describes the rate for the formation of **2.4** and H_2O from the condensation of bound aldehyde species with **2.2** (5.7×10^{-2} $M^{-1}s^{-1}$ at 180 ˚C). This incorporates more than one transformation (formation of imine from the bound aldehyde and its reduction to amine). The high selectivity for **2.4** (97%) was attributed to the high temperature and large reaction space afforded by adopting a flow reactor.

The same assumption that only bound aldehyde species generate the amine product was also made in the Au/ZrO_2 catalysed reaction of myrtenol with **2.2**.[80] The following kinetic and mechanistic model was formulated using the key steps outlined in the paper (Figure 3.2 and Scheme 3.2). The model also accounted for the adsorption of substrates and products to the catalyst surface (alcohol, amine, aldehyde, imine and amine product). However, it also includes a hemiaminal intermediate, which was proposed to be the species that undergoes hydrogen transfer (as opposed to the imine).

$$\text{Alcohol} \xrightarrow{k_1} \text{Bound Aldehyde} + \text{Bound } H_2$$

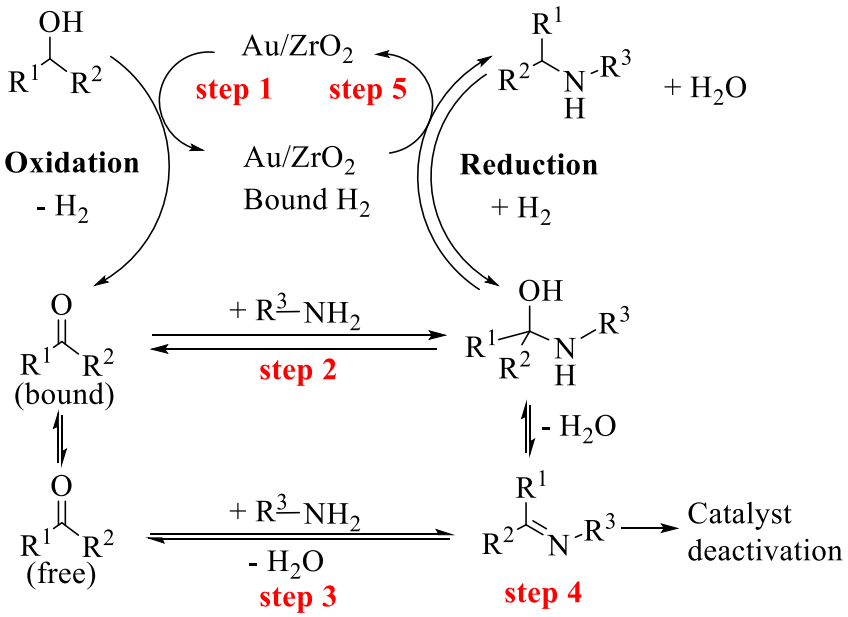
$$\text{Bound Aldehyde} + \text{Bound Amine} \xrightarrow{k_2} \text{Hemiaminal}$$

$$\text{Bound Aldehyde} \underset{}{\overset{K_3}{\rightleftharpoons}} \text{Free Aldehdye}$$

$$\text{Free Aldehyde} + \text{Amine} \underset{}{\overset{K_4}{\rightleftharpoons}} \text{Imine} + H_2O$$

$$\text{Hemiaminal} + \text{Bound } H_2 \xrightarrow{k_5} \text{Amine product} + H_2O$$

FIGURE 3.2. *Kinetic model for the amination of myrtenol with* ***2.2*** *using* Au/ZrO_2.



Step 1: Alcohol is oxidised to form bound aldehyde and hydride species.

Step 2: Bound aldehyde reacts with bound amine to produce hemiaminal.

Step 3: Free aldehyde reacts with amine to produce imine and H_2O.

Step 4: Imine can react with active sites and H_2O to produce hemiaminal.

Step 5: Hemiaminal undergoes hydrogen transfer, using the adsorbed hydride species, to form the amine product and H_2O. The amine product can be liberated from the catalyst to regenerate free active sites.

SCHEME 3.2. *Keys steps of the mechanistic and kinetic cycle for the amination of myrtenol with* ***2.2****.*

Similar to the previous study, the formation of bound aldehyde species from the oxidation of alcohol was postulated to be an irreversible process and the calculated rate for its formation was one of the slowest steps in the reaction (k_1) (7.4 x 10^{-2} s^{-1} at 180 ˚C). The activation energy for this transformation was comparable to that derived in the former study, with values of 87.7 and 93.7 kJ mol^{-1}, respectively.[77] The equilibrium constants K_3 and K_4 were combined to give an overall value of 9.5 x 10^3 M^{-1}, which describes the formation of imine from desorbed aldehyde. This is two orders of magnitude larger than the previously calculated values, where the equilibrium value for the formation of imine (K_2•K_3) was shown to be 1.5 at 180 ˚C. Additionally, it was demonstrated that imine acts to irreversibly deactivate Au/ZrO_2, through polymerisation on active catalyst sites. However, in this study the addition

of imine had no effect on the activity of Au/TiO_2 (Chapter 2). Thus these deactivation terms were not considered in the model.

The key findings from the mechanistic studies using Au/TiO_2 in 2-methyl-2-butanol under N_2 (detailed in Chapter 2) are highlighted below:

1. **H_2O is able to act as a reductant:**
   It was shown that the selectivity for **2.4** was slightly enhanced by 2% when using high H_2O concentrations (200 mM) in the solvent compared to using lower amounts (2 mM). This enhancement was attributed to H_2O acting as a reductant, presumably through dissociated H_2O species. As this effect was minimal, a term to account for it in the model was not essential.
2. **High H_2O concentrations in the solvent induces precipitation of 2.4:**
   It was shown that in the presence of high H_2O content (45, 180 and 200 mM), the mass balances for reactions was incomplete due to a deficiency of the amine product. However, the rate of disappearance of **2.1** remained consistent for these reactions. The decreased detection of amine product was assigned to the precipitation of **2.4** and/or the formation of an emulsion with H_2O, with the species becoming captured elsewhere in the system.

Berkeley Madonna™ software was used to model and analyse the reaction data working by numerically solving differential equations. Berkeley Madonna uses mathematical equations to model complex systems to:

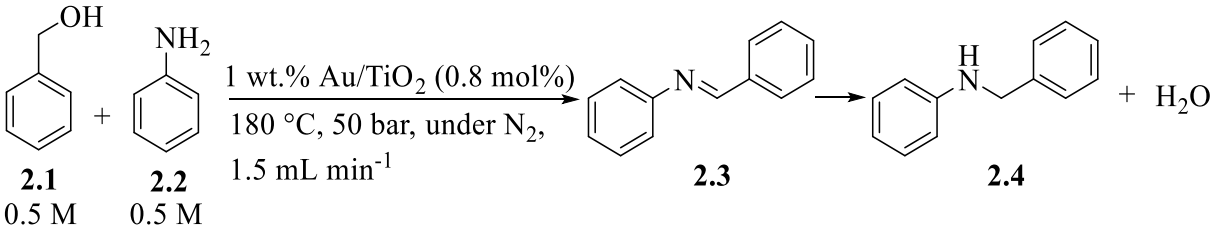
- Allow for the prediction of reaction profiles of future experiments.
- Support in the explanation of reaction results.
- Support in the understanding of the reaction mechanism.

The software is able to generate reaction models by applying the appropriate rate law and formulating kinetic equations following the manual input of proposed reaction steps. Once reaction data has been entered, the values of one or more parameters can be automatically found through a curve-fitting feature. This works to minimise the deviation between the models output and experimental data and allows for the simulation of reaction data, which can be viewed in graphical form.

3.2 Kinetic modelling of reaction data

The concentration-time profiles for experiments conducted with 2, 45, 180 and 200 mM of H_2O in 2-methyl-2-butanol were subjected to data modelling (Table 3.1). Although, 0.5 M of **2.1** and **2.2** were initially present in the reaction vessel, on starting the experiments, the internal volume of solvent present in the reactor (~4 mL) diluted the reaction mixtures to 0.4 M upon entering the reservoir.

TABLE 3.1. *Reactions modelled in this study showing the reaction conditions, mass balances and the rate of* ***2.1*** *disappearance.*



Entry	Solvent H_2O concentration (mM)	Mass balance (%)	d[1]/dt (M s^{-1})[a]
1	2	100	-1.3 x 10^{-3}
2	45	81	-1.3 x 10^{-3}
3	180	78	-1.4 x 10^{-3}
4	200	67	-1.2 x 10^{-3}

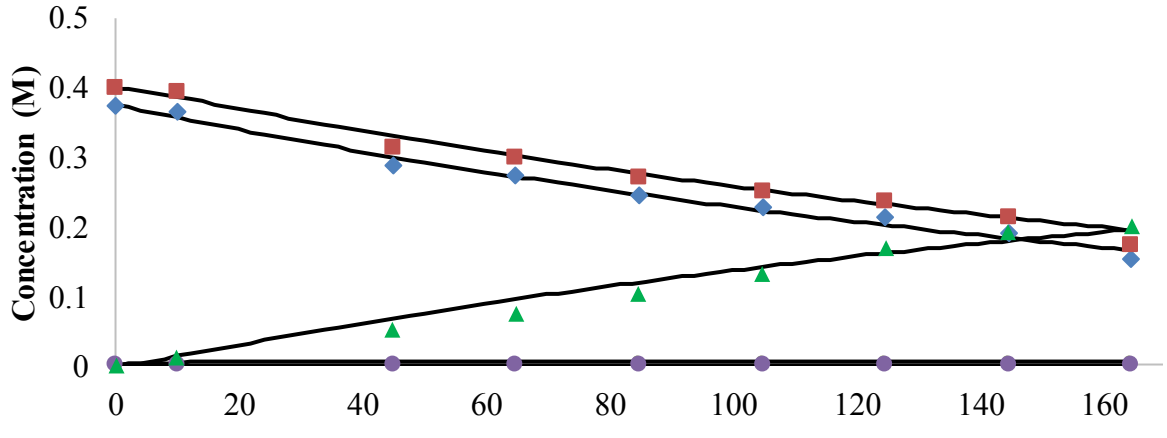
[a] *Conversion rate of* ***2.1*** *(M s^{-1}), calculated by linear regression of the concentration of* ***2.1*** *over the reaction time.*

The previously derived kinetic equations (Figure 3.1) were used to determine whether good fits were achievable when the toluene solvent (used for the reported kinetic model) was replaced with 2-methyl-2-butanol. The initial concentrations of reactants **2.1**, **2.2** and H_2O present in 2-methyl-2-butanol were entered as fixed values for each experiment and the curve-fitting feature used to find values for the rate equations.

It is generally accepted that the formation of aldehyde is irreversible and is the rate-limiting step in the AAA reaction; [77, 80, 92] therefore only the forward rate was considered (k_1). Two equilibria K_2 and K_3 were included for the formation of free aldehyde and imine, based on previous models.[77, 80] The generation of **2.4** (reduction step) was presumed to be irreversible in the previous model. However, it was shown in this work that when passing **2.4** over Au/TiO_2 in the presence of O_2, **2.3** and correspondingly PhCHO and **2.2** were formed

(Chapter 2). This was presumed to be due to the oxidation of **2.4** by O_2 and it was hypothesised that if the formation of **2.4** was reversible, the surface hydrides formed on generating **2.3** from **2.4** could be removed by O_2 (Scheme 2.10), thus making them inaccessible for the reduction of **2.3**. When the same experiment was performed under N_2, only small amounts of **2.3**, **2.2** and PhCHO were detected (1% total over 180 minutes), likely due to the insufficient purging of the system, and/or residual O_2 left on the catalyst surface. Therefore, the formation of **2.4** (k_4) was deemed to be essentially irreversible under N_2.

A good correlation between experimental and simulated data was produced for the reaction performed with 2 mM of H_2O in the solvent (Figure 3.3). Similar to the previous study, k_1 was found to be the rate-determining step with a value of 5.0×10^{-3} s^{-1}. This is faster than the value derived from the previous model, 4.5×10^{-4} s^{-1}, using the same reaction temperature of 180 ˚C. A different solvent system was used in this work (2-methyl-2-butanol vs. toluene) which could explain this result. In contrast, the value for k_1 in this study was slower compared to the rate reported for the amination of **2.2** with myrtenol (7.4×10^{-2} s^{-1} at 180 ˚C).[80] This is most likely attributed to the different catalyst and reagents used (Au/TiO_2 vs. Au/ZrO_2) as well as the larger amount of catalyst employed (1.4 mol% vs. 0.8 mol%). A large equilibrium value was calculated for the formation of **2.3** from desorbed PhCHO ($K_2 \bullet K_3$) (6.8×10^7) and the rate of the hydrogenation step was roughly two orders of the magnitude faster than the dehydrogenation of alcohol (7.0×10^{-1} M^{-1} s^{-1} vs. 5.0 10^{-3} s^{-1}).

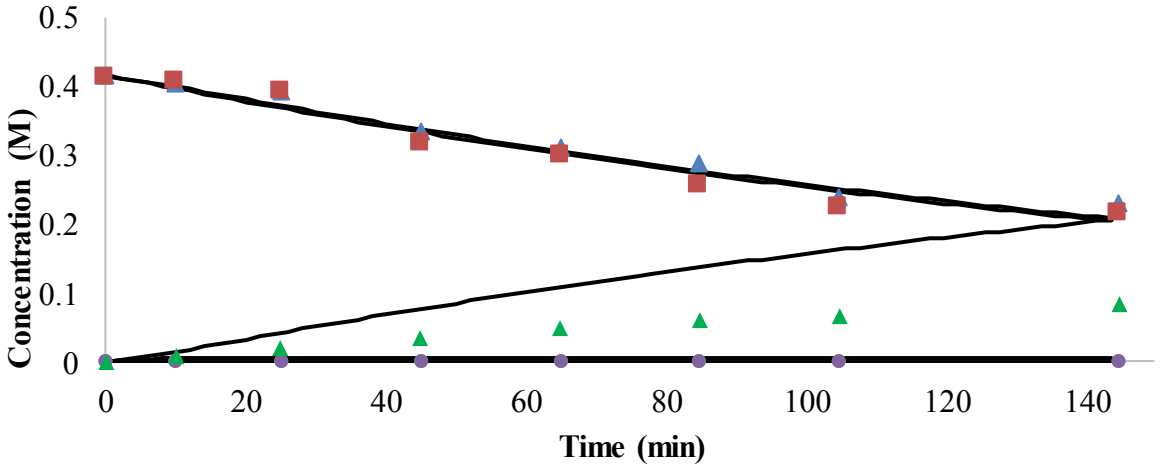


k_1/s^{-1}	$K_2 \bullet K_3$	$k_4/ M^{-1} s^{-1}$
5.0×10^{-3}	6.8×10^7	7.0×10^{-1}

FIGURE 3.3. *Simulated graph and derived kinetic parameters, Table 3.1, entry 1.* ***Legend:*** ♦*= benzyl alcohol* ***2.1****, (4 x10^{-8}),* ■ *= aniline* ***2.2****, (3 x10^{-8}),* ▲*= substituted amine* ***2.4****, (2 x10^{-3}),* ●*= imine* ***2.3****, (3 x10^{-3}),* ●*= PhCHO (2 x10^{-3}). Solid black lines= simulated reaction curves.*

The relative mean square (RMS) values for each reaction component are presented in the legend under the figure in parenthesis. This is a measure of the goodness-of-fit between the actual data and that predicted by the model and so gives an indication of how good the fits are. The closer the value is to 0, the smaller the error is. Overall, small error values were generated, however, errors were greater for products and intermediates (**2.3**, **2.4** and PhCHO). This can be ascribed to the involved equilibrium steps of these species. The model simulates reactions occurring at 180 ˚C in the reactor, but in practice, aliquots were taken from the vessel, which was held at room temperature. It is therefore reasonable to assume a difference in equilibrium constants for these steps, hence the larger error values associated with these components.

When the same rate and equilibrium constants were applied to experiments conducted with H_2O concentrations >2 mM (Table 3.1, entries 2-4), it was found that the model over predicted the formation of **2.4** (Figure 3.4, 180 mM of H_2O).



k_1/s^{-1}	$K_2 \bullet K_3$	$k_4/M^{-1}\ s^{-1}$
5.0×10^{-3}	6.8×10^{7}	7.0×10^{-1}

FIGURE 3.4. *Simulated graph and derived kinetic parameters, Table 3.1, entry 3.* ***Legend:*** ♦*= benzyl alcohol* ***2.1****, (4 x10^{-8}),* ■ *= aniline* ***2.2****, (2 x10^{-7}),* ▲*= substituted amine* ***2.4****, (2 x10^{-2})* ●*= imine* ***2.3****, (3 x10^{-2}),* ●*= PhCHO (2 x10^{-2}). Solid black lines= simulated reaction curves.*

The rate of disappearance of **2.1** was consistent for all experiments (Table 3.1, entries 1-4). However, the mass balances of reactions conducted with H_2O concentrations >2 mM were not complete (Table 3.1, entries 2-4), and the shortfall appeared to correlate with the amount

of H_2O present in the system. This was attributed to the precipitation of **2.4** with H_2O and/or the formation of an emulsion leading to decreases in its detection (Chapter 2). An additional term (k_5) was included in the model with its purpose to solely account for the loss of **2.4** (Figure 3.5). This step was considered to be reversible as the species may fall back into solution.

$$\text{Benzyl Alcohol} \xrightarrow{k_1} \text{Bound Aldehyde}$$

$$\text{Bound Aldehyde} \underset{}{\overset{K_2}{\rightleftharpoons}} \text{Free Aldehyde}$$

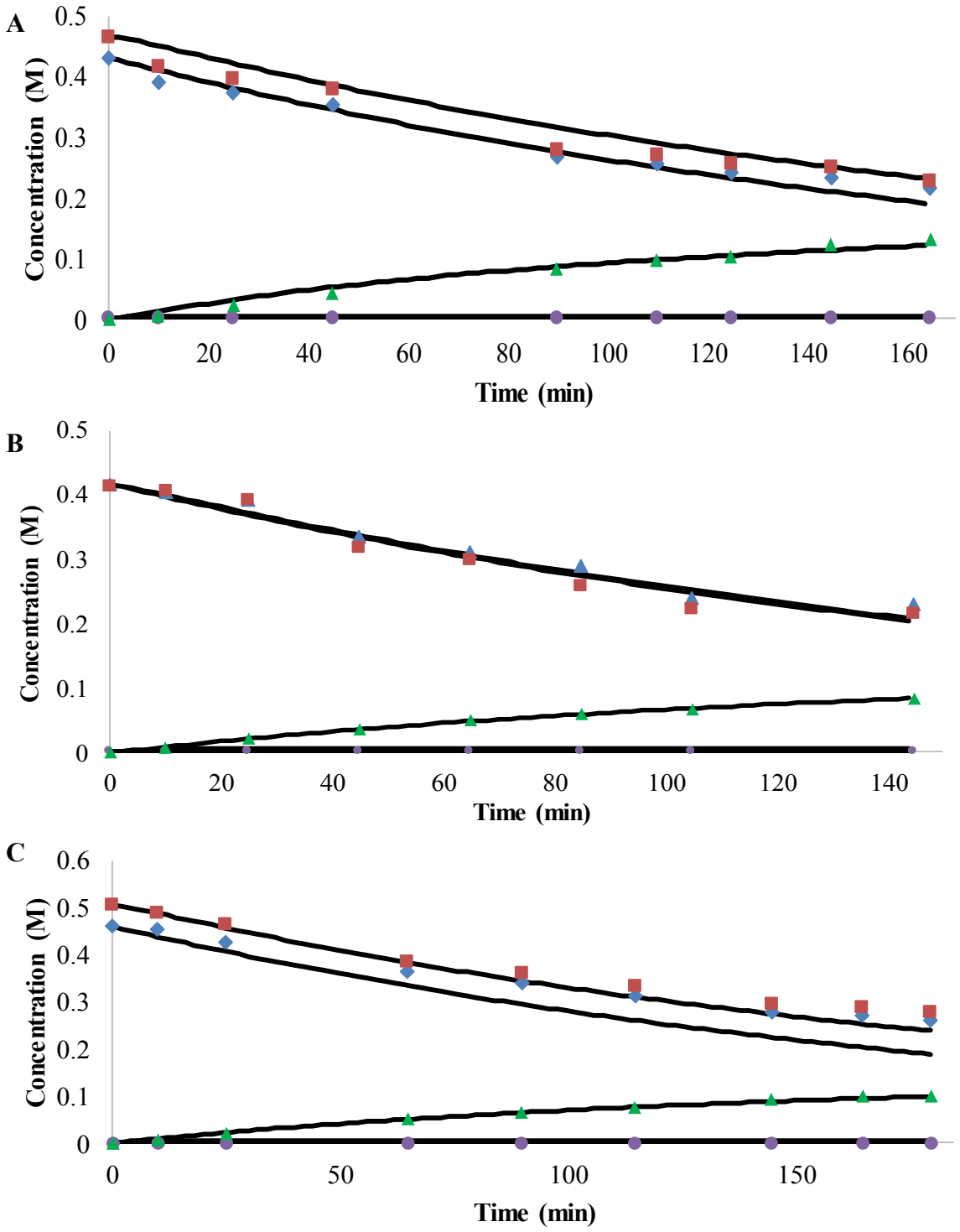
$$\text{Free Aldehyde} + \text{Aniline} \underset{}{\overset{K_3}{\rightleftharpoons}} \text{Imine} + H_2O$$

$$\text{Bound Aldehyde} + \text{Aniline} \xrightarrow{k_4} \text{Amine product} + H_2O$$

$$\text{Amine product} + H_2O \underset{}{\overset{k_5}{\rightleftharpoons}} \text{Precipitated Amine product}$$

FIGURE 3.5. *Derived kinetic equations with an additional term to account for the loss of* ***2.4****.*

The reactions employing 45, 180 and 200 mM of H_2O (Table 3.1, entries 2-4) were able to fit to this model by changing only the initial H_2O, **2.1** and **2.2** concentrations and keeping all other values constant (Figure 3.6 A-C). RMS values for these fits are presented in Table 3.2.



k_1/ s^{-1}	$K_2 \bullet K_3$	k_4/ M^{-1} s^{-1}	k_5/ M^{-1} s^{-1}	
5.0×10^{-3}	6.8×10^{7}	7.0×10^{-1}	$k_f = 4.6$	$k_r = 8.0 \times 10^{-1}$

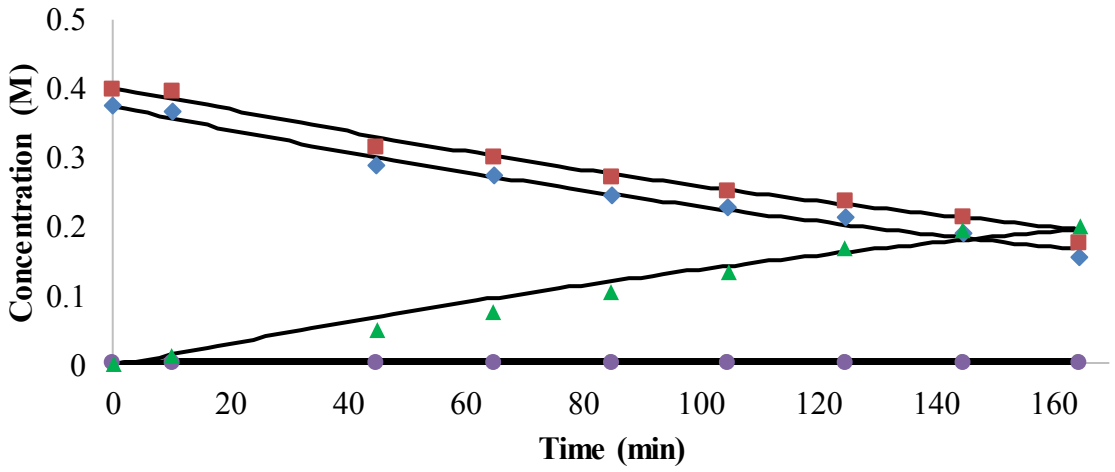
FIGURE 3.6. *Simulated graph and derived kinetic parameters,* ***A)*** *45 mM,* ***B)*** *180 mM,* ***C)*** *200 mM of H_2O (Table 3.1, entries 2-4).* ***Legend:*** ♦*= benzyl alcohol* ***2.1***, ■ *= aniline* ***2.2***, ▲ *= substituted amine* ***2.4***, ●*= imine* ***2.3***, ●*= PhCHO. Solid black lines= simulated reaction curves.*

TABLE 3.2. *RMS values for the data fits of reactions performed with 45, 180 and 200 mM of H_2O.*

Initial concentration of H_2O	2.1	2.2	2.3	2.4	Free PhCHO
45 mM	3×10^{-8}	3×10^{-8}	7×10^{-3}	5×10^{-3}	5×10^{-3}
180 mM	3×10^{-8}	3×10^{-8}	7×10^{-3}	5×10^{-3}	5×10^{-3}
200 mM	3×10^{-8}	3×10^{-8}	7×10^{-3}	5×10^{-3}	5×10^{-3}

The model is able to predict good fits to the reaction data and similar to the previous fits, the RMS values are higher for the intermediates (**2.3** and PhCHO) and **2.4**. As the rate constant and equilibrium values have remained unchanged (k_1, $K_2 \bullet K_3$ and k_4) it is unlikely that the precipitate and/or emulsion of **2.4** is deactivating Au/TiO_2, and is instead lost in the system. Indeed the reaction mixture was found to be cloudy in appearance when conducting these experiments, which could have been precipitated **2.4**.

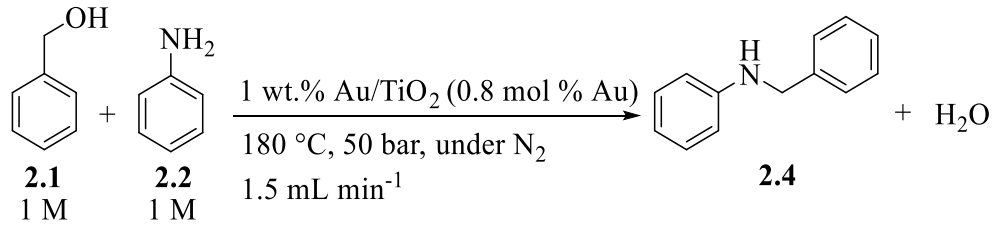
The updated model was used to fit data from the reaction performed with 2 mM of H_2O in 2-methyl-2-butanol, which achieved a complete mass balance (Table 3.1, entry 1). A poor fit was initially observed as the formation of **2.4** was under predicted, due to the fast forward rate of k_5 (4.6 M^{-1} s^{-1}), but by allowing the software to generate appropriate values for k_5, a better fit was achieved (Figure 3.7). The forward and reverse values derived for k_5 were fairly comparable, making k_5 a redundant term for this system. This is reasonable as we know that a complete mass balance is achieved when relatively dry solvent (2 mM of H_2O) was used (Table 3.1, entry 1). Fundamentally, k_5 is only acting to account for the loss of product, which is not observed when employing dry conditions.

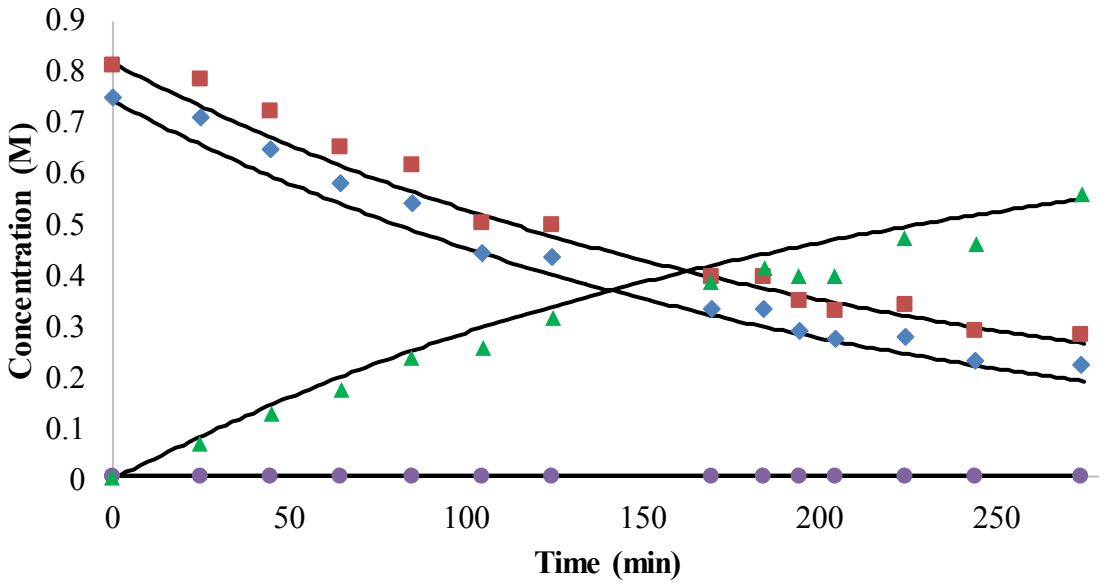


k_1/ s^{-1}	$K_2 \bullet K_3$	k_4/ M^{-1} s^{-1}	k_5/ M^{-1} s^{-1}	
5.0×10^{-3}	6.8×10^{7}	7.0×10^{-1}	$k_f = 1.0 \times 10^{2}$	$k_r = 5.0 \times 10^{2}$

FIGURE 3.7. *Simulated graph and derived kinetic parameters, Table 3.1, entry 1.* ***Legend:*** ♦= *benzyl alcohol* ***2.1****, (4 x10^{-8}),* ■ = *aniline* ***2.2****, (3 x10^{-8}),* ▲= *substituted amine* ***2.4****, (2 x10^{-3}),* ●= *imine* ***2.3****, (3 x10^{-3}),* ●= *PhCHO (2 x10^{-3}). Solid black lines= simulated reaction curves.*

To test the ability of the model to predict reaction profiles under dry conditions, an experiment conducted with **2.1** and **2.2** (1 M) using 2 mol% Au at 180 ˚C and 50 bar pressure (2 mM of H_2O 2-methyl-2-butanol) was modelled (Figure 3.8). Pleasingly, reaction curves with very good fits between simulated lines and the data points was found, demonstrating the models applicability for predicting reaction profiles with different initial H_2O concentrations in 2-methyl-2-butanol under N_2.





k_1/ s^{-1}	$K_2 \bullet K_3$	k_4/ M^{-1} s^{-1}	k_5/ M^{-1} s^{-1}	
5.0×10^{-3}	6.8×10^{7}	7.0×10^{-1}	$k_f = 1.0 \times 10^{2}$	$k_r = 5.0 \times 10^{2}$

FIGURE 3.8. *Simulated graph and derived kinetic parameters using 1M* ***2.1*** *and* ***2.2****.* ***Legend:*** ♦*= benzyl alcohol* ***2.1****, (4 x10^{-8}),* ■ *= aniline* ***2.2****, (4 x10^{-8}),* ▲*= substituted amine* ***2.4****, (4 x10^{-3}),* ●*= imine* ***2.3****, (5 x10^{-3}),* ●*= PhCHO (4 x10^{-3}). Solid black lines= simulated reaction curves.*

Overall a very simple model has been formulated which allows for the prediction of reaction profiles. Terms to account for mass transfer were not incorporated into the model; however, studies were performed to distinguish whether the system was under mass transfer limitations. Ultimately, the reaction rate is reliant on the effective mass transfer and diffusion between reagents and the catalyst surface. There are two fundamental types of diffusion that the reaction could be limited by, namely internal and external mass transfer. A catalytic reaction takes place following the diffusion of reagents through the fluid layer surrounding the catalyst particles (external mass transfer) and once they have passed into the pores within the particle (internal mass transfer) (Figure 3.9).[93]

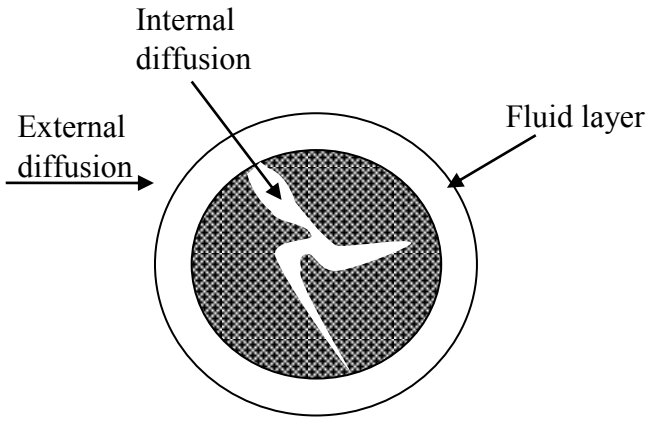


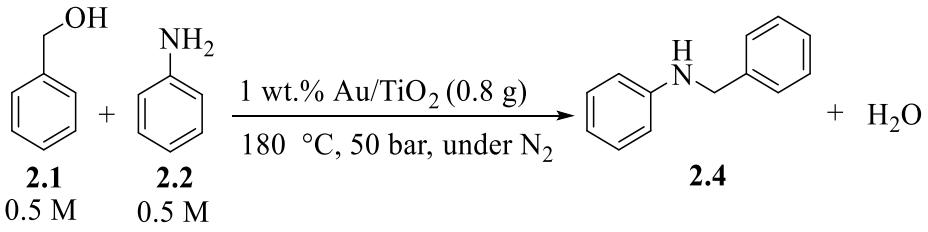
FIGURE 3.9. *Internal and external mass transfer in a porous catalyst.*

In this work, the flow rate could influence the effective transfer of reagents to the outer surface of the particles, and the size of the catalyst particles could affect the diffusion of reagents into the pores. Thus to investigate whether the system was limited by external and/or internal diffusion, the following experiments were devised:

External mass transfer:

A series of single pass reactions (Scheme 1.18) were performed using the model reaction of **2.1** with **2.2** at 5 different flow rates, giving 5 residence times (the average contact time of substrates with the catalyst surface) between 30 and 300 seconds (Scheme 3.3). Note that reactions which were subjected to kinetic modelling were performed with residence times of 30 seconds.

If the system is limited by external mass transfer, a dependency on the rate of **2.1** conversion is expected when plotted against the residence time.

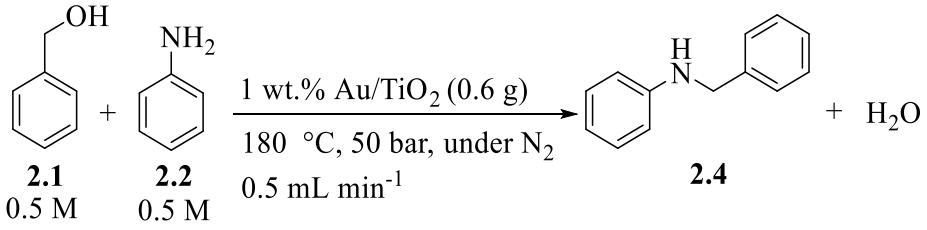


Performed in single pass mode at 5 different residence times:
30, 38, 60, 100 and 300 and seconds

SCHEME 3.3. *Experiments designed to assess whether reactions are limited by external mass transfer.*

Internal mass transfer:

A series of 3 single pass experiments using the model reaction of **2.1** with **2.2** were performed using the same flow rate (0.5 mL min^{-1}, residence time of 90 seconds) but employing different catalyst particle sizes (achieved by grinding and sieving the catalyst) (Scheme 3.4). These studies were performed at a slow flow rate in order to minimise any external mass transfer effects. Additionally, a lower pressure and catalyst loading was used (0.6 g vs. 0.8 g) compared to the studies investigating external mass transfer effects, as small catalyst particle sizes were found to increase the back pressure of the system. In our previous studies, we demonstrated that there are no effects on the catalytic reactivity of Au/TiO_2 when varying the pressure for the AAA reaction.[77] Note that reactions which were subjected to kinetic modelling were performed with an average catalyst particle size of (190 μm).
If the system is limited by internal mass transfer, a dependency on the rate of **2.1** conversion when plotted against the average particle size employed in the experiment is expected.



Performed in single pass with three different catalyst particle sizes:
70, 100 and 190 μm (average particle sizes)

SCHEME 3.4. *Experiments designed to assess whether reactions are limited by internal mass transfer.*

When the rate of **2.1** conversion is plotted against residence time, at first glance, there does not seem to be a dependency on the flow rate (Figure 3.10). However, on closer inspection it appears that there is a slight deviation between the residence times of 30 to 60 seconds (highlighted in Figure 3.10) As experiments were conducted using a residence time of 30 seconds, it can be suggested that the reactions are on the boundary of being limited by external mass transfer effects. If this is the case, the calculated rates may be slower than the inherent rates that would be achieved if the system was not influenced by diffusional effects.

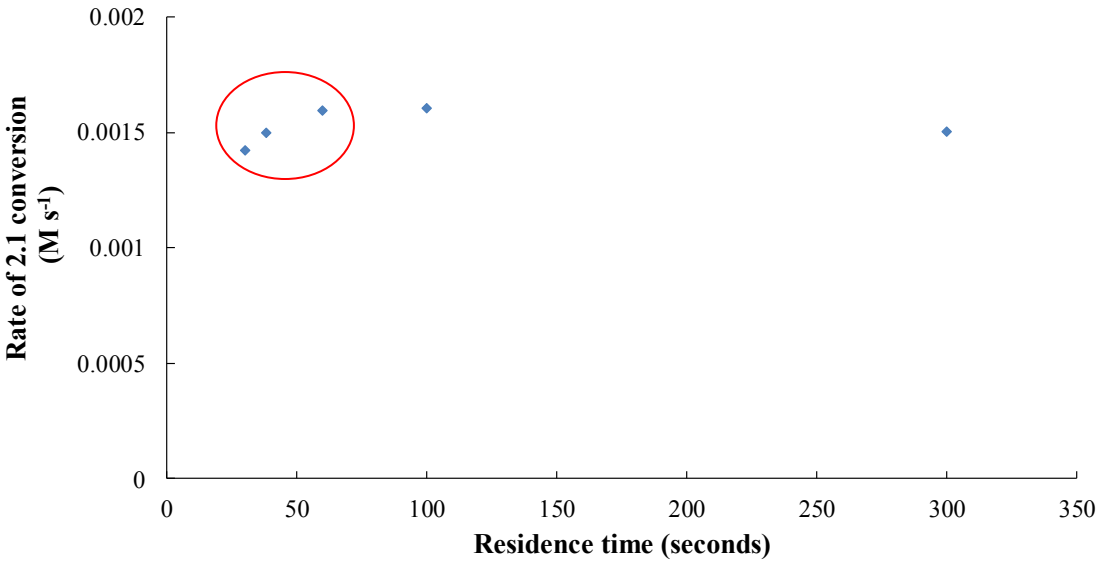


FIGURE 3.10. *Results of the external mass transfer studies showing the rate of* ***2.1*** *conversion against residence time.*

There does not appear to be any influence on the rate of **2.1** conversion when altering the catalyst particle size (Figure 3.11), indicating that the system is not limited by internal mass transfer effects.

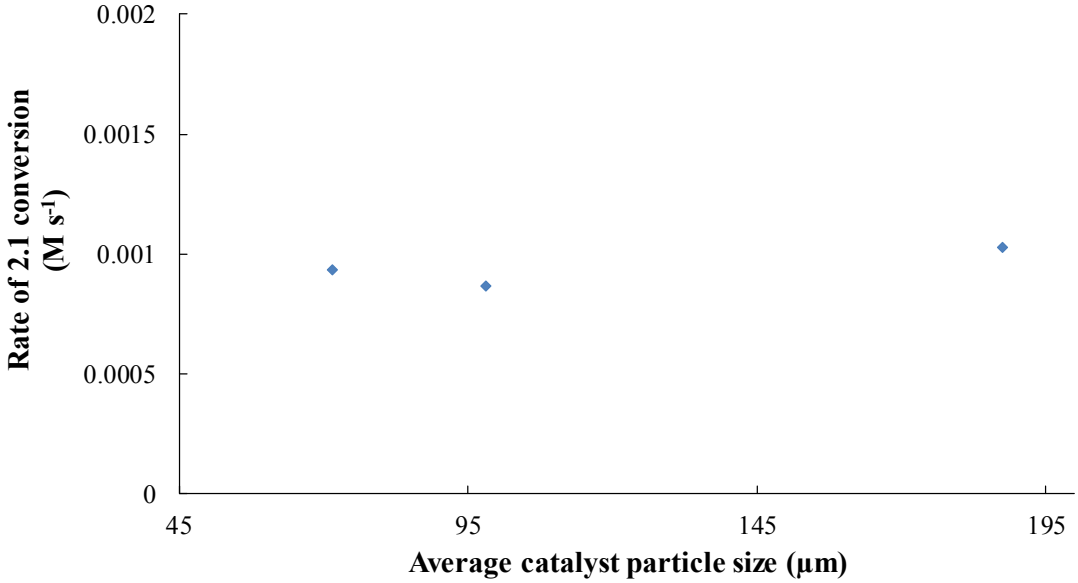


FIGURE 3.11. *Results of the internal mass transfer studies showing the rate of* ***2.1*** *conversion against the average catalyst particle size.*

3.3 Conclusion

A kinetic model was developed based on the rate equations previously derived[77] and the mechanistic findings detailed in this work (Chapter 2). Berkeley Madonna™ software was used to simulate rate constants for discreet steps of the catalytic cycle and the resulting model was able to predict concentration-time trends well with low RMS values, giving confidence in its accuracy. The formation of aldehyde was found to be the rate-determining step in the reaction, which is in line with what has previously been reported.

To account for the decreased detection of amine product (**2.4**) with experiments using H_2O concentrations higher than 2 mM, an additional term was included in the model (k_5). Essentially the term simulates a decreased formation of amine product, which is reliant on the amount of H_2O present in the system. The constant was redundant for experiments performed with dry solvent (2 mM of H_2O) as full mass balances were achieved for these reactions. The values of the other constants (k_1, $K_2 \bullet K_3$ and k_4) did not change upon introducing this term into the model, which highlights that the presumed amine precipitate and/or emulsion is not deactivating Au/TiO_2 but is instead being captured elsewhere in the system.

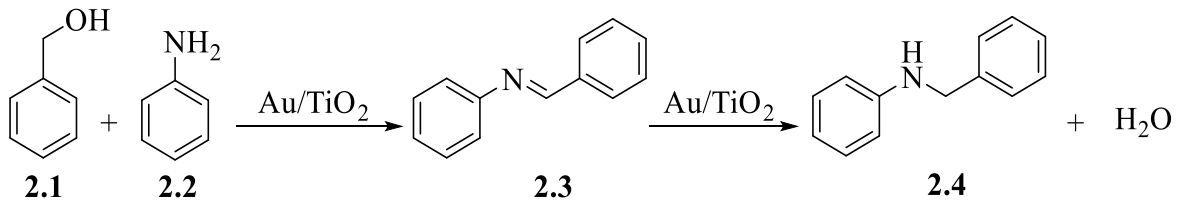
It was shown in Chapter 2 that H_2O is able to act as a reductant, however a term was not included in the model as the effects of this under N_2 were small (2% increase in the selectivity for **2.4** by using 200 mM of H_2O instead of 2 mM). Although mass transfer studies were performed, these terms were not included in the model. The studies demonstrated that the reactions are not limited by internal mass transfer effects but are likely to be on the boundary of external mass transfer influences. This means that the calculated rates may be slower than the true rates that could be achieved if such diffusion limitations were not in operation. Terms to account for the adsorption of species to the catalyst surface were not incorporated which could also influence the derived rates, as the adsorption of species is essential for catalytic activity. Nevertheless, the model is able to provide approximate predictions of the effects of using different initial H_2O and substrate (**2.1** and **2.2**) concentrations in 2-methyl-2-butanol (under N_2).

The simple model formulated may be used for the design of future experiments, for instance, to simulate the length of time a reaction requires to complete based on the starting concentrations of substrates. Future work could involve the incorporation of terms to account for the effects of mass transfer and the influence that O_2 has on the reaction (Chapter 2). This would allow for experiments conducted under aerobic conditions to be modelled. To test the

applicability of the model for the AAA reaction, the kinetic analysis of reactions using substrates other than **2.1** and **2.2** is necessary.

CHAPTER 4. Preparation, characterisation and catalytic screening of Au/TiO_2

It has previously been demonstrated that Au/TiO_2 is active and selective towards the AAA reaction.[77] The aim of this Chapter is to establish which catalyst preparation and calcination methods produce the most active catalysts for further catalyst development studies. Additionally, it is desirable to gain a deeper understanding of the influences that different techniques have on the structure and activity of Au/TiO_2. It is generally accepted that small Au particles (<10 nm) are most active in the AAA reaction,[73] however their size and distribution across the support are deeply affected by how they are prepared.[62, 75, 94-97] To analyse this, Au/TiO_2 was prepared using different synthetic and calcination methods and their structures characterised using a variety of techniques. The catalysts were assessed for their performance towards the alkylation of **2.2** by **2.1**, using a batch reactor (described in Section 4.3) (Scheme 4.1).



SCHEME 4.1. *The alkylation of* ***2.2*** *with* ***2.1*** *for the screening of* Au/TiO_2 *prepared by various techniques, using a batch reactor.*

To provide a background for the studies described in this Chapter, catalyst preparation methods are presented in the following Section (4.1). The effects of using different preparation techniques on the structure of Au/TiO_2 will be analysed subsequently in Section 4.2.

4.1 Background

There are numerous preparation methods reported for the synthesis of heterogeneous catalysts.[98, 99] Throughout this study some of these were employed to prepare Au/TiO_2, including impregnation (Section 4.1.1), deposition-precipitation (Section 4.1.2) and colloidal synthesis (Section 4.1.3). Additionally, spray drying (Section 4.1.4) was used for the preparation of Cu/TiO_2 (deployed in Chapter 6).

Each of these methods will be discussed, with a particular emphasis towards Au-based catalysts. The effects of thermal treatment on the structure of the catalyst will be discussed in Section 4.1.5.

4.1.1 Impregnation (IMP)

IMP is commonly used to prepare catalysts on a variety of supports. There are two ways that IMP can be performed; by incipient wetness impregnation (IWI) or wet impregnation (WI). The former involves the addition of the minimal amount of metal precursor solution to fill the support pores,[100] whereas the WI method involves the addition of an excess of metal precursor solution to the support, followed by evaporation so the concentrated solution remains in the pores.[100] In both cases, after the addition of the metal precursor to the support, the material is dried and calcined.

Both techniques generally lead to large particles; however the IWI method commonly leads to smaller metal particles compared to WI because of the close contact that is achieved between the metal precursor and support.[100] The metal precursor can reside on the outer surface of the support particles, consequently forming large crystals when the WI method is employed.[100] For Au catalysts, it was commonly found that systems prepared by the IMP method had poor activity when Au chloride complexes, e.g. $HAuCl_4$, $AuCl_3$ and $[Au(en)_2]Cl_3$, were used as precursors.[101-106] This was attributed to the mobility of chloride ions, which promotes the agglomeration of Au particles during thermal treatment, leading to the formation of large particles sizes (10-35 nm) that limits the number of accessible catalytic sites.[96, 107] In certain cases, chloride ions can be removed as HCl through thermal treatment under reducing conditions, but this was shown to lead to large Au particle sizes (10-30 nm) when Au/Fe_2O_3 was treated this way.[108]

4.1.2 Deposition- Precipitation (DP)

Haruta and co-workers have demonstrated that IMP techniques are unsuitable for producing highly dispersed Au systems, and that by using the DP method, highly active materials can be obtained.[108, 109] There are numerous variations of the DP method reported in the literature. A general procedure involves the addition of support to an aqueous solution of metal precursor, raising the pH to a fixed value by addition of base, washing the material to remove residual precursor (deionised H_2O), then drying and calcining the sample.[100] The washing of Au catalysts is very important for the removal of chloride ions to prevent particle agglomeration during thermal treatment, this commonly occurs with Au catalysts prepared by the IMP method where there is no washing step involved (Section 4.1.1).

There are many factors that can affect the final structure of the catalyst, such as the calcination conditions and the pH of the mixture during precipitation. For the preparation of Au/TiO_2 catalysts, it has been found that the loading of Au and the size of the particles decreases by using a high pH (8-10).[95, 110] It was shown that a maximum loading of Au is achieved at pH 6, thus to achieve good loadings without compromising particle size, careful consideration is required when choosing the pH.

4.1.3 Colloidal Synthesis (COL)

Colloidal synthesis involves the deposition of pre-formed metal nanoparticles of a defined size (stabilised by ligand or surfactant) onto a solid support.[111] The excellent control of particle shape and size (with narrow particle distributions) that can be achieved by the choice of stabiliser or ligand and the reducing agent are the main advantages of this technique. By fine-tuning these various parameters, reproducible preparations of catalysts can be achieved.[112]

There are some drawbacks to this technique, however, namely in the removal of ligands or surfactants, which are essential in preventing particle agglomeration. This is often carried out by thermal treatment, which can cause agglomeration of particles.[113] Nevertheless, it has been shown that this can be avoided by washing material in hot water (90 ˚C) for a short time period.[112]

4.1.4 Spray Drying (SD)

The SD procedure is similar to the WI IMP method, in that the metal precursor and support are mixed to form a slurry and there is no washing step involved. The main difference between the techniques resides in the procedure for drying the material. The SD method involves atomisation of the slurry, which is subsequently dried in a furnace to convert droplets to particles.[114, 115] By combining the straightforward principles of IMP with fast drying, agglomeration of catalyst particles may be reduced and catalyst can be prepared in a more controlled manner.[116] The SD method has been used to form catalysts with various nanoparticle morphologies including doughnut, spherical and hollow shapes.[114] The key parameters that affect particle morphology are the carrier gas flow rate and the temperature of drying.[114, 115]

4.1.5 Effect of thermal treatment conditions on particle size

It is well known that thermal treatment conditions (temperature, calcination atmosphere and gas flow rate) are important for determining the sizes of metal particles.[100] The combination of temperature and atmosphere used to dry and calcine Au/TiO_2 catalysts have been shown to have interesting effects on their particle sizes. When heating 'as-prepared' Au/TiO_2 under H_2 at 120 ˚C, complete reduction to Au^0 was achieved with small particle sizes (2 nm). Conversely, when Au/TiO_2 was heated in air at 125-170 ˚C, larger particles were formed (3 nm).[100] The explanations for this were that the H_2 could have removed residual chloride as HCl, whereas in air, chloride is still present which could have caused agglomeration.[100] Additionally, the lower temperature used in the former case could have initiated the reduction of the precursor to start at a lower temperature, inducing a stronger interaction between the particle and support, reducing the likelihood of Au agglomeration.

In terms of the flow rate, it has been shown that by employing faster rates during calcination (under air) larger Au particles were formed in the preparation of Au/Fe_2O_3.[117]

4.2 The effect of the preparation technique on the structure of $Au//TiO_2$

The aim of this study was to prepare Au/TiO_2 using different methods and to assess the effect this has on catalyst structure and performance in the alkylation of **2.2** by **2.1**. Table 4.1 gives a summary of the catalysts obtained from different preparation and calcination methods. Note that TEM images were recorded at Imperial College London and all other catalyst characterisation and calcination was performed by Johnson Matthey Plc, unless stated otherwise. Three methods (DP, IMP and COL) were used to synthesise as-prepared catalysts (oven dried only), and to understand the influence of calcination treatments, different thermal treatment conditions were applied to samples of each of the as-prepared catalysts. Both the as-prepared catalysts and thermally treated samples were characterised and screened for their activity (Section 4.3).

The DP method was chosen to assess the effects of using different temperatures (under air at 300, 500 and 800 ˚C) and not the IMP method (Table 4.1, entry 1). This is because there is no washing step involved in the IMP method and residual chloride from the metal precursor is known to cause agglomeration of Au particles, which is promoted by high temperatures (Section 4.1.1). To allow for comparisons of the IMP and DP methods, a sample of the catalyst prepared by the DP method was treated at 300 ˚C under a reducing atmosphere of H_2/N_2 (Table 4.1, entries 1 and 3).

The Au/TiO_2 catalyst prepared by the IMP method (employing the IWI technique) was calcined under different atmospheres to assess the effects this had on activity (Table 4.1, entry 3).

To avoid undesired agglomeration, the catalysts prepared using the COL method were treated with a hot washing step (refluxed at 90 ˚C for 2 hours) then oven dried at 100 ˚C for 24 hours (as-prepared). Additional samples were also calcined at a low temperature (200 ˚C) under a reducing atmosphere to understand whether thermal treatment is necessary for activity (Table 4.1, entry 4).

From this point forward, catalysts will be denoted as 'Au/TiO_2 (method of preparation)' for example, Au/TiO_2 (DP).

TABLE 4.1. *Au/TiO_2 catalysts synthesised using the COL, IMP and DP methods showing the metal loadings (wt.%) and the thermal treatments employed.*

				Calcination atmosphere (for 2 hours)		
Entry	**Catalyst**	**Metal loading (wt.%)**	**As-prepared catalyst**	**Air (˚C)**	**Ar (˚C)**	**H_2/N_2 (˚C)**
1	Au/TiO_2 (DP)	0.3	Yes[a]	300, 500, 800	-	300
2	Au/TiO_2 (DP2)	0.6	No	-	-	300
3	Au/TiO_2 (IMP)	0.9	Yes[a]	300	300	300
4	Au/TiO_2 (COL)	0.9	Yes[b]	-	-	200

[a] Dried in the oven at 100 ˚C for 24 hours, [b] Refluxed at 90 ˚C for 2 hours then oven dried at 100 ˚C for 24 hours.

The aim was to prepare catalysts with 1 wt.% loading of Au. It can be seen that the metal loading for the Au/TiO_2 (DP) system was much lower than expected (Table 4.1, entry 1). For this catalyst, a pH of 9 was employed in its synthesis, and it is known that using higher pH values can cause lower metal loadings (Section 4.1.2).[95, 110] Therefore, the procedure was repeated using a pH of 8, leading to a higher loading of 0.6 wt.% (Au/TiO_2 (DP2)) (Table 4.1, entry 2). Catalyst screening was performed using both Au/TiO_2 (DP) and Au/TiO_2 (DP2). As-prepared Au/TiO_2 (DP2) was thermally treated under one set of conditions (300 ˚C under H_2/N_2) because as-prepared Au/TiO_2 (DP) had already been calcined under varying conditions, and therefore could be used to assess the effects of different thermal treatments.

Au/TiO_2 prepared by the IMP and COL methods had much higher Au loadings compared to Au/TiO_2 (DP) and Au/TiO_2 (DP2) (Table 4.1, entries 3 and 4 vs. 1 and 2). Unlike the DP method there is no washing step involved with these techniques (Section 4.1.1 and 4.1.3) which could have facilitated in the removal of Au from catalysts prepared by the DP method. Although direct comparisons between methods cannot be made due to the different Au loadings and calcination treatments, the effect of thermal treatment and the effect of the preparation method on the catalyst structure can be made.

TEM images of as-prepared Au/TiO_2 (DP) and samples treated under the various conditions (300, 500, 800 ˚C (air) and 300 ˚C (H_2/N_2)) were recorded. Due to the low Au loading (0.2 wt.%), it was difficult to locate Au particles in samples calcined at temperatures <500 ˚C (Figure 4.1 A). However Au/TiO_2 (DP) treated at 800 ˚C, revealed significant sintering of Au particles (Figure 4.1 B), which may be attributed to the high temperature inducing mobility of the Au particles.

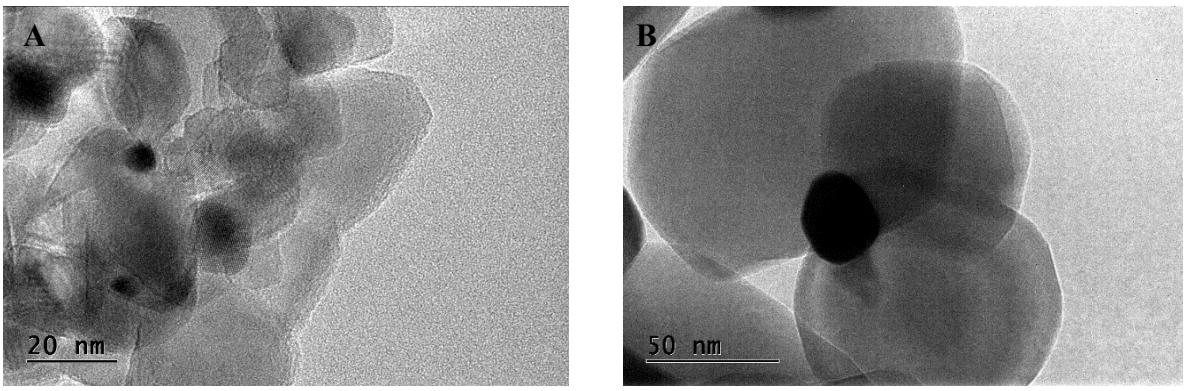


FIGURE 4.1. *TEM images of Au/TiO_2 (DP)* ***A)*** *As-prepared (oven dried at 100 ˚C),* ***B)*** *Calcined at 800 ˚C under air for 2 hours.*

To gauge if there were any differences in the size of Au nanoparticles for the Au/TiO_2 (DP) samples treated under the various calcination conditions, UV-Visible spectroscopy was performed.

Au nanoparticles exhibit a strong broad absorption band between 400-800 nm in the UV/Visible region. This originates from surface plasmon resonances (SPR) induced by the electromagnetic field as a result of the in-phase oscillations caused by the excitation of free electrons within the conduction band.[118] An absorption band results when the incident photon frequency is resonant with the collective oscillation of the conduction band electrons. Changes in Au nanoparticle sizes cause the absorption maxima to shift. As the Au nanoparticle diameter increases, the light can no longer polarise the nanoparticles homogeneously, causing a red shift of the plasmon maxima and a broadening of the band.[118]

There appears to be no difference in the plasmon band shape and position for the as-prepared catalyst compared to the samples heated at 300 ˚C under H_2/N_2 and air (Figure 4.2). It seems that calcination under reducing conditions makes little difference to the Au particle size. In contrast, materials calcined at temperatures >300 ˚C under air have a slight red-shift and broadening of the plasmon maxima. This corresponds to an increase in the diameter of the Au nanoparticles, and highlights the importance of keeping calcination temperature <300 ˚C, for producing small Au particle sizes. The peak observed for the Au/TiO_2 (DP) sample calcined at 800 °C shows a significant red shift and broadening, this agrees with the results from TEM analysis where large agglomerated particles where found (Figure 4.1 B).

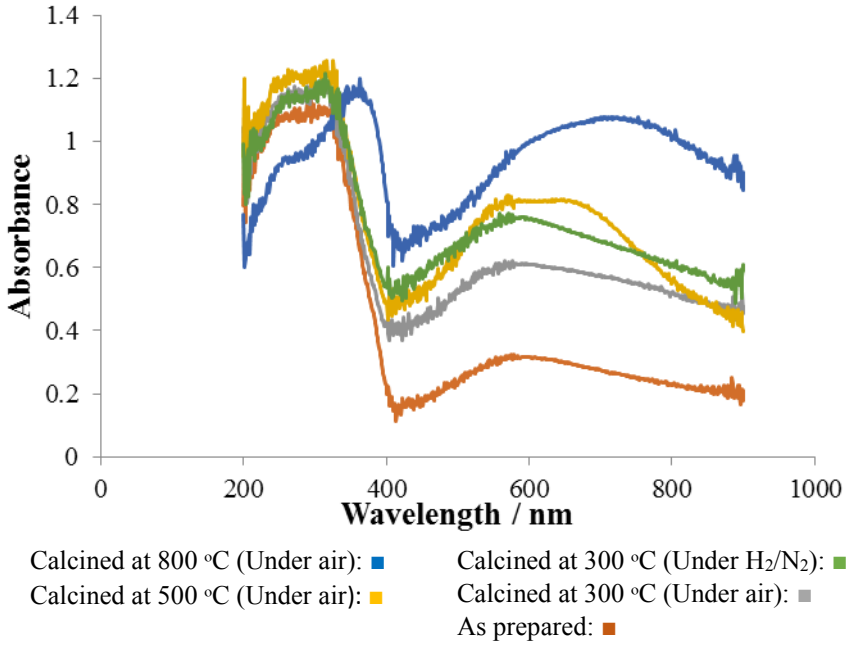


FIGURE 4.2. *UV-Visible spectra of Au/TiO_2 (DP) samples calcined under different conditions.*

TEM images of Au/TiO_2 (DP2) revealed small nanoparticles (mean size of 3.4 nm) following calcination at 300 ˚C under H_2/N_2 (Figure 4.3).

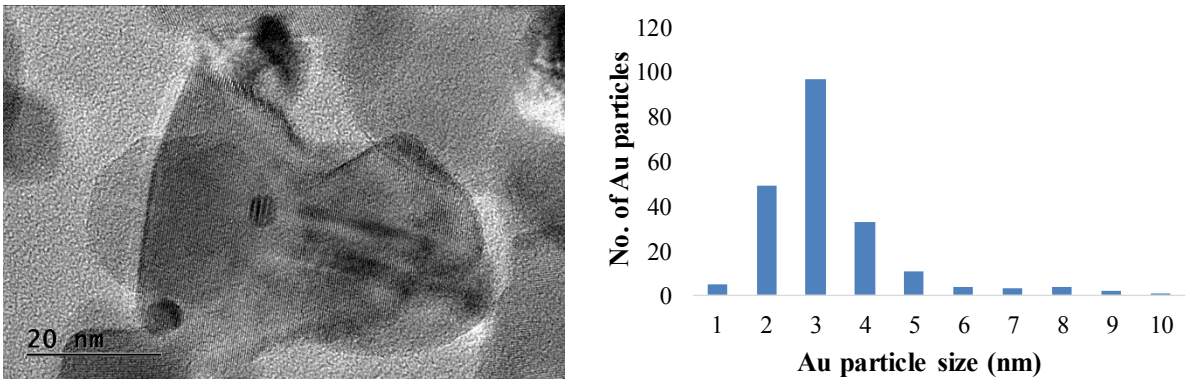


FIGURE 4.3. *TEM image of Au/TiO_2 (DP2) after calcination (at 300 ˚C) and the particle distribution graph showing a mean Au particle size of 3.4 nm (±0.2) (~200 Au particles were measured).*

TEM imaging of the as-prepared Au/TiO_2 (IMP) catalyst showed that some of the Au particles did not adhere to TiO_2, but were found on the TEM microscopy grid (Figure 4.4).

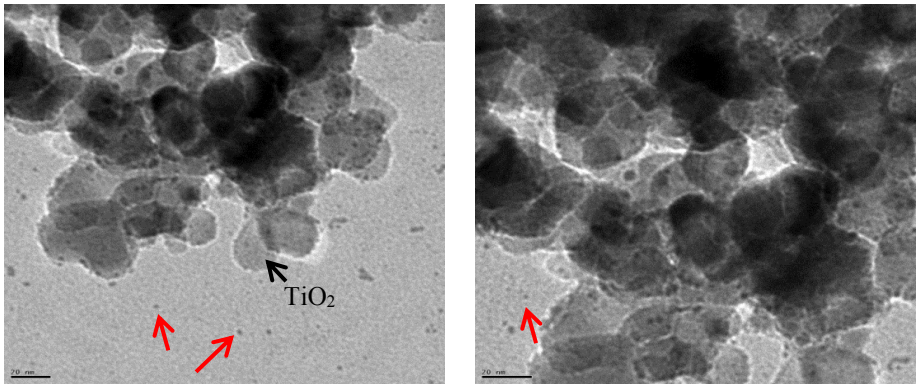


FIGURE 4.4. *TEM images of Au/TiO_2 (IMP). Red arrows pointing to Au particles.*

TEM images of the Au/TiO_2 (IMP) samples that were calcined under varying conditions (under Ar, H_2/N_2 and air for 2 hours at 300 ˚C) were also recorded, where drastic increases in Au particle sizes was observed (Figure 4.5 A-C). This was expected due to the poor adhesion of Au particles in the as-prepared catalyst (Figure 4.4) and the known issues of mobile chloride species inducing agglomeration of Au particles during thermal treatment (Section 4.1.1).

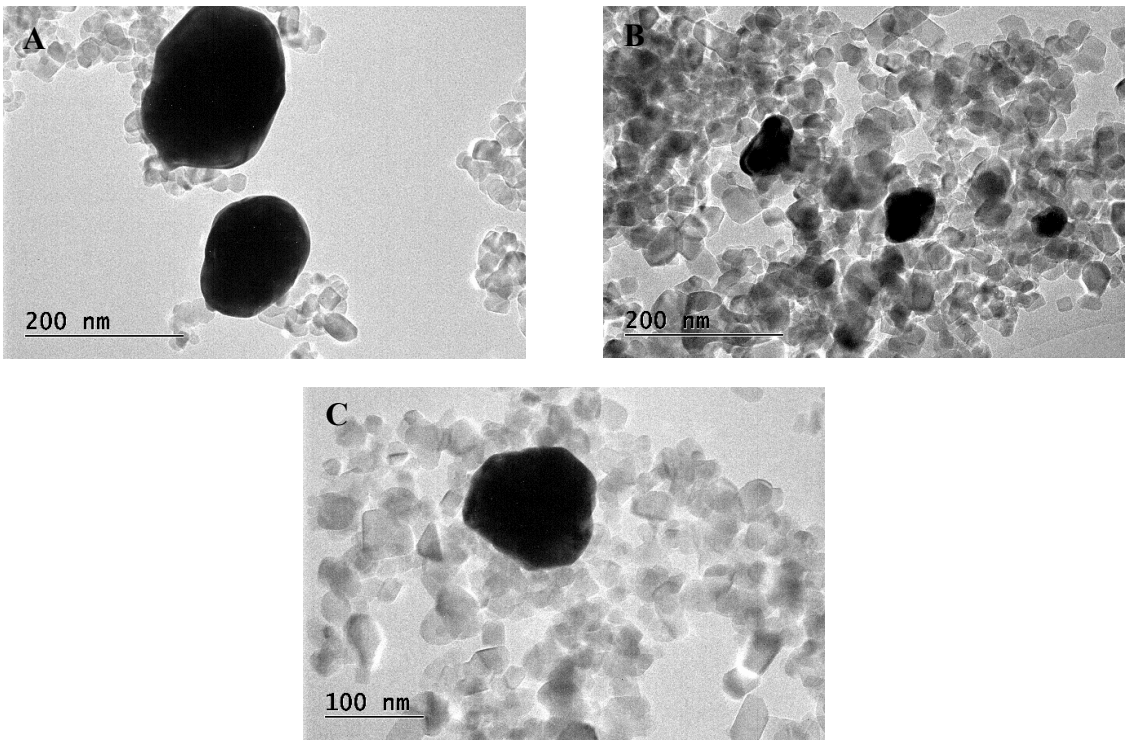


FIGURE 4.5. *TEM images of Au/TiO_2 (IMP) calcined under* ***A)*** *Argon,* ***B)*** *H_2/N_2,* ***C)*** *Air at 300 ˚C for 2 hours.*

As-prepared Au/TiO_2 (COL) exhibited particles with a mean diameter of 2.9 nm (Figure 4.6 A), however growth of the Au particles (mean size of 4.2 nm) was revealed following calcination at 200 ˚C (under H_2/N_2) (Figure 4.6 B). This was anticipated as it has previously been reported that thermal treatment of Au/TiO_2 prepared by the COL synthesis induces Au particle growth.[113]

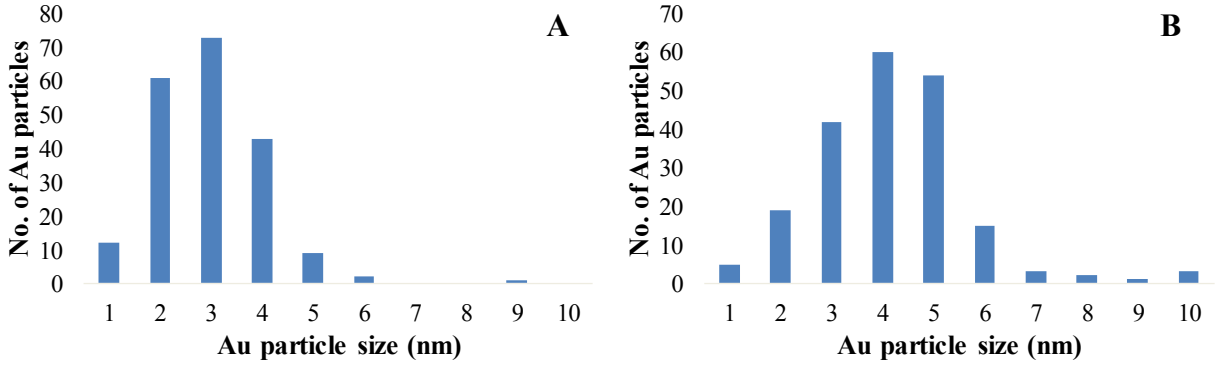


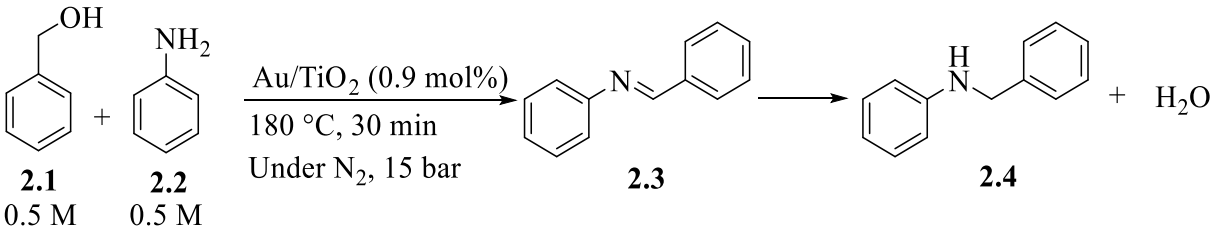
FIGURE 4.6. *Particle distribution graphs of Au/TiO_2 (COL) showing mean Au particle sizes for* ***A)*** *As-prepared sample (2.9 nm (±0.1)),* ***B)*** *Sample calcined at 200 ˚C under H_2/N_2 (4.2 nm (±0.1)). (~200 Au particles were measured).*

XRD analysis revealed the presence of anatase and rutile TiO_2 phases in all of the Au/TiO_2 catalysts prepared and confirms that calcination treatment has not invoked any major phase changes from anatase to rutile in the TiO_2 support employed (P25-Degussa TiO_2, 25% anatase and 75% rutile). This is a common phenomenon associated with TiO_2 usually occurring at temperatures from 500 ˚C.[119, 120] There were no diffraction lines for Au species in any of the patterns, which is most likely because the metal loadings were below the detection limit for the XRD.

4.3 Catalyst screening results and analysis

Reactions were performed using an Endeavor® catalyst screening system where up to 8 pressurised reactions can be run in parallel. The batch reactor automatically controls and maintains the temperature, gas flow and pressure of the 8 individual reactor vessels and ends the reactions by purging, venting or quenching. The reactor vessels are designed to maintain an inert seal up to 200 ˚ C and 34 bar pressure.

In this study, the model system of **2.1** with **2.2** was chosen to test the activity of the Au/TiO_2 catalysts (Scheme 4.2) using 2-methyl-2-butanol as the solvent and the conditions outlined in the scheme below:



SCHEME 4.2. *The alkylation of **2.2** with **2.1** for the screening of Au/TiO_2 catalysts prepared by the DP, COL and IMP techniques, using a batch reactor.*

A reaction temperature of 180 ˚C was employed in this work as we have previously demonstrated that this allows for good selectivity.[77] As conversion and selectivity was shown to be independent of pressure, 15 bar pressure was applied so that the mixture remained in the liquid phase. A Au loading of 0.9 mol% was used in all reactions and 30 minute reaction times, as preliminary investigations using Au/TiO_2 (Strem AUROlite™) showed that good conversion and selectivities could be achieved using these conditions (71% conversion of **2.1**, 95% selectivity for **2.4**).

As a control experiment, TiO_2 (P25-Degussa) was tested for its activity towards the reaction. Very low conversion of **2.1** (1%) was achieved, indicating that the presence of metal is necessary for catalytic activity. The catalyst screening results of the Au/TiO_2 systems prepared via the different routes and using different calcination treatments will now be discussed in turn.

4.3.1 Au/TiO_2 prepared by the DP method

As-prepared Au/TiO_2 has a low TOF and moderate selectivity for amine (**2.4**) (Table 4.2, entry 1), which was enhanced following thermal treatment at 300 ˚C under air (Table 4.2, entry 2).

TABLE 4.2. *Results for the conversion of* ***2.1*** *to products for Au/TiO_2 (DP) and (DP2) catalysts.*

				Selectivity (%)			
Entry	**Calcination Conditions**	**Conversion (%)[a]**	**TOF (h^{-1})[b]**	**2.4**	**2.3**	**PhCHO**	**Toluene**
1	As prepared	7	15	67	31	3	0
2	Under air (300 ˚C)	29	62	85	14	1	0
3	Under air (500 ˚C)	13	28	84	15	1	0
4	Under air (800 ˚C)	5	11	75	24	1	0
5	Under H_2/N_2 (300 ˚C)	32	69	83	16	1	0
6	Au/TiO_2 (DP2)[c]	89	192	95	2	0	3

[a] Determined by GC using 4-tert-butylphenol as an external standard, based on ***2.1****. Results are an average of 2 runs (error ± 2%).[b] TOF (h^{-1}) (moles of benzyl alcohol converted/moles of Au), [c] Treated under H_2/N_2 at 300 ˚C for 2 hours.*

This increase in activity could be due to reduction of Au (which is known to occur at temperatures as low as 100 ˚C) to form active metallic species. Indeed metallic Ni and Ag species are known to be essential for activity in the AAA reaction (Chapter 1).[59, 60, 66, 67] Using calcination temperatures >300 ˚C results in a reduction in activity and for material calcined at 800 ˚C, a decrease in the selectivity for **2.4** (Table 4.2, entry 2 vs. entries 3 and 4). This indicates that small Au particles are more active towards the reaction, certainly TEM and UV-Visible analysis revealed large Au particles for Au/TiO_2 (DP) calcined at 800 ˚C (Section 4.2).

There does not appear to be any effects of using different thermal atmospheres on catalytic activity (Table 4.2, entry 2 vs. entry 5), which suggests that the temperature at which material is calcined is the more important parameter to control.

Overall, the activity of Au/TiO_2 (DP) is not impressive, however, Au/TiO_2 (DP2) prepared using a lower pH (8), has a very high TOF and selectivity towards the alkylation of **2.2** by **2.1** (Table 4.2, entry 6). In fact, the activity is greater than that of commercially available Au/TiO_2 (Strem AUROlite™) tested under the same conditions (71% conversion of **2.1**, 95% selectivity for **2.4**). The main difference between Au/TiO_2 (DP) and Au/TiO_2 (DP2) is the Au loading, whereby there is a higher loading of Au in the Au/TiO_2 (DP2) catalyst (0.6

wt.% vs. 0.3 wt.%) (Section 4.2). Lower metal loadings result in a higher free TiO_2 surface with Au particles sparsely populated on the support and although the same Au mol% was used in the experiments, the result suggests that close proximity of well dispersed Au atoms is essential for activity.

It is well known that small Au particles (<5 nm) supported on oxides are very active catalysts for converting CO to CO_2, even below room temperature,[100] with the conversion-temperature plots often referred to as 'light-off' curves. For an active catalyst, a sudden increase in activity on heating is observed, due to the exponential dependence of the rate constant on temperature, followed by a slowing down of the reaction due to depletion of the reactant.[121] With this in mind, CO oxidation was performed on Au/TiO_2 (DP) samples to compare the effect of particle size towards the activity of CO oxidation (Figure 4.7).

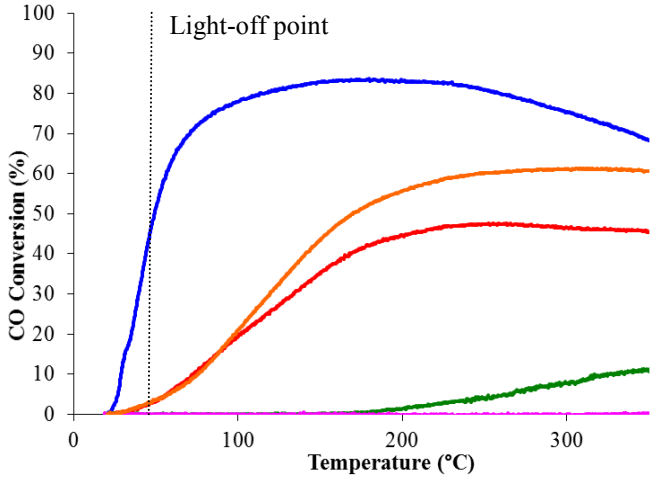


FIGURE 4.7. *CO conversion (%) for Au/TiO_2 catalysts (DP).*

Au/TiO_2 (DP) calcined at higher temperatures (>300 ˚C) shows decreased activity, indicated by the reduction in CO conversion. This is the same trend observed for the alkylation of **2.2** with **2.1** (Table 4.2) and may be ascribed to the larger Au particle sizes found in these systems (Section 4.2).

As-prepared Au/TiO_2 (DP) is the most active catalyst at the onset of the reaction (~50 ˚C), however the conversion decreases from 200 ˚C onwards. This may be due to sintering of Au particles as higher reaction temperatures were reached. Indeed the slower onset of activity observed for the calcined catalysts could be due to larger Au particles sizes. Although these systems are less active than the as-prepared catalyst, samples calcined at 300 ˚C under air and

H_2/N_2 show a steady conversion from ~200 ˚C onwards. It can be postulated that the calcination treatment has increased the adhesion and stability of Au particles to TiO_2, thus reducing the effects of sintering.

Overall, the results highlight the necessity of small Au particles sizes for the AAA reaction and choosing a suitable pH for the preparation of Au/TiO_2 by the DP method.

4.3.2 Au/TiO_2 prepared the IMP method

In general, the Au/TiO_2 (IMP) catalysts calcined under varying conditions at 300 ˚C, exhibit very poor activity towards the conversion of **2.1** (Table 4.3, entries 1-4). This may be due to the poor adhesion of Au to TiO_2 and the large agglomerated Au particles found during TEM analysis (Section 4.2).

TABLE 4.3. *Results for the conversion of **2.1** to products for Au/TiO_2 (IMP) catalysts.*

				Selectivity (%)			
Entry	**Calcination Conditions**	**Conversion (%)[a]**	**TOF (h^{-1})[b]**	**2.4**	**2.3**	**PhCHO**	**Toluene**
1	As prepared	5	11	75	24	1	0
2	Under air (300 ˚C)	3	6	91	9	0	0
3	Under argon (300 ˚C)	4	9	92	8	0	0
4	Under H_2/N_2 (300 ˚C)	2	4	82	18	0	0

*[a] Determined by GC using 4-tert-butylphenol as an external standard, based on **2.1**. Results are an average of 2 runs (error ± 3%).[b] TOF (h^{-1}) (moles of benzyl alcohol converted/moles of Au).*

The as-prepared sample shows comparable conversion to the calcined catalysts but affords the lowest selectivity for **2.4** (Table 4.3, entry 1 vs. entries 2-4). Increases in selectivity following calcination at 300 ˚C (under air and H_2/N_2) was also observed for Au/TiO_2 prepared by the DP method, and was attributed to the formation of active metallic Au species (Section 4.3.1).

There does not appear to be any differences in activity between samples calcined under air and argon (Table 4.3, entries 2 and 3), however thermal treatment under a reducing atmosphere (H_2/N_2) resulted in a decreased selectivity for **2.4** (Table 4.3, entry 4). A logical explanation for this is that slightly larger Au particles were present in this sample. This is supported by the reduction in the selectivity for **2.4** observed for Au/TiO_2 (DP) calcined at 800 ˚C (Table 4.2, entry 4), which was shown to have large Au particle sizes present (Section 4.2).

CO-oxidation experiments were performed; however all of the Au/TiO_2 (IMP) catalysts were found to be inactive, which is not surprising given the large Au particles present.

In summary, the IMP method is not a suitable technique for the preparation of active materials for the AAA reaction, due to the poor adhesion of Au to TiO_2 and the tendency for particles to agglomerate during calcination.

4.3.3 Au/TiO_2 prepared by the COL method

The activity of as-prepared Au/TiO_2 (COL) is practically identical to that of Au/TiO_2 (DP2), showing excellent activity towards the formation of **2.4** (Table 4.4, entry 1 vs. Table 4.2, entry 6). This is perhaps not surprising given that the average Au particle sizes were shown to be ~3 nm for both of these systems (Section 4.2).

TABLE 4.4. *Results for the conversion of **2.1** to products for Au/TiO_2 (COL) catalysts.*

				Selectivity (%)			
Entry	**Calcination Conditions**	**Conversion (%)[a]**	**TOF (h^{-1})[b]**	**2.4**	**2.3**	**PhCHO**	**Toluene**
1	As prepared	80	172	96	3	0	1
2	Under H_2/N_2(200 ˚C)	66	142	95	3	0	2

*[a] Determined by GC using 4-tert-butylphenol as an external standard, based on **2.1**. Results are an average of 2 runs (error ± 3%).[b] TOF (h^{-1}) (moles of benzyl alcohol converted/moles of Au).*

To determine whether the reaction conditions induced any changes in Au particle size for the as-prepared Au/TiO_2 (COL), TEM imaging was conducted following a typical reaction (alkylation of **2.2** by **2.1** at 180 ˚C for 30 minutes under 15 bar N_2). It was shown that on average Au particle sizes remained to be ~3.4 nm in diameter (Figure 4.8).

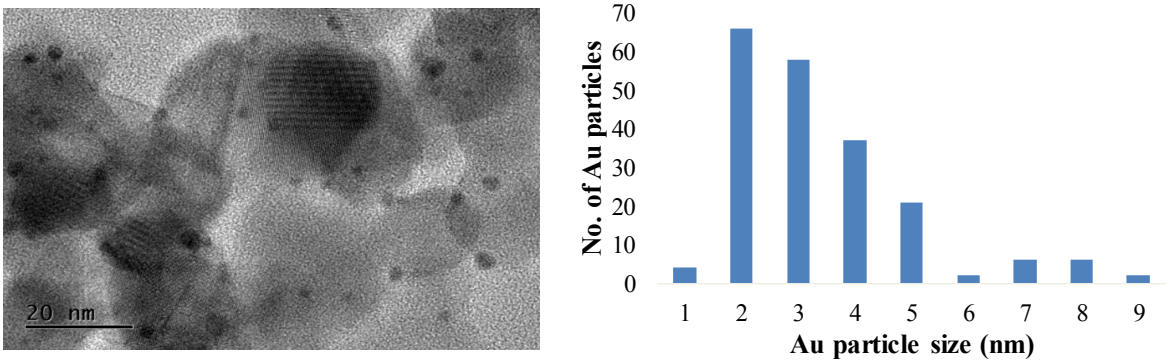


FIGURE 4.8. *TEM image of Au/TiO_2 (COL) after reaction and the particle distribution graph showing a mean Au particle size of 3.4 nm (±0.1) (~200 Au particles were measured).*

The TOF decreased substantially from 172 h^{-1} to 142 h^{-1} upon calcining the catalyst (Table 4.4, entry 2). The detrimental effect of the thermal treatment can be attributed to increases in Au particle size (4.2 nm), which was confirmed by TEM analysis (Section 4.2). The enhanced growth in Au particle size obtained during calcination, compared to Au/TiO_2 (COL) that had been used in a reaction, could be due to the increased time and temperature that the sample was subjected to heat for (2 hours at 200 ˚C vs. 30 minutes at 180 ˚C).

Overall, the use of a thermal treatment was unnecessary for producing active material by the COL method and catalysts exhibited comparable activity to analogous systems prepared by the DP technique.

4.4 Conclusion

Au/TiO_2 was prepared using the impregnation (IMP), deposition-precipitation (DP) or colloidal (COL) methods with samples of these catalysts thermally treated under various conditions and characterised using a range of techniques.

It was established through ICP analysis that by using a high pH in the DP method low Au loadings result (0.3 wt.%) but by using a lower pH (8), the Au loading and activity increased. In fact, one of the most active catalysts was generated in these studies using this method (Au/TiO_2 (DP2)). The Au/TiO_2 system prepared by the COL method had comparable Au particle sizes and activity to that of Au/TiO_2 (DP2), and although the Au particles exhibited good stability under the conditions employed, it was suggested that prolonged reaction times might induce particle sintering. Indeed calcination of this catalyst under reducing conditions resulted in particles size increases and a reduction in activity. Particle size was also shown to govern the activity of Au/TiO_2 (DP) systems, where high thermal treatment temperatures (>300 °C) resulted in increased Au particle sizes and reductions in activity and selectivity. Similarly, TEM analysis revealed significant agglomeration of Au particles in the Au/TiO_2 (IMP) catalysts and poor adhesion of Au to TiO_2. The as-prepared and calcined systems (under air, H_2/N_2 and argon) were poorly active in both the CO-oxidation experiments and the alkylation of **2.2** by **2.1**.

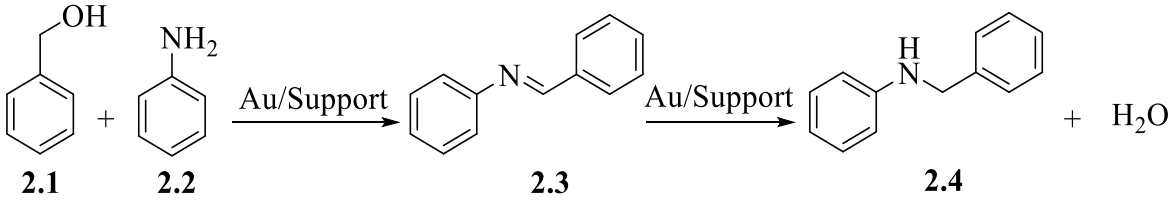
While calcination invoked increases in particle size, enhancements in activity was observed for Au/TiO_2 (IMP) and Au/TiO_2 (DP) catalysts that were treated at 300 ˚C, when contrasted against the as-prepared systems. This was attributed to the formation of active metallic Au species. In general, the calcination atmosphere did not influence catalytic activity.

The studies have highlighted the importance of employing appropriate reaction conditions, namely pH, when performing the DP procedure and using suitable calcination temperatures to allow for the formation of small Au particles. Both the DP and COL methods produced active systems, however future studies could compare the lifetime of Au/TiO_2 prepared by the COL and DP methods.

CHAPTER 5. Investigation of Au supported catalysts for the AAA reaction

The performance and stability of Au catalysts is known to be greatly dependent on the structure and interactions between Au and the support.[75, 95-97] However there have been only been a few attempts reported thus far to delineate the role of the support for Au based catalysts in the AAA reaction (discussed in Section 5.1).

The aims of this Chapter are to synthesise and characterise a variety of Au supported catalysts and to examine their activity towards the alkylation of **2.2** by **2.1** using the Endeavor® batch reactor (Section 4.3) (Scheme 5.1).



SCHEME 5.1. *The alkylation of* ***2.2*** *with* ***2.1*** *for the screening of Au supported catalysts prepared by the COL and DP techniques, using a batch reactor.*

By establishing whether the support contributes to and/or influences catalytic reactivity, the design of new catalysts will be aided, particularly for more active systems that can operate under mild conditions. At the same time, it will allow for a better understanding of what parameters may be important for activity, such as particle size. It was demonstrated in Chapter 4 that Au/TiO_2 catalysts prepared by the deposition- precipitation (DP) and colloidal (COL) methods exhibit very good activity towards the AAA reaction. Therefore, both of these methods were employed to prepare the various Au supported catalysts in this study.

To provide a background for the studies described in this Chapter, literature reports investigating the role of the support are discussed (Section 5.1) and following this, the effect of the support on catalyst structure will be presented (Section 5.2).

5.1 Background

It is known that small particle sizes are important for catalyst activity in the AAA reaction.[73] The catalyst support can influence the size of particles generated by reducing the mobility of metal nanoparticles and the tendency of agglomeration, thus changes in activity upon altering the support are often ascribed to the particle size effect.[122] However, supports have been shown to influence the intrinsic activity and selectivity of catalysts by strong-metal support interactions (SMSI).[73] SMSI's arise when atomic layers of support form across the surface of metal particles, which can lead to detrimental outcomes on activity due to the blockage of active sites.[73] Yet activity can be enhanced by the presence of special sites at the perimeter of metal particles, where electronic properties of both the metal and support atoms can influence the adsorbed species.[73, 123] Although C and SiO_2 are commonly used in industry because of their high surface area, they are considered to afford weak metal support interactions.[124] In recent years there has been increasing shift towards replacing these supports with the likes of porous TiO_2, CeO_2 and ZrO_2, which are believed to lead to stronger metal-support interactions allowing for increases in activity, selectivity and the lifetime of the deposited metal particles.[124]

Catalyst preparation and calcination methods can invoke variations in Au particle size when using different supports, especially ones with weak metal-support interactions such as SiO_2 and C, which often contain aggregated metal particles.[125] Thus the role of the support is difficult to isolate as it is intertwined with the influence of the metal particle size. Haruta and co-workers have reported on different Au supported catalysts for the alkylation of **2.2** by **2.1**, where it was found that the selectivity for **2.4** and conversion of **2.1** changed depending on the support employed.[75] This was attributed to the hydrogen bonding ability of catalysts, which was postulated to be important for the adsorption of **2.2**, and to differences in the adsorption of substrates and intermediates on to the catalyst surface. The acid and base properties of the metal oxide support was thought to be important for the adsorption of species on the catalyst, which was uncovered by plotting the conversion against the electronegativity of the metal ions (χi) in the support (Figure 5.1). χi is expressed as $\chi i=(1+2z)\ \chi_0$, where χ_0 is the Pauling's electronegativity of the metal element and z is the valence of metal ions.[75] The surface of metal oxides comprises of acidic and basic species, where the cationic metal centres act as Lewis acid sites and anionic oxygen centres as Lewis base sites.[126] It was hypothesised that alcohol dehydrogenation requires the presence of basic sites to abstract the hydroxyl hydrogen from alcohol to form the alkoxide species, and an

acidic site is needed to remove hydrogen from the alkoxide as a hydride.[61, 62] The plot shows that the conversion of **2.1** (to products and intermediates from the reaction with **2.2**), is highest for Au supported catalysts with a balance of acidic and basic sites. This suggests that there is a necessity for a balance of acid-base sites to facilitate the formation of the amine product and for the adsorption of substrates onto the catalyst surface. It can be suggested that SMSI's have also influenced the capacity for the adsorption of species in these studies due to the possible migration of support oxide over metal particles.

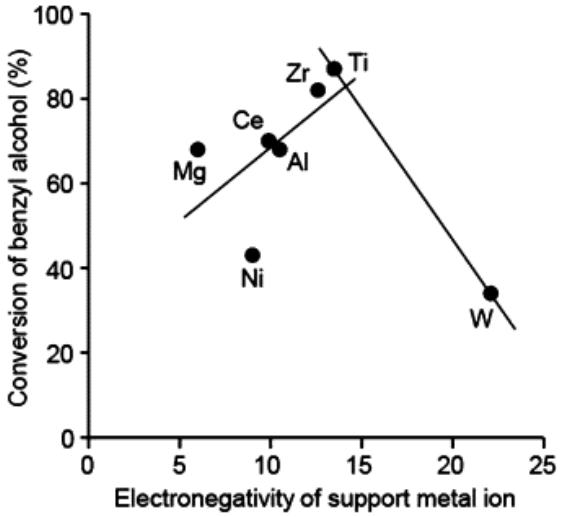


FIGURE 5.1. *Relationship between the electronegativity of metal ions (χi) in metal oxide supports and the conversion of* ***2.1****.*[75]

A direct correlation between the electronegativity of the metal oxide support ions and alcohol conversion was observed in a separate study investigating the amination of natural terpene myrtenol with **2.2** on different Au supported systems.[127] The conversion of myrtenol was shown to be higher for Au/ZrO_2 compared to Au/MgO and Au/Al_2O_3, much the same as in the study presented above.

5.2 The effect of the support on catalyst structure

Table 5.1 shows the Au supported catalysts synthesised in this study by the COL and DP methods along with the thermal treatments employed and Au loading results (wt.%). Note that BET and TEM analysis was conducted at Imperial College London and all other catalyst characterisation was performed by Johnson Matthey Plc. The Au/TiO_2 catalysts (Table 5.1, entry 1), are the Au/TiO_2 (DP2) and Au/TiO_2 (COL) systems which have previously been described in Chapter 4. Catalysts will be denoted as 'Au/Support (preparation technique)' from this point forward and the Au/TiO_2 catalyst prepared by the DP technique as Au/TiO_2 (DP2).

TABLE 5.1. *Au supported catalysts synthesised by the COL and DP methods showing the thermal treatments employed and metal loading results.*

		Deposition-precipitation		Colloidal	
Entry	**Catalyst**	**Thermal Treatment (˚C)**	**Metal Loading (wt.%)**	**Thermal Treatment (˚C)**	**Metal Loading (wt.%)**
1	Au/TiO_2	300[a]	0.6	200[a], 100[b]	0.9
2	Au/C	100[b]	1.0	100[b]	0.9
3	$Au/HFeO_2$	300[a]	0.9	200[a], 100[b]	1.0
4	Au/CeO_2	300[a]	1.0	200[a], 100[b]	0.8
5	$Au/\alpha\text{-}Al_2O_3$	-	-	100[b]	0.3
6	$Au/\gamma\text{-}Al_2O_3$	-	-	200[a], 100[b]	0.6
7	Au/SiO_2	-	-	100[b]	0.0

[a] *Under H_2/N_2 for 2 h,* [b] *Oven dried for 24 hours (as-prepared).*

Additional catalysts were synthesised using the COL method as opposed to employing the DP technique (Table 5.1, entries 5-7) due to the greater control of Au particle size by depositing pre-formed particles (Section 4.1.3). The COL method is commonly employed as aggregate growth can be avoided by depositing pre-reduced Au.[128] The DP technique does not work well for the synthesis of SiO_2 supported catalysts, because the high pH conditions required to hydrolyse $HAuCl_4$ induces weak interactions between the negatively charged SiO_2 surface and $[Au(OH)_nCl_{4-n}]^-$ species, which remain in solution.[129] Likewise, it is not the most effective route for the preparation of small Au particles sizes on carbon due to the hydrophobic nature of the support and low density of surface OH groups.[122] In this study both the DP and COL were employed for synthesis of Au/C catalysts for comparison purposes (Table 5.1, entry 2).

The aim was to prepare catalysts with 1 wt.% loading of Au. Apart from Au/TiO_2 (DP2), Au/α-Al_2O_3 (COL), Au/γ-Al_2O_3 (COL) and Au/SiO_2 (COL), (Table 5.1, entries 1, 5, 6 and 7), the metal loadings achieved were close to the expected value. It is known that Au loadings can be increased by using a higher pH in the preparation of Au/TiO_2, by the DP method, however this also results in larger Au particle sizes (Section 4.1.2). The low Au loading for Au/SiO_2 (COL), Au/α-Al_2O_3 (COL) and Au/γ-Al_2O_3 (COL) (Table 5.1, entries 5, 6 and 7) can be explained by the choice of surfactant (1 wt.% poly vinyl alcohol, PVA).[130] PVA has been shown to be an unsuitable surfactant for SiO_2 and Al_2O_3 supported catalysts in a previous study, with the primary problem being the strong dependency on the concentration of Au for efficient immobilisation.[128] Due to the absence of Au on SiO_2, studies were not progressed further with this catalyst.

The COL method employed relies on a washing step (refluxing material at 90 ˚C for 2 hours) to remove PVA. In order to determine whether the surfactant had been removed, elemental analysis (carbon, hydrogen and nitrogen) was conducted (performed by London Metropolitan University analytical department) (Table 5.2).

TABLE 5.2. *CHN analysis of Au supported catalysts synthesised using the COL method.*

Entry	Catalyst	Carbon (wt.%)
1	Au/TiO_2 (COL)	<0.1
2	Au/α-Al_2O_3 (COL)	<0.1
3	Au/γ-Al_2O_3 (COL)	<0.1
4	Au/C (COL)	N/A
5	Au/$HFeO_2$ (COL)	0.4
6	Au/CeO_2 (COL)	0.5

Very low amounts of carbon was present in the Au/TiO_2 (COL) and Au/Al_2O_3 (γ and α) (COL) catalysts (Table 5.2, entries 1-3), which implies that the reflux method has been successful in removing PVA from these systems. For Au supported on $HFeO_2$ and CeO_2 it was found that roughly 50% of carbon was still present (Table 5.2, entries 5 and 6), due to residual PVA. As a result, these catalysts were calcined (under H_2/N_2 at 200 ˚C for 2 hours), as this has been demonstrated to be an effective technique for the removal of PVA.[112] However, it can also cause increases in Au particle size, as demonstrated by Au/TiO_2 (COL) (Section 4.2). In order to compare differences in activity between calcined and as-prepared (oven dried only) catalysts, Au/γ-Al_2O_3 (COL) was also calcined under the same conditions and tested for its activity (Table 5.1, entry 6). As-prepared Au/C (COL), Au/α-Al_2O_3 (COL) and Au/SiO_2 (COL) (Table 5.1, entries 2, 5 and 7) were not thermally treated because of the

known difficulties in the preparation of small Au particle sizes using these supports and the particle growth that high temperatures can induce. Similarly, Au/C (DP) was not calcined for the same reasons. The other catalysts prepared by the DP method were calcined under reducing conditions at 300 ˚C, (Table 5.1, entries 1, 3 and 4) as this was shown to produce the most active Au/TiO_2 catalyst in Chapter 4.

BET analysis was conducted on the as-prepared catalysts synthesised by the COL method (Table 5.3, entries 1-6). The surface area of Au/TiO_2 (COL) is in good agreement with commercially available Au/TiO_2 (Strem AUROlite^{TM}) (47 m^2 g^{-1}) (Table 5.3, entry 1).[77] Likewise the values obtained for Au/Al_2O_3 (γ and α) (COL), Au/CeO_2 (COL) and $Au/HFeO_2$ (COL) are close to values reported in the literature (Table 5.3, entries 2-5).[131-134] The surface area of Au/C (COL) was lower than expected (Table 5.3, entry 6); activated charcoal generally has surface areas in the region of 700-1600 (m^2 g^{-1}).[135, 136] . It can be suggested that PVA has adhered to the support resulting in a lower than expected value or the charcoal support used (GSX) has an inherently low surface area.

TABLE 5.3. *BET surface area measurements of Au supported catalysts prepared by the COL method.*

Entry	Catalyst	BET surface area (m^2 g^{-1})
1	Au/TiO_2 (COL)	55 (±0.20)
2	$Au/HFeO_2$ (COL)	16 (±0.03)
3	Au/CeO_2 (COL)	242 (±1.25)
4	Au/α-Al_2O_3 (COL)	13 (±0.01)
5	Au/γ-Al_2O_3 (COL)	141 (±0.20)
6	Au/C (COL)	689 (±7.00)

TEM imaging and particle size measurements of the as-prepared Au/TiO_2 (COL), Au/C (COL), Au/γ-Al_2O_3 (COL) and $Au/HFeO_2$ (COL) catalysts revealed small mean Au particle sizes between 3-4 nm (Figure 5.2 A-D) compared to the Au/α-Al_2O_3 (COL) system (6.5 nm) (Figure 5.2 E). Small Au particles (3-4 nm) as well as very large aggregated Au species (up to 34 nm) where found on Au/α-Al_2O_3 (COL), which is contrast to the narrow size distribution observed for Au/γ-Al_2O_3 (COL) (mean Au particles size of 2.6 nm). The differences can be attributed to the much smaller surface area of α-Al_2O_3 compared to γ-Al_2O_3 (Table 5.3, entry 4 vs. entry 5). This is supported by the same observation and conclusion being reached in a separate study for the preparation Au supported on α-Al_2O_3.[137]

It was difficult to observe Au particles in the Au/CeO_2 (COL) sample due to the poor contrast between the dense support and Au species, and therefore particle size measurements were not possible.

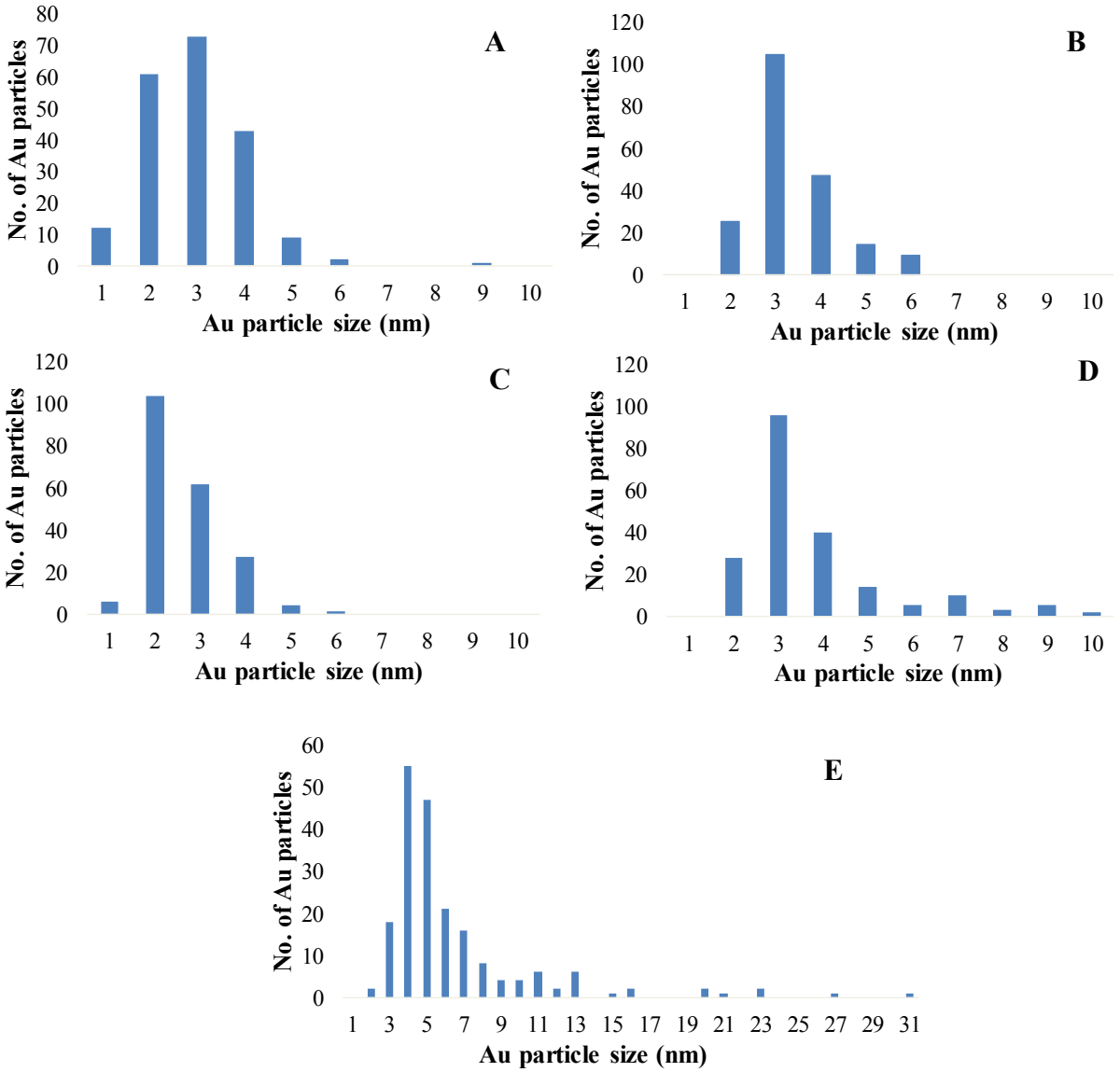


FIGURE 5.2. *Particle size distribution graphs of as- prepared* ***A)*** *Au/TiO_2 (COL),* ***B)*** *Au/C (COL),* ***C)*** *Au/γ-Al_2O_3 (COL),* ***D)*** *Au/$HFeO_2$ (COL),* ***E)*** *Au/α-Al_2O_3 (COL). (~200 Au particles were measured)*

Small and evenly distributed Au particles were found in the Au/TiO_2 (DP2) sample (mean size of 3.4 nm) (Figure 5.3 A). Large (up to 13 nm) and small (2-3 nm) Au particles were observed in the $Au/HFeO_2$ (DP) catalyst with a mean Au particle size of 4.8 nm (Figure 3 B). TEM imaging of Au/C (DP) revealed the presence of large (up to 39 nm) and small Au particles with a mean particle size of 15.4 nm (Figure 5.3 C). The formation of large Au species on this support is not unexpected, because as highlighted earlier, the DP method is not the most effective technique for the preparation of Au/C due to the hydrophobic nature of this support. Compared to the DP method, the COL method allowed for better control of particle size for this system, likely due to the deposition of pre-formed reduced Au particles.

Similar to the Au/CeO_2 catalyst prepared via the COL method, it was very difficult to observe Au particles in the Au/CeO_2 (DP) system due to the poor contrast between the dense support and Au species, and therefore particle size measurements were not possible.

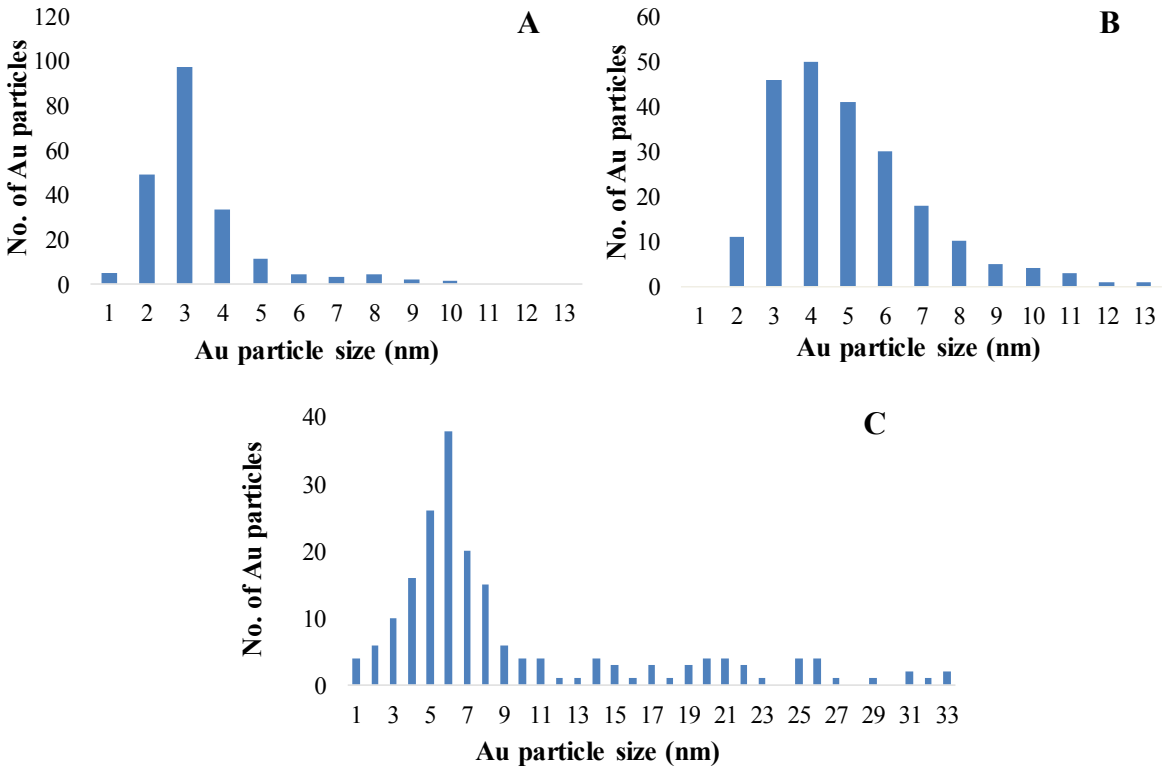
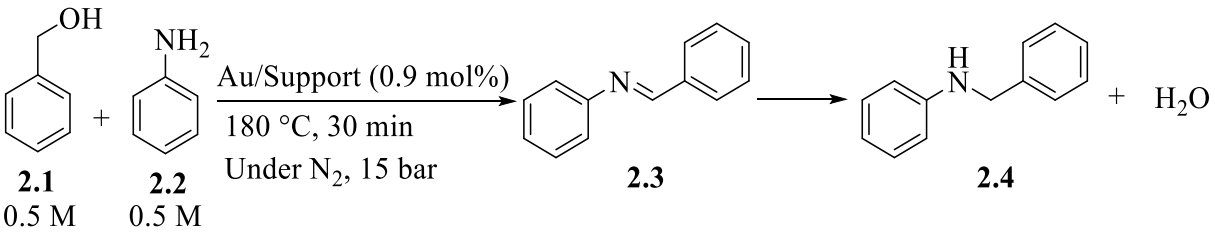


FIGURE 5.3. *Particle size distribution graphs of* ***A)*** *Au/TiO_2 (DP2),* ***B)*** *$Au/HFeO_2$ (DP),* ***C)*** *Au/C (DP) (~200 Au particles were measured).*

5.3 Catalyst screening results and analysis

The model system of **2.1** with **2.2** was chosen to test the activity of the Au supported catalysts using the Endeavor® batch reactor using the same conditions as those employed in Chapter 4 to allow for the comparison of results (Scheme 5.2).



SCHEME 5.2. *The alkylation of **2.2** with **2.1** for the screening of Au supported catalysts prepared by the COL and DP techniques, using a batch reactor.*

As a control experiment, supports were tested for their activity towards the reaction in the absence of Au. Very low conversions of **2.1** (1-2%) was achieved for TiO_2, $HFeO_2$ and C, whereas CeO_2 gave a slightly higher conversion of **2.1** (7%) to **2.3** and **2.4**. The acid-base properties and abundance of oxygen lattice vacancies in CeO_2[138] may have been factors which enhanced the conversion of **2.1**, particularly for the first step in the reaction whereby the alcohol is oxidised to the carbonyl species. Overall, the results indicate that the presence of metal is integral for catalytic activity.

5.3.1 Au supported catalysts prepared by the DP method

Catalytic screening of the Au supported catalysts prepared by the DP method revealed that the TOF and selectivity is significantly varied upon altering the catalyst support (Table 5.4).

TABLE 5.4. *Results for the conversion of* ***2.1*** *to products for Au supported catalyst prepared by the DP method.*

				Selectivity (%)			
Entry	**Catalyst**	**Conversion (%)[a]**	**TOF (h^{-1})[b]**	**2.4**	**2.3**	**PhCHO**	**Toluene**
1	Au/TiO_2 (DP2)	89	192	95	2	0	3
2	$Au/HFeO_2$ (DP)	47	101	90	9	1	0
3	Au/C (DP)	1	2	19	58	23	0
4	Au/CeO_2 (DP)	15	32	86	12	2	0

[a] Determined by GC using 4-tert-butylphenol as an external standard, based on ***2.1****. Results are an average of 2 runs (error ± 2%).[b] TOF (h^{-1}) (moles of benzyl alcohol converted/moles of Au).*

Au/TiO_2 (DP2) was the most active and selective system tested, followed by $Au/HFeO_2$ (DP) which showed good selectivity but a moderate TOF (Table 5.4, entries 1 and 2). Au/TiO_2 (DP2) had a mean Au particle size of 3.4 nm and a narrow particle size distribution; whereas $Au/HFeO_2$ (DP) had both large and small Au particle sizes present (Section 5.2). The mixture of particle sizes could explain the lower TOF afforded compared to the Au/TiO_2 (DP2) catalyst, as small particle sizes are known to be more active in the AAA reaction.[73] This is supported by the low activity obtained for Au/C (DP) (Table 5.4, entry 3) which had a mean Au particle size of 15.4 nm (Section 5.2). The selectivity for **2.4** achieved by Au/C (DP) was very low, which may highlight the necessity of having small particle sizes to facilitate the reduction of **2.3**. Indeed, the decrease in selectivity for **2.4** of the Au/TiO_2 catalyst (prepared by the DP method) following calcination at 800 ˚C (described in Chapter 4) was attributed to increases in Au particle size.

Justifying the low TOF value afforded by Au/CeO_2 (DP) (Table 5.4, entry 4), i.e. whether a support or particle size influence is in effect, was not possible due to the fact that the Au particle sizes could not be determined (Section 5.2). Given that the trend observed thus far shows that small particle sizes lead to higher selectivities and conversions, it is not unreasonable to assume that a mixture of small and large Au particles were present in the Au/CeO_2 (DP) catalyst. As the bare CeO_2 support was shown to convert **2.1** to products and intermediates (7%) it can be suggested that the support plays a role in catalysing the reaction perhaps through SMSI's. Apart from Au/CeO_2 (DP), it was difficult to comment on whether SMSI's were involved in catalysing the reaction for the other Au supported materials due to the varied Au particle sizes. To distinguish whether the differences in conversion could be attributed to changes in Au particle size, the TOF was plotted against the mean Au particle size for Au/TiO_2 (DP2), $Au/HFeO_2$ (DP) and Au/C (DP) (Figure 5.4).

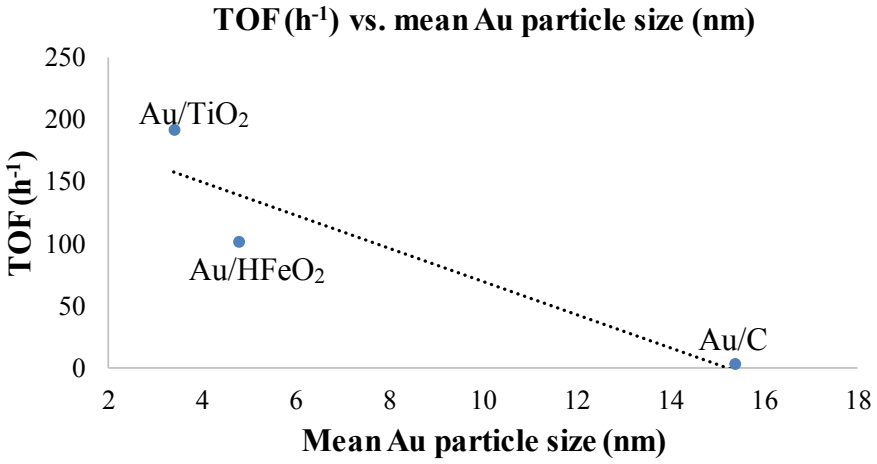


FIGURE 5.4. *TOF versus mean Au particle size for the Au supported catalysts. Note that the trend line is a guide and does not have any quantitative significance.*

A relationship of decreasing TOF with increasing particle size was revealed, indicating that variations in activity was influenced by changes in Au particle size. This implies that the main function of the support is to prevent Au agglomeration.

5.3.2 Au supported catalysts prepared by the COL method

As-prepared (oven dried at 100 ˚C for 24 hours) and calcined catalysts (under H_2/N_2 at 200 ˚C for 2 hours) were screened for their activity towards the amination of **2.2** with **2.1**, the results for calcined catalysts are shown in parenthesis.

It was found that conversion and selectivity varies significantly upon changing the catalyst support for the as-prepared systems (Table 5.5)

TABLE 5.5. *Results for the conversion of* ***2.1*** *to products for Au supported catalyst prepared by the COL method.*

						Selectivity (%)							
Entry	**Catalysts**	**Conversion (%)[a]**		**TOF (h^{-1})[b]**		**2.4**		**2.3**		**PhCHO**		**Toluene**	
1	Au/TiO_2 (COL)	**80**	*(66)*	**172**	*(142)*	**96**	*(96)*	**3**	*(3)*	**0**	*(0)*	**1**	*(1)*
2	$Au/\gamma\text{-}Al_2O_3$ (COL)	**84**	*(71)*	**181**	*(153)*	**95**	*(93)*	**4**	*(5)*	**1**	*(1)*	**1**	*(2)*
3	Au/C (COL)	**1**	-	**2**	-	**8**	-	**64**	-	**0**	-	**-**	*(27)*
4	$Au/\alpha\text{-}Al_2O_3$ (COL)	**6**	-	**13**	-	**74**	*(24)*	**-**	-	**1**	-	**1**	-
5	$Au/HFeO_2$ (COL)	**41**	*(54)*	**88**	*(116)*	**79**	*(81)*	**16**	*(12)*	**2**	*(0)*	**3**	*(6)*
6	Au/CeO_2 (COL)	**42**	*(28)*	**90**	*(60)*	**96**	*(82)*	**2**	*(13)*	**2**	*(1)*	**0**	*(4)*

[a] Determined by GC using 4-tert-butylphenol as an external standard, based on ***2.1****. Results are an average of 2 runs (error ± 3%).[b] TOF (h^{-1}) (moles of benzyl alcohol converted/moles of Au). Calcined catalyst results shown in parenthesis.*

As-prepared $Au/\gamma\text{-}Al_2O_3$ (COL) and Au/TiO_2 (COL) afforded the largest TOF's and selectivities with similar activities (Table 5.5, entries 1 and 2). This can be attributed to the small mean Au particle sizes (~3 nm) in these samples. Following calcination, the conversion of these two systems decreased (Table 5.5, entries 1 and 2); however, the selectivity for **2.4** remained constant. In previous work in Chapter 4 the decrease in activity of the Au/TiO_2 (COL) after calcination was attributed to increases in the mean Au particle size (from 2.9 nm to 4.2 nm) and thus it can be postulated that sintering has also occurred in the $Au/\gamma\text{-}Al_2O_3$ (COL) catalyst.

As-prepared Au/C (COL) had a mean Au particle size of 3.4 nm; however, it did not exhibit comparable activities to that achieved by $Au/\gamma\text{-}Al_2O_3$ (COL) and Au/TiO_2 (COL) (Table 5.5, entry 3 vs. entries 1 and 2). Agglomeration of Au particles could have occurred during the alkylation of **2.2** with **2.1**, which could explain this result. Therefore, TEM analysis was conducted of Au/C (COL) and the other as-prepared catalysts following the reaction (Table 5.6 and Figure 5.5). The mean Au particle size remained stable for $Au/\gamma\text{-}Al_2O_3$ (COL), Au/TiO_2 (COL), and $Au/HFeO_2$ (COL) (Table 5.6, entries 1-3) with a slight increase in particle size for $Au/\alpha\text{-}Al_2O_3$ (COL) (Table 5.6, entry 4). However, substantial growth of Au was revealed for the Au/C (COL) catalyst following the reaction (Table 5.6, entry 5). This may be attributed to the hydrophobic nature of the support and the known weak metal support interactions of carbon.[124, 139]

TABLE 5.6. *Mean Au particle sizes (nm) before and after the reaction of* ***2.1*** *with* ***2.2*** *for as-prepared colloidal catalysts.*

Entry	Catalyst	Before reaction (nm)	After reaction (nm)
1	Au/γ-Al_2O_3 (COL)	2.6 (± 0.1)	3.2 (± 0.1)
2	Au/TiO_2 (COL)	2.9 (± 0.1)	3.4 (± 0.1)
3	Au/$HFeO_2$ (COL)	3.7 (± 0.1)	4.3 (± 0.2)
4	Au/α-Al_2O_3 (COL)	6.5 (± 0.3)	8.4 (± 0.5)
5	Au/C (COL)	3.4 (± 0.2)	8.7 (± 0.1)
6	Au/CeO_2 (COL)*	-	-

* *Particle size measurements were not possible due to the poor contrast between Au and the support.*

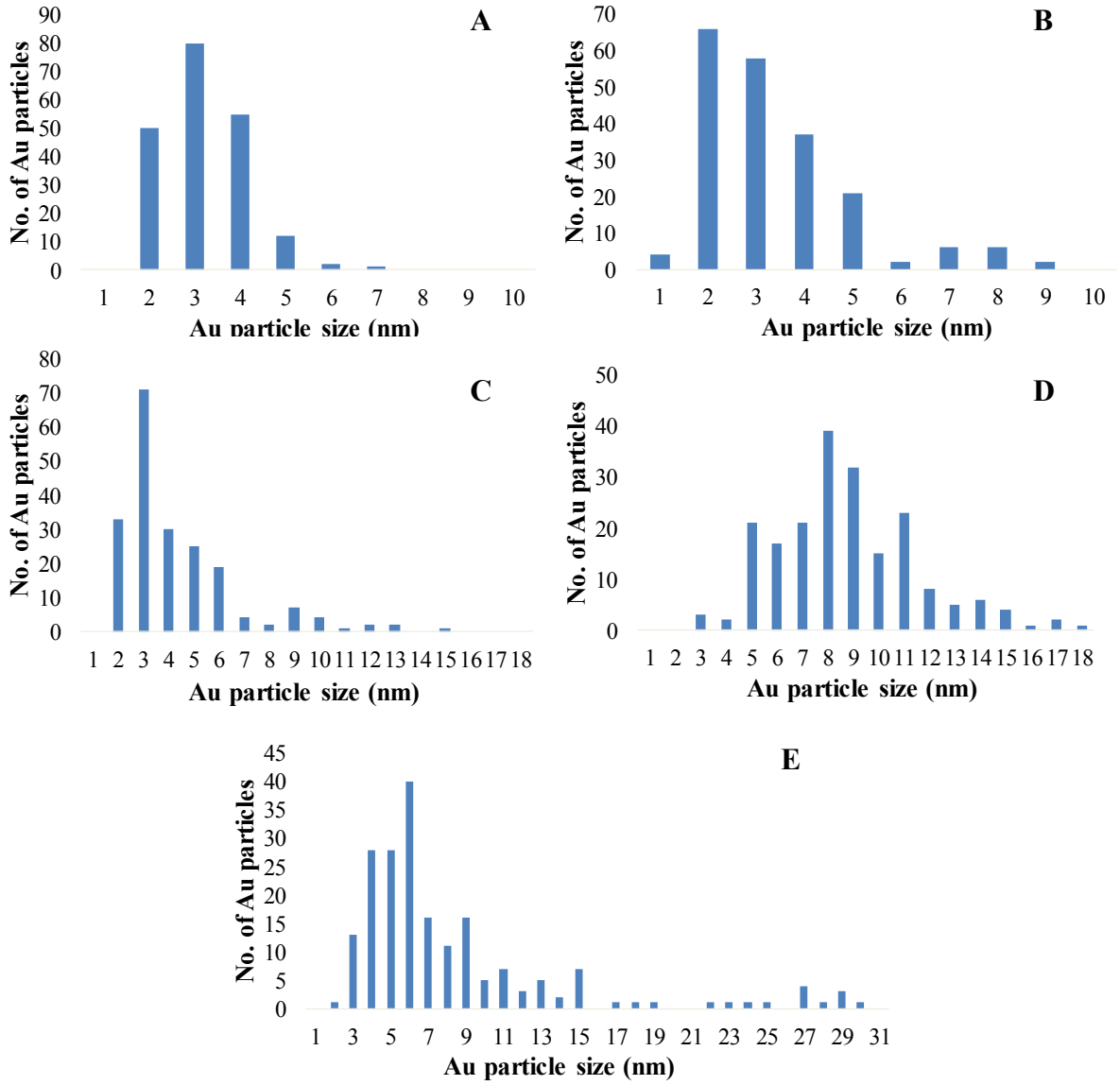


FIGURE 5.5. *Particle size distribution graphs of* ***A)*** *Au/γ-Al_2O_3 (COL),* ***B)*** *Au/TiO_2 (COL),* ***C)*** *Au/$HFeO_2$ (COL),* ***D)*** *Au/C (COL),* ***E)*** *Au/α-Al_2O_3 (COL), following the alkylation of* ***2.1*** *with* ***2.2*** *(180 ˚C, 15 bar, under N_2 for 30 min). (~200 Au particles were measured).*

The low TOF and selectivity generated by Au/α-Al_2O_3 (COL) (Table 5.5, entry 4) is not surprising given the large aggregates of Au observed by TEM analysis (mean particle size 6.5 nm) (Section 5.2).

Although small Au particle sizes were present in the as-prepared Au/$HFeO_2$ (COL) catalyst (3.7 nm), with no increases in size following the reaction (Table 5.6, entry 3), the selectivity for **2.4** was reduced compared to the same system synthesised by the DP method (79% vs. 90%) (Table 5.5, entry 5 vs. Table 5.4, entry 2), which had a mean particle size of 4.8 nm. The lower conversion afforded by Au/$HFeO_2$ (COL) could be due to residual PVA covering active sites. Indeed it was shown by CHN analysis that ~50% of carbon, was still present following the catalyst washing step (Section 5.2). Calcination was conducted to help facilitate the removal of PVA, which appears to have been successful as the conversion and selectivity for **2.4** increased (Table 5.5, entry 5).

Au/CeO_2 also had ~50% carbon present following the washing step, however the calcined sample generated a lower conversion and selectivity for **2.4** (Table 5.5, entry 6), which could be due to the sintering of Au particles. Overall the activity of Au/CeO_2 (COL) was much higher in contrast to the analogous system made by the DP method (Table 5.5, entry 6 vs. Tab1e 5.4, entry 4), thus it can be suggested that larger Au particle sizes were present in the Au/CeO_2 (DP) catalyst. Certainly, the TOF decreases as the mean Au particle size increases (prior to the reaction) (Figure 5.6). Note that significant agglomeration of particles was found following the reaction using Au/C (COL), hence the low TOF (Figure 5.6).

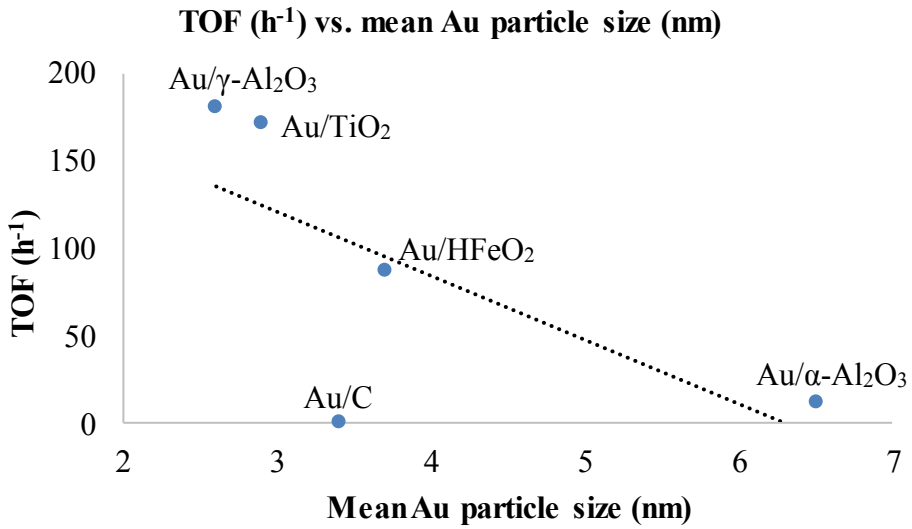


FIGURE 5.6. *TOF versus mean Au particle size for the Au supported catalysts. Note that the trend line is a guide and does not have any quantitative significance.*

As well as small particle sizes being integral for catalytic activity, it was postulated that a balance of acid-base support sites is important for the adsorption of substrates and formation of amine product in the AAA reaction (described in Section 5.1).[75] A volcano type relationship between the electronegativity of the metal support and conversion of alcohol was observed in these studies. In order to see whether the same trend is found in this study, the conversion of **2.1** afforded by as-prepared COL systems was plotted against the electronegativity of the metal support metal (χi) (Figure 5.7).

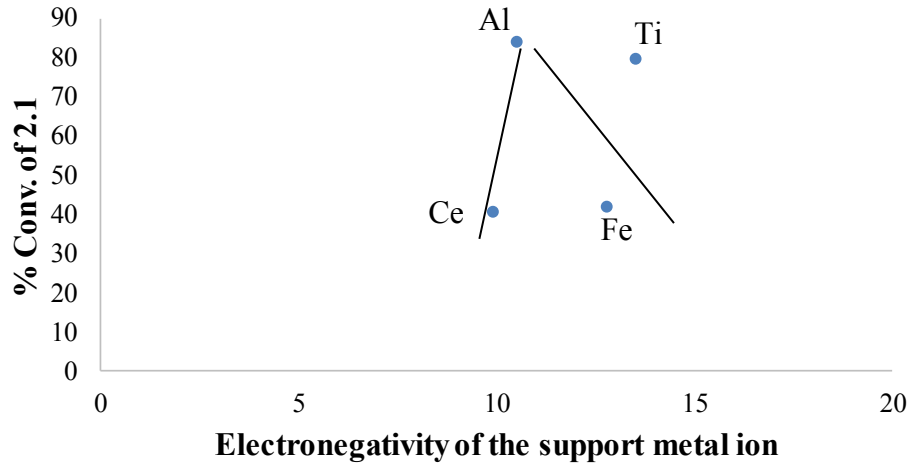


FIGURE 5.7. *Relationship between the electronegativity of metal ions (χi) in metal oxide supports and the conversion of* ***2.1****.*

A strong volcano type relationship was not observed in this work, and the activity seems to be mainly as a result of the Au particle size rather than the acid-base properties of the support. This is because the highest conversion was achieved using Au/TiO_2 (COL) and $Au/\gamma\text{-}Al_2O_3$ (COL), both of which had the smallest mean Au particle sizes (~3 nm) and appear at the top of the chart and $Au/HFeO_2$ (COL) which had slightly larger Au particles (~4 nm) appears in the middle of the chart. The acid-base sites could potentially be facilitating the reaction, however working alongside Au, because it was shown that in the absence of metal, the majority of the supports were inactive for the alkylation of **2.2** with **2.1** (Section 5.3).

The selectivity of the catalysts also seems to be a function of Au particle size, with smaller particles being more selective for **2.4**. Hydrogen temperature programmed desorption (H-TPD) was conducted (by Johnson Matthey Plc analytical department) to compare whether there were any differences in the binding of H_2 to the different as-prepared Au supported COL catalysts. The binding strength of H_2 on the catalyst surface is an important parameter to take into consideration for the reduction of imine in the AAA reaction. It can be imagined that decreases in the selectivity for **2.4** could arise for catalysts that bind H_2 too weakly or

strongly. In order to produce a crude binding energy, the peak integration values from H-TPD analysis were multiplied by the peak desorption temperatures, this was then compared against the selectivity for **2.4** (Figure 5.8, Table 5.7).

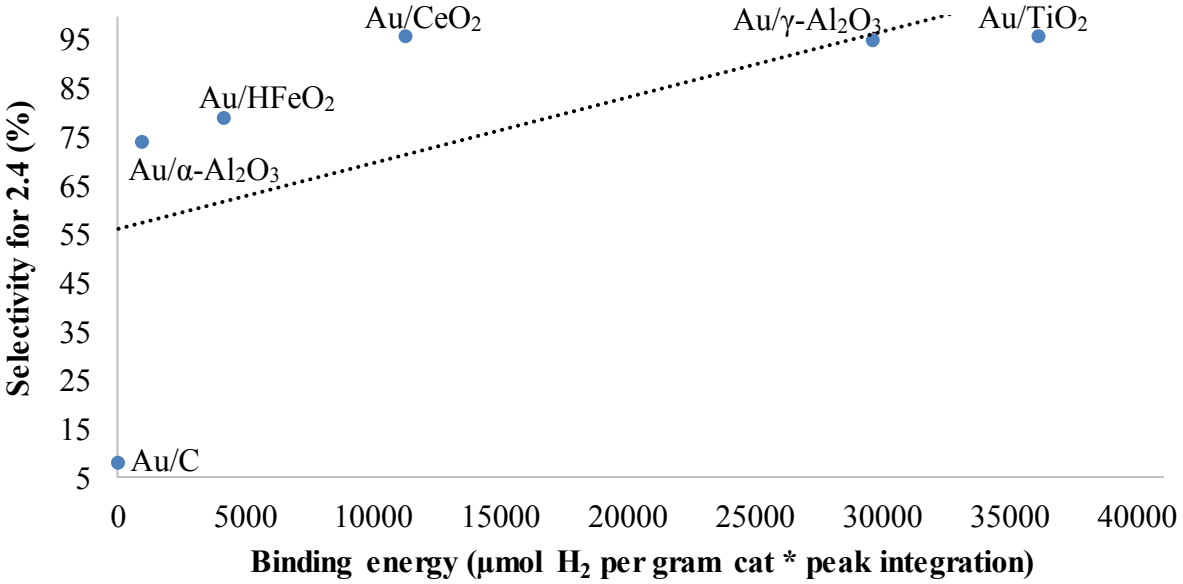


FIGURE 5.8. *Comparison of binding energy versus selectivity for* ***2.4*** *for the Au supported catalysts.*

TABLE 5.7. *Comparison of binding energy versus selectivity for* ***2.4*** *for the Au supported catalysts.*

Entry	Catalyst	Binding energy (µV K^{-1})	% Selectivity for 2.4
1	Au/TiO_2 (COL)	36136	96
2	Au/γ-Al_2O_3 (COL)	29610	95
3	Au/C (COL)	0	8
4	Au/α-Al_2O_3 (COL)	928	74
5	$Au/HFeO_2$ (COL)	4108	79
6	Au/CeO_2 (COL)	11231	96

As the selectivity for **2.4** increases, so the H_2 binding strength. The Au/TiO_2 (COL) and Au/γ-Al_2O_3 (COL) catalysts, both of which had the smallest mean Au particle sizes (~3 nm) and highest selectivities for **2.4** (Table 5.7, entries 1 and 2), displayed the strongest affinity for H_2. Whereas Au/C (COL), which exhibited agglomeration of particles following the reaction (mean particle size of 8.7 nm), and Au/α-Al_2O_3 (COL), which had large particle sizes prior to the reaction (mean particle size of 6.5 nm), afforded the lowest H_2 binding strengths and selectivities for **2.4** (Table 5.7, entries 3 and 4). Overall, the results suggest that the selectivity is a function of H_2 binding efficiency, which seems to be inherently related to

the Au particle size. Indeed, a Au particle size dependency has been reported for H_2 chemisorption, where it was suggested that only Au surface atoms of low coordination number form Au-H_2 complexes.[140]

Au/$HFeO_2$ (COL), which had a mixture of small and large Au particles (Section 5.2), shows a fairly low H_2 binding strength (Table 5.7, entry 5). Even though Au/CeO_2 (COL) had comparable selectivity for **2.4** to that of Au/TiO_2 (COL) and Au/γ-Al_2O_3 (COL) (Table 5.7 entry 6 vs. entries 1 and 2), the H_2 binding strength was significantly lower. Particle measurements were not possible with this system; however, a high selectivity indicates that small particles were present. CHN analysis did indicate that PVA was still present in this sample, which could be the reason for the reduced binding strength.

In order to assess the stability of Au particles on the support, as-prepared catalysts were used for the alkylation of **2.1** with **2.2** (180 ˚C, 30 minutes, 15 bar under N_2, 0.9 mol% Au), the catalyst was then filtered and the resulting solution subjected to ICP analysis.

Very low levels of Au was detected for all the systems analysed (Table 5.8, entries 1-6), if all Au species leached into the solution a value of 100% would be expected. This confirms the stability of Au to the various supports during the reaction.

TABLE 5.8. *ICP results showing the % of Au leached for as-prepared Au supported catalysts following the alkylation of* ***2.1*** *with* ***2.2****.*

Entry	Catalyst	Au that was found in solution (%)	ppm
1	Au/TiO_2 (COL)	0.1	0.02
2	Au/C (COL)	0.1	0.03
3	Au/$HFeO_2$ (COL)	0.2	0.04
4	Au/CeO_2 (COL)	0.3	0.05
5	Au/α-Al_2O_3 (COL)	0.2	0.03
6	Au/γ-Al_2O_3 (COL)	0.1	0.02

Similar to the conclusion drawn for the catalytic screening of materials prepared by the DP method, the variations in activity seem to be influenced by changes in Au particle size; implying that the main function of the support was to prevent Au agglomeration.

5.4 Conclusion

Overall, the differences in activity of the various catalysts synthesised by the DP and COL method was attributed to variations in Au particle size. It was shown that the larger the Au particles were, the lower the conversion and selectivity for **2.4**. The reduction in selectivity for catalysts prepared by the COL method was shown to be correlated to the H_2 binding efficiency, which was postulated to be inherently related to the Au particle size. This is because catalysts exhibiting larger Au particles showed a decreased affinity for H_2 and a lower selectivity for **2.4**. Thus, the results indicate that small Au particles are important for the binding of H_2 and accordingly, the reduction of **2.3**.

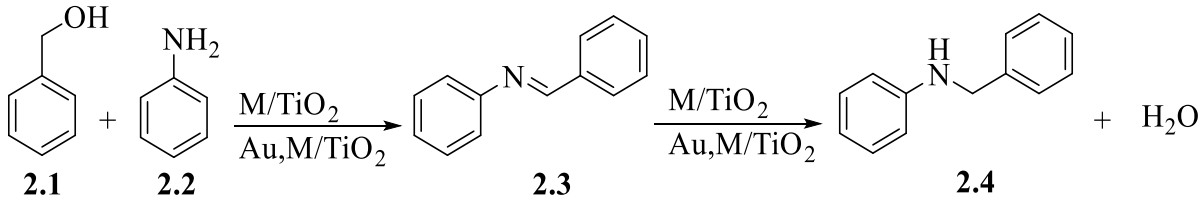
Due to the differences in particle size, it was difficult to establish whether the support was influencing catalytic activity as it is by nature interlinked with controlling the Au particle size. There was no correlation between alcohol conversion and the metal ion support electronegativity (which is a function of support acidity) observed for catalysts prepared by the COL method. It can be suggested that that the acid-base sites of the supports facilitate the reaction but working alongside Au (basic sites for the dehydrogenation of **2.1** and acid sites for the formation of **2.4**) because in the absence of metal, the majority of the supports were inactive for the alkylation of **2.2** with **2.1**. CeO_2 was active to a degree for the conversion of **2.1** (7 %) confirming that in some cases the support can take an active role in the reaction, perhaps through SMSI's, rather than acting as an inert particle stabiliser.

The DP method was unsuitable for forming small Au particles on carbon resulting in an inactive catalyst. The COL method was successful in preparing small Au particles with similar sizes for the majority of the systems, including Au/C. However, sintering of Au particles occurred during the reaction for this system. Similarly, it was found that Au agglomerated on α-Al_2O_3, likely due to the low surface area of this support. Thus in terms of designing a suitable catalyst for the AAA reaction, a support that prevents agglomeration of Au particles during the reaction and catalyst synthesis is important. In this context, Au/TiO_2 (prepared by the COL and DP method) and Au/γ-Al_2O_3 (prepared by the COL method) were shown to be the most active systems tested for the formation of **2.4** with stable Au particles, therefore TiO_2 and γ-Al_2O_3 are suitable supports for preparing Au catalysts to employ in the AAA reaction.

CHAPTER 6. Investigation of Au bimetallic and metal titania catalysts for the AAA reaction

As described in Chapter 1, there have been numerous heterogeneous catalysts reported for the AAA reaction. However, many of these processes are limited by their poor selectivity and high temperatures required (up to 400 ˚C) which can prevent their application for the synthesis of thermally-sensitive molecules (Chapter 1).

Previously, it has been demonstrated that Au/TiO_2 catalyses the selective transformations of a variety of amines and alcohols.[77] In this Chapter, other catalysts were examined, with the aim to discover if there is an alternative that may be more active and/or more cost effective. Bimetallic catalysts containing Au, as well as other metal catalysts supported on TiO_2, were synthesised and characterised. Their ability to facilitate the formation of C-N bonds in the alkylation of **2.2** by **2.1** was subsequently assessed in parallel using the Endeavor® batch reactor (Section 4.3) (Scheme 6.1).



SCHEME 6.1. *The alkylation of* ***2.2*** *with* ***2.1*** *for the screening of M/TiO_2 and $Au.M/TiO_2$ catalysts, using a batch reactor.*

A background for the choice of the metals, preparation technique and support selected is presented next, with the following Sections showing results from the characterisation and catalytic screening of the M/TiO_2 and $Au,M/TiO_2$ systems.

6.1 Background

The hydrogen borrowing mechanism constitutes two redox transformations. Namely, the oxidation of alcohol to form the carbonyl species and the reduction of imine to afford the amine product. Therefore, it is essential to select a metal that can facilitate both of these transformations in the design of a new catalytic system. In light of the broad applicability of Au/TiO_2 for the AAA reaction, other metals supported on TiO_2 from Group 11 (Cu and Ag) were chosen to be synthesised in this study to determine if they also exhibited activity for this reaction. Metals from Group 10 were selected (Pt, Pd and Ni) as they are known to be active towards oxidation and hydrogenation reactions,[77, 141-150] both of which are vital steps in the AAA reaction. Group 9 metals are already known to be active in the AAA reaction in the homogeneous form (Ru, Rh and Ir) (Chapter 1), and therefore were included in this study. Trends in periodicity are well known and metals from the *d*-block are widely employed in heterogeneous catalysis due to the range of oxidation states that can be achieved. It is of interest to analyse whether trends in activity are found, for example, whether increases in activity and metal stability are observed on descending a group due to the higher melting points and stability of oxidation states.

Au bimetallic catalysts, incorporating metals from Group 9, 10 and 11 were also supported on TiO_2 in order to see if the catalyst performance could be enhanced by introducing an additional metal. Indeed, there have been numerous investigations where Au bimetallic catalysts have been employed as a means of improving results. It was found that the addition of a second metal enables intrinsic problems related to Au to be overcome, such as the aggregation and sintering of nanoparticles at high temperatures.[151]

The selection of an appropriate support and method of synthesis are also fundamental considerations when designing a catalyst. In this study, catalysts were supported on TiO_2 and prepared primarily using the deposition-precipitation (DP) method. Spray drying (SD) was deployed for the synthesis of additional Cu/TiO_2 catalysts (Section 6.4), because Au supported systems made by this technique were shown to be active and selective for the formation of **2.4** (Chapter 4 and 5). Furthermore, there exists a strong metal-support interaction (SMSI) between TiO_2 and many metals (Chapter 5).[152, 153]

6.2 M/TiO_2 catalyst characterisation

Note that all catalyst characterisation and calcination was performed by Johnson Matthey Plc unless stated otherwise. Table 6.1 shows the M/TiO_2 catalysts prepared in this study by the DP method and their metal loading. The aim was to prepare systems with a 1 wt.% metal loading and it can be seen that for all catalysts synthesised the loadings reached the expected value or were close to it (Table 6.1, entries 1-8).

TABLE 6.1. *M/TiO_2 catalysts synthesised showing the metal loading results.*

Entry	Catalyst	Metal loading (wt.%)
1	Cu/TiO_2	1.0
2	Ni/TiO_2	1.0
3	Co/TiO_2	1.0
4	Ag/TiO_2	0.8
5	Rh/TiO_2	1.0
6	Pd/TiO_2	0.9
7	Pt/TiO_2	1.0
8	Ir/TiO_2	1.1

It was shown in Chapter 4 that high calcination temperatures (>300 ˚C) can cause particle sintering in Au/TiO_2, thus choosing a suitable pre-treatment is essential. The catalysts were calcined at 300 ˚C under a H_2/N_2 atmosphere to reduce the effects of particle agglomeration. As-prepared (dried in the oven at 100 ˚C for 24 hours) catalysts were also assessed for any differences in conversion and/or selectivity.

TEM images of calcined catalysts were recorded and for several systems, images of the as-prepared materials were taken to determine whether the calcination treatment invoked any changes in particle size. However, for all of the catalysts it was difficult to differentiate between the support and metal nanoparticles due to the low contrast. This was observed for the calcined Ir/TiO_2 catalyst in particular (Figure 6.1 A), where the Ir particles are highlighted in red, confirmed by elemental dispersive x-ray analysis (EDX). This has been reported previously for Ir/TiO_2, where it was concluded that, as a consequence of the SMSI's, the calcination procedure invoked partially reduced TiO_2 moieties to cover Ir particles causing difficulties in distinguishing metal species.[154]

The large dark structures highlighted by yellow arrows are likely to be TiO_2 crystals. This is supported by a TEM image of TiO_2 (P25 Degussa) presented in the literature, showing regions of dense TiO_2 crystal structures (Figure 6.1 B).[155]

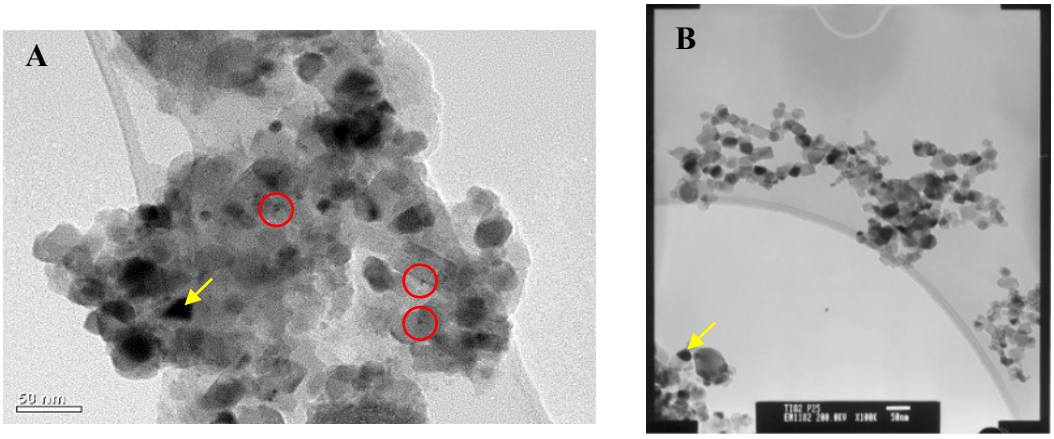


FIGURE 6.1. A) *Calcined Ir/TiO_2 and* ***B)*** *TEM photograph of TiO_2 (P25-Degussa) from the literature.*[155]

In contrast, TEM imaging of the calcined Ag/TiO_2 catalyst showed that a considerable amount of Ag particles did not adhere to TiO_2, but were instead found deposited on the TEM microscopy grid (Figure 6.2). This result can be explained by the TEM sample preparation method, whereby the catalyst is initially suspended in solvent before being transferred onto the microscopy grid. This slight washing effect may have freed any loosely bound Ag particles from the support.

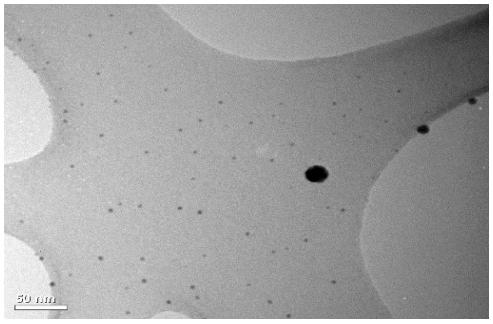
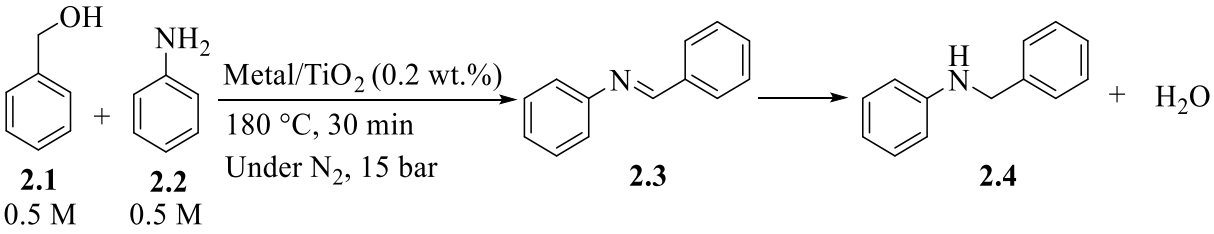


FIGURE 6.2. *TEM photograph of calcined Ag/TiO_2 showing leached Ag species on the TEM grid.*

XRD analysis revealed the presence of anatase and rutile TiO_2 phases in the calcined forms of all catalysts, confirming that calcination treatment has not invoked any major phase changes (from anatase to rutile) in the TiO_2 support employed (P25-Degussa TiO_2, 25% anatase and 75% rutile). This is a common phenomenon associated with TiO_2, usually occurring at temperatures from 500 °C.[119, 120] There were no diffraction lines observed for metal species in any of the patterns, which is most likely because the metal loadings were below the detection limit for the XRD.

6.3 M/TiO_2 screening results and analysis

The model system of **2.1** with **2.2** was chosen to test the activity of the metal supported catalysts employing the Endeavor® batch reactor and using the same general conditions as those employed in Chapter 4 and 5 to allow for the comparison of results (Scheme 6.2). 0.2 wt.% of metal was used in the experiments, thus turnover frequencies (TOF, h^{-1}) based on the moles of benzyl alcohol converted by per mole of metal have been calculated to normalise the results.



SCHEME 6.2. *The alkylation of **2.2** with **2.1** for the screening of M/TiO_2 catalysts prepared by the DP technique, using a batch reactor.*

As mentioned in Chapter 4, bare TiO_2 exhibited very low conversion of **2.1** (1-2%) under these conditions. The Au/TiO_2 catalyst prepared by the DP method in Chapter 4 (Au/TiO_2 (DP2)) was used as a benchmark to compare the activity of the M/TiO_2 catalysts against.

6.3.1 Group 9: M/TiO_2 screening results

It can be seen that Au/TiO_2 was the most active catalyst in terms of its selectivity for **2.4** and turn over frequency (TOF) (Table 6.2, entry 1 vs. entries 2-7).

TABLE 6.2. *Results for the conversion of **2.1** to products for the calcined and as-prepared M/TiO_2 catalysts.*

				Selectivity (%)			
Entry	**Catalyst**	**Conversion (%)[a]**	**TOF (h^{-1})[b]**	**2.4**	**2.3**	**PhCHO**	**Toluene**
1	**Au/TiO_2**	**89**	**192**	**95**	**2**	**0**	**3**
2	Rh/TiO_2	97	109	39	18	0	41
3	Rh/TiO_2 calc.	97	109	39	15	0	46
4	Co/TiO_2	2	1	52	39	0	9
5	Co/TiO_2 calc.	1	0	22	28	0	50
6	Ir/TiO_2	5	11	18	80	1	0
7	Ir/TiO_2 calc.	47	99	76	19	1	4

*[a] Determined by GC using 4-tert-butylphenol as an external standard, based on **2.1**. Results are an average of 2 runs (error ± 2%).[b] TOF (h^{-1}) (moles of benzyl alcohol converted/moles of metal).*

Although both the as-prepared and calcined forms of Rh/TiO_2 exhibited excellent TOF's (Table 6.2, entries 2 and 3), the selectivity for **2.4** was poor and toluene was formed as a by-product in significant quantities (by the disproportionation of **2.1**, described in Chapter 1). There was no effect on the overall activity following calcination of this system, which is in contrast to Co/TiO_2, which had a high selectivity for toluene after thermal treatment (Table 6.2, entry 4 vs. 5). It has been reported that the metal-support interface is important for the disproportionation reaction[156] thus it can be postulated that calcination has invoked changes in the metal-surface interface and/or increased the size of Co particles making toluene formation favourable.

Similarly, the conversion and selectivity for **2.4** was substantially increased after Ir/TiO_2 had been thermally treated (Table 6.2, entries 6 and 7). This effect has been reported previously in the oxidation of alcohols reaction, where it was suggested that the high temperature catalyst pre-treatment (450 ˚C) of Ir/TiO_2 formed oxygen vacancies that allowed for the adsorption and/or activation of alcohol by bringing it within close proximity to the Ir metal centre.[154] Although Ir/TiO_2 was not reduced at temperatures as high as 450 ˚C in this study, it is likely that calcination had a similar effect on the catalyst structure based on the increase in activity observed.

There appears to be no trend in TOF or selectivity within this group. The low activity of the supported Ir and Rh systems in comparison to Au/TiO_2 is surprising given the widespread use and activity of the homogeneous analogues using these metals in the AAA reaction (Chapter 1). Different supports could be tested to see if this enhances the activity, for example, it has been shown that toluene formation can be 'switched off' for Pd based catalysts by using MgO instead of TiO_2 during **2.1** oxidation.[72, 157] This was attributed to differences in the mode of adsorption of **2.1** on the metal-support interface due to the higher basicity of the MgO support.

6.3.2 Group 10: M/TiO_2 screening results

There were no improvements in activity by using Group 10 metals supported on TiO_2 (Table 3, entries 2-6) compared to the Au/TiO_2 catalyst (Table 6.3, entry 1 vs. entries 2-6).

TABLE 6.3. *Results for the conversion of **2.1** to products for the calcined and as-prepared M/TiO_2 catalysts.*

				Selectivity (%)			
Entry	**Catalyst**	**Conversion (%)[a]**	**TOF (h^{-1})[b]**	**2.4**	**2.3**	**PhCHO**	**Toluene**
1	**Au/TiO_2**	**89**	**192**	**95**	**2**	**0**	**3**
2	Pd/TiO_2	100	116	17	20	0	63
3	Pt/TiO_2	66	140	54	11	0	35
4	Pt/TiO_2 calc.	58	124	61	12	0	27
5	Ni/TiO_2	3	2	32	65	2	0
6	Ni/TiO_2 calc.	4	3	67	32	1	0

*[a] Determined by GC using 4-tert-butylphenol as an external standard, based on **2.1**. Results are an average of 2 runs (error ± 2%).[b] TOF (h^{-1}) (moles of benzyl alcohol converted/moles of metal).*

Although the TOF's of Pd and Pt supported on TiO_2 were high (Table 6.3, entries 2, 3 and 4), large amounts of toluene were produced. As mentioned above (Section 6.3.1) basic supports have shown to suppress toluene formation, which could be tried for these systems. Even so, the selectivity for **2.3** afforded by these catalysts was still higher than that of Au/TiO_2 (Table 6.3, entries 2-4 vs. entry 1). Thus, it can be suggested that the hydrogenation of **2.3** is slow for these catalysts. The calcination treatment did not invoke any significant changes in activity for the Pt/TiO_2 catalyst (Table 6.3, entry 3 vs. entry 4).

The low TOF generated for both the as-prepared and calcined Ni catalysts could be due to the absence of a high temperature catalyst pre-treatment, which has been reported to important for the activity of heterogeneous Ni catalysts in the AAA reaction (Chapter 1).[59, 60]

Given that unsupported TiO_2 can catalyse this reaction with a comparable result (1-2% conversion of **2.1**), these catalysts are effectively inactive.

There does not seem to be a trend in activity within this group, however it can be observed that the TOF's of the base metal systems prepared (Ni and Co supported on TiO_2) are considerably lower than the catalysts synthesised using metals from periods 5 and 6 (Rh, Ir, Au, Pd and Pt). As mentioned above, this could be due to the absence of high temperature catalyst pre-treatment, but could also be due to sintering of Ni and Co particles due to their lower melting points when contrasted to the other metals within their respective groups.

6.3.3 Group 11: M/TiO_2 screening results

Au/TiO_2 remained the most active catalyst, when compared to the catalysts synthesised using Group 11 metals (Table 6.4, entry 1 vs. entries 2-5).

***TABLE 6.4**. Results for the conversion of **2.1** to products for the calcined and as-prepared M/TiO_2 catalysts.*

				Selectivity (%)			
Entry	**Catalyst**	**Conversion (%)[a]**	**TOF (h^{-1})[b]**	**2.4**	**2.3**	**PhCHO**	**Toluene**
1	**Au/TiO_2**	**89**	**192**	**95**	**2**	**0**	**3**
2	Ag/TiO_2	2	1	17	83	0	0
3	Ag/TiO_2 calc.	3	2	25	75	0	0
4	Cu/TiO_2	29	20	80	17	1	2
5	Cu/TiO_2 calc.	14	10	61	36	2	1

*[a] Determined by GC using 4-tert-butylphenol as an external standard, based on **2.1**. Results are an average of 2 runs (error ± 2%).[b] TOF (h^{-1}) (moles of benzyl alcohol converted/moles of metal).*

As-prepared and calcined Ag/TiO_2 displayed very poor performance in the reaction (Table 6.4, entries 2 and 3). TEM analysis revealed that Ag particles were found on the microscopy grid (Section 6.2), thus the low activity could be explained by the poor adhesion of Ag on the TiO_2. It may also be due to the absence of a pre-reduction treatment before the start of the reaction. Certainly, reduction of Ag to form metallic Ag species was essential for the activity of other Ag based catalysts reported for the AAA reaction (Chapter 1).[67, 71] Thermal treatment of as-prepared Ag/TiO_2 did increase the selectivity for **2.4** slightly (Table 6.4, entry 2 vs. entry 3) but the overall conversion remained low. Similar to the conclusion drawn for the Ni/TiO_2 catalyst, Ag/TiO_2 is practically inactive as unsupported TiO_2 achieved 1-2 % conversion of **2.1**.

Although Au/TiO_2 remains to be the most active system tested, among the cheaper metal catalysts prepared (Co, Ni and Cu), Cu/TiO_2 displayed the best selectivity for **2.4** (Table 6.4, entry 4 and 5). While the TOF afforded by this catalyst was modest, it was decided that additional studies of Cu/TiO_2 would be carried out, as Cu is substantially cheaper than Au. Further probing of Cu/TiO_2 began with an experiment to prove the heterogeneity of the catalyst, starting with a preliminary investigation of the as-prepared Cu/TiO_2 system (Table 6.4, entry 4). The catalyst was reacted with **2.1** and **2.2** at 180 ˚C, 15 bar under N_2 for 20 minutes, yielding 13% conversion of **2.1**. The catalyst was then filtered off and the supernatant solution placed back into the reactor under the same reaction conditions. It was found that a further 15% of **2.1** was converted in the absence of Cu/TiO_2. This indicates leaching of active catalyst into the solution, and that unsupported Cu species are catalytically active. Leaching of a Cu catalyst supported on magnetite has previously been observed in the synthesis of aromatic imines using alcohols and amines (or nitroarenes), where it was found that 17-18% of metal was lost to the liquid phase after quinoline and aniline were used in the reaction mixture.[158] In the study it was found that when the catalyst was subjected to **2.1** and NaOH (at 100 ˚C for 4 days under Ar) leaching was reduced to 10% (identified by ICP-MS). Thus, it was concluded that nitrogen-containing species facilitated in the leaching of Cu.
In light of this, the Cu/TiO_2 catalysts synthesised in this study were subjected to solutions of:

2-methyl-2-butanol and *N*-phenylbenzylamine (**2.4**) (0.5 M)

and

2-methyl-2-butanol only

at 180 ˚C, 15 bar under N_2 for 1h 30 minutes, with the resulting solutions analysed by ICP analysis (Table 6.5).

TABLE 6.5. *Leaching studies of Cu/TiO_2 catalysts (calcined and as-prepared) subjected to solutions of **2.4** and 2-methyl-2-butanol.*

Entry	Experimental conditions	Cu/TiO_2 (% of Cu detected)[a]	Cu/TiO_2 calc. (% of Cu detected)[a]
1	2-methyl-2-butanol	0.04	0.01
2	**2.4** in 2-methyl-2-butanol	0.99	0.73

[a] *% of Cu detected in the solution following filtration of the reaction mixtures.*

Negligible leaching was detected overall. If all Cu species leached into solution, a value of 100% would be expected. However, the presence of **2.4** was shown to result in increased

amounts of Cu being detected (Table 6.5, entry 1 vs. entry 2), which indicates that amine facilitates the leaching of Cu.

In an attempt to increase the overall activity of the Cu/TiO_2 catalysts, additional systems were prepared using different preparation and calcination methods (Section 6.4).

6.4 Preparation, characterisation and catalytic screening of additional Cu/TiO_2 catalysts

The DP and SD methods were used for the preparation of additional Cu systems (described in Chapter 4). Furthermore, two different calcination atmospheres (under H_2/N_2 and under air) at high temperatures (500 ˚C for 4 hours) were employed to gauge whether the calcination procedure invoked any changes in particle size. Note that all catalyst characterisation and calcination was performed by Johnson Matthey Plc unless stated otherwise

To assess the effects of metal loading, for each method 5 wt.% and 1 wt.% Cu catalysts were made. For all systems, the metal loadings were close to, or achieved the expected values. From this point forward, catalysts will be denoted as 'metal loading % Cu/TiO_2 (preparation method)' e.g. 1% Cu/TiO_2 (DP).

The metal nanoparticles and overall catalyst structures were determined by XRD and TEM analysis and compared against the 1% Cu/TiO_2 (DP) catalysts prepared earlier (Section 6.3.3). As there was poor contrast between Cu and support, particle size distribution graphs were not possible. However, the measurement of particles that could be observed for the 1% Cu/TiO_2 (DP) calcined under H_2/N_2 showed that there were small Cu particles present 1-2 nm (Figure 6.3 A). Particles in the 4% Cu/TiO_2 (DP) (calcined under H_2/N_2) contained slightly larger particles (2-3 nm) (Figure 6.3 B), likely due to agglomeration of Cu because of the increased metal loading and high calcination temperatures. Certainly, it is known that calcination of Cu based catalysts exceeding temperatures of 300-350 ˚C leads to sintering.[159]

Cu particle sizes between 1-5 nm were found in the 5% Cu/TiO_2 (SD) sample (calcined under H_2/N_2), with the 1% Cu/TiO_2 (SD) (calcined under H_2/N_2) containing slightly smaller particles (2-3 nm) (Figure 6.3 C and D, respectively). Therefore, it seems that the SD method has produced larger Cu particles in comparison to the DP method. This result is not unexpected given that the SD technique is similar to the impregnation method, which is known for forming large particle sizes (Chapter 4).

In terms of the effect of the calcination atmosphere, from the particles that could be observed there did not seem to be a significant variation in Cu particle sizes for the 5% Cu/TiO_2 samples (SD) calcined under air and H_2/N_2 (Figure 6.3 C vs. E).

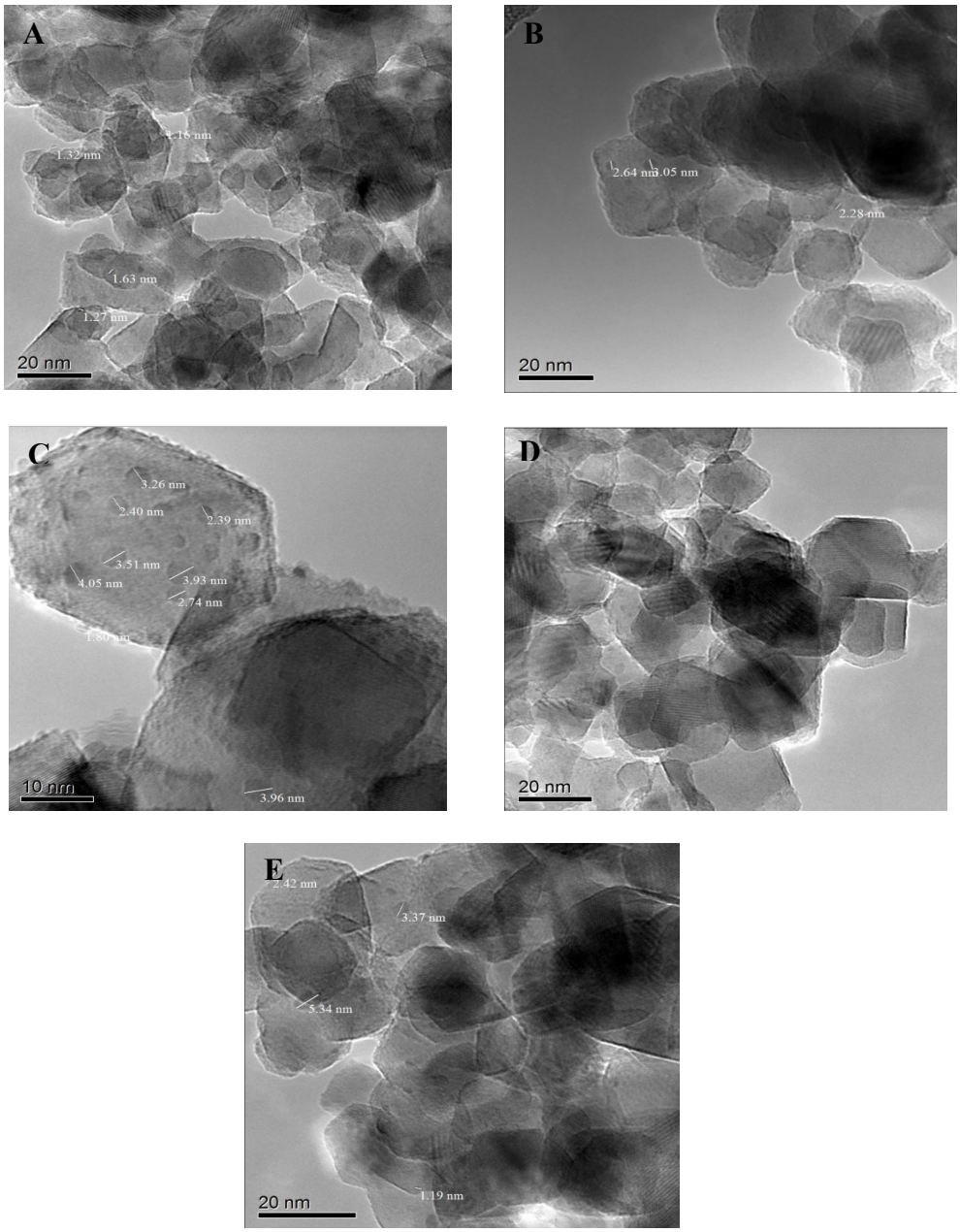


FIGURE 6.3. *TEM photographs of the various Cu/TiO_2 catalysts prepared by the DP and SD methods,* ***A)*** *Cu/TiO_2 (1% DP, calc. under H_2/N_2),* ***B)*** *Cu/TiO_2 (4% DP, calc. under H_2/N_2),* ***C)*** *Cu/TiO_2 (5% SD calc. under H_2/N_2),* ***D)*** *Cu/TiO_2 (1% SD, calc. under H_2/N_2),* ***E)*** *Cu/TiO_2 (5% SD calc. under air).*

Diffraction lines for Cu species were not identifiable in the XRD patterns for both of the 1% Cu/TiO_2 catalysts made by the DP and SD procedures. This is most likely due to the metal loading being below the detection limit for XRD. However, CuO crystallites were detected in samples of the 4% Cu/TiO_2 (DP) and 5% Cu/TiO_2 (SD) (Figure 6.4, CuO peaks highlighted in the red boxes). Not surprisingly, the CuO crystallite sizes were larger for

catalysts calcined under air (determined by Rietveld analysis by Johnson Matthey Plc analytical department) (Table 6.6, entries 1 and 2 vs. 3 and 4).

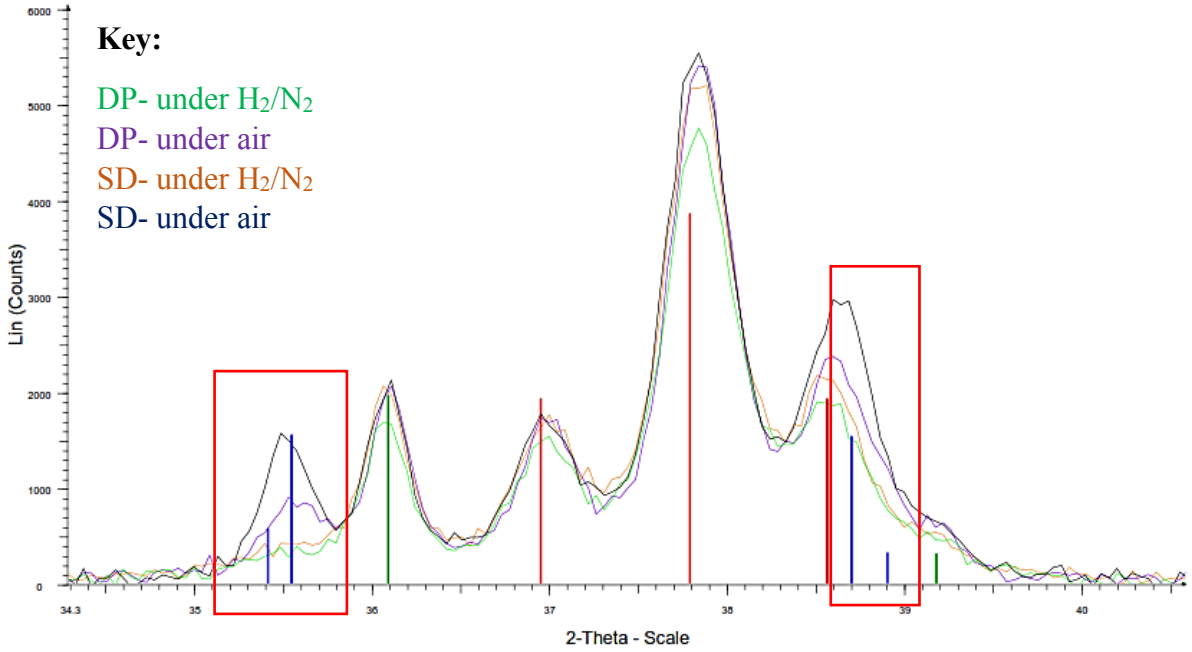


FIGURE 6.4. *Comparison of XRD patterns for Cu/TiO_2 catalysts calcined under air and H_2/N_2, prepared by DP and SD.*

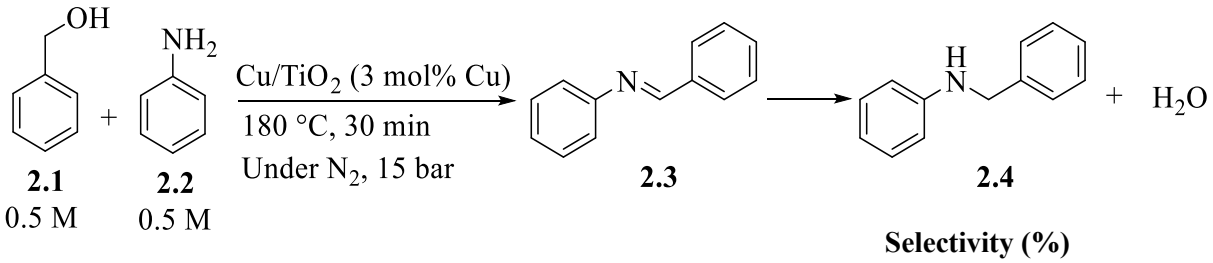
TABLE 6.6. *CuO crystallite sizes of the 4% and 5% Cu/TiO_2 made by DP and SD methods, respectively.*

Entry	Catalyst	Calcination atmosphere (500 ˚C)	CuO size (nm)
1	5 % Cu/TiO_2 (SD)	air	24
2	4% Cu/TiO_2 (DP)	air	17
3	5 % Cu/TiO_2 (SD)	H_2/N_2	11
4	4% Cu/TiO_2 (DP)	H_2/N_2	14

6.4.1 Cu/TiO_2 screening results

In general, the activity and selectivity of the newly prepared Cu/TiO_2 catalysts were low (Table 6.7, entries 3-8), compared to the original Cu/TiO_2 systems described in Section 6.3 (Table 6.7, entries 1 and 2).

TABLE 6.7. *Results for the conversion of* ***2.1*** *to products for the Cu/TiO_2 catalysts.*



Entry	Catalyst and calcination atmosphere	Conversion (%)[a]	TOF (h^{-1})[b]	Selectivity (%) 2.4	2.3	PhCHO	Toluene
1	**1% Cu/TiO_2 DP (as.prep)**	**29**	**10**	**80**	**17**	**1**	**2**
2	**1% Cu/TiO_2 DP (H_2/N_2)**	**14**	**20**	**61**	**36**	**2**	**1**
3	4% Cu/TiO_2 (DP) (air)	6	4	15	73	1	10
4	4% Cu/TiO_2 (DP) (H_2/N_2)	10	7	32	61	1	6
5	5% Cu/TiO_2 (SD) (air)	6	4	13	77	1	10
6	5% Cu/TiO_2 (SD) (H_2/N_2)	6	4	10	79	1	9
7	1% Cu/TiO_2 (SD) (air)	6	4	11	78	1	10
8	1% Cu/TiO_2 (SD) (H_2/N_2)	5	3	13	72	1	14

[a] *Determined by GC using 4-tert-butylphenol as an external standard, based on* ***2.1****. Results are an average of 2 runs (error ± 2%).*[b] *TOF (h^{-1}) (moles of benzyl alcohol converted/moles of Cu).*

All of the newly synthesised catalysts exhibited similar TOF's and selectivities regardless of the preparation method employed and metal loading. The lower activity of the systems could be due to the larger Cu particle sizes present in these systems, as confirmed by TEM analysis (Section 6.4). Indeed, it was demonstrated that Au/TiO_2 catalysts that had larger Au particles present, afforded decreased selectivities for **2.4** (Chapter 4). The larger Cu particles may also be the cause for the increased selectivity for toluene and/or the higher calcination temperature used (500 ˚C vs. 300 ˚C) may have invoked changes to the metal-support interface making toluene formation more favourable. There was no significant influence on catalytic activity by using different calcination atmospheres (Table 6.7, entries 2, 4, 6 and 8 vs. entries 3, 5 and 7).

To understand whether the preparation and calcination procedures enhanced the adhesion of Cu to TiO_2, systems were subjected to the same solutions and reaction conditions employed in the previous leaching experiments for testing the 1% Cu/TiO_2 (DP) catalyst (Section 6.3.3). Namely, 2-methyl-2-butanol and *N*-phenylbenzylamine (**2.4**) (0.5 M) and 2-methyl-2-butanol only at 180 ˚C, 15 bar under N_2 for 1h 30 minutes, with the resulting solutions analysed by ICP analysis. Note that if all Cu species leached into solution a value of 100% would be expected. In the previous studies it was found that solutions of **2.4** induced higher levels of leaching compared to using solvent only, 0.99% and 0.73% of Cu was detected for the as-prepared and calcined samples, respectively. Compared to the 1% Cu/TiO_2

(DP) system, leaching was reduced when the systems are subjected to solutions of **2.4** (Table 6.8, entries 1-6). This could be due to the higher calcination temperatures used for these systems (500 ˚C vs. 300 ˚C) invoking better adhesion of Cu to the support.

TABLE 6.8. *Leaching studies of Cu/TiO_2 catalysts subjected to solutions of* ***2.4*** *and 2-methyl-2-butanol.*

Entry	Catalyst and calcination atmosphere	ICP (% of Cu) solvent[a]	ICP (% of Cu) 2.4 in solvent[a]
1	4% Cu/TiO_2 (DP) (H_2/N_2)	0.01	0.26
2	4% Cu/TiO_2 (DP) (air)	0.09	0.54
3	5% Cu/TiO_2 (SD) (H_2/N_2)	0.01	0.22
4	5% Cu/TiO_2 (SD) (air)	0.11	0.63
5	1% Cu/TiO_2 (SD) (H_2/N_2)	0.06	0.26
6	1% Cu/TiO_2 (SD) (air)	0.22	0.35

[a] *% of Cu detected in the solution following filtration of the reaction mixtures.*

On the whole, increased levels of Cu were detected for materials calcined under air compared to under H_2/N_2 (Table 6.8, entries 1, 3 and 5 vs. 2, 4 and 6). The stability of catalysts calcined under H_2/N_2 could be attributed to the increased formation of metallic Cu species, which may form stronger bonds to TiO_2 compared to CuO species. Although larger particle sizes were observed for catalysts prepared by the SD technique, compared to systems made by the DP method, this does not seem to have had an influence in the adhesion of Cu particles to the support (Table 6.8, entries 1 and 2 vs. 3 and 4).

Attempts to improve the activity of Cu/TiO_2 did not prove to be successful; nonetheless, enhancements in Cu stability were achieved. The higher activity observed for the original 1% Cu/TiO_2 (DP) catalysts prepared could be due to a homogeneous reaction of the leached species being more catalytically active and/or due to the small Cu particle sizes.

So far, the discussion has been focussed on the use of monometallic catalysts in the AAA. It has been shown that the introduction of a second metal often allows for more active and selective systems. Furthermore, they are less prone to deactivation, a problem that is frequently highlighted in the oxidation of alcohols.[147, 160, 161] Improvements in activity and stability are understood to arise from a combination of ensemble effects, whereby additional components may act as spacers, isolating active sites, or as electronic modifiers due to the vicinity of the active atoms.[151, 162]

6.5 Au,M/TiO_2 catalyst characterisation

In this part of the work, various Au bimetallic catalysts supported on TiO_2, synthesised by the DP method are examined (Table 6.9). Note that all catalyst characterisation and calcination was performed by Johnson Matthey Plc unless stated otherwise.

The catalysts were calcined at 300 ˚C under a H_2/N_2 atmosphere and as-prepared (dried in the oven at 100 ˚C for 24 hours) catalysts were also screened for their activity to assess if there was any differences in conversion and/or selectivity.

A total metal loading of 1 wt.% with a 1:1 molar ratio of each metal was aimed for when preparing the systems. Half the desired metal loading was found for Au,Pd/TiO_2 and Au,Cu/TiO_2 (Table 6.9, entries 1 and 2), while the other catalysts afforded metal loading slightly lower than 1 wt.% (Table 6.9, entries 2-5). The deposition of two metals onto TiO_2 may have been a factor that resulted in the lower loadings; however, it is known that higher metal loadings can be achieved by increasing the pH when preparing Au/TiO_2, but this can lead to larger particle sizes (demonstrated in Chapter 4). The metal: Au ratio for the Au,Ag/TiO_2 and Au,Cu/TiO_2 systems was higher than expected (Table 6.9, entries 2 and 3). To avoid the precipitation of silver chloride when preparing Au,Ag/TiO_2 ($HAuCl_4$ was used as the Au precursor), Au was deposited onto the support first, and after a washing step, Ag was deposited. Thus it can be suggested that leaching of Au occurred during the washing step, before the addition of Ag. This was previously observed in the synthesis of a Au,Ag/TiO_2 catalyst in the literature, where it was found that up to 50% less of the expected Ag was deposited, in this case Ag was deposited first and then Au.[163] In the case of the Au,Cu/TiO_2 the results suggest that under the preparation conditions employed (deposition of both metals simultaneously, Chapter 7), Cu had a stronger affinity to TiO_2.

TABLE 6.9. *Au,M/TiO_2 catalysts synthesised showing the metal loading results and metal: Au molar ratio.*

Entry	Catalyst	Metal loading (wt.%)	M:Au ratio
1	Au,Pd/TiO_2	0.6	1
2	Au,Cu/TiO_2	0.6	3
3	Au,Ag/TiO_2	0.7	4
4	Au,Ni/TiO_2	0.9	1
5	Au,Co/TiO_2	0.7	2

TEM imaging of the calcined catalysts (conducted at Johnson Matthey Plc and Imperial College London), showed that in general the particles sizes fell in the range between 5-10

nm, with larger particles found on the Au,Ni/TiO_2 (mean particle size of 8.5 nm) and Au,Ag/TiO_2 catalysts (mean particle size of 6.8 nm) (Figure 6.5 A and B). The Au,Pd and Au,Co TiO_2 supported catalysts contained slightly smaller metal sizes; both materials had a mean particle size of 5.5 nm (Figure 6.5 C and D). Note that the production of a particle size distribution graph for the Au,Cu/TiO_2 system was not possible due to the limited number of species that could be found. There was a larger amount of Cu present in this catalyst, which could be the reason for this (Table 6.9, entry 2). Indeed, there was poor contrast between Cu and TiO_2, when analysing the Cu/TiO_2 catalysts (Section 6.4).

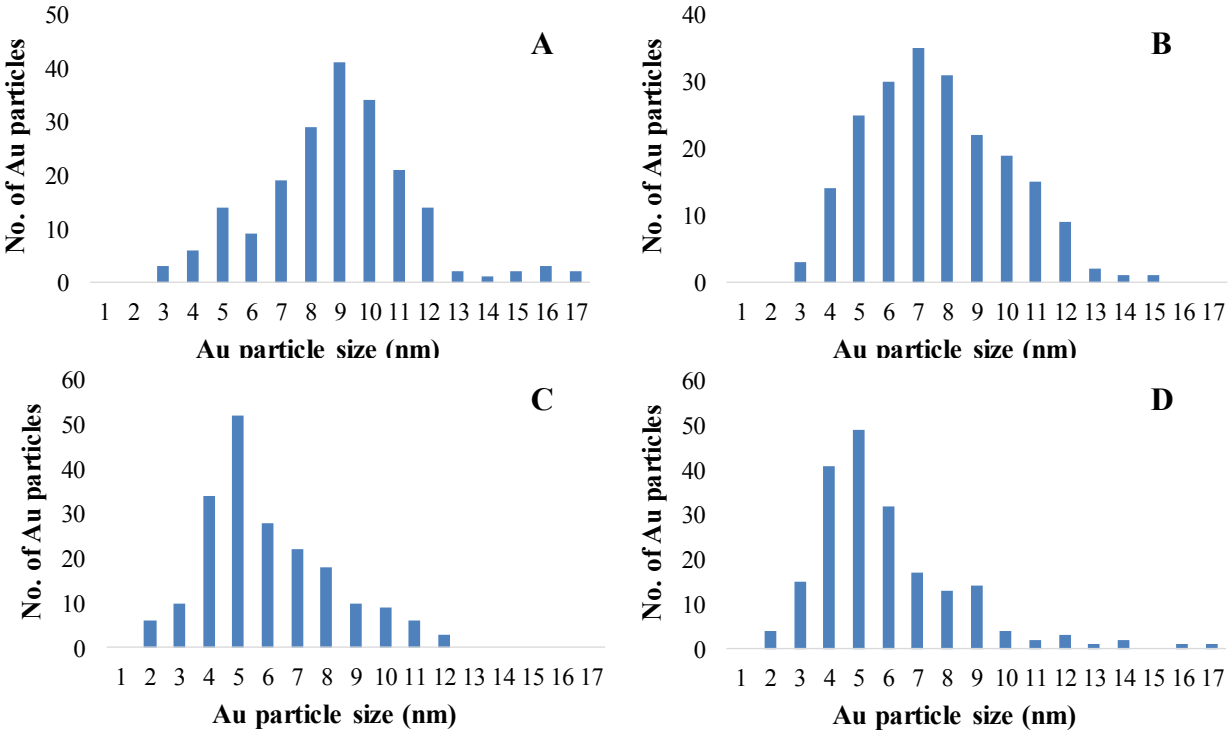


FIGURE 6.5 *Particle size distribution graphs of* ***A)*** *Au,Ni/TiO_2,* ***B)*** *Au,Ag/TiO_2,* ***C)*** *Au,Pd/TiO_2,* ***D)*** *Au,Co/TiO_2.*

To determine the nanostructure compositions, i.e. whether alloys and/or monodispersed particles were present, EDX (elemental dispersive x-ray) analysis was performed. It was difficult to determine the exact structure, as individual nanoparticles that were assessed showed the presence of both metals. This could be due to the close vicinity of monodispersed particles or alloy formation. For example, Figure 6.6 shows the EDX analysis of particles in the calcined Au,Ni/TiO_2 catalyst. The highlighted particles in the red boxes were examined, which correspond to areas 1-3 in the graphs under the image. All three areas show the

presence of both Ni and Au. Cu was also detected which is most likely due to the holey carbon Cu coated TEM microscopy grid.

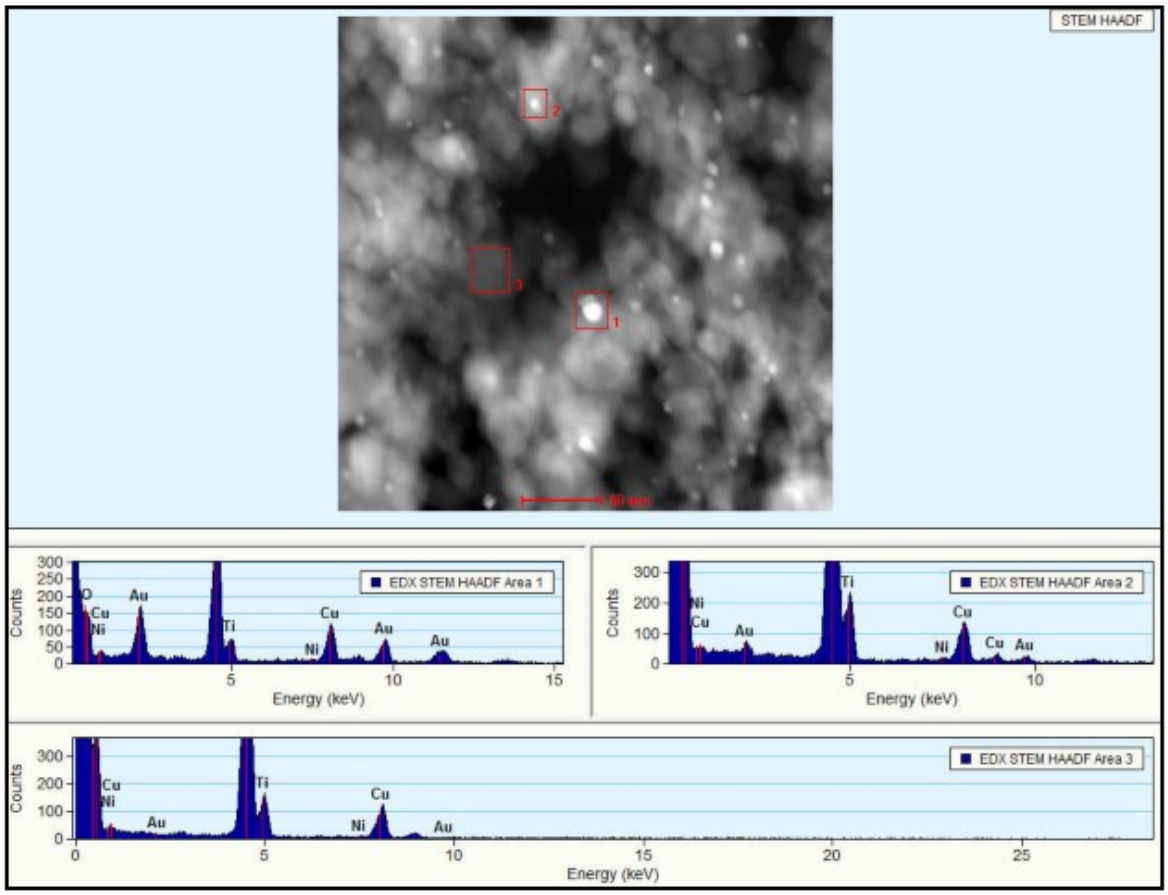


FIGURE 6.6. *EDX analysis of calcined Au,Ni/TiO₂.*

XRD analysis was performed on the calcined catalysts, where the presence of anatase and rutile TiO_2 was confirmed in all samples, indicating that a phase change of anatase to rutile had not occurred (P25-Degussa TiO_2 employed, anatase -25% and rutile -75%). However, there were no diffraction peaks for metal species in any of the samples.

6.6 Au,M/TiO_2 screening results and analysis

The model system of **2.1** with **2.2** was chosen to test the activity of the bimetallic supported catalysts employing the Endeavor® batch reactor and using the same conditions as those employed in Sections 6.3 (Scheme 6.2) to allow for the comparison of results.

6.6.1 Group 9: Au,M/TiO_2 screening results

The addition of Co to Au/TiO_2 has not made any enhancements towards the activity of the catalyst (Table 6.10, entries 2 and 3 vs. entry 1).

TABLE 6.10. *Results for the conversion of **2.1** to products for the calcined and as-prepared Au,M/TiO_2 catalysts.*

				Selectivity %			
Entry	**Catalyst**	**Conversion (%)[a]**	**TOF (h^{-1})[b]**	**2.4**	**2.3**	**PhCHO**	**Toluene**
1	**Au/TiO_2**	**89**	**192**	**95**	**2**	**0**	**3**
2	Au,Co/TiO_2	51	62	90	7	0	3
3	Au,Co/TiO_2 calc.	52	62	92	5	0	2

*[a] Determined by GC using 4-tert-butylphenol as an external standard, based on **2.1**. Results are an average of 2 runs (error ± 4%).[b] TOF (h^{-1}) (moles of benzyl alcohol converted/moles of total metal).*

Improvements in TOF and selectivity were observed for the bimetallic version of the Co system compared to the monometallic catalysts (Table 6.2, entries 4 and 5). However, this could mainly be due to the presence of Au rather than a cooperative effect between the two metals. This is supported by the observation that there is no effect on the selectivity following calcination of Au,Co/TiO_2 (Table 6.10, entry 2 vs. entry 3), whereas for the monometallic Co/TiO_2 systems the selectivity for toluene increased after thermal treatment. This suggests that Au was the dominant species during the reaction, controlling the selectivity.

6.6.2 Group 10: Au,M/TiO_2 screening results

Au/TiO_2 remained the most active catalyst in terms of its conversion and selectivity for **2.4** (Table 6.11, entry 1).

TABLE 6.11. *Results for the conversion of **2.1** to products for the calcined and as-prepared Au,M/TiO_2 catalysts.*

				Selectivity %			
Entry	**Catalyst**	**Conversion (%)[a]**	**TOF (h^{-1})[b]**	**2.4**	**2.3**	**PhCHO**	**Toluene**
1	**Au/TiO_2**	**89**	**192**	**95**	**2**	**0**	**3**
2	Au,Ni/TiO_2	38	49	90	8	0	2
3	Au,Ni/TiO_2 calc.	71	92	95	3	0	2
4	Au,Pd/TiO_2 calc.	98	126	24	28	0	48

*[a] Determined by GC using 4-tert-butylphenol as an external standard, based on **2.1**. Results are an average of 2 runs (error ± 4%).[b] TOF (h^{-1}) (moles of benzyl alcohol converted/moles of total metal).*

Particularly notable was the substantial enhancement in TOF when the as-prepared Au,Ni/TiO_2 catalyst was calcined (Table 6.11, entry 2 vs. entry 3). This may be ascribed to the formation of active metallic Ni species, which are known to be important for the activity of heterogeneous Ni catalysts in the AAA reaction (Chapter 1).[59, 60] The increase in conversion following thermal treatment implies that Au and Ni may have been working together to catalyse the reaction.

Significant toluene formation was observed when employing the calcined Au,Pd/TiO_2 catalyst (Table 6.11, entry 4). This was not unexpected due to the known formation of this species (by the disproportionation of **2.1**) when using Pd based systems (Chapter 1). The drastic change in selectivity for this catalyst compared to using Au only (Table 6.11, entry 4 vs. entry 1) implies that Pd is governing the activity in the reaction. As previously mentioned, (Section 6.3.1) basic supports have shown to suppress toluene formation which could be tried for this bimetallic system.

6.6.3 Group 11: Au,M/TiO_2 screening results

Similarly, Au,M/TiO_2 systems using Group 11 metals were screened for their activity in the alkylation of **2.2** by **2.1**. Yet again, Au/TiO_2 remained the most active in terms of its conversion and selectivity for **2.4** (Table 6.12, entry 1).

TABLE 6.12. *Results for the conversion of **2.1** to products for the calcined and as-prepared Au,M/TiO_2 catalysts.*

				Selectivity %			
Entry	**Catalyst**	**Conversion (%)[a]**	**TOF (h^{-1})[b]**	**2.4**	**2.3**	**PhCHO**	**Toluene**
1	**Au/TiO_2**	**89**	**192**	**95**	**2**	**0**	**3**
2	Au,Ag/TiO_2	7	10	42	57	1	0
3	Au,Ag/TiO_2 calc.	7	10	35	64	1	0
4	Au,Cu/TiO_2	13	14	71	28	1	0
5	Au,Cu/TiO_2 calc.	13	14	75	24	1	0

*[a] Determined by GC using 4-tert-butylphenol as an external standard, based on **2.1**. Results are an average of 2 runs (error ± 4%).[b] TOF (h^{-1}) (moles of benzyl alcohol converted/moles of total metal).*

The low activity of the as-prepared and calcined Au,Ag/TiO_2 systems (Table 6.12, entry 3) was most likely due to the decreased molar ratio of Au compared to Ag (Section 6.5). Indeed monometallic Ag/TiO_2 displayed very poor activity in this reaction (Table 6.4, entries 2 and 3). Similarly, the low molar ratio of Au in the Au,Cu/TiO_2 catalysts may explain the poor activity observed, certainly the monometallic Cu/TiO_2 materials displayed similar conversion and selectivities to the Au,Cu/TiO_2 materials (Table 6.12, entries 4 and 5 vs. Table 6.4, entries 4 and 5). There was no influence on activity following calcination of both of the Au,Ag and Au,Cu supported systems (Table 6.12, entries 2 and 4 vs. entries 4 and 5).

Although Au/TiO_2 was the most active system it was of interest to determine whether there were any correlations in activity by including a second metal. Thus data from hydrogen temperature programmed desorption (H-TPD) of several calcined bimetallic catalysts was compared against the catalyst screening results (Section 6.6.4).

6.6.4 Comparison of H-TPD data and screening results

The reduction of imine is a key step in the AAA in order to produce amine product, thus the ability of the catalyst to bind H_2 may be critical for its selectivity. To identify whether this was true, the peak integration values from H-TPD analysis were multiplied by the peak

desorption temperatures to get a crude binding energy, this was then compared against the selectivity for **2.4** (Figure 6.7 and Table 6.13).

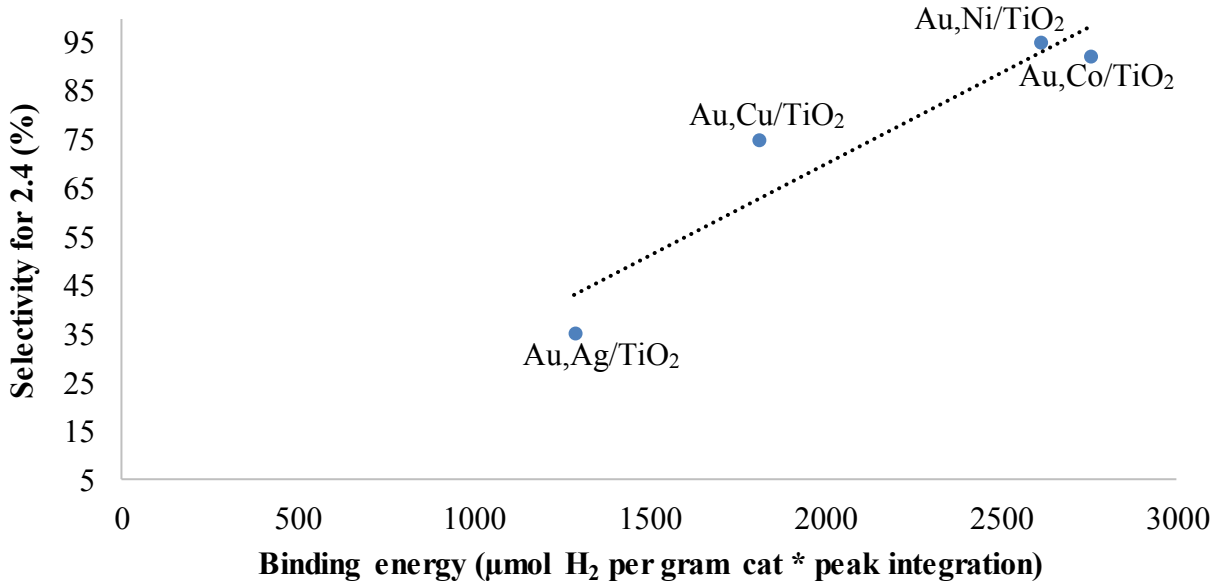


FIGURE 6.7. *Comparison of binding energy versus selectivity for* ***2.4*** *for the Au,M/TiO₂ catalysts.*

TABLE 6.13. *Comparison of binding energy versus selectivity for* ***2.4*** *for the Au,M/TiO₂ catalysts.*

Entry	Catalyst	Binding energy (µV K^{-1})	% Selectivity for 2.4
1	Au,Co/TiO_2	2758	92
2	Au,Ni/TiO_2	2612	95
3	Au,Cu/TiO_2	1814	75
4	Au,Ag/TiO_2	1287	35

A relationship between the H_2 binding energy and selectivity for **2.4** was observed, where catalysts that bind H_2 more strongly show an increase in selectivity (Table 6.13, entry 1 and 2 vs. entries 3 and 4). Indeed, Au,Co/TiO_2 and Au,Ni/TiO_2 display similar binding strengths and selectivities for **2.4**, indicating that catalysts which have stronger affinities for H_2 are more selective in the AAA reaction. This trend was established earlier in Chapter 5 for the Au supported catalysts, where the H_2 binding affinity was postulated to be inherently related to Au particle size. Given that the production of individual size particle distribution graphs for the Au and metal species was not possible and due to the difficulties in determining whether the metals were acting cooperatively to facilitate the reaction, it was not possible to delineate whether the particle size was influencing the H_2 binding strengths in this study.

6.7 Conclusion

In this Chapter, 13 metal catalysts using Group 9, 10 and 11 metals were prepared and tested in the AAA reaction. Overall, Au/TiO_2 remained the most active and selective system than all of the M/TiO_2 and $Au,M/TiO_2$ catalysts prepared. Although the bimetallic systems exhibited higher activity than the monometallic catalysts, the inclusion of a second metal was shown to be detrimental to catalytic activity (Section 6.6). The increased activity for Au,Co and Au,Ni supported on TiO_2 was proposed to be due mainly to the presence of Au and the decreases in activity for Au,Ag and Au,Cu catalysts due to the low molar ratio of Au. H-TPD analysis highlighted that the ability of catalysts to bind H_2 was important for the selectivity of the catalysts, with systems showing a lower H_2 affinity affording lower selectivities for **2.4**.

It was surprising that Group 9 metals on TiO_2 (Ir, Rh) did not prove to be successful alternatives to using Au/TiO_2 given the known activity of homogeneous systems using these metals in the AAA reaction (Chapter 1). This could be due to large metal particles, which were difficult to determine using TEM because of the poor metal-support contrast. There were no noticeable trends in activity within the monometallic Group 9, 10 and 11 metal catalysts prepared, however in general systems using base metals (Cu, Ni and Co on TiO_2) showed lower TOF's contrasted to the period 5 and 6 transition metal catalysts synthesised (Ir, Rh, Pd and Pt on TiO_2). This was attributed to the increased likelihood of these metals to sinter because of the lower melting points and/or due to catalyst pre-reduction being necessary.

Although these studies did not lead directly to a better catalyst, many important parameters for catalyst activity and stability have been identified, which may be helpful for further design of catalysts. In particular, the choice of catalytic loading, calcination treatment and atmosphere were shown to be important for the catalyst stability of Cu-based systems. It was demonstrated that by employing a reducing atmosphere, metal leaching can be decreased.

Future experiments could involve the synthesis of metals on supports other than TiO_2 as it has been demonstrated for Pd based catalysts in the oxidation of alcohols that toluene formation can be avoided by using basic supports. This would be particularly interesting for Pd and Rh systems, which afforded significant amounts toluene formation but high TOF's in this study.

6.8 Project summary and Future work

The AAA reaction is used to synthesise a wide range of products for the pharmaceutical and agrochemical industries, as well as finding applications in the formation of household products. Consequently, the field receives great interest, with the current focus being on ways to achieve these transformations with greener and safer methods. Indeed many reported systems for this reaction operate at high temperatures with the inclusion of base and have poor substrate scope and selectivity. In this light, a previously reported system using Au/TiO_2 in flow with toluene as a solvent is able to catalyse the AAA reaction in the absence of base.[77] The use of a flow reactor enables reactions to be performed safely, as small quantities of reagents are reacted at a given time, and by operating the reactor in single pass mode, there is greater control over the selectivity of the reaction.

In this project, further studies of Au/TiO_2 were undertaken using the flow reactor and the model reaction between benzyl alcohol (**2.1**) and aniline (**2.2**) in a greener solvent system (2-methyl-2-butanol vs. toluene). Studies were designed to interrogate the influence of H_2O. Additionally, as reactions are commonly performed under anaerobic conditions, the effect of O_2 on the model reaction was investigated. It was found that H_2O is able to act as a reductant for the formation of *N*-phenylbenzylamine (**2.4**) from *N*-benzylideneaniline (**2.3**). A secondary role of H_2O was uncovered when experiments were performed under N_2. The detection of **2.4** decreased as higher H_2O concentrations were employed in 2-methyl-2-butanol, and was attributed to the precipitation of **2.4** with H_2O and/or the formation of an emulsion. Surprisingly, when performing reactions under aerobic conditions this effect was negated, which was attributed to an increased solubility of **2.4**. In order to fully delineate the influence of H_2O under inert conditions, the solubility of **2.4** in 2-methyl-2-butanol/H_2O mixtures needs to be investigated.

The selectivity for the amine product (**2.4**) was lower when reactions were conducted in the presence of O_2, which was ascribed to the oxidation of **2.4** to **2.3**, and/or the removal of surface of hydride species that are required for the reduction of **2.3**.

The stability and possible deactivation routes of Au/TiO_2 was explored were it was found that reaction intermediates and products (**2.3**, **2.4** and H_2O) had no influence in deactivating the catalyst. Au/TiO_2 showed excellent stability when using the model reaction, with slow deactivation observed over the course of 10 hours. Increases in Au particle size were the likely cause for the gradual deactivation.

One of the aims of this project was to develop a kinetic model by using the conversion-time data from the mechanistic studies performed under N_2. A predicative model was generated using previously derived kinetic equations, but introducing a term to account for the loss of **2.4** at high H_2O concentrations in 2-methyl-2-butanol. Mass transfer studies indicated that the system was not under the influence of internal diffusion, however it may be on the limit of external mass transfer effects. Even so, the model was able to simulate reaction profiles, with low RMS values generated. In terms of future work, the inclusion of terms for mass transfer effects and adsorption of species could be incorporated, as well as equations to account for the effect of O_2, so that experiments performed under aerobic conditions can be modelled.

A key challenge in the AAA reaction is the use of non-noble metal catalysts that are able to perform under mild conditions with high activity. The exploration of a new catalytic system began with examining the influence that different preparation and calcination treatments had on Au/TiO_2. Catalysts made by the impregnation method (IMP) were shown to be inactive, which was attributed to the large Au particle sizes present. In the AAA reaction, small particle sizes are known to be more active.[73] The deposition-precipitation (DP) and colloidal method (COL) produced active catalysts with small Au particle sizes (2 nm). Calcination at 300 ˚C resulted in more active and selective systems for Au/TiO_2 prepared by the DP method, presumed to be due to the formation of metallic Au. Yet, temperatures >300 ˚C resulted in decreases in activity, likely due to the increases in Au particle size. The calcination atmosphere had no significant effect on the activity of the catalysts.

In order to study the effect that changing the support has on the activity of the system, a range of Au supported catalysts were made by the DP and COL method. The differences in activity were found to be correlated with the Au particle size. The larger the Au particles were, the lower the conversion and selectivity for **2.4**, which was concluded to be related to a decreased affinity for H_2 from the results of H-TPD analysis. It was difficult to delineate the exact role of the support, as it is interlinked with controlling the particle size.

Au/TiO_2 (prepared by the COL and DP method) and $Au/\gamma\text{-}Al_2O_3$ (prepared by the COL method) were the most selective and active catalysts tested, and the Au particles remained stable following reactions. Further studies could test the stability of the Au particles over a longer time in flow (single pass) and the applicability of the systems to catalyse transformations other than the model reaction could be carried out.

Other metal and Au bimetallic catalysts supported on TiO_2 were synthesised to explore whether a better catalyst, in terms of activity and cost, could be prepared rather than using Au based systems. Cu/TiO_2 showed promising results in terms of its selectivity and it is lower in cost than Au, however the TOF was modest. Attempts to increase the activity of the system by using other preparation techniques, catalyst loading and calcination treatments proved unsuccessful. Although the activities of the Au bimetallic catalysts were good, this was attributed to the presence of Au.

Similar to the study of the Au/Supported catalysts, H-TPD analysis revealed that the ability of the systems to bind H_2 is important for the selectivity for **2.4**. Further studies could interrogate metals anchored on supports other than TiO_2.

Overall, the studies have highlighted the importance of the careful control and choice of reaction conditions, the catalyst preparation and calcination method, as all three parameters greatly affect the activity of the catalyst. Even though Au/TiO_2 remained to be the most active system, the studies have led to a better understanding of factors that are important for AAA reaction, such as particle size and H_2 binding affinity. Thus, the studies can be used in the design of future catalyst for the AAA reaction.

CHAPTER 7. Experimental

7.1 General

All reagents were sourced commercially and used without further purification (Aldrich). Au/TiO_2 employed in Chapters 1-3 was sourced from Strem (AUROlite^{TM}). All other metal salts and catalyst supports were procured from Johnson Matthey Plc. Reactions were performed in anhydrous 2-methyl-2-butanol. The conversion of substrates to products was monitored using a HP 6890 Gas Chromatograph equipped with a H_2 flame ionisation detector and an HP5 Agilent column (30 m × 320 μm × 0.25 μm). A Mettler Toledo DL38 Karl Fischer Titrator was used to determine the H_2O content in 2-methyl-2-butanol. ^1H NMR were obtained on a Bruker Avace at 400 MHz.

7.1.1 GC method

The percentage of conversion and selectivity was determined by comparison with known standards, using calibration plots and 4-tert-butylphenol (50 mM in methanol) as an external standard.

1.0 μL of analyte solution was injected into the inlet, which was heated to 250 ˚C with a split ratio of 25:1. The system was operated under a constant pressure of 15 psi with an initial column temperature of 50 ˚C, which was held for 30 s and then heated at 70 ˚C per min to 300 ˚C and held for a further two min.

Table 7.1, shows the retention times of the reaction components.

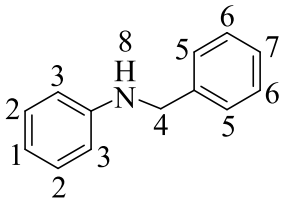
TABLE 7.1. *Retention times of reaction components.*

Components	Retention time (min)
Benzyl alcohol (**2.1**)	2.3
Aniline (**2.2**)	2.1
Benzaldehyde	1.9
N-benzylideneaniline (**2.3**)	3.8
N-phenylbenzylamine (**2.4**)	4.0
Toluene	1.4

7.1.2 ^{1}H NMR characterisation of *N*-phenylbenzylamine (2.4)

The ^{1}H NMR spectra of a commercial sample of **2.4** was ran, and the signals used to confirm the presence of **2.4** in reaction samples.

Commercial *N*-phenylbenzylamine:



^{1}H NMR (400 MHz, $CDCl_3$): δ 7.39-7.25 (m, 5H, *1-3*), 7.20 (t, *J*=8 Hz, 2 H, *2*), 6.77 (t, *J*=7 Hz, 1 H, *1*), 6.64 (d, *J*=8 Hz, 2 H, *3*), 4.35 (s, 2 H, *4*), 4.09 (br, 1 H, *8*).

7.2 Catalyst characterisation

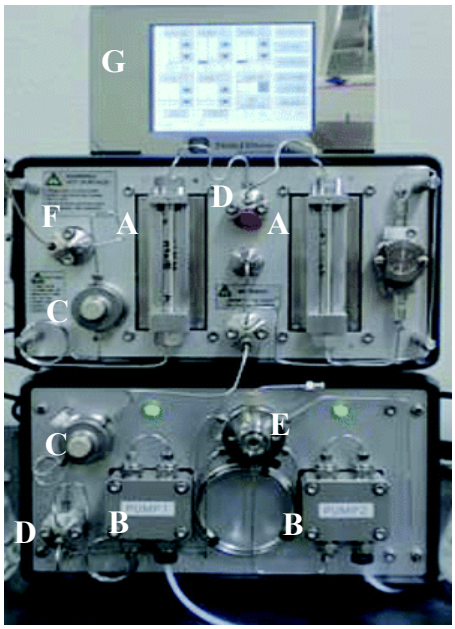
TEM photographs were obtained either on a JEOL 2010 TEM instrument at Imperial College London or at Johnson Matthey Plc using a Tecanai F20 TEM instrument. A UV-Vis-Unicam UV4 instrument was used for UV-Visible analysis at Johnson Matthey Plc. The CO-oxidation experiments were performed on home-made apparatus at Johnson Matthey Plc. Calcinations were conducted at Johnson Matthey Plc using a Carbolite STF tube furnace with a flow rate of 200 mL min^{-1} of Ar or 5% H_2/N_2; other calcinations were performed in static air in a Carbolite RHF1400 furnace at Johnson Matthey Plc. XRD analysis was conducted at Johnson Matthey Plc by using a Bruker AXS D8 diffractometer. The BET surface area and mean pore size of the catalysts was obtained by low temperature N_2 adsorption studies at 77 K using a Micromeritics Tristar 3000 instrument at Imperial College London. ICP analysis was conducted at Johnson Matthey Plc using a Perkin Elmer Optima instrument. H-TPD was performed at Johnson Matthey Plc using Altamira AMI-200 apparatus. CHN microanalysis was performed at London Metropolitan University using a Thermo Scientific (Carlo Erba) Flash 2000 Elemental Analyser, configured for %CHN. FTIR analysis was performed using a Perkin-Elmer Spectrum 100 FTIR Spectrometer.

7.3 Catalytic reactions

Experiments were performed using either a ThalesNano X-cube™ flow reactor (Chapters 2 and 3) or an Endeavor® batch reactor (Argonaut) (Chapter 4, 5 and 6). All reactions conducted in flow employed dried (at 150 ℃, for 24 hours under static air) 1 wt.% Au/TiO_2 (Strem AUROlite™) catalyst.

7.3.1 Components of the Thalesnano X-CUBE™ flow reactor

Figure 7.1 shows the general features of the flow reactor employed in these studies. In general the catalyst was loaded into a cylindrical cartridge (measuring 4 mm x 70 mm, up to two catalyst cartridges can be used in tandem) and then heated and pressurised up to the desired reaction conditions (Figure 7.1 A) with the reaction mixture being delivered by a piston pump (Figure 7.1 B and C). Two reaction mixtures can be delivered at the same time (at flow rates between 0.1 to 3 mL min^{-1}), however, in this work, only one pump was employed. The reactor allows for reactions to be conducted with temperatures and pressures up to 200 ˚C and 100 bar, respectively.



A: Heating units
B: Piston pumps
C: Pressure sensors
D: Mixing units
E: Injection port
F: System valve
G: Touch screen control panel

FIGURE 7.1. *Components of the ThalesNano X-cube™ flow reactor.*

*7.3.1.1 Typical procedure for the alkylation of aniline (**2.2**) with benzyl alcohol (**2.1**) using the flow reactor in batch-recycle mode*

Either anhydrous 2-methyl-2-butanol (2 mM of H_2O) or 2-methyl-2-butanol with added deionised H_2O was used to condition the flow reactor up to the desired temperature and pressure (180 ˚C at 50 bar). For reactions performed with a H_2O content >2 mM, the desired amount of H_2O was added to the solvent and the concentration of H_2O determined using a Karl Fischer titrator (Section 7.1). The same solvent (10 mL) was used to generate a reaction mixture of alcohol (0.5 M) and amine (0.5 M), which was purged with either air or N_2 (prior to and during the reaction) and (re)circulated through the heated cartridge containing 1 wt.% Au/TiO_2 (Strem AUROlite^{TM}) (0.8 g, 190 μm average particle size) at a flow rate of 1.5 mL min^{-1}. The progress of the reaction was monitored by GC using 4-tert-butylphenol (50 mM in methanol) as an external standard.

*7.3.1.2 Typical procedure for the alkylation of aniline (**2.2**) with benzyl alcohol (**2.1**) using the flow reactor in single pass mode*

Anhydrous 2-methyl-2-butanol (2 mM of H_2O) was used to condition the flow reactor up to the desired temperature and pressure (180 ˚C at 50 bar). The same solvent (200 mL) was used to generate a solution of alcohol (0.5 M) and amine (0.5 M), which was purged with either air or N_2 (prior to and during the reaction) and was passed through the heated cartridge containing 1 wt.% Au/TiO_2 (Strem AUROlite^{TM}, 190 μm average particle size) (0.8 g) at a flow rate of 0.2 mL min^{-1}. Collected fractions were analysed by GC using 4-tert-butylphenol (50 mM in methanol) as an external standard.

Note that the same procedure was followed for the external and internal mass transfer experiments (Chapter 3), however different flow rates (0.1-1.5 mL min^{-1}) and different particle sizes (70, 100 and 190 μm average particle sizes) using a flow rate of 0.5 mL min^{-1} were employed for the external and internal mass transfer studies, respectively.

*7.3.1.3 Method for the experiment conducted with N-benzylideneaniline (**2.3**) in flow using batch-recycle mode*

Either anhydrous 2-methyl-2-butanol (2 mM of H_2O) or 2-methyl-2-butanol with the addition of deionised H_2O (200 mM) was used to condition the flow reactor up to the desired temperature and pressure (180 ˚C at 50 bar). The same solvent (10 mL) was used to generate

a solution of the imine (0.2 M), which was purged with N_2 (prior to and during the reaction) and (re)circulated through the heated cartridge containing 1 wt.% Au/TiO_2 (Strem AUROlite^{TM}) (0.8 g, 190 μm average particle size) at a flow rate of 1.5 mL min^{-1}. The progress of the reaction was monitored by GC using 4-tert-butylphenol (50 mM in methanol) as an external standard.

*7.3.1.4 Method for the experiment conducted with N-phenylbenzylamine (**2.4**) in flow using batch-recycle mode*

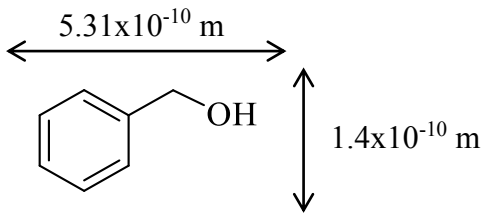
Anhydrous 2-methyl-2-butanol (2 mM of H_2O) was used to condition the flow reactor up to the desired temperature and pressure (180 ˚C at 50 bar). The same solvent (10 mL) was used to generate a solution of *N*-phenylbenzylamine (0.5 M), which was purged with either air or N_2 (prior to and during the reaction) and (re)circulated through the heated cartridge containing 1 wt.% Au/TiO_2 (Strem AUROlite^{TM},190 μm average particle size) (0.8 g) at a flow rate of 1.5 mL min^{-1}. The progress of the reaction was monitored by GC using 4-tert-butylphenol (50 mM in methanol) as an external standard.

7.3.1.5 Method for catalyst deactivation studies in flow using single pass mode

Anhydrous 2-methyl-2-butanol (2 mM of H_2O) was used to condition the flow reactor up to the desired temperature and pressure (180 ˚C at 50 bar). The same solvent (500 mL) was used to generate a solution of benzyl alcohol (**2.1**) (0.5 M) and aniline (**2.2**) (0.5 M), which was purged with N_2 (prior to and during the reaction) and was passed through the heated cartridge containing 1 wt.% Au/TiO_2 (Strem AUROlite^{TM}, 190 μm average particle size) (0.8 g) at a flow rate of 0.3 mL min^{-1}. After 2 hours either H_2O, *N*-phenylbenzylamine (**2.4**) or *N*-benzylideneaniline (**2.3**) (all 16 mM) was added to the reaction vessel. The progress of the reaction was monitored by GC using 4-tert-butylphenol (50 mM in methanol) as an external standard.

16 mM of species (H_2O, **2.3** and **2.4**) was added to the starting solution based on calculations performed to determine the concentration required to cover a monolayer of Au/TiO_2:

Using average bond lengths, the rough area of a molecule of alcohol (**2.1**) was calculated to be 7.4 x 10^{-20} m^2.



Area = width x length

$= 1.4 \times 10^{-10} \times 5.3 \times 10^{-10} = 7.4 \times 10^{-20}$ m^2

The BET surface area of Au/TiO_2 was 47 m^2 g^{-1}, thus to cover this area, 6.3×10^{20} molecules of **2.1** are required:

$= 47 \div 7.4 \times 10^{-20} = 6.3 \times 10^{20}$ molecules of **2.1**

In 1 mole there is 6×10^{23} molecules, therefore to cover the surface area of 0.8 grams of Au/TiO_2, 0.8 mmol are required. As 500 mL of solvent was used in experiments with the reactor operated in single pass mode, 16 mM of **2.1** was used in the experiment to ensure a constant coverage of **2.1** over the catalyst surface:

$= (0.8 \div 6.0 \times 10^{23}) \times 6.3 \times 10^{20} = 0.8$ mmol of **2.1**

7.3.2 Typical procedure for the alkylation of aniline (2.2) with benzyl alcohol (2.1) using the Endeavor® batch reactor

The Endeavor® batch reactor allows for up to 8 reactions to be conducted with temperatures and pressures up to 200 ˚C and 34 bar, respectively. Experimental parameters can be entered using the Endeavor® software. Reactions can be stirred by disposable impellers in the overhead stirrer system, with adjustable speeds up to 1000 rpm.

In general, catalyst (0.2 wt.%, mol% shown in Table 7.2, 190 μm average particle size) or support (0.3 g) was loaded into a glass reaction vessel (15 mL total volume, with a working volume of 5 mL), which were then placed inside the stainless steel reactor. Anhydrous 2-methyl-2-butanol (2 mL) was used to make a solution of aniline (**2.2**) (0.5 M) and alcohol (**2.1**) (0.5 M), which was then added to the catalyst contained in the glass reaction vessel. The overhead stirrer system was then clamped into position and the desired programme for performing reactions selected and started.

The following programme was used in this work:

Reactions were purged with N_2 (3 cycles), the mixtures were then heated up to 180 ˚C under a pressure of 15 bar (N_2) under continuous stirring at 250 rpm for 30 min. The reactions were allowed to cool to 25 ˚C and were subsequently vented. Reaction mixtures were analysed by GC using 4-tert-butylphenol (50 mM in methanol) as an external standard.

TABLE 7.2. *Mol% of catalyst employed in the Endeavor® batch reactions.*

Catalyst	mol%
Au/TiO_2	0.9
Au/CeO_2	0.9
$Au/HFeO_2$	0.9
Au/C	0.9
$Au/\alpha\text{-}Al_2O_3$	0.9
$Au/\gamma\text{-}Al_2O_3$	0.9
Cu/TiO_2	3.0
Ni/TiO_2	3.0
Co/TiO_2	3.0
Ag/TiO_2	2.0
Rh/TiO_2	2.0
Pd/TiO_2	2.0
Pt/TiO_2	0.9
Ir/TiO_2	0.8
$Au,Ni/TiO_2$	2.0
$Au,Co/TiO_2$	2.0
$Au,Pd/TiO_2$	1.0
$Au,Cu/TiO_2$	2.0

7.3.2.1 Leaching study of Cu/TiO_2 catalysts using the Endeavor® batch reactor

Two portions of Cu/TiO_2 (3 mol% Cu) were loaded into separate glass reaction vessel, which were then placed inside the stainless steel reactor. Anhydrous 2-methyl-2-butanol (2 mL) was added to one of the glass vessels containing Cu/TiO_2, to the other a solution of *N*-phenylbenzylamine (0.5 M) in 2-methyl-2-butanol (2 mL). Reactions were then started using the programme described in Section 7.3.2, but with a reaction time of 1 h 30 min. Following the cooling and venting of the reaction, the mixture was filtered and the solutions analysed by ICP analysis (Section 7.2).

7.4 Catalyst synthesis and calcination

This section details the catalyst preparation and calcination methods employed for the materials described in Chapters 4, 5 and 6.

7.4.1 Preparation of Au/TiO_2 by the incipient wetness impregnation method (IMP)

A solution of $HAuCl_4.3H_2O$ (41.2% Au assay, 1.21 g $HAuCl_4.3H_2O$, 2.5 mmol of Au) made in 26 mL of deionised H_2O was added to TiO_2 (Degussa P25, 50 g), stirring the mixture with a glass rod until all the liquid was absorbed onto the support. The catalyst was then dried in an oven at 100 ˚C for 24 hours before samples were calcined under air, H_2/N_2 and argon at 300 ˚C (see Section 7.4.5).

7.4.2 Preparation of Au supported, metal and Au bimetallic catalysts using the deposition-precipitation method (DP) [62]

7.4.2.1 Preparation of Au supported catalysts

Deionised H_2O (1 L) was added to a beaker containing support (50 g). The mixture was vigorously stirred (500 rpm) and heated to 75 ˚C. The pH was adjusted to 8 (in the case of Au/TiO_2 two catalysts were prepared, using pH values of 8 and 9, see Chapter 4) by the addition of a NaOH solution (2.5 g in 100 mL of deionised H_2O, 63 mmol of NaOH). A solution of $HAuCl_4.3H_2O$ (41.2% assay, 1.21 g, 2.6 mmol of Au) made in 100 mL of deionised H_2O was then added drop-wise along with the NaOH solution (63 mM) to maintain a pH of 8 (or 9). After the addition of all the $HAuCl_4.3H_2O$ solution, the slurry was left under vigorous stirring (500 rpm) for 30 min at 75 ˚C. The Au catalyst was then collected by filtration and exhaustively washed with deionised H_2O. The catalyst was then dried in an oven at 100 ˚C for 24 hours before calcination under air, H_2/N_2 and argon at temperatures between 300-800 ˚C (see Section 7.4.5 and Tables 4.1 and 5.1). Au/C was oven dried only.

7.4.2.2 Preparation of Cu/TiO_2

Deionised H_2O (400 L) was added to a beaker containing TiO_2 (Degussa P25, 19 g). The mixture was vigorously stirred (500 rpm) and heated to 75 ˚C. The pH was adjusted to 8 by the addition of a NaOH solution (2.5 g in 100 mL of deionised H_2O, 63 mmol of NaOH). A solution of $Cu(NO_3)_2.3H_2O$ (26.3% assay, 3.80 g and 0.76 g for a 5 and 1 wt.% loading, respectively) in 40 mL of deionised H_2O was then added drop-wise along with the NaOH solution (63 mM) to maintain a pH of 8. After the addition of all the $Cu(NO_3)_2.3H_2O$ solution, the slurry was left under vigorous stirring (500 rpm) for 30 min at 75 ˚C. The resulting mixture was filtered and exhaustively washed with deionised H_2O (1 L). The catalyst was then dried in an oven at 100 ˚C for 24 h before samples were calcined under air and H_2/N_2 at 300 and 500 ˚C between 2 and 4 h (see Section 7.4.5 and 6.4).

7.4.2.3 Preparation of other monometallic catalysts

The same procedure used for preparing the Cu/TiO_2 catalysts (Section 7.4.2.2) was employed for the synthesis of other monometallic systems (M/TiO_2), where loadings of 1 wt.% were aimed for. Table 7.3 shows the amount of metal salts employed. Samples of all systems were calcined at 300 ˚C under H_2/N_2 for 2 hours (Section 7.4.5).

TABLE 7.3. *Weights of metal salts employed in the synthesis of the M/TiO_2 catalysts.*

Catalyst	Metal Salt	Metal assay (%)	Grams	Mmol
Ni/TiO_2	$Ni(NO_3)_2.6H_2O$	20.2	0.99	3.4
Co/TiO_2	$Co(NO_3)_2.6H_2O$	20.3	0.99	3.4
Ag/TiO_2	$AgNO_3$	63.5	0.31	1.8
Rh/TiO_2	$Rh(NO_3)_3$	12.3	1.63	1.9
Pd/TiO_2	$PdCl_2$	23.8	0.84	1.9
Pt/TiO_2	$Pt(NO_3)_2$	16.5	1.22	1.0
Ir/TiO_2	$IrCl_3$	52.1	0.38	1.0

7.4.2.4 Preparation of the Au bimetallic catalysts

The same procedure used for preparing Cu/TiO_2 (Section 7.4.2.2) was employed for the synthesis of the majority of the bimetallic catalysts (Au,M/TiO_2), where a total metal loading of 1 wt.% and a 1:1 molar ratio of each metal was aimed for. Au,Ag/TiO_2 was prepared following the procedure outlined in Section 7.4.2.5 and Au,Pd/TiO_2 was made in a 50 g batch using the same procedure outlined in Section 7.4.2.1 (at pH 8). Table 7.4 shows the amount

of metal salts employed. In all cases, $HAuCl_4.3H_2O$ was used as the Au precursor (41.2% assay). Samples of all systems were calcined at 300 ˚C under H_2/N_2 for 2 hours (Section 7.4.5).

TABLE 7.4. *Weights of metal salts employed in the synthesis of Au,M/TiO_2 catalysts.*

Catalyst	Metal Salt	Metal assay (%)	Grams (metal)	Mmol (metal)	Grams (Au)	Mmol (Au)
Au,Ni/TiO_2	$Ni(NO_3)_2.6H_2O$	20.2	0.23	0.79	0.37	0.79
Au,Co/TiO_2	$Co(NO_3)_2.6H_2O$	20.3	0.23	0.79	0.37	0.79
Au,Pd/TiO_2	$PdCl_2$	23.8	0.73	1.60	0.79	1.60
Au,Cu/TiO_2	$Cu(NO_3)_2.3H_2O$	26.3	0.19	0.79	0.37	0.79

7.4.2.5 Preparation of Au,Ag/TiO_2

Deionised H_2O (400 L) was added to a beaker containing TiO_2 (Degussa P25, 19 g). The mixture was vigorously stirred (500 rpm) and heated to 75 ˚C. The pH was adjusted to 8 by the addition of a NaOH solution (2.5 g in 100 mL of deionised H_2O, 63 mmol of NaOH). A solution of the $HAuCl_4.3H_2O$ (41.2% assay, 0.31 g, 0.65 mmol of Au) made in 40 mL of deionised H_2O was then added drop-wise along with the NaOH solution (63 mM) to maintain a pH of 8. After the addition of all the $HAuCl_4.3H_2O$ solution, the slurry was left under vigorous stirring (500 rpm) for 30 min at 75 ˚C. The resulting mixture was filtrated and exhaustively washed with deionised H_2O (1 L). The catalyst was then dried in an oven at 100 ˚C for 24 h. The procedure was repeated, using the same pH but adding a solution of $AgNO_3$ (63.5% assay, 0.11 g, 0.65 mmol of Au) to the Au/TiO_2 catalyst to form the bimetallic Au,Ag/TiO_2 system. A sample was calcined under air and H_2/N_2 at 300 ˚C for 2 hours (see Section 7.4.5).

7.4.3 Preparation of Au supported catalysts by the colloidal method (COL) [112]

A solution of poly(vinyl alcohol) (PVA) (0.12 g in 12 mL H_2O) was added to a solution of $HAuCl_4.3H_2O$ (41.2% assay, 0.24 g, 0.50 mmol of Au) made in 500 mL of H_2O. A freshly prepared solution of $NaBH_4$ (13 mM) was added to the PVA-Au mixture to form a dark-brown sol. After 30 min, the colloid was added to the support (10 g, TiO_2, CeO_2, Al_2O_3, C, $HFeO_2$) under vigorous stirring (500 rpm). The resulting mixture was filtered and

exhaustively washed with deionised H_2O (1 L). The catalyst was then dried in an oven at 100 ˚C for 24 h. Following the drying step, catalysts were refluxed in deionised H_2O in a round bottomed flask at 90 ˚C, under vigorous stirring (500 rpm) for 2 h. The resulting slurry was filtered, washed thoroughly with deionised H_2O (1 L) and dried at 100 ˚C for 24 h. Samples of Au/TiO_2, Au/CeO_2, $Au/HFeO_2$ and $Au/\gamma\text{-}Al_2O_3$ were subjected to calcination under H_2/N_2 at 200 ˚C for 2 h (See Sections 5.2 and 7.4.5).

7.4.4 Preparation of Cu/TiO_2 by the spray drying method (SD)

$Cu(NO_3)_2.3H_2O$ (26.3% assay, 3.80 g and 0.76 g for 5 and 1 wt.% loading, respectively) was added to a mixture of TiO_2 (19 g) suspended in 100 mL of deionised H_2O. The mixture was stirred to form a slurry and then introduced into a Büchi B-290 spray dryer using a peristaltic pump. The nozzle temperature was 200 ˚C. Samples of the resulting catalyst precursor were calcined under flowing 5% H_2/N_2 in a tube furnace or under static air at 500 ˚C for 4 h (See Section 6.4 and Section 7.4.5).

7.4.5 Typical procedure for catalyst calcination

A ramp rate of 10 ˚C min^{-1} up to 300 or 500 ˚C either under air, argon or H_2/N_2 was used for the prepared catalysts. The temperature was then held for 2 h (4 hours when using 500 ˚C) and cooled down back to room temperature.

REFERENCES

1. V. Hessel, D. Kralisch and N. Kockmann, *Novel Process Windows: Innovative Gates to Intensified and Sustainable Chemical Processes,* Wiley-VCH, 2015.
2. G. Guillena, J. Ramón Diego and M. Yus, *Chem. Rev.,* 2010, **110**, 1611-1641.
3. P. T. Anastas and N. Eghbali, *Chem. Soc. Rev.,* 2010, **39**, 301-312.
4. P. T. Anastas and M. M. Kirchhoff, *Acc. Chem. Res.,* 2002, **35**, 686-694.
5. P. J. Dunn, D. J. C. Constable, J. D. Hayler, G. R. Humphrey, J. Leazer Johnnie L., R. J. Linderman, K. Lorenz, J. Manley, B. A. Pearlman, A. Wells, A. Zaks and T. Y. Zhang, *Green Chem.,* 2007, **9**, 411-420.
6. M. Hornby and J. Peach, *Foundations of Organic Chemistry,* Oxford University Press: Oxford, 1993.
7. J. S. Carey, D. Laffan, C. Thomson and M. T. Williams, *Org. Biomol. Chem.,* 2006, **4**, 2237-2347.
8. S. Schreiber, A. Bleich and C. G. Pick, *J. Mol. Neurosci.,* 2002, **18**, 143-149.
9. C. P. Ong, C. L. Ng, H. K. Lee and S. F. Li, *J. Chromatogr.,* 1991, **588**, 335-339.
10. M. J. Millan, *J. Pharmacol. Exp. Ther*., 2010, **128**, 229-273.
11. A. Cid, J. A. Manso, O. Moldes, J. Morales, G. Astray, A. Cid and J. Quintás, *CyTA: Journal of Food*, 2011, **9**, 252-256.
12. M. A. Rosenow, C. L. Magee, J. C. Williams and J. P. Allen, *Acta Cryst*., 2002, **58**, 2076-2081.
13. R. N. Salvatore, C. H. Yoon and K. W. Jung, *Tetrahedron,* 2001, **57**, 7785-781.
14. M. D. Argentine, P. K. Owens and B. A. Olsen, *Adv. Drug Delivery Rev.,* 2007, **59**, 12-28.
15. K. G. Carson, B. D. Harris, C. A. Maryanoff, R. D. Shah, A. Abdel-Magid, *J. Org. Chem.,* 1996, **61**, 3849-3862.

16. D. Chusov and B. List, *Angew. Chem. Int. Ed.,* 2014, **53**, 5199-5201.
17. I. Bytschkov and S. Doye, *Eur. J. Org. Chem.,* 2003, 935-946.
18. Y. Yang, S. Shi, D. Niu, P. Liu and S. L. Buchwald, *Science,* 2015, **349**, 62-66.
19. T. Müller E., K. C. Hultzsch, M. Yus, F. Foubelo and M. Tada, *Chem. Rev.,* 2008, **108**, 3795-3892.
20. A. J. A. Watson and J. M. J. Williams, *Science,* 2010, **329**, 635-636.
21. R. Grigg, T. R. B. Mitchell, S. Sutthivaiyakit and N. Tongpenyai, *J. Chem. Soc.,* 1981, **12**, 611-612.
22. Y. Watanabe, Y. Tsuji and Y. Ohsugi, *Tetrahedron Lett.,* 1981, **22**, 2667-2670.
23. Y. Watanabe, Y. Tsuji, H. Ige, Y. Ohsugi and T. Ohta, *J. Org. Chem.,*1984, 49, 3359-3363.
24. Y. Watanabe, Y. Morisaki, T. Kondo and T. Mitsudo, *J. Org. Chem.,* 1996, **61**, 4214-4218.
25. S. Ganguly and D. M. Roundhill, *Polyhedron,* 1990, **9**, 2517-2526.
26. D. Hollmann, A. Tillack, D. Michalik and M. Beller, *Tetrahedron Lett.,* 2006, 47, 8881-8885.
27. M. H. Hamid, C. L. Allen, G. W. Lamb, A. C. Maxwell, H. C. Maytum, A. J. A. Watson and J. M. J. Williams, *J. Am. Chem. Soc.,* 2009, **131**, 1766-1774.
28. D. Hollmann, A. Tillack, D. Michalik, R. Jackstell and M. Beller, *Chem. Asian. J.,* 2007, **2**, 403-410.
29. S. Ganguly, F. L. Joslin and D. M. Roundhill, *Polyhedron,* 1989, **9**, 2517-2526.
30. S. Imm, S. Bähn, L. Neubert, H. Neumann and M. Beller, *Angew. Chem. Int. Ed.,* 2010, 49, 8126-8129.
31. J. Gal, *Helv. Chim. Acta,* 2013, **96**, 1617-1657.
32. S. Demir, F. Coşkun and İ Özdemir, *J. Organomet. Chem.,* 2014, **755**, 134-140.

33. A. N. Kharat and B. T. Jahromi, *J. Coord. Chem.,* 2013, **66**, 3498-3508.

34. Z. Z. Li, K. Fujita, Z. Li, N. Ozeki and R. Yamaguchi, *Tetrahedron Lett.,* 2003, **44**, 2687-2690.

35. R. Kawahara, K. Fujita and R. Yamaguchi, *Adv. Synth. Catal.,* 2011, **353**,1161-1168.

36. O. Saidi, A. J. Blacker, G. W. Lamb, S. P. Marsden, J. E. Taylor and J. M. J. Williams, *Org. Process Res. Dev.,* 2010, **14**, 1046-1049.

37. Y. Zhang, C. Lim, D. S. B. Sim, H. Pan and Y. Zhao, *Angew. Chem., Int. Ed.,* 2014, **53**, 1399-1403.

38. A. Martínez-Asencio, D. J. Ramón and M. Yus, *Tetrahedron,* 2011, **67**, 3140-3149.

39. J. J. Garcia, G. Reyes-Rios, *Inorg. Chim. Acta.*, 2012, **392**, 317-321.

40. T. T. Dang, B. Ramalingam, S. P. Shan and A. M. Seayad, *ACS Catal.,* 2013, **3**, 2536-2540.

41. H. Yang, R. Mao, C. Luo, C. Lu and G. Cheng, *Tetrahedron,* 2014, **70**, 8829-8835.

42. T. Yan, B. L. Feringa and K. Barta, *Nat. Commun.,* 2014, **5**, 5602.

43. X. Guo, D. Wang, C. Wang, Y. Wang, R. Zhong, X. Zhu, L. Cai, Z. Gao and X. Hou, *Adv. Synth. Catal.,* 2013, **355**, 1117-1125.

44. T. D. Tuan, A. M. Seayad, B. Ramalingam, S. Pei Shan and T. T. Dang, *ChemCatChem,* 2014, **6**, 808-814.

45. C. H. Bartholomew, *Appl. Catal., A.,* 2001, **212**, 17-60.

46. G. W. Lamb, F. A. Al Badran, J. M. J. Williams and S. T. Kolaczkowski, *Chem. Eng. Res. Design,* 2010, 88, 1533-1540.

47. *"New Prescription For Drug Makers: Update the Plants",* L. Abboud and S. Hensley, The Wall Street Journal, September 3, 2003.

48. A. B. Brown and E. E. Reid, *J. Am. Chem. Soc.,* 1924, **46**, 1836-1839.

49. K. N. Tayade, M. Mishra, M. K. and R. S. Somani, *J. Mol. Catal. A: Chem.,* 2014, **390**, 91-96.
50. M. A. Kumar, M. M. Reddy, P. Swamy, M. Naresh, K. Srujana, L. Satyanarayana, A. Venugopal and N. Narender, *Green Chem.,* 2013, **15**, 3474-3483.
51. P. R. Likhar, R. Arundhathi, M. L. Kantam and P. S. Prathima, *Eur. J. Org. Chem.,* 2009, 5383-5389.
52. R. G. Rice and E. J. Kohn, *J. Am. Chem. Soc.,* 1955, **77**, 4052- 4054.
53. E. J. Schwoegler and H. Adkins, *J. Am. Chem. Soc.,* 1939, **61**,3499-3502.
54. A. Baiker and W. Richarz, *Tetrahedron Lett.,* 1977, **18**, 1937-1938.
55. E. F. Pratt and E. J. Frazza, *J. Am. Chem. Soc.,* 1954, **76**, 6174-6179.
56. M. Mishra, M. Dixit, P. A. Joshi and D. O. Shah, *Catal. Commun.,* 2013, **33**, 80-83.
57. J. Sun, X. Jin, F. Zhang, W. Hu, J. Liu and R. Li, *Catal. Commun.,* 2012, **24**, 30-33.
58. A. Mehta, A. Thaker, V. Londhe and S. R. Nandan, *Appl. Catal., A.,* 2014,**478**, 241-251.
59. K. Shimizu, N. Imaiida, K. Kon, Hakim Siddiki S.M.A. and A. Satsuma, *ACS Catal.,* 2013, **3**, 998-1005.
60. K. Shimizu, S. Kanno, K. Kon, S. M. A. Hakim Siddiki, H. Tanaka and Y. Sakata, *Catal. Today,* 2014, **232**, 134-138.
61. R. N. Spitz, J. E. Barton, M. A. Barteau, R. H. Staley and A. W. Sleight, *J. Phys. Chem.,* 1986, **90**, 4067-4075.
62. A. Abad, A. Corma and H. García, *Chem. Eur. J*., 2008, **14**, 212 – 222 .
63. X. Cui, X. Dai, Y. Deng and F. Shi, *Chem. Eur. J.,* 2013, **19**, 3665-3675.
64. V. Gyollai, T. Sipocz, G. Dorman, L. Kocsis, G. Sipos, T. Sipőcz, G. Dormán, L. Kocsis, R. V. Jones and F. Darvas, *J. Flow. Chem.,* 2013, **3**, 51-58.
65. X. Cui, Y. Zhang, F. Shi and Y. Deng, *Chem. Eur. J.,* 2011, **17**, 1382-1382.
66. G. Chuah, H. Liu and S. Jaenicke, *J. Catal.,* 2012, 292, 130-137.

67. F. Vermoortele, I. Geukens, M. Meledina, S. Turner, G. Van Tendeloo and D. E. De Vos, *Appl. Catal., A.,* 2014, **469**, 373-379.

68. A. Corma, T. Ródenas and M. Sabater, *Chem. Eur. J.,* 2010, **16**, 254-260.

69. M. Ousmane, G. Perrussel, Z. Yan, J. Clacens, F. De Campo and M. Pera-Titus, *J. Catal.,* 2014, **309**, 439-452.

70. Y. Zhang, X. Qi, X. Cui, F. Shi and Y. Deng, *Tetrahedron Lett.,* 2011, **52**, 1334-1338.

71 . X. Cui, Y. Zhang, F. Shi and Y. Deng, *Chem. Eur. J.*, 2011, **17**, 1021-1028.

72. M. Sankar, E. Nowicka, R. Tiruvalam, Q. He, S. H. Taylor, C. J. Kiely, D. Bethell, D. W. Knight and G. J. Hutchings, *J. Catal.,* 2011, **17**, 6524-6532.

73. C. T. Campbell, *Nat. Chem.,* 2012, **4**, 597-598.

74. N. Kawakita, *Gold Bull.,* 2009, **42**, 267-274.

75. R. Takamura, T. Takei, T. Akita, M. Haruta and T. Ishida, *Appl. Catal., A.,* 2012, **413**, 261-266.

76. L. He, X. Lou, J. Ni, Y. Liu, Y. Cao, H. He and K. Fan, *Chem. Eur. J.,* 2010, 16, 13965-13969.

77. F. J. Roberts, N. Zotova, G. H. Kelsall, A. S. Jessiman, K. Hellgardt and K. K. Hii, *Green Chem.,* 2012, **14**, 226-232.

78. R. K. Henderson, C. Jiménez-González, D. J. C. Constable, S. R. Alston, G. G. A. Inglis, G. Fisher, J. Sherwood, S. P. Binks and A. D. Curzons, *Green Chem.,* 2011, **13**, 854-862.

79. L. Petrov, Y. Alhamed and A. Alzahrani, *J. Catal. ,* 2011, 32, 387-404.

80. I. L. Simakova, Y. Demidova, J. Wärnå, A. Simakov and D. Y. Murzin, *Chem. Eng. J.,* 2014, **238**, 164-171.

81. A. Corma, C. Gonzalez-Arellano, M. Iglesias, F. Sanchez, *Chem. Commun.,* 2005, **15**, 3451-3453.

82. L. Liu, A. Selloni, G. Q. Lu, C. Sun and S. C. Smith, *J. Mater. Chem.,* 2010, **20**, 10319-10334.

83. C. Michel, F. Delbecq, C. Pinel, S. Chibani, F. Delbecq and M. Besson, *Catal. Sci. Technol.,* 2013, **3**, 339-350.

84. B. N. Zope, D. D. Hibbitts, M. Neurock and R. J. Davis, *Science,* 2010, **330**, 74-78.

85. X. Zhang, H. Shi and B. Xu, *J. Catal.,* 2011, 279, 75-87.

86. X. Yang, X. Wang, C. Liang, W. Su, C. Wang, Z. Feng, C. Li and J. Qiu, *Catal. Commun.,* 2008, **9**, 2278-2281.

87. M. Li, X. Wang, N. Perret and M. A. Keane, *Catal. Commun. ,* 2014, **46**, 187-191.

88. C. Powell, B. Panthi, J. Saavedra, C. J. Pursell and B. D. Chandler, *J. Catal.,* 2013, **307**, 37-47.

89. Y. Wang, L. Yan and G. Wang, *Phys. Chem. Chem. Phys.,* 2015, **17**, 8231-8238.

90. J. Gong and C. B. Mullins, *Acc. Chem. Res.,* 2009, **42**, 1063-1073.

91. B. Zhu, M. Lazar, B. G. Trewyn and R. J. Angelici, *J. Catal.,* 2008, **260**, 1-6.

92. M. Nishimura, A. Satsuma and K. Shimizu, *ChemCatChem,* 2009, **1**, 497-503.

93. L. Forni, *Catal. Today,* 1999, **52**, 147-152.

94. S. He, M. Yin, Z. Yu, K. Wu, L. Wang and C. Sun, *J. Catal. ,* 2013, **34**, 1534-1542.

95. F. Schuth and A. Wolf, *Appl. Catal., A.,* 2002, **226**, 1-13.

96. M. Haruta, *CATTECH,* 2002, **6**, 102-115.

97. N. Zheng and G. D. Stucky, *J. Am. Chem. Soc.,* 2006, **128**,14278-14280.

98. K. Ebitani, T. Mizugaki, K. Mori and K. Kaneda, *Bull. Chem. Soc. Jpn.,* 2006, **79**, 981-1016.

99. I. Mabaso, E. Viljoen, C. Welker, M. Claeys, D. Barkhuizen, E. van Steen and J. C. Q. Fletcher, *Pure. Appl. Chem.,* 2006, **78**, 1759-1769.

100. C. G. Bond, C. Louis and T. D. Thompson, *Catalysis by Gold,* Imperial College Press, 2006.

101. P. A. Sermon, G. C. Bond and P. B. Wells, *J. Chem. Soc.,* 1979, **75**, 385-394.

102. T. D. Mitrelias, J. Hargreaves, G. J. Hutchings and R. W. Joyner, *Catal. Lett.,* 1998, **50**, 211-218.

103. N. W. Cant and W. K. Hall, *J. Phys. Chem.,* 1971, **75**, 2914-2921.

104. D. Cunningham, K. Tanaka, M. Haruta and W. Vogel, *Catal. Lett.,* 1996, **40**, 175-181.

105. M. Bollinger and M. A. Vannice, *Catal. Lett.,* 1993, **17**, 245-262.

106. J. Schwank and J. Lee, *J. Catal.,* 1986, **102**, 207-215.

107. M. C. Kung, C. K. Costello and H. Kung, *J. Catal.,* 2003, **216**, 425-432.

108. S. Tsubota, T. Kobayashi, H. Kageyama, M. J. Genet and M. Haruta, *J. Catal.,* 1993, **144**, 175-192.

109. A. Ueda, K. Tanaka and M. Haruta, *J. Catal.,* 1997, 168, 125-127.

110. D. Cunningham, Y. Bando and M. Haruta, *Stud. Surf. Sci. Catal.,*1995, **91**, 227-235.

111. Q. Zhang, G. A. Somorjai, K. Na and G. A. Somorjai, *J. Custer. Sci.,* 2014, **25**, 83-114.

112. J. Lopez-Sanchez, N. Dimitratos, C. Hammond, G. L. Brett, L. Kesavan, S. White, P. Miedziak, R. Tiruvalam, R. L. Jenkins, A. F. Carley, D. Knight, C. J. Kiely and G. J. Hutchings, *Nature Chem.*, 2011, **3**, 551-556.

113. H. Yin, C. Wang, H. Zhu, S. H. Overbury, S. Sun and S. Dai, *Chem. Commun.,* 2008, 36, 4357-4359.

114. A. B. D. Nandiyanto and K. Okuyama, *Adv. Powder Technol.,* 2011, **22**, 1-19.

115. K. Okuyama and I. Wuled Lenggoro, *Chem. Eng. Sci.,* 2003, **58**, 537-547.

116. M. Santiago, A. Restuccia, F. Gramm and J. Pérez-Ramírez, *Micropor. Mesopor. Mat.,* 2011, **146**, 76-81.

117. A. P. Kozlova, K. Asakura, Y. Matsui, T. Kogure, A. I. Kozlov, A. P. Kozlova, T. Shido and Y. Iwasawa, *J. Catal.,* 2000, **196**, 56-65.

118. S. K. Ghosh and T. Pal, *Chem. Rev.,* 2007, **107**, 4797-4862.

119. N. Wetchakun, B. Incessungvorn, K. Wetchakun and S. Phanichphant, *Mater. Lett.,* 2012, **82**, 195-198.

120. M. A. Debeila, M. C. Raphulu, E. Mokoena, M. Avalos, V. Petranovskii, N. J. Coville and M. S. Scurrell, *Mater. Sci. Eng. A.,* 2005, **396**, 61-69.

121. F. Duprat, *Chem. Eng. Sci.*, 2002, **57**, 901-911.

122. A. Corma and H. Garcia, *Chem. Soc. Rev.,* 2008, **37**, 2096-2126.

123. J. L. C. Fajín, A. Bruix, M. N. D. S. Cordeiro, J. R. B. Gomes and F. Illas, *J. Chem. Phys.,* 2012, **137**, 34701.

124. A. Wieckowski, E. Savinova.R and G. V. Constantinos, *Catalysis and Electrocatalysis at Nanoparticles Surfaces,* Taylor and Francis, 2003.

125. X. Liu, M. Liu, Y. Luo, C. Mou, S. D. Lin, H. Cheng, J. Chen, J. Lee and T. Lin, *J. Am. Chem. Soc.*, 2012, **134**, 10251-10258.

126. N. S. Kotsarenko, T. S. Glazneva, N. S. Kotsarenko and E. A. Paukshtis, *Kinetics & Catal.,* 2008, **49**, 859-867.

127. I. L. Simakova, Y. Demidova, M. Estrada, S. Beloshapkin, E. V. Suslov, D. V. Korchagina, K. P. Volcho, N. F. Salakhutdinov, A. V. Simakov and D. Y. Murzin, *Appl. Catal., A.,* 2013, **464**, 348-356.

128. L. Prati, M. Rossi, S. Coluccia, G. Martra and F. Porta, *Catal. Today,* 2000, **61**, 165-172.

129. G. Pantaleo, A. M. Venezia, L. F. Liotta, H. Wu, A. Venezia and L. Liotta, *Catalysts,* 2013, **3**, 774-793.

130. L. Ortiz-Soto, B. Lee, M. D. Amiridis, S. H. Overbury, H. Zhu, B. Lee and S. Dai, *Catal. Lett.,* 2004, **95**, 99-106.

131. R. Leppelt, V. Plzak, J. Cai, A. Chuvilin, A. Karpenko, B. Schumacher, U. Kaiser and R. J. Behm, *Top. Catal.,* 2007, **44**, 183-198.

132. R. M. Cornell, and U. Schwertmann, U. Introduction to the Iron Oxides, in: The Iron Oxides: Structure, Properties, Reactions, Occurences and Uses, Second Edition, Wiley-VCH, Weinheim, 2003.

133. M. Trueba and S. P. Trasatti, *Eur. J. Inorg. Chem.,* 2005, **17**, 3393-3403.

134. E. Yalamaç, A. Trapani and S. Akkurt, *Eng. Sci. & Tech.,* 2014, **17**, 2-7.

135. L. E. Wolf, *Application of Graphene: An Overview,* Springer Science & Business Media, 2014.

136. J. Raaymakers, A. van Dillen, K. de Jong and M. G. Nijkamp, *Appl. Phys. A.,* 2001, 72, 619-623.

137. S. A. Nikolaev and V. V. Smirnov, *Catal. Today,* 2009, 147, S336-S341.

138. C. Breitkopf, N. El Kolli, J. Krafft, C. Louis, M. C. I. Bezen and J. A. Lercher, *Chem. Eur. J.,* 2011, **25**, 7095-7104.

139. T. Zhu, N. Li and C. Xu, *Int. J. Electrochem. Sci.,* 2013, **8**, 9508-9517.

140. P. Claus, *Appl. Catal., A. ,* 2005, **291**, 222-229.

141. A. Corma, M. Iglesias, C. González-Arellano and F. Sánchez, *Adv. Synth. Catal.,* 2004, **346**, 1316-1328.

142. S. Liu, J. Li, X. Tian, X. Zhen, Y. Yang and J. Han, *Syn. Commun.,* 2012, **42**, 2540-2554.

143. M. Irfan, E. Petricci, T. N. Glasnov, M. Taddei and C. O. Kappe, *Eur. J. Org. Chem.,* 2009, 1327-1334.

144. S. Saaby, K. R. Knudsen, M. Ladlow and S. V. Ley, *Chem. Commun.,* 2005, **23**, 2909-2911.

145. Y. Shinozuka, Y. Ohishi, T. Shishido, K. Takaki and T. Kawabata, *J. Mol. Catal.*, 2005, **236**, 206-215.

146. A. M. Venezia, G. Deganello, A. Longo, A. Martorana, L. F. Liotta, Z. Schay and L. Guczi, *Catal. Today,* 2001, **66**, 271-276.

147. T. Mallat and A. Baiker, *Chem. Rev.,* 2004, **104**, 3037-3058.

148. W. Lei, Y. Ji, L. Wu and Q. Fan, *Acta. Chim. Sinica.,* 2014*,* 72*,* 798-808.

149. Z. Guo, B. Liu, Q. Zhang, W. Deng, Y. Wang and Y. Yang, *Chem. Soc. Rev.,* 2014, 43, 3480-3524.

150. P. Atkins, R. Overton, J. Rourke, M. Weller and F. Armstrong, *Inorganic Chemistry 4th Edition,* Oxford University Press, Oxford, 2006.

151. A. Wang, X. Y. Liu, C. Mou and T. Zhang, *J. Catal.,* 2013, **308**, 258-271.

152. S. Bagheri, N. Muhd Julkapli and A. H. Bee, *The Scientific World Journal,* 2014, **2014**, 1-21.

153. D. W. Goodman, *Catal. Lett.,* 2005, **99**, 1-4.

154. A. Yoshida, Y. Mori, T. Ikeda, K. Azemoto and S. Naito, *Catal. Today,* 2013, **203**, 153-157.

155. Y. G. Li, J. F. Porter, Y. Li and C. K. Chan, *J. Mater. Sci.,* 1999, **34**, 1523-1531.

156. S. Sadasivan, R. M. Bellabarba and R. P. Tooze, *Nanoscale,* 2013, **5**, 11139-11146.

157. E. Cao, M. Sankar, E. Nowicka, Q. He, M. Morad, P. J. Miedziak, S. H. Taylor, D. W. Knight, D. Bethell, C. J. Kiely, A. Gavriilidis and G. J. Hutchings, *Catal. Today,* 2013, 203, 146-152.

158. R. Cano, J. Pérez M., M. Yus and D. Ramón J, *Eur. J. Org. Chem.,* 2012, **24**, 4548-4554.

159. M. V. Twigg and M. S. Spencer, *Appl. Catal., A.,* 2001, **212**, 161-174.

160. R. J. Davis, M. S. Ide and D. D. Falcone, *J. Catal.,* 2014, **311**, 295-305.

161. V. R. Gangwal, J. Van der Schaff, B.F.M. Kuster, J. C. Schouten, *J. Catal.,* 2005, **232**, 432-443.

162. V. Ponec, *Appl. Catal., A.,* 2001, **222**, 31-45.

163. A. Sandoval, A. Aguilar, C. Louis, A. Traverse and R. Zanella, *J. Catal.,* 2011, **281**, 40-49.